Qualitative and quantitative analyses of the composition and dynamics of light harvesting complex I in eukaryotic photosynthesis

Dissertation

zur Erlangung des akademischen Grades *doctor rerum naturalium* (Dr. rer. nat.)

vorgelegt dem Rat der Biologisch-Pharmazeutischen Fakultät
der Friedrich-Schiller-Universität Jena

von

Diplombiologe Einar Jamandre Stauber
geboren am 22. August 1973 in Moscow (Idaho, USA)

November 2007

Abbreviations

ADP	adenosine diphosphate
ATP	adenosine triphosphate
CAB	chlorophyll a/b binding protein
CC424	arginine auxotrophic *Chlamydomonas reinhardtii* strain
CV	coefficient of variation
DEAE	(diethylamino)ethyl
1-DE	one-dimensional gel electrophoresis
2-DE	two-dimensional gel electrophoresis
EST	expressed sequence tag
IEF-PAGE	isoelectic focusing/SDS-PAGE
IRLhca3	RNA*i* mutant of Lhca3
LC-MS	liquid chromatography-mass spectrometry
LC-MS/MS	liquid chromatography-tandem mass spectrometry
Lhc	light harvesting complex protein
Lhca	light harvesting complex protein of photosystem I
Lhcb	light harvesting complex protein of photosystem II
LHCI	light harvesting complex of photosystem I
LHCII	light harvesting complex of photosystem II
MS	mass spectrometry
NADP	nicotinamide adenine dinucleotide phosphate
P_i	inorganic phosphate
PSI	photosystem I
PSI-LHCI	holocomplex of photosystem I and light harvesting complex I
PSII	photosystem II
SILAC	stable isotope labelling by amino acids in cell culture
RNA*i*	ribonucleic acid interference technology
SDS-PAGE	sodium dodecyl sulfate – polyacrylamide gel electrophorhesis

Table of contents

1. Introduction

The accessory light-harvesting complexes (LHCs) enable land plants and green algae to live in highly variable environments. The LHCs form an antenna around photosystem I (PSI) (called LHCI) and photosystem II (PSII) (called LHCII) that gather solar energy and transfer it to the reaction centers where the energy drives electron transport (Jansson, 1999; Koziol, 2007). LHCI and LHCII are each composed of several pigment binding proteins called Lhca and Lhcb, respectively. Lhca and Lhcb belong to a multi-gene family encoding proteins with one to four transmembrane helices and several conserved chlorophyll and xanthophyll binding sites (Pichersky, 1996; Koziol, 2007). They likely evolved through gene duplication of high-light inducible proteins of cyanobacteria which function in acclimation to light stress (Dolganov, 1995; Jansson, 1999; Montané, 2000; Koziol, 2007). LHCI is tightly associated with the PSI core complex. It exhibits low temperature fluorescence emission shifted toward longer wavelengths as compared to LHCII.

Despite its central role in photosynthesis, the exact composition of LHCI and our understanding of the role of the single Lhca proteins and their function in adaptation of the photosynthetic capacity to varying environmental conditions is far from complete. For example, genome sequence information has provided valuable data on the number and structure of *lhca* genes, however, their corresponding proteins have not always been identified. This is partly due to the difficulty of separating the different Lhca. Quantitative determinations of Lhca have been hampered by the lack of methods for absolute quantification of proteins in complexes.

In the present study, two eukaryotic organisms, the green alga *Chlamydomonas reinhardtii* (Chlamydomonas) and *Lycopersicon esculentum* (*Solanum lycopersicum*, tomato) as a land plant, were studied with respect to composition of their LHCI and the association of LHCI with PSI. A detailed study of Chlamydomonas LHCI was aimed at determining its qualitative composition and the stoichiometry of its Lhca with respect to the PSI core complex.

The LHCI-PSI complex has a remarkable ability to adjust itself to changing environmental conditions. Under iron deficiency, PSI levels are drastically reduced, and LHCI is remodelled and becomes energetically uncoupled from PSI (Moseley, 2002a). In this thesis, the

remodelling of the LHCI-PSI complex occuring under iron deficiency was investigated in detail with special focus on the mechanism of the uncoupling of LHCI from PSI.

With the advances in mass spectrometry (MS) techniques, proteomics have become an important tool in the analysis of protein complexes. Two-dimensional gel electrophoresis (2-DE) and one-dimensional gel electrophoresis (1-DE) have been applied throughout this study to identify and quantify single Lhca obtained from purified complexes or thylakoid preparations. As a method for protein quantification, stable isotope labelling was established for use in Chlamydomonas and successfully applied in the determination of the Lhca-PSI stoichiometry.

2. Background

2.1 Photosystem I is a light-driven plastocyanin or cytochrome c_6 – ferredoxin oxidoreductase

Light-dependent electron flow from H_2O to NADPH in the photosynthetic apparatus is carried out by the concerted action of four multiprotein complexes of the thylakoid membrane; PSII, the cytochrome *b_6f* complex, PSI-LHCI and the adenosine triphosphate (ATP) synthase (Dekker, 2005; Nelson, 2006). PSII initiates the process by the light-driven removal of electrons from H_2O in the lumenal compartment of the thylakoids and transferring them to a pool of mobile lipophilic electron carriers referred to as the plastoquinone pool. Plastoquinol does not deliver electrons directly to PSI, but instead delivers them to the cytochrome *b_6f* complex which transfers them to either of the soluble lumenal electron carriers plastocyanin or cytochrome *c_6* which can donate electrons to PSI (Cramer, 2006). Plastocyanin serves as an electron donor for land plants, algae and most photosynthetic prokaryotes. In contrast to land plants (Weigel, 2003), green algae and cyanobacteria can also use cytochrome *c_6* as an electron donor to PSI. Thus the cytochrome *b_6f* complex mediates electron flow between the two photosystems and also plays a key role in processes such as state transitions and cyclic electron flow that tune PSII and PSI activity to chloroplast requirements (Finazzi, 2004; Rochaix, 2007).

In PSI, light energy absorbed by antenna pigments is used to drive transmembrane electron transport from plastocyanin or cytochrome *c_6* in the lumen to ferredoxin on the stromal side of the thylakoid membrane. Excitation energy from the antenna system proceeds to the electron transport chain through a pair of connecting chlorophylls associated with each of its branches (Jordan, 2001; Gobets, 2003; Vasil'ev, 2004). Excitation of the primary donor P700 and subsequent donation to the primary acceptor (A_0) result in “trapping” through stable charge separation. Electrons on the acceptor side of PSI are transferred to ferredoxin, a powerful reductant, which provides electrons for NADPH production, nitrate assimilation and several other chloroplast reactions. Most of the reducing power of ferredoxin is used for CO_2 fixation. The redox cycle is completed when plastocyanin or cytochrome *c_6* donate electrons to $P700^+$ from the luminal side of PSI. Alternatively electrons can be transferred back to the cytochrome *b_6f* complex during cyclic electron flow (Cramer, 2006).

Luminal protons set free by H_2O oxidation and electron transfer through the cytochrome b_6f complex are used to convert ADP + P_i into ATP in the stromal compartment by the ATP synthase.

Excess light energy can damage the photosynthetic apparatus leading to a decrease in photosynthetic efficieny with increasing illumination (photoinhibition). Although photoinhibition has been most intensively studied in PSII (Krieger-Liszkay, 2005), PSI is also subject to photoinhibition when electron flow through PSI is impaired (Hippler, 2000; Sommer, 2003b; reviewed in Rochaix, 2000; Sommer, 2003a). At low temperatures (Zhang, 2004) when CO_2 fixation rates are low, a shortage of oxidized ferredoxin causes electrons to be trapped at the acceptor side of PSI which also leads to photoinhibition. Interestingly, under iron deficiency when PSI levels are strongly diminished, PSI is not subject to photoinhibition (Moseley, 2002a).

2.2. Light-harvesting complex I delivers excitation energy to photosystem I

Lhca proteins belong to the superfamily of chlorophyll and carotenoid binding proteins (Lhc) that function in gathering solar energy and transferring it to photosynthetic reaction centers (Jansson, 1999; Koziol, 2007; Fig. 1). Crystal structures of the major LHCII components have been solved at atomic resolution in *Pisum sativum* (pea; Kühlbrandt, 1994; Standfuss, 2005) and *Spinacia oleracea* (spinach; Liu, 2004). Because of the similarity between Lhca and Lhcb, these structures provide a basis for understanding Lhca structure and function.

The first study biochemically characterizing LHCI identified four proteins (Lhca1-Lhca4) with molecular masses between 20 and 24 kDa which specifically associate with PSI in *Cucumis sativus* (cucumber) and *Hordeum vulgare* (barley) seedlings (Mullet, 1980). Lhca1/Lhca4 purify together as a dimer (Lam, 1984) while Lhca2 and Lhca3 exist as monomers. However, if mild conditions are used, a heterodimer of Lhca2 and Lhca3 (or possibly a homodimer of Lhca3) can also be obtained (Ihalainen, 2000). Expression of two additional genes (*lhca5* and *lhca6*) has been shown at the transcript level (Jansson, 1999; Koziol, 2007). Each Lhca protein/pigment complex has distinct spectral and functional properties (Croce, 2002). In some species such as tomato the main types are represented by two genes whose products differ in one or several amino acid(s): *cab 6a* and *cab 6b* both encode Lhca1 proteins (Hoffman, 1987; Pichersky, 1987; Zolla, 2002) and *cab 11* and *cab 12*

both encoding Lhca4 proteins (Schwartz, 1991). The situation is similar in poplar where isoforms of *lhca1* and *lhca2* exist (Klimmek, 2005). The inability to detect both isoforms is likely due to high level of identity between the two proteins and the lack of sufficiently sensitive methods.

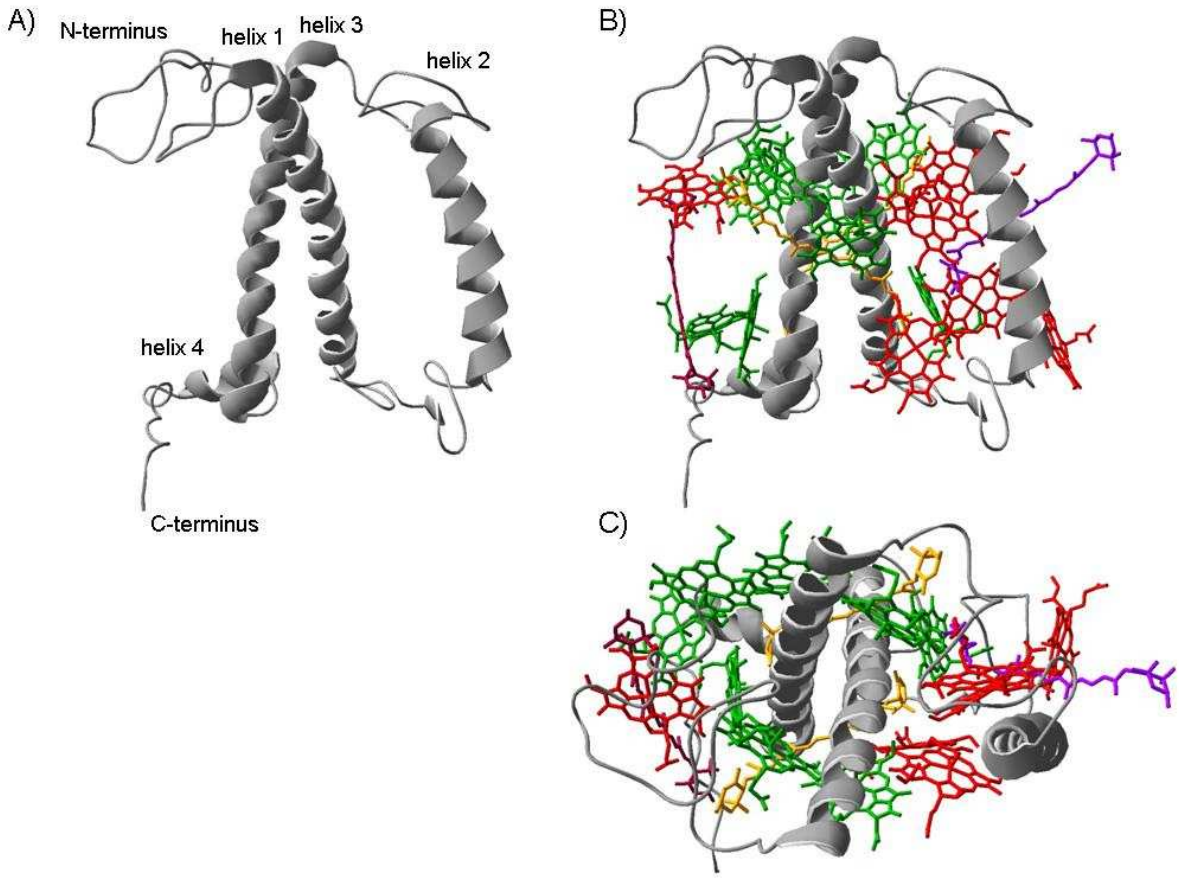

Figure 1. Model of a *Spinacia oleracea* (spinach) major Lhcb1 complex (Liu, 2004) exemplifies the common structure shared by Lhca and Lhcab proteins. A) The backbone of Lhcb1. Lhcs share the same basic structure defined by three membrane-spanning helices (helix 1 = helix B), (helix 2 = helix C), (helix 3 = helix A) and a short amphipathic helix (helix 4 = helix D). **B)** Fourteen chlorophyll molecules (eight chlorophyll *a* (*green*) and six chlorophyll *b* (*red*)) are coordinated by one monomeric Lhcb complex. Two central carotenoids (*orange*) assigned as lutein molecules associate closely with helix 1 and helix 2 at sites L1 and L2. These two carotenoids are necessary for proper *in vitro* folding of the Lhcb proteins. A third carotenoid (*purple*) assigned as neoxanthin is located in the chlorophyll *b* rich region around helix 1 at site N1. A fourth xanthophyll molecule (*crimson*), is located at the interface between interacting monomers at site V1 and shows mixed occupancy by violaxanthin and zeaxanthin. The xanthophyll at the V1 position likely plays a role in non-photochemical quenching in the xanthophyll cycle. **C)** View along the axes of the α-helices.

X-ray diffraction structures of pea PSI-LHCI crystals show that Lhca1, Lhca2, Lhca3, and Lhca4 cooperatively associate with PSI on the PSI-F side of the complex (Ben-Shem, 2003; Amunts, 2007). Gap pigments between the individual LHCI subunits and between LHCI and PSI enable rapid excitation energy transfer between LHCI and the core and also physically stabilize the entire complex. In line with biochemical data, the crystal structures show close association between Lhca1 and Lhca4 while association between Lhca2 and Lhca3 is weaker. Biochemical studies with antisense and knockout *Arabidopsis thaliana* plants have shown that PsaK is important for stabilization of the Lhca2/Lhca3 dimer (Jensen, 2000; Varotto, 2002). The first plant crystal structure data show an interaction between PsaK and Lhca3 (Ben-Shem, 2003) but this interaction is missing in the new structural model (Amunts, 2007). A possible explanation for the discrepancy is that structural models do not always correspond with native protein conformation. Structural models also show close interaction of PsaG and Lhca1, however, biochemical data from *A. thaliana* lacking PsaG did not have a decreased functional antenna size in comparison with wild-type plants (Jensen, 2002; Varotto, 2002).

PSI-LHCI possesses low energy "red" chlorophylls which have energy states lower than those of P700. The low energy states arise from excitionic coupling between two or more chlorophylls (Gobets, 2001) and may also arise from monomeric chlorophylls that are in an appropriate protein environment (Byrdin, 2002). They likely function in channeling excitation energy and, depending on their location, can direct energy toward P700 or toward non-photosynthetic carotenoids (Fig. 1). Transfer of energy from these chlorophylls is thus an uphill energy transfer by thermal activation and represents the slowest component in excitation energy transfer. Exitons can travel back and forth between the core an peripheral antenna multiple times before being trapped by P700 or dissipated from antenna pigments. The net flow of excitons is therefore significantly affected by the presence and location of red chlorophyll clusters.

Land plants do not have far red shifted chlorophylls in the PSI core. Instead, the most far red shifted chlorophylls are located in LHCI where Lhca3 and Lhca4 contain the lowest energy chlorophylls. Mutagenesis studies have been sucessful in identifying conserved chlorophyll binding residues responsible for the low energy forms (Morosinotto, 2002, 2003; Croce, 2004; Morosinotto, 2005b; Mozzo, 2006). Because PSI and LHCI are nearly isoenergetic with one another, the low energy "red" chlorophylls compete with P700 for exitation energy in the steady state (Croce, 1996; Ihalainen, 2005b; Englemann, 2006). Another important role that

they play is likely the dissipation of excitation energy (Nield, 2004; Melkozernov, 2006; Jensen, 2007). Exitons can travel back and forth between the core and peripheral antenna multiple times before being trapped by P_{700} or dissipated by non-light harvesting carotenoids. Red chlorophylls likely play an important role in determining the dynamics of this balance because they appear to interact with carotenoids that form triplet states. Carotenoids have the ability to quench triplet chlorophyll states and thereby prevent the formation of highly reactive singlet oxygen which makes them indispensable components of Lhcs. The finding that the presence of red chlorophylls enhances quenching of chlorophyll triplet states by carotenoids in recombinant land plant Lhca4 provides evidence for the role of red chlorophylls in photoprotection of PSI-LHCI (Carbonera, 2005).

2.3. Light-harvesting complex I plays an important role in acclimation of the photosynthetic apparatus to iron deficiency

Iron deficiency leads to a paling of photosynthetic tissue (chlorosis) due to a reduction in the amount of chlorophyll. Several adaptations in PSI photochemistry have evolved that allow photosynthetic organisms to cope with limited iron availability. Cyanobecteria can use flavodoxin as an electron acceptor to replace ferredoxin (an iron coordinating protein) during iron scarcity (Laudenbach, 1988a; La Roche, 1996). Green algae and photosynthetic prokaryotes have the ability to use plastocyanin (which coordinates copper) instead of cytochrome c_6 as an electron donor to PSI. This ability likely evolved from selective pressures exerted by both iron and copper deficiency in aquatic environments (Merchant, 2006; Peers, 2006). LHCI also plays an important role in the adaptation to iron deficiency. Photosynthetic prokaryotes express an iron stress induced PSI antenna which an likely serve both to increase light harvesting capacity and mediate photooxidative stress (Laudenbach, 1988b; Bibby, 2001; Boekema, 2001; Bibby, 2003; Melkozernov, 2003; Ihalainen, 2005a).

Physiological studies with *Beta vulgaris* (sugar beet) showed that iron deficiency limits the photochemical capacity with increasing light intensity. This is due to i) a reduction in electron transport chain components (Spiller, 1980; Terry, 1980) and ii) a reduction of the ability of leaves to absorb incident light (Terry, 1983). The decreased light absorption can be explained by the lower leaf chlorophyll content. PSI and the cytochrome b_6f complex, which contain most of the iron in the photosynthetic complex are more severely affected than PSII (Nishio, 1985). At low light intensities, iron deficient leaves convert incoming light into chemical

energy with the same yield as iron sufficient leaves (photochemical efficiency), despite reduced chlorophyll content. However, as light intensities increase, the iron deficient leaves are much less efficient in utilizing incoming quanta for electron transport. Sugar beet as well as *Pyrus communis* (pear) and *Prunus persica* (peach) are able to reduce rates of Rubisco carboxylation to coincide with reduced capacity in the electron transport chain in a highly coordinated and regulated manner (Larbi, 2006).

Chlamydomonas has recently been used as a model organism to uncover the molecular mechanisms that control changes in the photosynthetic apparatus during iron deficiency (Moseley, 2002a) and to understand the interplay between the photosynthetic and repiratory electron transport chains (Naumann, 2007). In addition to increased expression of the FOX1 ferroxidase to increase iron assimilation, spectroscopic measurements showed that functional changes to PSI-LHCI occured. Fluorescence induction and decay measurements indicated a block in electron transport downstream of PSII, indicating that the cytochrome b_6f complex and/or PSI were functionally comprimised. 77 K fluorescence emission measurements of thylakoid membranes showed increased fluorescence and a blue shift in emission from 709 to 705 nm at 1 µM Fe indicating that LHCI is energetically uncoupled from PSI (Wollman, 1982; Jensen, 2000; Morosinotto, 2005a). In contrast, the functional antenna of PSII increased in size indicating that most of the thylakoid chlorophyll must be associated with LHCII (Naumann, 2007).

Immuno-blotting and 2DE showed that changes in the thylakoid proteome occur in a graded manner to progressively decreasing iron content (Moseley, 2002a). Ferredoxin, the PsaK subunit of PSI, and Lhca3 were the most sensitive subunits. Analysis of mRNA for PSI (*psaF, psaK*), the cytochrome b_6f complex (*petA*) and the ATP synthase complex (*Cβlp*) showed unchanged transcript levels which demonstrated that the observed decrease in protein amounts were under post-transcriptional control. At the same time, novel proteins were induced some of which were shown to be LHCI-like proteins using immuno-blotting. In contrast, the major PSII trimeric light harvesting complexes (LHCII) were not affected by iron deficiency (Moseley, 2002a).

Interestingly, iron deficient cells were not sensitive to high light despite low PSI levels and unchanged LHCII levels as are PSI-deficient mutants (Spreitzer, 1981; Redding, 1999;

Moseley, 2002a). This finding suggests that under iron deficient conditions LHCI adapts a configuration that favours dissipation of excess light energy to prevent photoinhibition.

To test if energetic uncoupling of LHCI can protect PSI from photoinhibition, the PSI-F deficient strain Δ*psaF*, which is sensitive to high light (Hippler, 2000) was crossed with the *crd1* strain (copper response defect) which has an energetically uncoupled LHCI (Hippler, 2000; Moseley, 2002a; Moseley, 2002b). Culture of the Δ*psaF* strain under photoautotrophic conditions in the presence and absence of iron showed that the cells were less light sensitive under iron deficient conditions (Moseley, 2002a). The double mutant *crd1/psaF* showed decreased light sensitivity as compared with the *psaF* strain under both iron sufficient and iron deficient conditions (Moseley, 2002a). Taken together, these results indicate that energetic uncoupling of LHCI during iron deficiency allows the complex to function preferentially in dissipating excitation energy and thereby protects the photosynthetic apparatus from photoinhibition.

2.4. Chlamydomonas and tomato as eukaryotic model organisms to study light-harvesting complex I

Chlamydomonas reinhardtii (Chlamydomonas) is a unicellular biflagelate green alga found in soil or brackish freshwater. It has long been used as a laboratory model organism for studying the photosynthetic apparatus because it is easily cultured and amenable to molecular manipulation and biochemical purification (Hippler, 1998; Harris, 2001; Rochaix, 2001; Merchant, 2006). It is a facultative phototroph with the ability to use acetate as a respiratory energy source which has allowed the isolation of numerous photosynthetic mutants (Rochaix, 2001). For iron deficiency studies, it is well suited because trace element levels in the culture medium can be easily controlled and because molecular markers for iron deficiency exist. A vast array of molecular resources are now available such as an extensive mutant collection, technologies for transformation of the nuclear and organelle genomes, and a genome project (Grossman, 2003). These resources provide the foundation for the use of proteomics for studying Chlamydomonas.

Chlamydomonas LHCI is different from the land plant complex in several aspects. Early work on LHCI in Chlamydomonas showed that in contrast to the case in land plants, LHCI could be isolated as a large oligomeric complex from a PSI deficient mutant (Wollman, 1982). In a

later study, Bassi and colleagues isolated oligomeric LHCI that had been biochemically separated from PSI (Bassi, 1992). Analysis of the Lhca proteins using immunoblotting and 1-DE as well as 2-DE demonstrated a larger number of Lhca proteins than in land plants. N-terminal amino acid sequencing identified six different Lhca; p14 (Lhca4), p14.1 (Lhca3), p15.1 (Lhca5), p18 (Lhca8), p18.1 (Lhca6), p22.1 (Lhca1). Chlamydomonas also differs from land plants in that it has a smaller percentage of red chlorophylls which are of higher energies (Melkozernov, 2004; Ihalainen, 2005b). The location of these chlorophylls is at present not clear.

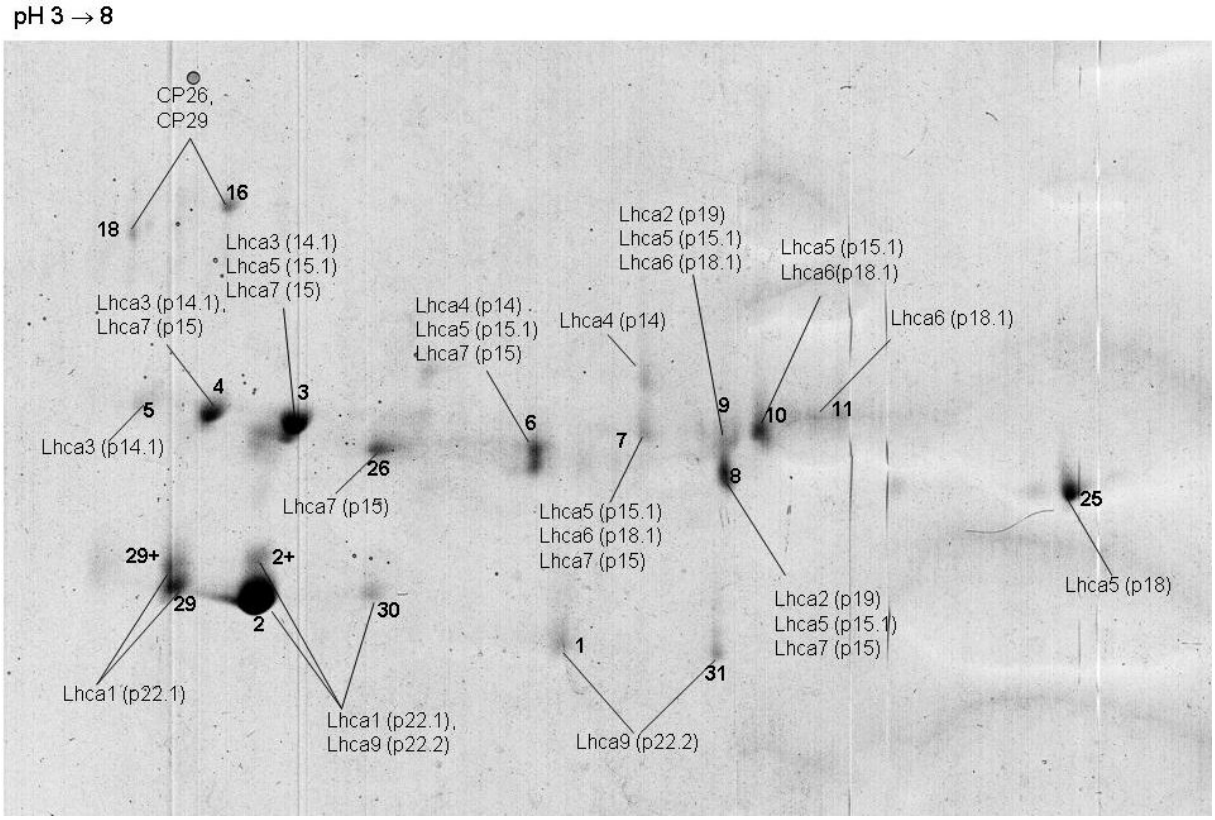

Figure 2. Two-dimensional map of Lhca proteins from *C. reinhardtii*. 2-DE separation and LC-MS/MS analysis of PSI–LHCI particles from *C. reinhardtii*. Each of the spots was excised from a Coomassie-stained gel, treated with trypsin, and subjected to LC-MS/MS analysis and database searching. Spots are labelled with the protein name, including the relative mobility identifiers in SDS-PAGE in parentheses. Newly identified Lhca proteins are named Lhca2 (p19), Lhca7 (p15), and Lhca9 (p22.2). Taken from Stauber (2003) with permission.

Further biochemical investigation of Chlamydomonas LHCI was carried out by Hippler and coworkers using high-resolution 2-DE (Hippler, 2001). With this procedure, reproducible 2-DE maps of thylakoid membrane proteins and PSI-LHCI were obtained. In a subsequent study, MS and genomic and expressed sequence tag (EST) information were used to annotate

the 2D gels of the LHCI proteins (Stauber, 2003), and it was demonstrated that all nine Chlamydomonas *lhca* genes (Koziol, 2007) are expressed on the protein level (Lhca1 – Lhca9, Fig. 2).

Structural data from electron microscopy show that Chlamydomonas LHCI is larger than the land plant complex, consistent with the higher number of Lhca proteins as compared with land plants (Germano, 2002; Kargul, 2003). The images also indicate that LHCI proteins might bind to the side of PsaA between PsaK and PsaL, or on the side of PsaB between PsaG and PsaH (Germano, 2002; Kargul, 2003, 2005; Jensen, 2007).

Although the tomato genome has not been sequenced, the composition of the tomato LHCI complex is of interest because it contains a diverse set of *lhca* genes (Pichersky, 1996; Jansson, 1999). In addition, tomato is amenable to biochemical isolation procedures and over 150,000 EST sequences are available from The Institute for Genomic Research (TIGR).

2.5. Proteomics and mass spectrometry as tools for qualitative and quantitative analyses of protein complexes

The chloroplast proteome probably consist of about 2200 proteins (Richly, 2004). In addition to photosynthetic subunits, many proteins are also likely involved in the assembly, maintenance and regulation of the photosynthetic apparatus (Sommer, 2003a). High resolution 2-DE provides an effective tool for proteome analysis because thousands of proteins can be resolved and visualized during a single analysis (Luck, 1977; Görg, 2004).

Application of 2-DE to membrane proteins has been difficult (Santoni, 2000) but techniques for solubilization of membrane-bound proteins made functional proteomics of thylakoid proteins possible (Hippler, 2001). Often 2-DE is used in conjunction with MS (Aebersold, 2003) and software tools such as SEQUEST (Eng, 1994) or Mascot (Perkins, 1999) for determination of protein sequence (Fig. 3). Technical advancements such as the linear ion trap mass spectrometer have significantly increased the sensitivity and speed of MS analysis (Schwartz, 2002).

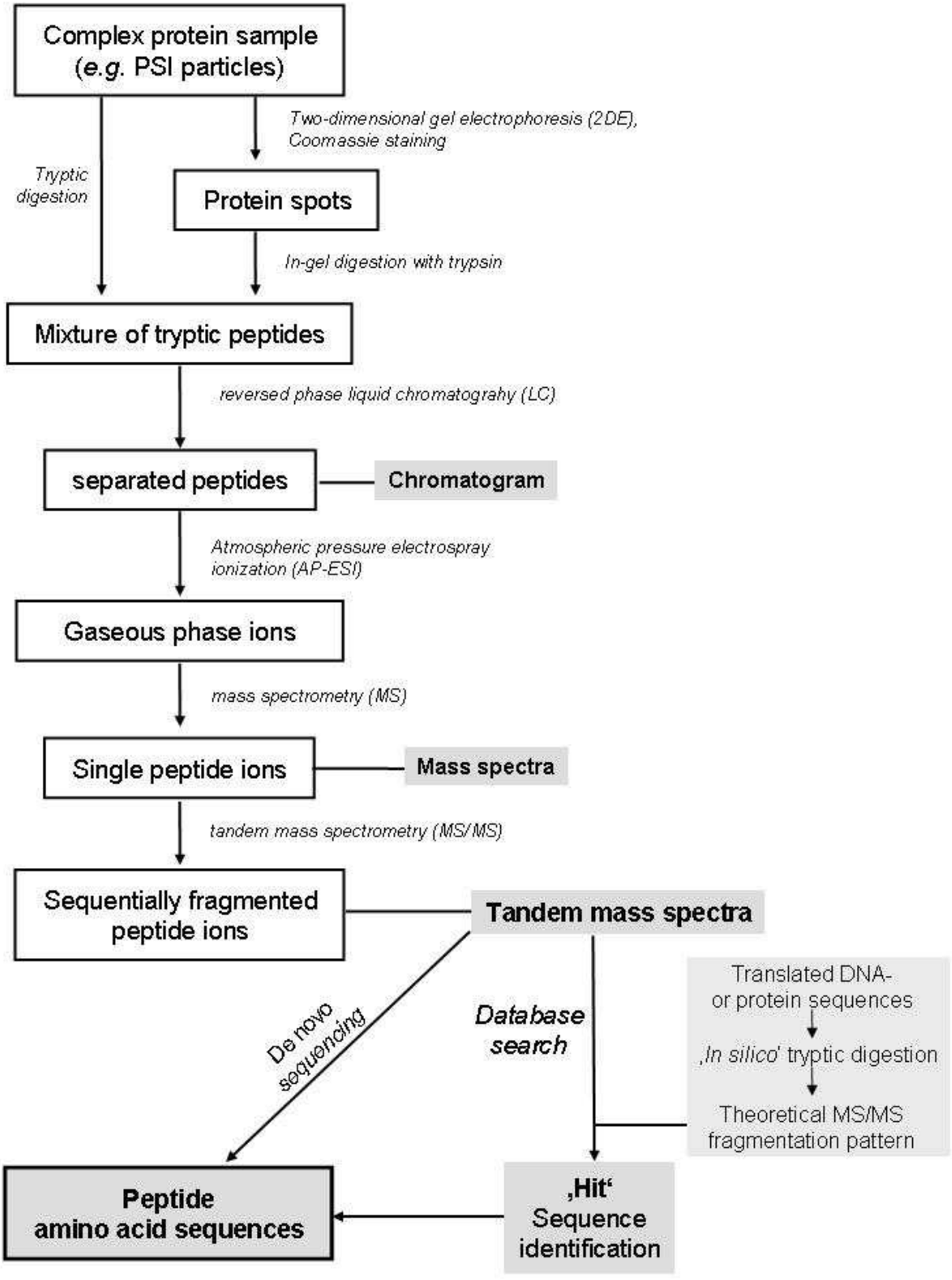

Figure 3. The use of LC-MS for peptide amino acid sequencing. Schematic overview of the steps leading from complex protein samples to amino acid sequence tags.

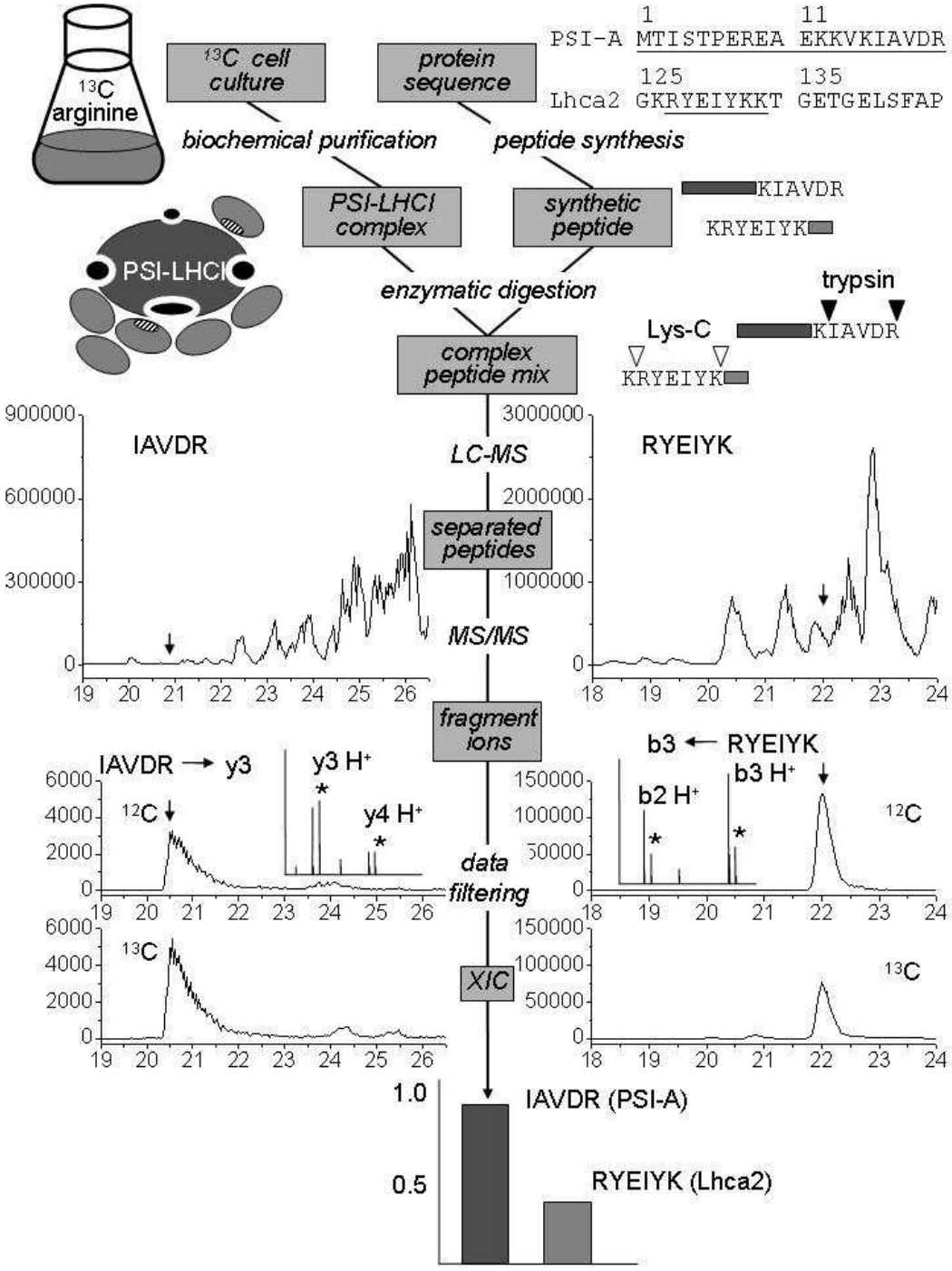

Figure 4. The use of stable isotope labelling and MS/MS for determining the stoichiometry between PSI and Lhca as exemplified with PsaA and Lhca2. The arginine auxotrophic strain CC424 is metabolically labelled using the SILAC approach (Ong, 2002) with $^{13}C_6$-arginine in liquid culture. From the cell culture, $^{13}C_6$-labelled PSI-LHCI is biochemically isolated. Standard peptides ($^{12}C_6$) are chemically synthesized. PSI-LHCI and synthetic peptides are combined and enzymatically digested with proteases Lys-C and/or trypsin. After sample cleanup, the native ($^{13}C_6$) and internal standard ($^{12}C_6$) peptides are analyzed by HPLC. Native ($^{13}C_6$) and internal standard ($^{12}C_6$) peptides are then fragmented concurrently by MS/MS. By filtering the data for arginine-containing fragments ($^{13}C_6$ isotopomer denoted with an asterisk), extracted ion chromatograms (XIC) for each peptide are constructed. By comparing the signal intensities of the native ($^{13}C_6$) and internal standard ($^{12}C_6$) peptides, it is possible to determine the stoichiometry between PsaA and Lhca2.

2-DE is also often used for quantitative comparison of protein expression profiles (Görg, 2004; Wagner, 2004). It provides a robust method for analyzing thousands of protein spots simultaneously, but has its limitations for analyzing complex samples because of overlap in protein migration (Westbrook, 2001). Another limitation is that the accuracy of 2-DE-based quantitation is limited to about 20 % (Koller, 2005; Uitto, 2007). Difference gel electrophorhesis (DIGE) (Alban, 2003) or radiolabelling (Görg, 2004) reduce inaccuracy, but do not enable co-migrating proteins originating from the same sample to be distinguished. Although several Chlamydomonas Lhca can be well separated by 2-DE, many proteins co-migrate (Stauber, 2003).

Techniques for comparative quantitation using MS and stable isotopes have been developed recently (reviewed in Ong, 2005). Techniques for determining protein stoichiometry with synthetic isotopically labelled peptides have also been described (Barndridge, 2003; Gerber, 2003). A standard approach is to label the proteome of an organism from one experimental condition with a stable isotope and then quantify changes in protein expression using MS. Usually, proteins are quantified on the basis of proteolysis products (proteotypic peptides) after they have been hydrolyzed with an enzyme such as trypsin. Two widely used methods for introduction of a metabolic label exist. One utilizes isotopically labelled chemical probes which are chemically linked to specific amino acids such as cysteine, or methionine (Gygi, 1999). Another approach known as SILAC (stable isotope labelling by amino acids in cell culture, Fig. 4) takes advantage of amino acid auxotrophy to introduce an isotopic label metabolically (Ong, 2002).

3. Aims of the study

This thesis was aimed at gaining a better understanding of the qualitative and quantitative composition of LHCI in eukaryotic organisms and its dynamic changes during varying environmental conditions. As the green alga Chlamydomonas can be easily cultured and manipulated in the laboratory, it was chosen as a model organism to study the composition and stoichiometry of LHCI and its association with PSI in detail. In order to relate the results to the conditions in higher plants, the study was extended with a proteomic analysis of tomato LHCI. The following questions were addressed:

- Which Lhca mediate the physical interaction of LHCI with the PSI core?
- What is the stoichiometry of the individual Lhca with the PSI core in Chlamydomonas?
- What proportion of Lhca that potentially contribute to far red fluorescence constitute Chlamydomonas LHCI?
- What is the qualitative composition of tomato LHCI?

One environmental factor that has been in the focus of research in the Hippler laboratory is the effect of varying iron concentrations on the photosynthetic apparatus. It has been established that iron deficiency induces an uncoupling of LHCI from PSI. One aim of the present study was to examine the mechanism responsible for this remodelling in detail using a combination of quantitative proteomics and RNA*i* techniques.

The following questions were addressed:

- What are the quantitative changes on the protein level in LHCI that underlie the adaptation of Chlamydomonas to iron deficiency under heterotrophic growth conditions?
- What functional changes to the photosynthetic apparatus accompany these changes?

A prerequisite for addressing the aims presented above was the availability of means to quantify changes in PSI-LHCI during iron deficiency and to determine the stoichiometry of each Lhca protein with PSI. Therefore, one major technical goal of this thesis was to establish methods for MS-based quantification of proteins using stable isotopes to complement gel-based methods.

4. Published papers and manuscripts under submission

Manuscript 1.

Einar J. Stauber and Michael Hippler (2004) *Chlamydomonas reinhardtii* proteomics. **Plant Physiology and Biochemistry** 42, 989-1001.

Manuscript 1 reviews current developments and progress of proteomics in the model organism Chlamydomonas. The manuscript compiles the most important results of the analysis of sub-proteomes and gives an overview of available computer programs and databases for proteomics in Chlamydomonas as well as of novel methods for quantitative proteome analysis.

The content of the manuscript was planned by both authors and was based on a draft written by E. Stauber. Both authors edited the manuscript. E. Stauber prepared figs. 1 and 2. Figs. 3 and 4 were prepared by Jens Allmer, who was thanked.

Manuscript 2.

Yuichiro Takahashi, Taka-aki Yasui, Einar J. Stauber, and Michael Hippler (2004) Comparison of the subunit compositions of the PSI-LHCI supercomplex and the LHCI in the green alga *Chlamydomonas reinhardtii*. **Biochemistry** 43, 7816-7823.

In manuscript 2, the oligomeric structure of Chlamydomonas LHCI is analyzed. By comparing a PSI mutant (Δ*psaB*) with the wild-type, Lhca2, Lhca3, and Lhca9 are demonstrated to not be required for a stable oligomeric structure of LHCI. Furthermore, the results show that the PSI core complex allows the association of all LHCI proteins.

Y. Takahashi and M. Hippler planned the project. T. Yasui grew and harvested cultures and performed initial purification and Western blotting. Y. Takahashi performed the DEAE-sepharose chromatography, Western blotting, and fluorescence emission measurements and prepared the respective figures. The above experiments were performed in the laboratory of Y. Takahashi at the Okayama University. E. Stauber performed the 2-DE, quantitative analysis of the 2-DE gel spot volumes, MS and database searching and prepared the figure and table for these data as part of the group of M. Hippler at the Friedrich Schiller University in Jena. The manuscript was based on a draft written by Y. Takahashi with contributions from M. Hippler. E. Stauber wrote the methods and results sections of the manuscript regarding his experimental contributions.

Manuscript 3.

Stefanie Storf, Einar J. Stauber, Michael Hippler, and Volkmar H.R. Schmid (2004) Proteomic analysis of the photosystem I light-harvesting antenna in tomato (*Lycopersicon esculentum*). **Biochemistry** 43, 9214-9224.

Manuscript 3 shows for the first time that LHCI of land plants is heterogenously composed using tomato as a model plant. For each of the four most prominent Lhca polypeptides, four to five isoforms are detected at the protein levels, some of them for the first time in land plants.

V. Schmid and M. Hippler planned the project. S. Storf grew the plants, isolated the thylakoids, PSI and LHCI and carried out isoelectric focusing, gel electrophoresis and Western blotting, prepared the figures and tables and wrote the methods for these parts of the manuscript. She also prepared proteins for MS analyses and analyzed data. These experiments were carried out in the group of V. Schmid at the Johannes Gutenberg-University in Mainz. 2-DE experiments were established in the Hippler lab and were also later done in Mainz. E. Stauber helped transfer the methods for preparation of proteins for MS analysis, prepared proteins for MS analyses, especially Lhca2, performed MS analyses, carried out database searches for modifications, analyzed data and prepared figure 2. S. Storf also perfomed database searches. These experiments were carried out in the Hippler lab in Jena. The manuscript was mainly written by V. Schmid with contributions from M. Hippler. E. Stauber contributed to writing the methods for his experimental work and to the discussion regarding the modifications of proteins and helped with editing the manuscript.

Manuscript 4.

Bianca Naumann*, Einar J. Stauber*, Andreas Busch, Frederik Sommer, and Michael Hippler (2005) N-terminal processing of Lhca3 is a key step in remodeling of the photosystem I-Light-harvesting complex under iron deficiency in *Chlamydomonas reinhardtii*. **Journal of Biological Chemistry** 280, 20431-20441, * Both authors contributed equally.

Manuscript 4 describes the structural changes of LHCI of Chlamydomonas that occur under iron deficient conditions. N-terminal processing of Lhca3 plays a key role in the remodelling by reducing the efficiency of energy transfer between LHCI and the PSI core complex. Remodelling of LHCI under iron deficiency is also associated with a depletion of Lhca5 and an increase in the content of Lhca4 and Lhca9.

M. Hippler planned the project. E. Stauber established the method for quantitative MS/MS that was used in the study. At the time the experimental work was being done, this was a novel technique and hadn't yet been published. He identified and quantified the truncated form of Lhca3 in the thylakoids with MS/MS and prepared the respective parts of figure 1 and figure 3. He also established the culture conditions for the arginine auxotrophic strain, performed preliminary experiments on the quantitation of changes of the photosynthetic apparatus due to iron deficiency and transferred knowledge to B. Naumann. B. Naumann established and carried out the chloropolast isolation procedure as well as the Bradford assay, performed Western blotting, established the LC-MS system at the University of Pennsylvania and performed all other quantitative MS measurements and data analysis for proteins of the thylakoid membranes, isolated PSI-LHCI particles, and for thylakoids and PSI-LHCI particles from the Lhca3 RNAi strain and prepared the respective figures. A. Busch designed primers and produced the Lhca3 RNAi strain, performed fluorescence measurements, wrote the methods and prepared the figures these experimental contributions. F. Sommer performed sucrose gradient centrifugation for isolation of PSI-LHCI and low temperature fluorescence spectroscopy. The manuscript was based on a draft written by M. Hippler, with contributions from E. Stauber, both these authors edited the manuscript.

Manuscript 5.

Einar J. Stauber, Andreas Busch, Bianca Naumann, Aleš Svatoš, and Michael Hippler (2007) Proteotypic profiling of LHCI from *Chlamydomonas reinhardtii* provides new insights into structure and function of the complex. **In preparation for Proteomics**.

In manuscript 5, the stoichiometric ratio between the LHCI proteins and PSI is determined in Chlamydomonas using stabile isotope labelling and MS analysis. It is demonstrated that several populations of LHCI exist which differ in their stoichiometric composition. The stoichiometry between PSI and every Lhca polypetide is determined. These results provide insight into the fluorescence characteristics of Chlamydomonas LHCI.

M. Hippler planned the project and elaborated the experiments together with E.Stauber. E. Stauber established the LC-MS system in Jena. He designed the peptides and established the experimental procedures for enzymatic digestion of the samples, peptide purification and quantitative MS. He performed the experimental work and data analysis for the 23 February 2005 and 23 July 2005 PSI-LHCI samples and prepared the figures in the manuscript. These experiments were performed at the Max-Planck Institute of Chemical Ecology Jena in the group of A. Svatoš. A. Svatoš guided the establishment of the LC-MS system in Jena and discussed peptide modification, chromatography and fragmentation with E. Stauber. A. Busch performed most of the experimental work and data analysis for the 30 May 2006 PSI-LHCI purification. B. Naumann performed some of the MS measurements for the 30 May 2006 purification and established the LC-MS system in the group of M. Hippler at the Westfälische Wilhelms-Universitat Münster. The manuscript was based on a draft written by E. Stauber and was edited primarily by E. Stauber and M. Hippler with comments from A. Svatoš.

Manuscript 1

Einar J. Stauber and Michael Hippler (2004) *Chlamydomonas reinhardtii* proteomics. **Plant Physiology and Biochemistry** 42, 989-1001.

Available online at www.sciencedirect.com
SCIENCE DIRECT®
Plant Physiology and Biochemistry 42 (2004) 989–1001
Plant Physiology and Biochemistry
www.elsevier.com/locate/plaphy

Review

Chlamydomonas reinhardtii proteomics

Einar J. Stauber [a], Michael Hippler [b,*]

[a] *Lehrstuhl für Pflanzenphysiologie, Friedrich-Schiller Universität Jena, Dornburger Street 159, 07743 Jena, Germany*
[b] *Department of Biology, University of Pennsylvania, Philadelphia, PA 19104, USA*

Received 4 August 2004; accepted 27 September 2004

Available online 19 December 2004

Abstract

Proteomics, based on the expanding genomic resources, has begun to reveal new details of *Chlamydomonas reinhardtii* biology. In particular, analyses focusing on subproteomes have already provided new insight into the dynamics and composition of the photosynthetic apparatus, the chloroplast ribosome, the oxidative phosphorylation machinery of the mitochondria, and the flagellum. It assisted to discovered putative new components of the circadian clockwork as well as shed a light on thioredoxin protein–protein interactions. In the future, quantitative techniques may allow large scale comparison of protein expression levels. Advances in software algorithms will likely improve the use of genomic databases for mass spectrometry (MS) based protein identification and validation of gene models that have been predicted from the genomic DNA sequences. Although proteomics has only been recently applied for exploring *C. reinhardtii* biology, it will likely be utilized extensively in the near future due to the already existing genetic, genomic, and biochemical tools.

Keywords: Proteomics; Mass spectrometry; Quantitative proteomics; Subproteome analysis

1. Introduction

The unicellular biflagellate green alga *Chlamydomonas reinhardtii* has been explored as a eukaryotic model organism for decades. Aspects of fundamental biological processes of both the plant and animal kingdoms, including the biogenesis and function of the chloroplast, the assembly and function of flagella and the basal body and their relevance for human diseases, the mechanisms of photosensory and chemosensory processes, the assimilation and utilization of nutrients, as well as the circadian control of cellular physiology and behavior have been elucidated in *C. reinhardtii*.

A draft of the *C. reinhardtii* genomic sequence as well as sequence information from approximately 250,000 complementary DNA (cDNA) clones allow the application of a number of global methodologies in *C. reinhardtii*. Proteomic investigations aim to provide insight into biological processes on the protein level through large scale protein identification and protein–protein interaction studies. In addition to identifying as many of the expressed gene products as possible that are present in an organism at a particular time point, many proteomic investigations aim to identify post-translational modifications of proteins, as well as the organization of proteins in multi-protein complexes and their localization in tissues. In addition, proteomic techniques, in conjunction with other global approaches, such as transcriptome and metabolome profiling, will be key in exploring the integrated behavior of *C. reinhardtii*'s biological systems. A recent overview article highlights several aspects of proteomics research [73].

Advances in high throughput mass spectrometry (MS) based proteomics approaches have increased the number of proteins that can be identified in a single experiment. Despite these advances, subproteome analysis is still necessary for achieving comprehensive coverage of individual components of multi-protein complexes. Even in purified organelles, such as the chloroplast, or subfractions of it, complete coverage of all the predicted proteins is far from being achieved. In addition to increasing the sensitivity of analyses, the isola-

Abbreviations: IEF-PAGE, isoelectric focusing-polyacrylamide gel electrophorhesis; IFT, intraflagellar transport; LC-MS/MS, liquid chromatography coupled to mass spectrometry; LHC, light harvesting complex; MALDI-TOF, matrix assisted laser desorption ionization-time of flight; MS, mass spectrometry; MS/MS, tandem mass spectrometry; PSI, photosystem I.

* Corresponding author. Tel.: +1 215 898 4974; fax: +1 215 898 8780.
E-mail address: mhippler@sas.upenn.edu (M. Hippler).

0981-9428/$ - see front matter © 2005 Elsevier SAS. All rights reserved.
doi:10.1016/j.plaphy.2004.09.008

tion of protein fractions based on biochemical properties yields valuable information about the proteins being studied.

In this article, we will discuss progress that has been made in proteomic investigations in *C. reinhardtii*. First, we will cover cellular compartments or functional groups of proteins for which proteomics experiments have already been carried out in *C. reinhardtii*. Concurrently, we will comment on advances that have been made in proteomics investigations in other organisms where they appear relevant to *C. reinhardtii* proteomics. Finally, we will discuss advances in quantitative proteomics and software tools as well as considerations for archiving and dissemination of proteomic data.

2. *C. reinhardtii* as a model organism

Several factors facilitate genetic and molecular manipulation of *C. reinhardtii*. (*a*) The well understood haploid genetics allow the genetic dissection of phenotypes. (*b*) A large collection of mutants with mutations in the nuclear, plastid and mitochondrial genomes are available for characterizing gene function using forward genetic approaches. (*c*) The nuclear and organelle genomes can be manipulated by genetic transformation. (*d*) Genomic information enables the determination of gene function using reverse genetics. (*e*) The availability of molecular markers and bacterial artificial chromosome clones will allow map based cloning to be used for identification of genes [32]. (*f*) The possibility to carry out large scale protein purification in *C. reinhardtii* enables efficient analysis on the protein level. Several review articles highlight various aspects of *C. reinhardtii* biology as well as tools that have aided experimental investigation [20,43,58]. Genomic information as well as extensive cDNA clones, genetic tools and the possibility for large scale biochemical purification of proteins from *C. reinhardtii* will facilitate proteomic techniques in this organism.

3. Genomic resources

A second draft version (chlre2) of the ~100 million base pair *C. reinhardtii* nuclear genome has been completed by the Department of Energy (USA) funded Joint Genome Institute (JGI). A finished sequence is expected to be available by the end of 2004. Tools to access the sequence are available from the JGI website http://www.genome.jgi-psf.org/chlre2/chlre2.home.html. In addition, extensive cDNA resources exist. Expressed sequence tag (EST) information from approximately 51,000 cDNAs were generated by the Kazusa DNA Research Institute in Japan and are available from the website http://www.kazusa.or.jp/en/plant/chlamy/EST/index.html [2]. Additionally, over 200,000 cDNAs have been produced from a variety of physiological conditions by National Science Foundation (USA) funded projects. Alignment of the 200,000 ESTs has yielded approximately 8700 assemblies of contiguous EST's [64]. Information from ESTs is accessible through the *Chlamydomonas* Genetics Center website (http://www.biology.duke.edu/chlamy_genome/.

The plastid genome with a size of 203.8-kbp has been fully sequenced (National Center for Biotechnology Information accession BK000554) and encodes 99 genes [44]. The 5.7-kbp mitochondrial genome (accession U03843), encoding eight genes has also been sequenced. Further information on the *C. reinhardtii* genome projects are given in detail in a recent review [21].

4. Chloroplast proteomics

4.1. The chloroplast and its proteome

Plastids are plant cell organelles that are derived from prokaryotic endosymbionts, not unlike today's cyanobacteria. They retain remnants of the original prokaryotic genome, however, most chloroplast proteins are encoded by nuclear genes and imported into the chloroplast. Each *C. reinhardtii* cell contains a single chloroplast that occupies approximately two thirds of the cellular volume. In addition to the reactions of photosynthesis, a large number of other essential or important biochemical reactions take place in the chloroplast. Chloroplasts are surrounded by an outer and inner envelope membrane and are permeated by the thylakoid membrane. The membrane systems define three soluble phases; the intermembrane space, the stroma, and the thylakoid lumen. In addition to the thylakoid membranes, other important features of the *C. reinhardtii* chloroplast include the DNA containing nucleoids as well as parts of the visual apparatus. The proteome of the *A. thaliana* chloroplast probably contains the products of at least 2200 [57] genes and possibly more since several published estimates are higher. No systematic bioinformatic analysis of the *C. reinhardtii* chloroplast proteome has yet been carried out, but the figure is possible higher, since the chloroplast harbours the visual apparatus, that is absent from plastids of vascular plants.

Proteomics has also begun to increase our understanding of the function and dynamics of the chloroplast. To date, proteomics has provided extensive knowledge of the light harvesting complex proteins (LHC) of the photosynthetic apparatus in *C. reihardtii*. In addition, proteomics has made the molecular characteristics of the dynamic behavior of the photosynthetic apparatus due to nutrient stress or limitation accessible to experimental investigation.

The identification of protein sorting will give clues into the biogenesis and function of chloroplast compartments. As has been demonstrated in several investigations of higher plant chloroplast compartments [51] proteomics has been valuable for determining protein sorting and localization.

Most of our knowledge of protein sorting stems from algorithms which predict protein localization from signal sequences of pre-protein sequences, for example PSORT [47] TargetP [12], Predotar [67]. Because complete proteome cov-

erage of the chloroplast has not yet been achieved through experimental approaches, these programs will continue to be important. These programs have been trained using sequences from higher plants. Since *C. reinhardtii* chloroplast targeting peptides are known to differ from those of higher plants [16] it is expected that they will initially have difficulties making correct predictions for *C. reinhardtii* sequences. The overall accuracy of TargetP and Predotar for predicting intracellular sorting is only around 56% as measured on a set of *C. reinhardtii* proteins for which location is known or deduced by homology. (O. Vallon, C. Hauser, O. Emanuelsson, I. Small, personal communication). The result is particularly poor for chloroplast-targeted proteins. These programs are being re-trained, in hope of generating better prediction tools. Experimentally determined data are valuable for training these programs and for verifying their predictions.

4.2. Photosynthetic thylakoid proteins

The thylakoid membranes are the site of oxygenic photosynthesis. Genetic approaches have been used for over 40 years to study the mechanisms of photosynthesis in *C. reinhardtii* [28]. It is foreseeable that proteomics will provide a deeper understanding of the building blocks of the photosynthetic apparatus and will enable the characterization of the remarkable flexibility of the photosynthetic apparatus to changing environmental conditions.

To analyze the thylakoid proteome, a procedure was developed that enables the separation of hydrophobic proteins with high resolution IEF and polyacrylamide gel electrophoresis (IEF-PAGE). This procedure allowed the separation of approximately 400 reproducible protein spots from *C. reinhardtii* thylakoids [27]. Using polyclonal and peptide-specific antibodies, two-dimensional maps of the major LHCI and LHCII proteins were produced and Sequence tags [42] from tandem mass spectrometry (MS/MS) data were used to identify selected proteins. Analysis of the photosystem I (PSI) deficient mutant *Δycf4* and the *crd1* mutant, which is deficient in PSI and LHCI under copper deficiency, demonstrated the utility of IEF-PAGE for displaying the differential effects of these two mutations on the LHC associated with PSI (LHCI).

In a subsequent study, the LHC were systematically analyzed using liquid chromatography coupled to mass spectrometry (LC-MS/MS) [68] resulting in the identification of all nine of the LHCI proteins that are predicted from genomic data [11] (see Fig. 1). In addition, eight of the nine major LHCII proteins were identified on the protein level. For the two LHCII proteins, namely Lhcbm3 and Lhcbm6, differential N-terminal processing was determined by a combination of IEF-PAGE and LC-MS/MS. In the case of Lhcbm6 the N-terminal processing was confirmed by analysis of a hemagglutinin tagged form of Lhcbm6. The mass spectrometric analysis also identified phosphorylation of a Thr residue in the N-terminal part of Lhcbm3. The phosphorylation site was found in the longer N-terminal processed form of Lhcbm3, thus, formation of the second shorter N-terminal processed Lhcbm3 product would lead to a removal of the phosphorylation site and therefore may represent a novel regulatory mechanism. In total, 17 different major LHC were identified in this study. Another study reported that the transit peptide of Lhcb4 (CP29) from *C. reinhardtii* is not removed after import into the chloroplast but undergoes acetylation and phosporylation [72]. This demonstrates that processing of the

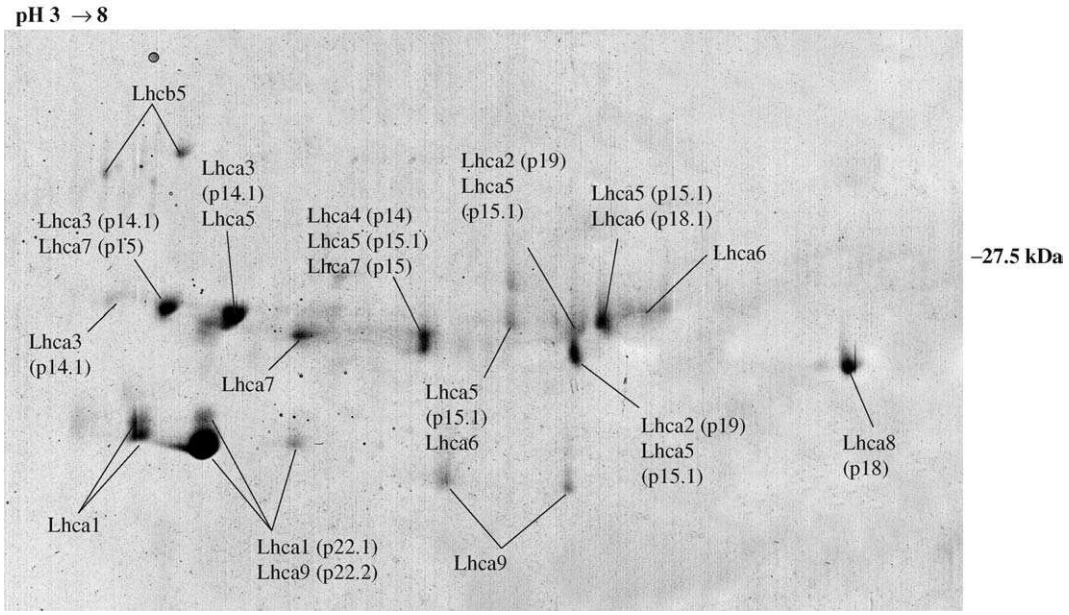

Fig. 1. Two-dimensional map of Lhca proteins from *C. reinhardtii*. Two dimensional electrophorhesis and LC-MS/MS analysis of PSI–LHCI particles from *C. reinhardtii*. Each of the spots was excised from a Coomassie-stained gel, treated with trypsin, and subjected to LC-MS/MS analysis and database searching. Spots are labeled with the protein name, including the relative mobility identifiers in SDS-PAGE in parentheses. Newly identified Lhca proteins are named: Lhca2 (p19), Lhca7 (p15), and Lhca9 (p22.2). Taken from [68] with permission.

transit peptide after protein import into the chloroplast is not mandatory in *C. reinhardtii*.

Further insight into the structure of the LHCI complex was provided through the isolation of the LHCI complex from a PSI-deficient mutant using chromatography on an (diethylamino)ethyl (DEAE) column in combination with IEF-PAGE and LC-MS/MS [71]. The isolated LHCI complex consisted primarily of six individual proteins (called Lhca proteins) as compared to nine in the PSI–LHCI complex, indicating that these three Lhca require PSI for stable association with the LHCI complex. Interestingly, the crystal structure of the *Pisum sativum* PSI–LHCI [6] shows that four Lhca proteins bind asymmetrically to one side of PSI. The fact that a stable LHCI complex can be isolated from *C. reinhardtii* is surprising in the light of the *Pisum* PSI structure and suggests that the *Clamydomonas* Lhca antenna is probably larger as compared to that of vascular plants. Alternatively the *Pisum* PSI structure could represent a minimal PSI–LHCI composition.

Investigation of the adaptation of the photosynthetic machinery to iron-deficiency and iron-limitation in *C. reinhardtii* using IEF-PAGE in conjunction with immunochemical analyses revealed that iron-deficiency induces a remodeling of the photosynthetic apparatus [46]. The photosynthetic apparatus responded in a graded manner by degradation of some light harvesting proteins as well as induction of novel ones. While some of the light harvesting proteins of PSI decreased dramatically in abundance, those associated with PSII remained quite stable. The iron-deficiency mediated responses were detected before chlorosis, which is a diagnostic symptom of iron-deficiency in plants. This indicates that the restructuring of the pigment and protein complexes of the photosynthetic apparatus may be a programmed cell response rather than a secondary consequence of the inhibition of chlorophyll synthesis due to iron-deficiency.

The response of the thylakoid membrane proteins to photoautotrophic and photoheterotrophic conditions was investigated by means of a combination of blue-native gel electrophoresis using Coomassie blue dye, and denaturing PAGE and matrix assisted laser desorption ionization-time of flight (MALDI-TOF) MS [56]. In total, 30 proteins were identified, 14 of which contained at least one transmembrane domain, showing that this method as the potential to elucidate the thylakoid protein composition. The fact that LHCI was found completely dissociated from PSI in photoheterotrophic conditions, however, points to artefacts using this methodical combination in determination of protein complex composition isolated from thylakoid membranes. It is well documented that PSI–LHCI can be isolated as supercomplex under these physiological conditions [3,26,70,71].

Recent investigations of the *A. thaliana* integral thylakoid membrane proteome, identified 154 proteins [17]. Several extraction and separation techniques, combined with LC-MS/MS and MALDI-TOF analyses, were used in this study. Out of the 154 proteins, 27 had not been identified previously. Based on these results, a curated proteome database was developed [69] (http://www.cbsusrv01.tc.cornell.edu/users/ppdb/).

4.3. Lumenal proteins

Proteomic investigations in higher plants have shown that in addition to the proteins involved in water splitting and electron transfer, the lumen contains a number of proteins that are involved in the mediation of oxidative stress. Proteins involved in proteolysis and protein folding, such as protein disulfide isomerses and petidyl–prolyl *cis-trans* isomerases, were also prominent components of the lumen. Analyses of peripheral thylakoid and luminal proteins have identified 36 proteins [62] from (*Pisum sativum* and *A. thaliana*) and 81 proteins [51] from (*A. thaliana*). Bioinformatics can be used to predict lumenal proteins based on characteristic lumenal transit peptide for the Δ pH-twin-arginine translocation pathway, and to a lesser extent, the ATP-driven Sec pathway. Such analyses, aided by a set of experimentally identified proteins, predicted approximately 201 lumenal proteins [51]. No systematic analysis of the thylakoid lumen from *C. reinhardtii* has been carried out to date.

4.3.1. Envelope membrane

The envelope membranes are responsible for the import of proteins into the chloroplast. The translocases of the outer and inner chloroplast membranes are two multi-protein complexes that are known to function in protein import. In addition, the envelope membrane is involved in the biosynthesis of metabolites as well as the transport of various molecules [31]. The low abundance of envelope proteins, especially proteins of the intermembrane space, makes it difficult to study them biochemically.

No analysis of the *C. reinhardtii* envelope membrane has been reported to date, however, several proteomic investigations have been done in higher plants. These studies provide a range of techniques that may be useful for later studies in *C. reinhardtii*.

Proteomic analyses of *A. thaliana* envelope membranes identified 112 proteins [15]. Interestingly, comparison of data from the analysis of the chloroform/methanol extracts of the envelope membranes of *S. oleracea* from a previous study and *A. thaliana* demonstrate the advantage of using more than one model organism for proteomic investigations. More than 20 proteins were identified exclusively using MS/MS data from *S. oleracea* samples, whereas 15 proteins were identified exclusively from *A. thaliana* samples.

In an investigation of *A. thaliana* inner and outer envelope fractions, in which strong cation exchange chromatrography of peptides was implemented, 392 proteins were identified [18].

In another study, 137 proteins were identified in an envelope membrane enriched fraction that was analyzed as part of an investigation of the complete chloroplast proteome [35]. The differences in the number of proteins identified in the envelope membrane preparations in these studies may reflect,

among others, differences in extraction procedures used as well as purity of the protein fraction. There is probably a tradeoff between accuracy and sensitivity of a preparative procedure. Additionally protein contamination from other compartments can potentially increase the number of proteins identified for a subproteome like the envelope membrane. Therefore, annotation of proteins to a subproteome must bare this contamination argument in mind when only based on identification by highly sensitive proteomic techniques until the localization of a given protein is not confirmed by an independent method.

In these studies, most of the proteins of the protein translocase complexes were identified. Many metabolic proteins, such as those involved in prenylquinone biosynthesis, were not reported in any of these investigations. This may reflect the low abundance of these proteins as well as the fact that some proteins are only expressed at particular time points.

4.3.2. Chloroplast ribosomal proteomics

Chloroplast ribosomes consist of chloroplast encoded ribosomal RNA and proteins, which are encoded by both the plastid and nuclear genomes [24]. The chloroplast ribosome functions in the translation of plastid mRNA into proteins. Plastid ribosomes share many similarities with prokaryotic ribosomes. The chloroplast 70S ribosome can be divided into a large (50S) and a small (30S) subunit. The small subunit serves in mRNA binding, and the large subunit serves in peptidyl bond formation between amino acids during protein synthesis.

Proteomic investigation of the total proteins of the 70S ribosome (TP70) in *C. reinhardtii*, [78] revealed differences to bacterial and *S. oleracea* 70S ribosomes. The 30S subunit is responsible for this variability, while the 50S subunit seems to have been conserved throughout evolution.

The large and small subunits were purified by serial sucrose gradient centrifugation and then analyzed using 1D-PAGE and LC-MS/MS as well as with two dimensional LC-MS/MS. For 22 TP30 proteins overlapping EST sequences could be identified. Four of the *C. reinhardtii* TP30 proteins were more than twice as large as compared with the corresponding proteins from *S. oleracea* or *E. coli* due to N- or C-terminal extensions or an insertion sequence. The presence of unusually large proteins associated with TP30 from *C. reinhardtii* had been demonstrated previously with experiments utilizing IEF-PAGE [23]. Comparison based on sequence homology with other proteins, suggests that the additional motifs serve in translational regulation via mRNA binding. In addition, a novel 66 kDa protein, named plastid-specific ribosomal protein 7 (PSRP-7) was identified. This protein contains an S1 domain, which is known to participate in mRNA binding.

In contrast, the TP50 proteins were conserved when compared with the proteins from *S. oleracea* or *E. coli*, in accordance with the conserved function of TP50. These results correspond with previous experiments using two dimensional electrophoresis and immuno-blotting [54]. Twenty-eight TP50 proteins were identified from the 31 predicted from *C. reinhardtii* EST sequences or plastid open reading frames [78]. Two additional proteins, named ribosomal-associated protein 38 (RAP38) and RAP41 were recognized. These proteins associate with TP70, but not with TP50 or TP30 alone and have sequence similarity with RNA-binding proteins with ribonuclease activity from other organisms.

5. Basal body and flagellum proteomics

Each *C. reinhardtii* cell possesses a basal body and two flagella. Many known flagella and basal body proteins have been conserved throughout evolution. Analysis of these proteins in *C. reinhardtii* has in several cases been instrumental in identifying their homologues in other organisms, including humans. Basal body and cilia defects are implicated in a number of human diseases, such as situs inversus, hydrocephalous, and certain kinds of kidney defects.

The basal bodies, which are essential for cilia and flagella formation, and centrioles, which are necessary for centrosome formation, are two versions of the same organelle which play important roles in eukaryotic cells [43]. Basal bodies are also responsible for defining structrual assymetry within the cell as well as the direction of flagellar motion [4]. A recent investigation of basal bodies from *C. reinhardtii* revealed the presence of a marker for the rotational asymmetry of basal bodies and probasal bodies [19]. Biochemical analysis of the basal body is complicated because it is difficult prepare contaminant free fractions [37], which would also complicate proteomic identification of *bonafide* basal body proteins.

Eukaryotic flagella and cilia are structurally related organelles, which protrude from the cell surface and serve in cellular motility, movement of fluid over cell surfaces, and also have sensory functions [66]. The protein core of the flagella, called the axoneme, is surrounded by a flagellar membrane.

Precursors from the flagellum must be transported to the tip where assembly occurs. Processes which serve in the assembly and maintenance of flagella and cilia have been intensively investigated since the process of intraflagellar transport (IFT) was first discovered in *C. reinhardtii* [36]. This process is most likely essential for cila assembly and maintenance for all organisms, which possess cilia [59].

5.1. Flagellum proteomics

Recently, the *C. reinhardtii* flagellum has been subjected to a MS based proteomic analysis (G. Pazour, N. Agrin, J. Leszyk, G.B. Witman, personal communication). Extracts from biochemically fractioned flagella were separated by 1D SDS-PAGE and gel slices from the entire gel lane were used for LC-MS/MS analyses. In this investigation, over 400 proteins and were identified, representing 90% of known flagellar proteins. Based on these results, an open access website

of identified proteins is being established. A comparison of these results with those of the analysis of axonemes from human cilia [50] will provide more information on how highly conserved flagellum/cilia have remained throughout evolution.

Quantitative proteomics has recently been used in an investigation of flagellar assembly mutants. Isotope coded affinity tagging of proteins was used in conjunction with LC-MS/MS to detect decreases in the levels of an adenylate kinase in the outer dynein arm (ODA) assembly mutants 5 and 10 [77]. The decreases in the adenylate kinase levels appear to be specific for these two mutants.

Isoelectric focusing combined with PAGE has been instrumental for the analysis of axonemal proteins for many years. Investigations of the two flagellar mutants *pf14* and *pf1*, [41] and several subsequent studies implemented IEF-PAGE to differentially display the protein components of wildtype and mutant axonemes. The use of $H_2{}^{35}SO_4$ to metabolically labeled sulfur containing proteins provided a very sensitive means for protein detection, allowing the visualization of over 200 protein spots from three micrograms of protein as starting material. Based on these investigations, the number of axonemal proteins in *C. reinhardtii* was estimated to be between 250 and 300. Moreover, in experiments in which either of the mutant phenotypes were rescued by wildtype proteins during mating (dikaryon rescue), the ^{35}S-isotopic marker was useful in differentiating between proteins that had been primarily affected and those that had been secondarily affected by the mutation [41]. The *pf14* and *pf1* genes have been cloned [76] and [9], respectively.

The assembly and maintenance of flagellum is dependent on the process of IFT, which was first observed as the rapid bidirectional movement of particles along the length of the flagella [36]. The particles are transported in the space between the axonemal tubules and flagellar membrane. This process, which probably occurs in all organisms that possess cilia was first documented in *C. reinhardtii*. Mutant analyses have revealed that anterograde IFT particles are composed of aproximately 16 proteins. Kinesin-II was identified as the motor for anterograde transport and dynein 1b as the motor for retrograde transport [7].

In several investigations characterizing IFT particles as well as their motors, IEF-PAGE was useful defining their composition. For example, in a detailed study of the identity of intraflagellar particles and their anterograde motor, IEF-PAGE was used to resolve the presence of 15 distinct gel spots from a 17S IFT particle [8]. Microsequencing of some of these proteins and database searching identified homologous proteins from *Caenorhabditis elegans*, which are necessary for ciliar assembly in sensory neurons.

5.2. Basal body proteomics

Already existing centrioles nucleate the formation of new centrioles, however, how this process takes place and how it is regulated in a cell-cycle specific manner is unknown. Identification of proteins in the basal body may reveal proteins involved in centriole assembly and function. Biochemical isolation of basal bodies indicates the presence of over 200 proteins [10].

The *Chlamydomonas* genome project enables as one of its benefits the application of comparative genomics approaches. Such a strategy was used to identify genes encoding for flagellar and basal body proteins [39]. Dutcher and coworkers employed a comparative genomics approach in which the non-flagellated proteome of *Arabidopsis* was substracted from the shared proteome of the ciliated/flagellated organisms *Chlamydomonas* and human. Hereby 688 genes were identified that are present exclusively in organisms with flagella and basal bodies. By using the outcome of the comparative approach in the study of human ciliation disorders, a new gene for which a defective allele causes the human ciliation disorder Bardet–Biedl syndrome was identified. This approach, similar to the identification of nuclear encoded eukaryotic plastid genes of prokaryotic origin, together with proteomic analyses will provide powerful means for defining the basal body and flagellar proteomes.

6. Mitochondrial proteomics

Mitochondria are also from prokaryotic origin and were derived by endosymbiosis. Like the chloroplast, they have lost most of their genes throughout evolution, but probably contain the products of over 1000 genes [67], most of which are encoded by the nuclear genome. In addition to energy production, mitochondria carry out a number of other important functions such as amino acid, nucleotide, and lipid metabolism and also involved in apoptosis. They are also involved in the process of iron sulfur cluster formation [40], which is the only function, which all known types of mitochondria have in common.

The mitochondrial genome of *C. reinhardtii* contains 15.8 kbp DNA and encodes the cytochrome b protein, six subunits of the NADH dehydrogenase complex and a reverse-transcriptase like protein.

Mitochondria of *C. reinhardtii* are much smaller than their chloroplasts and occupy approximately 3% of the cellular volume [5] A method for the isolation of mitochondria from a cell wall less strain has been published [14]. Another method utilizes the J12 “yellow in the dark” mutant to reduce thylakoid membrane contamination from dark grown cells [5].

Recently, the *C. reinhardtii* mitochondrial proteins were analyzed using two dimensional blue-native electrophoresis and PAGE in combination with Edmann sequencing [74]. The five complexes of the oxidative phosphorylation system were resolved by two dimensional gel electrophoresis and 20 different proteins were identified from sequence tags. In this study, it was shown that a mitochondrial ATP-synthase associated protein (MASAP) associates with subunit V, even after solubilization with 5% (w/v) Triton X-100 and 0.5 M potassium phosphate. Thus, this protein, for which the function is

unknown, associates tightly with the F_1F_0-ATP synthase. This protein may contribute to the strong tendency for dimerization of this complex in mitochondria. MS-based approaches will increase the sensitivity of protein identification and expand our knowledge of the mitochondrial proteome in *C. reinhardtii*.

A proteomic analysis of mitochondria from *A. thaliana* has been used to identify 492 proteins [25]. The information from this investigation were used to create a mitochondrial protein database (http://www.mitoz.bcs.uwa.edu.au/).

From a proteomic investigation of *S. cerevevisiae*, 750 mitochondrial proteins, representing approximately 90% of the predicted mitochondrial proteome were identified [65]. Interestingly, bioinformatic analyses of these protein sequences indicate that 25% of them are involved the expression and regulation of the eight proteins encoded for by the mitochondrial genome. In this study, 10 mg of highly pure mitochondrial proteins were used as starting material.

7. Circadian oscillators

Cyanobacteria and numerous eukaryotes, have internal circadian oscillators, which regulate behavior, and cell physiology in rhythms that have a period of about 24 h. Circadian oscillators are characterized by (*a*) a period of *circa* 24 h, (*b*) an entrainment mechanism based on external stimuli, (*c*) relative insensitivity to temperature. Circadian clocks probably increase fitness of organisms by initiating behavior or metabolism in anticipation of daily or seasonal rhythms of nature [30].

For example, expression of *li818r1* [61] mRNAs in *C. reinhardtii* has been shown to be under circadian control. Supercoiling of regions of the *C. reinhardtii* chloroplast genome containing the *psaB* gene was likewise shown to be controlled by a circadian oscillator [60].

In *C. reinhardtii* the proteins of the CHLAMY1 complex [79] bind UG *cis*-acting elements in the 3′ untranslated regions of mRNA molecules for proteins involved in early steps of primary metabolism, such as nitrogen uptake and metabolism and carbon dioxide metabolism. Nucleic acid binding proteins are important components of circadian systems. However, many individual components of the circadian oscillator are still not known.

Recently, functional proteomics was used to identify new nucleic acid binding proteins that oscillate in a circadian manner in *C. reinhardtii* [75]. Proteins from whole cell extracts were purified with Heparin affinity fast performance liquid chromatography. Differential display of the heparin affinity purified proteins using two dimensional electrophoresis, which had been modified for resolution of basic proteins, resolved two proteins, which showed a more than fourfold increase during subjective night as compared with subjective day. Analysis of the protein spots with LC-MS/MS and database searching identified one of them as a member of the protein disulfide isomerase family. Members of this family generally act in the isomerization of disulfide bonds during protein folding, and have also been shown to influence the rate of translation of *psbA* mRNA in *C. reinhardtii* [34]. The second protein was determined to be a member of the tetratricopeptide repeat family of proteins, which are known to participate in protein–protein interactions.

8. Proteomics of the thioredoxin protein–protein interaction

Thioredoxins mediate the activity of a variety of enzymes by changing the redox state through disulfide/dithiol interchange reactions. In plants, they have been found to regulate enzymes of carbon assimilation, but are also present in the mitochondria and cytoplasm, [63]. An elegant proteomic approach has been developed to isolate and identify disulfide proteins that can be reduced by thioredoxin in *C. reinhardtii* [38]. A mutated form of the cytosolic heterotrophic thioredoxin, CrTrxh, in which the less reactive cysteine had been replaced (C39S), was used to prepare an affinity column that specifically binds to disulfide proteins. Isolated proteins were then identified using MALDI-TOF analyses. Fifty-five proteins were identified, 26 of which had not been previously identified. Enzymes involved in the biosynthesis of six amino acids were implicated as thioredoxin targets. Biochemical analysis of isopropylmalate dehydrogenase, which is involved in leucine biosynthesis, demonstrated that this enzyme is only active in the presence of a reductant (thioredoxin or dithiothreitol). The activity of the antioxidant enzyme catalase was shown to be negatively effected by the presence of thioredoxin, in contrast to catalase from *A. thaliana*, which was unaffected by reducing agents.

9. Quantitative proteomics

Quantitative proteomics is defined as the systematic comparison of the absolute abundance of proteins in a proteome or subproteome, or the relative abundance of proteins in the sample of interest relative to a control sample. Stable isotopes have been used increasingly in the past few years in MS-based proteomic studies, because they enable accurate quantification of peptides using MS.

In our laboratory, we have established a method for comparative proteomics. We use comparative quantification of isotopically labeled and unlabeled peptides with LC-MS/MS (Stauber, Naumann, Hippler, unpublished results) (see Fig. 2). This strategy is commonly referred to as Stable Isotope labeling by amino acids in cell culture [49]. We are employing this technology to investigate changes of the chloroplast proteome, which are induced by the onset of iron-deficiency. Fig. 2 shows an example of the experimental procedure. Arginine auxotrophic *Chlamydomonas* cells were grown in the presence of L-arginine in iron-replete conditions and transferred for 5 days to iron limiting conditions. In parallel the

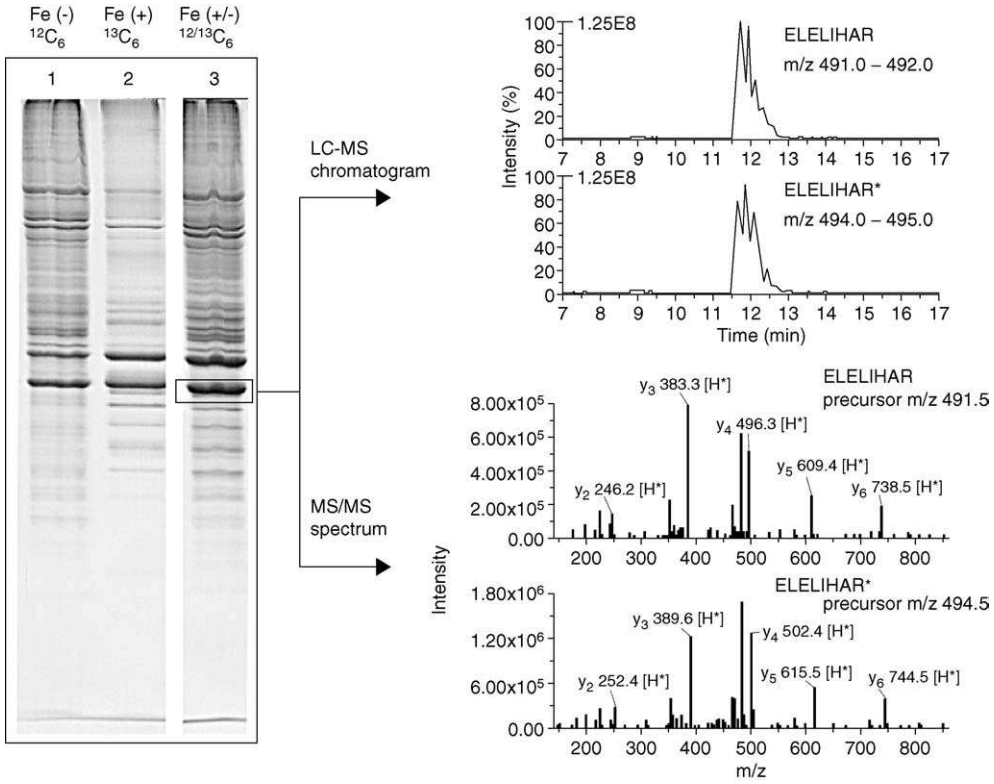

Fig. 2. The use of isotopically labeled cultures to compare changes in protein levels is possible with *C. reinhardtii*. Thyakoids were isolated from CC24 mt(–) cells grown under iron limiting conditions in the presence L-arginine (174.2 Da) (100 ug/ul) and from cells grown in media containing 18 um Fe EDTA to which isotopically labeled L-arginine with six 13C atoms (180.2 Da), had been added. Samples were mixed on an equal protein basis and separated by SDS-PAGE and stained with Coomassie blue. Lanes 1 and 2 show equal loading of the two samples. A protein band corresponding to the Lhcbm proteins was excised (lane 3), the proteins were digested with trypsin, and analyzed by LC-MS (left, upper panels) and MS/MS (left, lower panels). Resolution of the doubly charged peptide ions ELELIHAR and ELELIHAR [+6 Da] using the data filters in the full scan mode for *m/z* 491.0–492.0 and 494.0–495.0 shows that the protein is present at equal amounts in both conditions. The fragmentation of the precursor ions 491.5 (upper MS/MS) and 494.5 (lower MS/MS) reveals a y-ion series differing in 6 Da due to the presence of isotopically labeled arginine.

auxotrophic strain was grown under iron-sufficient conditions in the presence of isotopically labeled L-arginine, harboring six ^{13}C atoms. Chloroplasts were isolated from both conditions and separated into thylakoid and envelope membranes and stroma proteins. Thylakoid samples are mixed on an equal protein basis and separated by SDS-PAGE. A protein band corresponding to the Lhcbm proteins was excised the proteins were digested with trypsin, and analyzed by LC-MS and MS/MS (Fig. 2). Resolution of the doubly charged peptide ions ELELIHAR and ELELIHAR [+6 Da] using the data filters in the full scan mode for *m/z* 490.4–491.6 and 493.4–494.6 shows approximately equal protein amounts in iron-sufficient and -deficient conditions in line with previous results [46]. The fragmentation of the precursor ions 491.5 (upper panel of MS/MS in Fig. 2) and 494.5 (lower panel of MS/MS in Fig. 2)) reveals a y-ion series differing in 6 Da due to the presence of isotopically labeled arginine. Incorporation of labeled arginine into proteins of this strain demonstrates the suitability of this method for comparative proteomic analyses in *C. reinhardtii*.

To our knowledge this is the first application of this powerful technique in a photosynthetic eukaryotic organism. One of the difficulties that we have observed when using this procedure is that the $^{13}C_6$-arginine can be further metabolized by the cell and incorporated into other amino acids, which complicates the quantitative analysis. Therefore, isotope swapping experiments have to be performed to validate comparative quantifications. In summary we are convinced that this technique will allow extensive quantitative proteomic studies in *Chlamydomonas*, which will prove very valuable for the evaluation of protein dynamics in the context of environmental changes or varying genetic backgrounds.

This quantitative proteomics data could be combined with transcriptomic data from DNA chips (version 1.1 of the *C. reinhardtii* microarry is currently available, within the CC425 background, [21] and data from the newly emerging field of *C. reinhardtii* metabolomics (Bölling and Fiehn, 2004). These data could be used to create a systems biology perspective of the transcript, protein, and metabolic state of an organism when it has been perturbed by a stress condition or by a mutation. Such an integrated approach to analyze transcriptomic and proteomic responses has already been taken in yeast to analyze the global response to nutrient availability [29].

A different strategy utilizes, isotopically labeled chemical probes which can be chemically linked to specific amino acids such as cysteine, methionine, tryptophan, or N-terminal amino acids of proteins or peptides. One of the most widely used

chemical probes of this kind is called the isotope coded affinity tag [22], which can be commercially purchased. An advantage of this technique is that it significantly reduces sample complexity, and thus results in a higher dynamic range of the analytical procedure. However, many peptides with potentially interesting features, such as post-translational modifications, may be missed.

10. Software tools for *C. reinhardtii* proteomics

The genomic resources for *C. reinhardtii* provide the informatic and material infrastructure that will enable protein identification and protein–protein interaction studies to be carried out on a global scale. The complete genomic sequence should contain the information necessary to deduce all genes, however, intron/exon boundaries and post-translational splicing events introduce difficulties for the prediction of protein sequences.

Most approaches for identifying proteins from MS/MS data do not rely solely on de novo deduced sequences. Commonly used approaches utilize nucleotide or protein databases for correlation and subsequent identification of an amino acid sequence from tandem mass spectral data, [13,42,52]. Thus, the presence and nature of a database is critical. If a peptide sequence is not represented in the given database, then it cannot be identified. Introns in genomic databases present such a problem because they render a database sequence effectively "invisible" to a searching algorithm that compares MS/MS data only to information from directly translated genomic sequences.

Until now, non of the commercially available approaches is able to identify peptides that are split by an intron when deduced from genomic DNA. However, an algorithm has been recently developed that is designed to fulfill this task [1]. This algorithm, named GenomicPeptideFinder (GPF), uses short spans of peptide sequence, which can be derived from algorithmic or manual de novo sequencing, together with the molecular mass of the precursor ion (see Fig. 3). These are known as sequence tags [42]. The sequence predictions are based on selected MS/MS spectra. Fragments of the predicted amino acid sequence are aligned with each of the six frames of the translated genome and the precursor mass information is used to assemble the corresponding tryptic peptides using the sequence as a matrix. Hereby, intron-split peptides or peptides that originate from alternative splicing can be gathered and in turn verified by mass spectrometric data interpretation tools like Sequest [13].

In addition to this published algorithm, additional tools are being developed to use MS/MS data to assist in the definition of exon/intron boundaries. The French consortium Génopole Rhône-Alpes in Grenoble has undertaken a systematic study of the chloroplast proteome. Their analysis uses the program suite Pepline, being developed in collaboration between the DRDC/CP-CEA (http://www.dsv.cea.fr/cp) and Helix-Institut National de Recherche Informatique et en Automatique (INRIA) laboratories (http://www.helix.inrialpes.fr). This program is comprised of two modules, aimed, respectively, at generating sequence tags from MS/MS data and mapping them onto a proteome, cDNA or genome database. In the latter application, it has the abil-

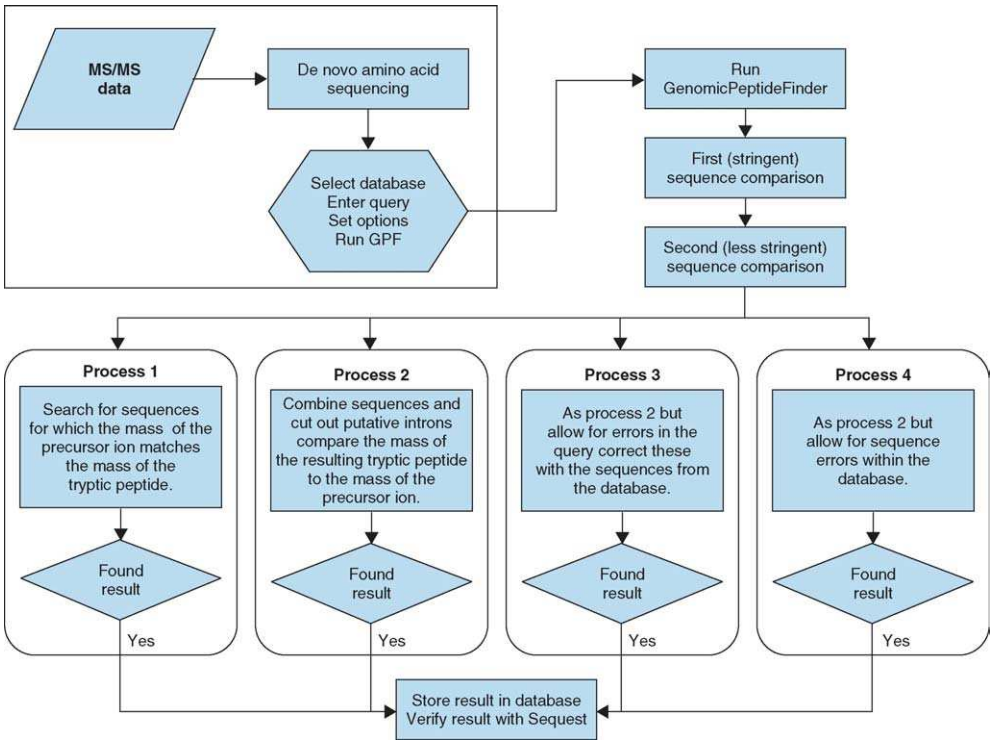

Fig. 3. Schematic work flow of GPF [1] (taken with permission).

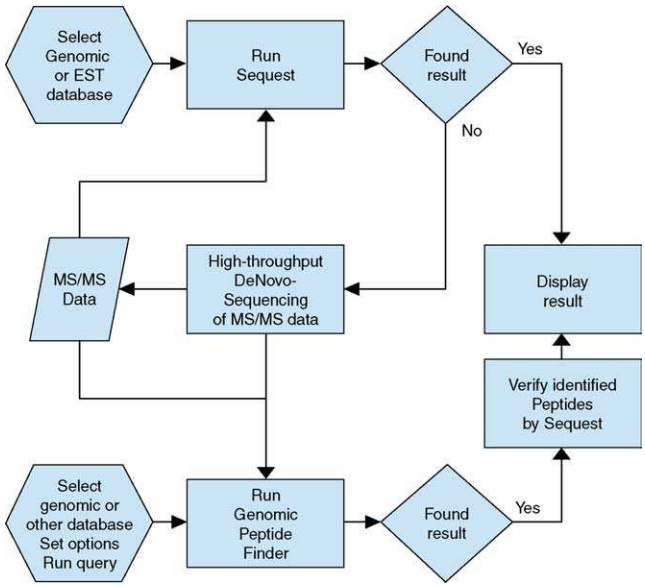

Fig. 4. Schematic work flow to assess the mass spectrometric data obtained by LC-MS/MS.

ity to handle intron-split peptides. (Communicated by Olivier Vallon, Norbert Rolland, Marianne Tardif, Jerome Garin).

In cases the *Chlamydomonas* genomic database is used to mine mass spectrometric data obtained from *Chlamydomonas* proteins we suggest to operate mass spectrometric evaluation tools like Sequest or Mascot in parallel with the GPF (Fig. 4). The rationale behind this is that the use of GPF will allow the identification of intron split peptide sequences, when deduced from the genomic DNA, as well as peptides sequences that derived from alternative splicing, which would be missed by Sequest or Mascot analyses otherwise, so that the parallel usage will permit to extract more information from the data. It is foreseeable that a successful integration of GPF and with other commercial available algorithm like Sequest will be widely applicable to proteomics studies that deal with genomic database from organism that possess genes with exon–intron structures.

Determining the identity and number of genes from a genomic sequence is an immense task. cDNA sequences for *A. thaliana* covered about 60% of predicted genes (Seki et al., 2003). In order to obtain additional clones and annotate more genes, strategies for cloning open reading frames have been implemented. A recent study was carried out in *C. elegans* [55]. Additionally, numerous gene-finding algorithms are used for identifying coding regions in genomic sequences. Currently, the success rate is reported to be generally maximally around 50% [53], a figure which is also supported by open reading frame cloning studies [55].

MS data, in conjunction will software tools such as GPF, may make valuable contributions to the annotation of the *C. reinhardtii* genome. Genomic databases will be indispensable for the identifying proteins using MS-based proteomics, especially those that are expressed at low levels. Software tools that increase the probability and reliability for identifying low abundance proteins will be valuable. Many proteins that are expressed at low levels, although hard to detect, possess interesting biological functions. It is of note that about 40% of the *H. sapiens* genes are alternatively spliced [45]. It appears that alternative splicing plays also an important role in generating proteome diversity in plants [33]. Although the extent of splicing in *C. reinhardtii* is currently not known, the generations of tools that determine and elucidate alternative splicing will be important for the future.

11. Archiving and dissemination of proteomic data

Large amounts of proteomic data will be gathered in the near future, as more proteomic investigations in *C. reinhardtii* get under way. An important outcome of these investigations would be the generation of high quality open access databases. Several examples of curated databases exist, which were initiated based on investigations in *A. thaliana*, for membrane bound proteins (http://www.aramemnon.botanik.uni-koeln.de), the chloroplast (http://www.cbsusrv01.tc.cornell.edu/users/ppdb/), and mitochondrial proteins (http://www.mitoz.bcs.uwa.edu.au/).

In addition, statistical criteria for assessing MS-based proteomics data would be useful for allowing comparison of data between different laboratories [48]. Databases, such as the open proteomics database (http://www.bioinformatics.icmb.utexas.edu/OPD/) containing raw mass spectral data may facilitate the development of new algorithms as well as the refinement of old algorithms.

12. Conclusions

Because proteins are involved in nearly all aspects of biological function, proteomics has the potential to significantly increase our understanding of *C. reinhardtii* biology. This hope has begun to be realized for the elucidation of *Chlamy-*

domonas subproteomes as outlined above. The proteomic investigations that have been reported to date have primarily implemented MS based identification of proteins, however, protein–protein interaction studies in *C. reinhardtii*, analyses of multi-protein complexes composition as well as quantitative protein profiling will in the future add another dimension of knowledge of protein function. Challenges in the future will be to increase the sensitivity of analytical procedures for MS and to link the information to powerful bioinformatic tools that help in the identification of proteins. In line with that, validation of gene models as predicted from the *Chlamydomonas* genomic data as well as elucidation of alternative protein splicing by MS will be major tasks for the future.

Acknowledgements

We thank J. Allmer for help with Fig. 4. Funding was provided by the Deutsche Forschungsgemeinschaft and the University of Pennsylvania to M.H.

References

[1] J. Allmer, C. Markert, E.J. Stauber, M. Hippler, A new approach that allows identification of intron-split peptides from mass spectrometric data in genomic databases, FEBS Lett 562 (2004) 202–206.

[2] E. Asamizu, Y. Nakamura, K. Miura, H. Fukuzawa, S. Fujiwara, M. Hirono, et al., Establishment of publicly available cDNA material and information resource of Chlamydomonas reinhardtii (Chlorophyta), to facilitate gene function analysis, Phycologia (2004).

[3] R. Bassi, S.Y. Soen, G. Frank, H. Zuber, J.D. Rochaix, Characterization of chlorophyll a/b proteins of photosystem I from *Chlamydomonas reinhardtii*, J. Biol. Chem. 267 (1992) 25714–25721.

[4] J. Beisson, M. Jerka-Dziadosz, Polarities of the centriolar structure: morphogenetic consequences, Biol. Cell. 91 (1999) 367–378.

[5] P. Bennoun, A. Atteia, Y. Pierre, M. Delosme, Etiolated cells of *Chlamydomonas reinhardtii*: choice material for characterization of mitochondrial membrane polypeptides, Proc. Natl. Acad. Sci. USA 92 (1995) 10202–10206.

[6] A. Ben-Shem, F. Frolow, N. Nelson, Crystal structure of plant photosystem I, Nature 426 (2003) 630–635.

[7] D.G. Cole, The intraflagellar transport machinery of Chlamydomonas reinhardti, Traffic 4 (2003) 435–442.

[8] D.G. Cole, D.R. Diener, A.L. Himelblau, P.L. Beech, J.C. Fuster, J.L. Rosenbaum, *Chlamydomonas* kinesin-II-dependent intraflagellar transport (IFT): IFT particles contain proteins required for ciliary assembly in *Caenorhabditis elegans* sensory neurons, J. Cell Biol. 141 (1998) 993–1008.

[9] A.M. Curry, B.D. Williams, J.L. Rosenbaum, Sequence analysis reveals homology between two proteins of the flagellar radial spoke, Mol. Cell. Biol. 12 (1992) 3967–3977.

[10] S. Dutcher, Purification of basal bodies and basal body complexes from *Chlamydomonas reinhardtii*, Methods Cell Biol. 47 (1995) 323–334.

[11] D. Elrad, A.R. Grossman, A genomes-eye view of the light-harvesting polypeptides of *Chlamydomonas reinhardtii*, Curr. Genet 45 (2004) 61–75.

[12] O. Emanuelsson, H. Nielsen, S. Brunak, G. Von Heijne, Predicting subcellular localization of proteins based on their N-terminal amino acid sequence, J. Mol. Biol. 300 (2000) 1005–1016.

[13] J.K. Eng, A.L. McCormack, J.R. Yates, An approach to corrrelate tandem mass spectral data of peptides with amino acid sequences in a protein database, J. Am. Soc. Mass Spectrom. 5 (1994) 976–989.

[14] M. Eriksson, P. Gardestrom, G. Samuelsson, Isolation, purification, and characterization of mitochondria from *Chlamydomonas reinhardtii*, Plant Physiol. 107 (1995) 479–483.

[15] M. Ferro, D. Salvi, S. Brugiere, S. Miras, S. Kowalski, M. Louwagie, et al., Proteomics of the chloroplast envelope membranes from *Arabidopsis thaliana*, Mol. Cell Proteomics 2 (2003) 325–345.

[16] L. Franzen, J. Rochaix, G. Von Heijne, Chloroplast transit peptides from the green alga *Chlamydomonas reinhardtii* share features with both mitochondrial and higher plant chloroplast presequences, FEBS Lett. 260 (1990) 165–168.

[17] G. Friso, L. Giacomelli, A.J. Ytterberg, J.-B. Peltier, A. Rudella, Q. Sun, et al., In-depth analysis of the thylakoid membrane proteome of *Arabidopsis thaliana* chloroplasts: new proteins, new functions, and a plastid proteome database, Plant Cell 16 (2004) 478–499.

[18] J. Froehlich, C. Wilkerson, W. Ray, R. McAndrew, K. Osteryoung, D. Gage, et al., Proteomic study of the *Arabidopsis thaliana* chloroplastic envelope membrane utilizing alternatives to traditional two-dimensional electrophoresis, J. Proteome Res. 2 (2003) 413–425.

[19] S. Geimer, M. Melkonian, The ultrastructure of the *Chlamydomonas reinhardtii* basal apparatus: identification of an early marker of radial asymmetry inherent in the basal body, J. Cell. Sci. 117 (2004) 2663–2674.

[20] U.W. Goodenough, Green yeast, Cell 70 (1992) 533–538.

[21] A.R. Grossman, E.E. Harris, C. Hauser, P.A. Lefebvre, D. Martinez, D. Rokhsar, et al., *Chlamydomonas reinhardtii* at the crossroads of genomics, Eukaryotic Cell 2 (2003) 1137–1150.

[22] S.P. Gygi, B. Rist, S.A. Gerber, F. Turecek, M.H. Gelb, R. Aebersold, Quantitative analysis of complex protein mixtures using isotope-coded affinity tags, Nat. Biotechnol. 17 (1999) 994–999.

[23] M. Hanson, J. Davidson, L.B. Mets, Characterization of chloroplast and cytoplasmic ribosomal proteins of *Chlamydomonas reinhardi* by two-dimensional gel electrophoresis, Mol. Gen. Genet. 132 (1974) 105–118.

[24] E.H. Harris, J.E. Boynton, N.W. Gillham, Chloroplast ribosomes and protein synthesis, Microbiol. Rev. 58 (1994) 700–754.

[25] J.L. Heazlewood, J.S. Tonti-Filippini, A.M. Gout, D.A. Day, J. Whelan, A.H. Millar, Experimental analysis of the Arabidopsis mitochondrial proteome highlights signaling and regulatory components, provides assessment of targeting prediction programs, and indicates plant-specific mitochondrial proteins, Plant Cell 16 (2004) 241–256.

[26] M. Hippler, F. Drepper, J. Farah, J.D. Rochaix, Fast electron transfer from cytochrome c6 and plastocyanin to photosystem I of *Chlamydomonas reinhardtii* requires PsaF, Biochemistry 36 (1997) 6343–6349.

[27] M. Hippler, J. Klein, A. Fink, T. Allinger, P. Hoerth, Towards functional proteomics of membrane protein complexes: analysis of thylakoid membranes from Chlamydomonas reinhardtii, Plant J. 28 (2001) 595–606.

[28] M. Hippler, K. Redding, J. Rochaix, *Chlamydomonas* genetics, a tool for the study of bioenergetic pathways, Biochim. Biophys. Acta 1367 (1998) 1–62.

[29] T. Ideker, V. Thorsson, J.A. Ranish, R. Christmas, J. Buhler, J.K. Eng, et al., Integrated genomic and proteomic analyses of a systematically perturbed metabolic network, Science 292 (2001) 929–934.

[30] C.H. Johnson, Precise circadian clocks in prokaryotic cyanobacteria, Curr. Issues Mol. Biol. 6 (2004) 103–110.

[31] J. Joyard, E. Teyssier, C. Miege, D. Berny-Seigneurin, E. Marechal, M.A. Block, et al., The biochemical machinery of plastid envelope membranes, Plant Physiol. 118 (1998) 715–723.

[32] P. Kathir, M. LaVoie, W.J. Brazelton, N.A. Haas, P.A. Lefebvre, C.D. Silflow, Molecular map of the *Chlamydomonas reinhardtii* nuclear genome, Eukaryotic Cell 2 (2003) 362–379.

[33] K. Kazan, Alternative splicing and proteome diversity in plants: the tip of the iceberg has just emerged, Trends Plant Sci. 8 (2003) 468–471.

[34] J. Kim, S.P. Mayfield, Protein disulfide isomerase as a regulator of chloroplast translational activation, Science 278 (1997) 1954–1957.

[35] T. Kleffmann, D. Russenberger, A. Von Zychlinski, W. Christopher, K. Sjolander, W. Gruissem, et al., The *Arabidopsis thaliana* chloroplast proteome reveals pathway abundance and novel protein functions, Curr. Biol 14 (2004) 354–362.

[36] K. Kozminski, K. Johnson, P. Forscher, J. Rosenbaum, A motility in the eukaryotic flagellum unrelated to flagellar beating, Proc. Natl. Acad. Sci. USA 90 (1993) 5519–5523.

[37] P.A. Lefebvre, C.D. Silflow, *Chlamydomonas*: the cell and its genomes, Genetics 151 (1999) 9–14.

[38] S.D. Lemaire, B. Guillon, P. Le Marechal, E. Keryer, M. Miginiac-Maslow, et al., New thioredoxin targets in the unicellular photosynthetic eukaryote *Chlamydomonas reinhardtii*, Proc. Natl. Acad. Sci. 101 (2004) 7475–7480.

[39] J. Li, J. Gerdes, C. Haycraft, Y. Fan, T. Teslovich, H. May-Simera, et al., Comparative genomics identifies a flagellar and basal body proteome that includes the BBS5 human disease gene, Cell 117 (2004) 541–552.

[40] R. Lill, G. Kispal, Maturation of cellular Fe–S proteins: an essential function of mitochondria, Trends Biochem. Sci. 25 (2000) 352–356.

[41] D. Luck, G. Piperno, Z. Ramanis, B. Huang, Flagellar mutants of *Chlamydomonas*: studies of radial spoke-defective strains by dikaryon and revertant analysis, Proc. Natl. Acad. Sci. USA 74 (1977) 3456–3460.

[42] M. Mann, M. Wilm, Error-tolerant identification of peptides in sequence databases by peptide sequence tags, Anal. Chem. 66 (1994) 4390–4399.

[43] W. Marshall, J. Rosenbaum, How centrioles work: lessons from green yeast, Curr. Opin. Cell Biol. 12 (2000) 119–125.

[44] J.E. Maul, J.W. Lilly, L. Cui, C.W. Depamphilis, W. Miller, E.H. Harris, et al., The *Chlamydomonas reinhardtii* plastid chromosome: islands of genes in a sea of repeats, Plant Cell 14 (2002) 2659–2679.

[45] B. Modrek, C.J. Lee, Alternative splicing in the human, mouse and rat genomes is associated with an increased frequency of exon creation and/or loss, Nat. Genet. 34 (2003) 177–180.

[46] J.L. Moseley, T. Allinger, S. Herzog, P. Hoerth, E. Wehinger, S. Merchant, et al., Adaptation to Fe-deficiency requires remodeling of the photosynthetic apparatus, EMBO J. 21 (2002) 6709–6720.

[47] K. Nakai, P. Horton, PSORT: a program for detecting sorting signals in proteins and predicting their subcellular localization, Trends Biochem. Sci. 24 (1999) 34–35.

[48] A.I. Nesvizhskii, R. Aebersold, Analysis, statistical validation and dissemination of large-scale proteomics datasets generated by tandem MS, Drug Discov. Today 9 (2004) 173–181.

[49] S.-E. Ong, B. Blagoev, I. Kratchmarova, D.B. Kristensen, H. Steen, A. Pandey, et al., Stable isotope labeling by amino acids in cell culture, SILAC, as a simple and accurate approach to expression proteomics, Mol. Cell Proteomics 1 (2002) 376–386.

[50] L.E. Ostrowski, K. Blackburn, K.M. Radde, M.B. Moyer, D.M. Schlatzer, A. Moseley, et al., A proteomic analysis of human cilia: identification of novel components, Mol. Cell Proteomics 1 (2002) 451–465.

[51] J.-B. Peltier, O. Emanuelsson, D.E. Kalume, J. Ytterberg, G. Friso, A. Rudella, et al., Central functions of the lumenal and peripheral thylakoid proteome of Arabidopsis determined by experimentation and genome-wide prediction, Plant Cell 14 (2002) 211–236.

[52] D.N. Perkins, D.J.C. Pappin, D.M. Creasy, J.S. Cottrell, Probability-based protein identification by searching sequence databases using mass spectrometry data, Electrophoresis 20 (1999) 3551–3567.

[53] M. Pertea, S. Salzberg, Computational gene finding in plants, Plant Mol. Biol. 48 (2002) 39–48.

[54] B. Randolph-Anderson, N. Gillham, J. Boynton, Electrophoretic and immunological comparisons of chloroplast and prokaryotic ribosomal proteins reveal that certain families of large subunit proteins are evolutionarily conserved, J. Mol. Evol. 29 (1989) 68–88.

[55] J. Reboul, P. Vaglio, J.-F. Rual, P. Lamesch, M. Martinez, C.M. Armstrong, et al., C. elegans ORFeome version 1.1: experimental verification of the genome annotation and resource for proteome-scale protein expression, Nat. Genet. 34 (2003) 35–41.

[56] S. Rexroth, J.M.W.M.z. Tittingdorf, F. Krause, N.A. Dencher, H. Seelert, Thylakoid membrane at altered metabolic state: challenging the forgotten realms of the proteome, Electrophoresis 24 (2003) 2814–2823.

[57] E. Richly, D. Leister, An improved prediction of chloroplast proteins reveals diversities and commonalities in the chloroplast proteomes of Arabidopsis and rice, Gene 329 (2004) 11–16.

[58] J.-D. Rochaix, Assembly, function, and dynamics of the photosynthetic machinery in Chlamydomonas reinhardtii, Plant Physiol. 127 (2001) 1394–1398.

[59] J.L. Rosenbaum, G.B. Witman, Intraflagellar transport, Nat. Rev. Mol. Cell. Biol. 3 (2002) 813–825.

[60] M.L. Salvador, U. Klein, L. Bogorad, Endogenous fluctuations of DNA topology in the chloroplast of *Chlamydomonas reinhardtii*, Mol. Cell. Biol. 18 (1998) 7235–7242.

[61] F. Savard, C. Richard, M. Guertin, The *Chlamydomonas reinhardtii* LI818 gene represents a distant relative of the cabI/II genes that is regulated during the cell cycle and in response to illumination, Plant Mol. Biol. 32 (1996) 461–473.

[62] M. Schubert, U.A. Petersson, B.J. Haas, C. Funk, W.P. Schroder, T. Kieselbach, Proteome map of the chloroplast lumen of Arabidopsis thaliana, J. Biol. Chem. 277 (2002) 8354–8365.

[63] P. Schurmann, J.-P. Jacquot, Plant thioredoxin systems revisited, Ann. Rev. Plant Physiol. Plant Mol. Biol. 51 (2000) 371–400.

[64] J. Shrager, C. Hauser, C.-W. Chang, E.H. Harris, J. Davies, J. McDermott, et al., Chlamydomonas reinhardtii genome project. A guide to the generation and use of the cDNA information, Plant Physiol. 131 (2003) 401–408.

[65] A. Sickmann, J. Reinders, Y. Wagner, C. Joppich, R. Zahedi, H.E. Meyer, et al., The proteome of Saccharomyces cerevisiae mitochondria, Proc. Natl. Acad. Sci. 100 (2003) 13207–13212.

[66] C.D. Silflow, P.A. Lefebvre, Assembly and motility of eukaryotic cilia and flagella. Lessons from Chlamydomonas reinhardtii, Plant Physiol. 127 (2001) 1500–1507.

[67] I. Small, N. Peeters, F. Legeai, C. Lurin, Predotar: a tool for rapidly screening proteomes for N-terminal targeting sequences, Proteomics 4 (2004) 1581–1590.

[68] E.J. Stauber, A. Fink, C. Markert, O. Kruse, U. Johanningmeier, M. Hippler, Proteomics of Chlamydomonas reinhardtii light-harvesting proteins, Eukaryotic Cell 2 (2003) 978–994.

[69] Q. Sun, O. Emanuelsson, K.J. Van Wijk, Analysis of curated and predicted plastid subproteomes of Arabidopsis. Subcellular compartmentalization leads to distinctive proteome properties, Plant Physiol. 135 (2004) 723–734.

[70] Y. Takahashi, M. Goldschmidt-Clermont, S.Y. Soen, L.G. Franzen, J.D. Rochaix, Directed chloroplast transformation in *Chlamydomonas reinhardtii*: insertional inactivation of the psaC gene encoding the iron sulfur protein destabilizes photosystem I, EMBO J. 10 (1991) 2033–2040.

[71] Y. Takahashi, T.A. Yasui, E.J. Stauber, M. Hippler, Comparison of the subunit compositions of the PSI–LHCI supercomplex and the LHCI in the green alga Chlamydomonas reinhardtii, Biochemistry 43 (2004) 7816–7823.

[72] M.V. Turkina, A. Villarejo, A.V. Vener, The transit peptide of CP29 thylakoid protein in Chlamydomonas reinhardtii is not removed but undergoes acetylation and phosphorylation, FEBS Lett. 564 (2004) 104–108.

[73] M. Tyers, M. Mann, From genomics to proteomics, Nature 422 (2003) 193–197.

[74] R. Van Lis, A. Atteia, G. Mendoza-Hernandez, D. Gonzalez-Halphen, Identification of novel mitochondrial protein components of Chlamydomonas reinhardtii. A proteomic approach, Plant Physiol. 132 (2003) 318–330.

[75] V. Wagner, M. Fiedler, C. Markert, M. Hippler, M. Mittag, Functional proteomics of circadian expressed proteins from Chlamydomonas reinhardtii, FEBS Lett. 559 (2004) 129–135.

[76] B. Williams, M. Velleca, A. Curry, J. Rosenbaum, Molecular cloning and sequence analysis of the *Chlamydomonas* gene coding for radial spoke protein 3: flagellar mutation pf-14 is an ochre allele, J. Cell Biol. 109 (1989) 235–245.

[77] M. Wirschell, G. Pazour, A. Yoda, M. Hirono, R. Kamiya, G.B. Witman, Oda5p, a novel axonemal protein required for assembly of the outer dynein arm and an associated adenylate kinase, Mol. Biol. Cell 15 (2004) 2729–2741.

[78] K. Yamaguchi, M.V. Beligni, S. Prieto, P.A. Haynes, W.H. McDonald, J.R. Yates, et al., Proteomic characterization of the Chlamydomonas reinhardtii chloroplast ribosome: identification of proteins unique to the 70S ribosome, J. Biol. Chem. 278 (2003) 33774–33785.

[79] B. Zhao, C. Schneid, D. Iliev, E.-M. Schmidt, V. Wagner, F. Wollnik, M. Mittag, The circadian RNA-binding protein CHLAMY 1 represents a novel type heteromer of RNA recognition motif and lysine homology domain-containing subunits, Eukaryotic Cell 3 (2004) 815–825.

Manuscript 2

Yuichiro Takahashi, Taka-aki Yasui, Einar J. Stauber, and Michael Hippler (2004) Comparison of the subunit compositions of the PSI-LHCI supercomplex and the LHCI in the green alga *Chlamydomonas reinhardtii*. **Biochemistry** 43, 7816-7823.

Comparison of the Subunit Compositions of the PSI−LHCI Supercomplex and the LHCI in the Green Alga *Chlamydomonas reinhardtii*†

Yuichiro Takahashi,*,‡ Taka-aki Yasui,‡ Einar J. Stauber,§ and Michael Hippler§

Department of Biology, Faculty of Science, Okayama University, 3-1-1, Tsushima-naka, Okayama, 700-8530, Japan, and Lehrstuhl für Pflanzenphysiologie, Friedrich-Schiller-Universität Jena, Dornburger Str. 159, 07743 Jena, Germany

Received November 6, 2003; Revised Manuscript Received March 25, 2004

ABSTRACT: Although the light-harvesting chlorophyll protein complex I (LHCI) of photosystem I (PSI) is intimately associated with the PSI core complex and forms the PSI−LHCI supercomplex, the LHCI is normally synthesized in PSI-deficient mutants. In this paper, we compared the subunit compositions of the PSI−LHCI supercomplex and the LHCI by immunoblot analysis and two-dimensional gel electrophoresis combined with mass spectrometry. The PSI−LHCI supercomplex and the LHCI were purified by sucrose density gradient centrifugation and (diethylamino)ethyl column chromatography from *n*-dodecyl-*β*-D-maltoside-solubilized thylakoids of the wild-type and Δ*psaB* mutant of the green alga *Chlamydomonas reinhardtii*. The PSI−LHCI supercomplex contained all of the nine Lhca polypeptides (Lhca1−9) that are detected in wild-type thylakoids. In contrast, the LHCI retained only six Lhca polypeptides, whereas Lhca3 and two minor polypeptides, Lhca2 and Lhca9, were lost during the purification procedure. Sucrose density gradient centrifugation showed that the purified LHCI retains an oligomeric structure with an apparent molecular mass of 300−400 kDa. We therefore concluded that Lhca2, Lhca3, and Lhca9 are not required for the stable oligomeric structure of the LHCI and that the association of these polypeptides in the LHCI is stabilized by the presence of the PSI core complex. Finally, we discuss the possible localization and function of Lhca polypeptides in the LHCI.

Light energy used to drive photosynthetic electron transport is absorbed by antenna pigments located in the thylakoid membranes. In higher plants and green algae, antenna pigments reside in core and accessory antenna systems. The core antenna system is fused with reaction center proteins such as the PsaA/PsaB heterodimer in photosystem I (PSI)[1] or is intimately associated with the reaction center complex like CP43 and CP47 in photosystem II (PSII). The accessory antenna systems are called the light-harvesting chlorophyll a/b complexes (LHC). LHCI is functionally related to PSI as is LHCII to PSII. It is known that LHCI is tightly associated with the PSI core complex, and thus the PSI−LHCI supercomplex is easily purified after solubilizing thylakoids with nonionic detergents (*1*). On the contrary, LHCII is loosely associated with the PSII core complex, and thus the PSII−LHCII supercomplex can be isolated only under mild conditions (*2*).

LHCI forms an oligomer and consists of several distinct Lhca polypeptides (*3*). Two types of LHCI have been isolated from higher plants: LHCI-680, which consists of Lhca2 and Lhca3 and emits 77 K fluorescence peaking at 680 nm, and LHCI-730, which consists of Lhca1 and Lhca4 and emits fluorescence at 730 nm (*4*). The number of Lhca polypeptides present in the PSI−LHCI supercomplex currently remains controversial. The three-dimensional structure of the PSI−LHCI supercomplex, as characterized by single particle analysis with electron microscopy, suggests that 8−14 Lhca polypeptides are present (*5*−*7*). Because the Lhca polypeptide is estimated to bind 10−12 chlorophyll molecules, there must be 100 or more chlorophyll molecules bound to LHCI in the supercomplex (*8*). The structure of the PSI−LHCI supercomplex also suggests that Lhca polypeptides form a half-ring structure and are bound at one side of the PSI core complex (*5*). Recently, the crystal structure of plant PSI−LHCI supercomplex has been determined at a 4.4-Å resolution (*9*). The structure revealed that the supercomplex contains only 4 Lhca polypeptides. It is of interest that the PSI−LHCI supercomplex from *Chlamydomonas reinhardtii* is significantly larger than the corresponding complex in spinach (*6*). However, the assignment and function of individual Lhca polypeptides in the PSI−LHCI supercomplex remain to be elucidated.

The LHCI complex of *C. reinhardtii* was initially identified as CPO (chlorophyll protein O) by nondenaturing lithium dodecyl sulfate polyacrylamide gel electrophoresis (*10*). The relative electrophoretic mobility on the gel was lower than that of CPI (PSI reaction center complex), suggesting that CPO forms a high molecular weight complex. Because the structure of the PSI−LHCI supercomplex appears similar in *C. reinhardtii* and higher plants, the oligomeric structure

† This research was supported by a grant in aid for General Research (C) (2) (15570037) to Y.T. and by grants from the Deutsche Forschungsgemeinschaft and the Freistaat Thüringen to M.H.

* To whom correspondence should be addressed. Tel: +81-86-251-7861. Fax: +81-86-251-7876. E-mail: taka@cc.okayama-u.ac.jp.

‡ Okayama University.

§ Friedrich-Schiller-Universität Jena.

[1] Abbreviations: Chl, chlorophyll; CPO, chlorophyll protein O; DM, *n*-dodecyl-*β*-D-maltoside; LHCI, light-harvesting complex I; LHCII, light-harvesting complex II; PSI, photosystem I; PSII, photosystem II; 2DE, two-dimensional electrophoresis.

10.1021/bi035988z CCC: $27.50
Published on Web 05/26/2004

of *C. reinhardtii* LHCI is rather stable compared with that of higher plants. It was also found that CPO accumulates normally in the PSI-deficient mutant (*10*). This indicates that assembly of the LHCI is independent of the PSI complex and that the oligomeric form of the LHCI accumulates stably in vivo even in the absence of the PSI core complex. Two types of the LHCI, LHCI-680 and LHCI-705, which emit 77 K fluorescence at 685 and 705 nm, respectively, have been isolated from the PSI−LHCI supercomplex of *C. reinhardtii*. In contrast to LHCI-680 and LHCI-730 in higher plants, the polypeptide composition of LHCI-680 and LHCI-705 is very similar (*3*). Detailed biochemical analyses revealed that there are nine distinct Lhca polypeptides in *C. reinhardtii* (*11*).

In the present paper, we purified the PSI−LHCI supercomplex and the LHCI from *C. reinhardtii* wild-type and Δ*psaB* cells and compared the polypeptide compositions by SDS−PAGE and Western blotting. In addition, to compare the polypeptides in the PSI−LHCI supercomplex and LHCI at high resolution and sensitivity, we employed two-dimensional gel electrophoresis (2DE) combined with tandem mass spectrometry (MS/MS). We found that the LHCI from the Δ*psaB* mutant still contained most of the major Lhca polypeptides found in the PSI−LHCI supercomplex. Immunoblotting, however, revealed that Lhca3 (p14.1) is lost during the preparation of the LHCI from Δ*psaB* cells. The 2DE identified two additional minor polypeptides that were decreased in the purified LHCI. In conclusion, the association of these Lhca proteins with the LHCI is stabilized by the presence of the PSI core complex, but the presence of these polypeptides is not required for stabilizing the oligomeric structure of the LHCI.

EXPERIMENTAL PROCEDURES

Strains and Growth Conditions. In these studies, we used the *C. reinhardtii* wild-type strain 137C and the *psaB*-deficient mutant (Δ*psaB*). Cells were grown to mid-log phase [$(2-5) \times 10^6$ cells mL^{-1}] in a Tris-acetate-phosphate (TAP) medium at 25 °C.

Purification of Chlorophyll−Protein Complexes. Thylakoid membranes were purified by discontinuous sucrose density gradient centrifugation as described previously (*12*). The thylakoid membranes (0.8 mg Chl mL^{-1}) were solubilized with 0.8% (w/v) *n*-dodecyl-*β*-D-maltoside (DM), and the resulting extracts were fractionated by sucrose density gradient centrifugation as described previously (*13*). The sucrose gradient contained a linear concentration of sucrose from 0.1 to 1.3 M in 5 mM Tricine-NaOH at pH 8.0 and 0.05% DM, and centrifugation was carried out at 141000*g* (SW28, Beckman) at 4 °C for 24 h. The chlorophyll−protein complexes were further separated by column chromatography on (diethylamino)ethyl (DEAE) Toyopearl 650S (Tosoh, Tokyo, Japan). Fractions were eluted with a linear gradient of NaCl (25−175 mM) in 50 mM Tris-HCl at pH 8.0 and 0.05% DM. Chlorophyll concentrations were determined as described in ref *14*.

Western Blotting. Polypeptides were solubilized with 2% SDS and 0.1 M dithiothreitol at 100 °C for 1 min and separated by SDS−PAGE according to ref *15*. D1 was resolved by urea−SDS−PAGE as described in ref *13*. To improve the separation of LHCI polypeptides around 20−30 kDa, an SDS−PAGE system with a high Tris buffer and gradient acrylamide concentration (15−22.5%) was used in the resolving gel (*16*). Separated polypeptides were electrophoretically transferred to nitrocellulose filters and then probed with specific polyclonal antibodies. The signals were visualized by enhanced chemiluminescence.

2DE and MS. The 2DE was performed as described in ref *17*, and mass spectrometric analyses were conducted as described in ref *11*.

Measurement of Fluorescence Emission Spectra. Fluorescence emission spectra were measured at 77 K with a Hitachi fluorescence spectrophotometer F-4500. Samples were excited with an actinic light at 430 nm.

RESULTS

Purification of PSI−LHCI Supercomplex from Wild-Type Cells. LHCI is tightly bound to the PSI core complex so that the PSI−LHCI supercomplex can be isolated from thylakoids solubilized with nonionic detergents under moderate conditions (*15*). Figure 1A shows the separation profile of the chlorophyll−protein complexes. The thylakoids purified from wild-type cells were solubilized with 0.8% DM, and the resulting extracts were separated by sucrose density gradient centrifugation. The gradient was collected from the bottom, and the fractionation profile was monitored by measuring the absorption at 670 nm. Three major peaks were clearly detected (A-1, A-2, and A-3 from the top of the gradient). Western blotting using anti-PsaD antibody indicates that most of the PSI is present in A-3 (fractions 6−8), and a small amount of PSI is in A-2 (fractions 9 and 10). PSII was exclusively present in A-2, while LHCII was separated in A-1 as described in refs *15* and *18*. Western blotting using LHCI antibodies (anti-p14.1, p15, and p18.1) revealed that the separation profile of LHCI is almost identical to that of PSI, indicating that LHCI is copurified with PSI on the sucrose density gradient. Two signals in A-1 (fractions 11−15), which were visualized with anti-p15, are ascribed to its cross-reaction to LHCII proteins.

Fraction A-3 was subsequently loaded onto a DEAE column and separated with a buffer containing a linear gradient of NaCl (Figure 1B). We identified a single peak containing both PSI and LHCI proteins, indicating that the PSI and LHCI are stably associated to form a homogeneous PSI−LHCI supercomplex. In addition, this chromatographical purification step improved the fluorescence emission spectrum at 77 K; a shoulder peak at 685 nm, which may be ascribed to a small contamination of the LHCII and/or PSII, was almost removed (data not shown). The chlorophyll a/b ratio was estimated to be 5.1, which is consistent with the reported value of 4.4−5.1 (*3*, *6*).

Purification of LHCI from Δpsa B Cells. The LHCI is synthesized normally and stably accumulated in the absence of the PSI core complexes (*10*). The *C. reinhardtii* LHCI consists of several distinctive polypeptides (*3*, *11*), and as shown in Figure 1, all of the LHCI polypeptides detected in the present study are associated with the PSI complex. We compared the polypeptide compositions of the wild-type PSI−LHCI supercomplex and the LHCI from the PSI-deficient mutant Δ*psaB* (*19*). Thylakoids from Δ*psaB* cells were solubilized under the same conditions as wild-type thylakoids and were separated by sucrose density gradient

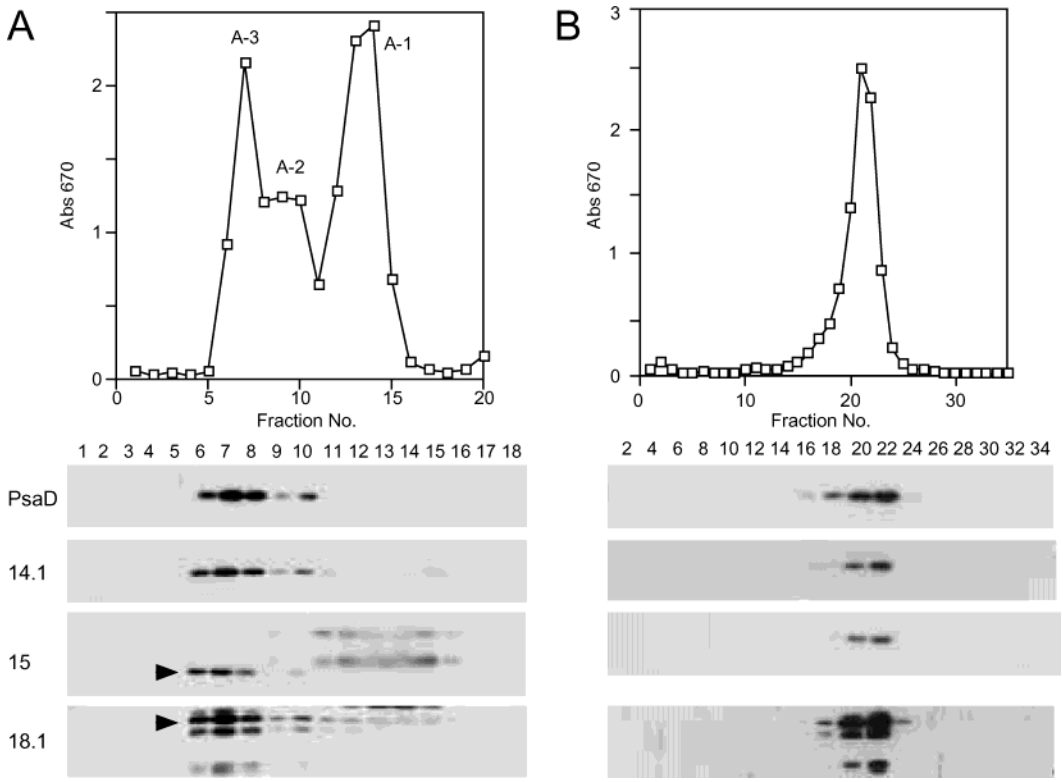

FIGURE 1: Purification of the PSI−LHCI supercomplex from wild-type cells. Thylakoids purified from wild-type cells (0.8 mg chl/mL) were solubilized with 0.8% DM and subsequently separated by sucrose density gradient centrifugation (A). The gradient was collected from the bottom to the top, and the fractionation profile was monitored by an absorption at 670 nm. The resulting fractions were analyzed by Western blotting using antibodies against PsaD and LHCI polypeptides (p14.1, p15, and p18.1). Anti-p15 and anti-p18.1 antibodies cross-reacted against other Lhca polypeptides; arrowheads indicate p15 and p18.1 bands. Fraction A-3, which is enriched in the PSI−LHCI supercomplex, was further purified by DEAE column chromatography (B). The fractions were eluted with a linear gradient of NaCl (25−150 mM) in 50 mM Tris-HCl at pH 8.0 and 0.05% DM, and they were monitored by an absorption at 670 nm. The collected fractions were analyzed by Western blotting using the same antibodies as in A.

centrifugation (Figure 2A). We found two major bands (A-1 and A-2) as well as a shoulder (A-3). Band A-1 contained the LHCII, while A-2 consisted of the PSII core complex. Western blotting using LHCI antibodies indicated that LHCI is present in A-3 (fractions 5−12). Because this mutant lacks PSI, A-3 was detected as a shoulder. The apparent molecular mass of the LHCI on the sucrose density gradient was estimated to be 300−400 kDa, indicating that the LHCI polypeptides form a large complex even in the absence of PSI. Of great interest is that the majority of the p14.1 (Lhca3) polypeptide was separated at a slightly higher position than the LHCII (fraction 16). Other LHCI polypeptides were not detected in this fraction. This indicates that most of the p14.1 polypeptide was present as a monomer in the thylakoids or was easily dissociated from the oligomeric form of LHCI during solubilization and purification. Whether this polypeptide still binds pigments is unknown.

Because A-3 was still contaminated by other polypeptides, we subjected this fraction to DEAE column chromatography to further purify the LHCI. The LHCII separated into fractions 2−16, which contained low concentrations of NaCl, and a small amount of LHCI eluted into factions 8−18 (Figure 2B). The main portion of LHCI eluted at approximately 100 mM NaCl (fractions 24−30). In these fractions, Lhca3 remaining in the LHCI-enriched fraction copurified with other LHCI polypeptides. The third peak, eluting at a higher concentration of NaCl, contained the PSII complex. These observations indicate that the DEAE column chromatography effectively removed the contaminating LHCII and PSII complex from the LHCI (Figure 2B). The chlorophyll a/b ratio of the purified LHCI was estimated to be 2.7, which is more similar to the ratio of 2.8 in LHCI-705 than 2.1 in LHCI-680 (*3*).

More severe treatment of the PSI−LHCI supercomplex generates two types of LHCI, LHCI-680 and LHCI-705 (3). However, one main type of LHCI was isolated from the PSI-deficient mutant (Figure 2). Fluorescence emission spectrum measured at 77 K showed a peak at 708 nm and a shoulder at 685 nm, reminiscent of those of LHCI-705 and LHCI-680, respectively (Figure 3). The fluorescence peaking at 708 nm may correspond to a typical emission band from an oligomeric form of LHCI, and the fluorescence at 685 nm might be derived from a more modified form of LHCI (*3*). This suggests that, during the purification process, there is a small modification to the structural integrity of the purified LHCI.

We next compared the polypeptide profile of the PSI−LHCI and LHCI preparations. The left panel in Figure 4 shows the polypeptides separated on the SDS−polyacrylamide gel, which has an improved resolution in the 20−30-kDa range (*15*, *16*). In addition to PsaD and PsaF in the PSI−LHCI supercomplex, this gel resolved at least seven polypeptide bands (a−g). Band e appeared as a diffuse band migrating above f, and re-electrophoresis of the excised gel containing bands e and f clearly showed two distinct bands. These bands from a to g are assigned as Lhca4 (p14), Lhca6 (p18.1), Lhca3 (p14.1), Lhca5 (p15.1), Lhca7 (p15), Lhca8 (p18), and Lhca1 (p22.1), respectively (Table 1) (*20*).

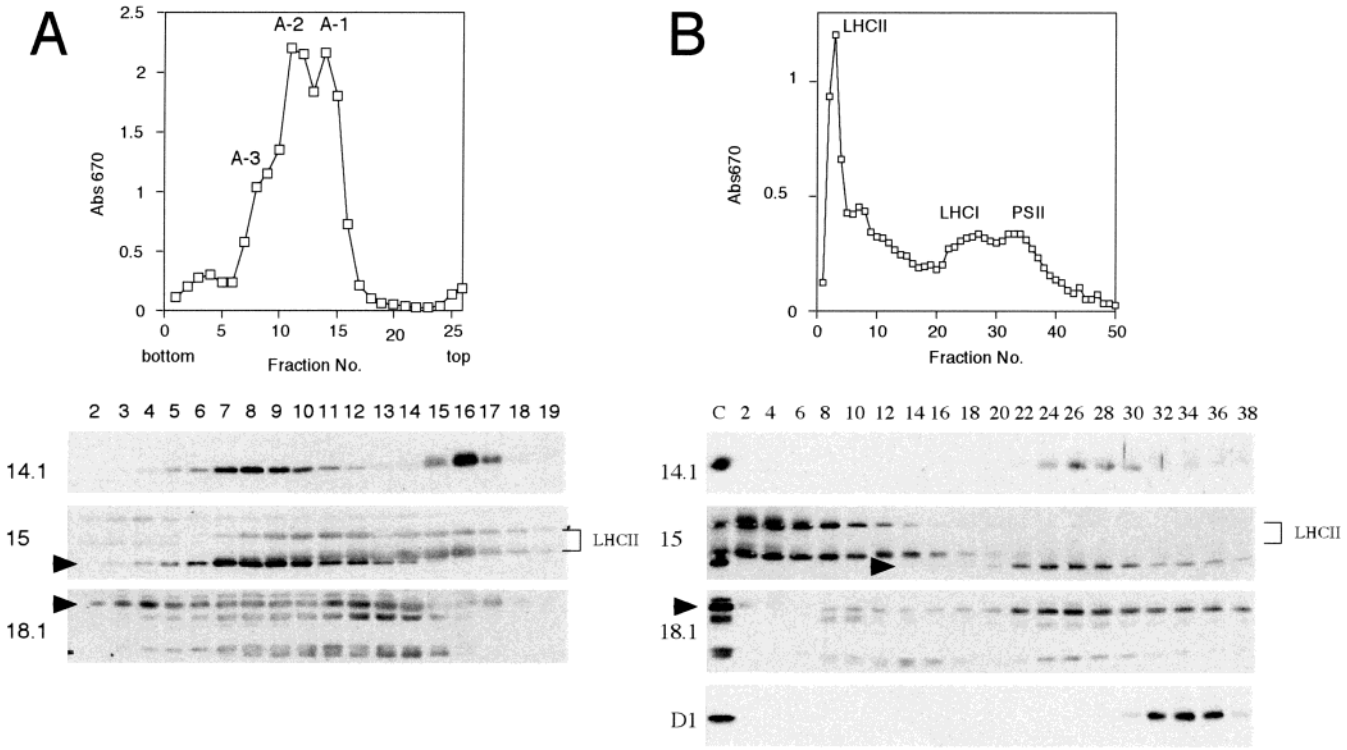

FIGURE 2: Separation of the LHCI from Δ*psaB* cells. Thylakoids purified from the Δ*psaB* cells (0.8 mg chl/mL) were solubilized with 0.8% DM and subsequently separated by sucrose density gradient centrifugation as described in Figure 1A. The gradient was collected from the bottom to the top, and the fractionation profile was monitored by an absorption at 670 nm. The resulting fractions were analyzed by Western blotting using antibodies against PsaD and LHCI polypeptides (p14.1, p15, and p18.1). Anti-p15 and anti-p18.1 antibodies cross-reacted against other Lhca polypeptides; arrowheads indicate p15 and p18.1 bands (A). Fraction A-3, which is enriched in LHCI, was further purified by DEAE column chromatography (B). The fractions were eluted with a linear gradient of NaCl concentration (25−175 mM) in 50 mM Tris-HCl at pH 8.0 and 0.05% DM, and they were monitored by an absorption at 670 nm. The collected fractions were analyzed by Western blotting using the same antibodies as in A.

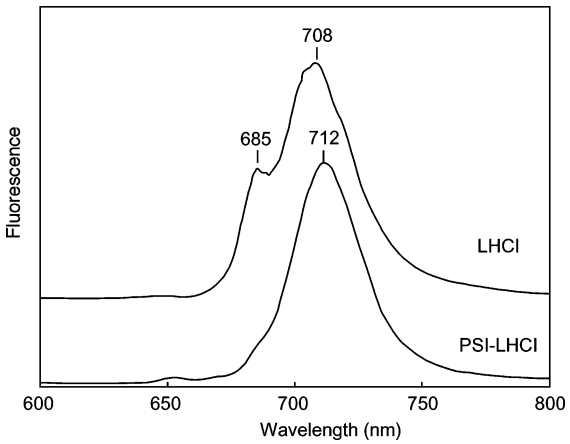

FIGURE 3: Fluorescence emission spectra of the PSI−LHCI supercomplex and LHCI at 77 K. These complexes were purified as described in Figures 1B and 2B, suspended in 50 mM Tris-HCl at pH 8.0 and 0.05% DM, and excited with an actinic light at 430 nm.

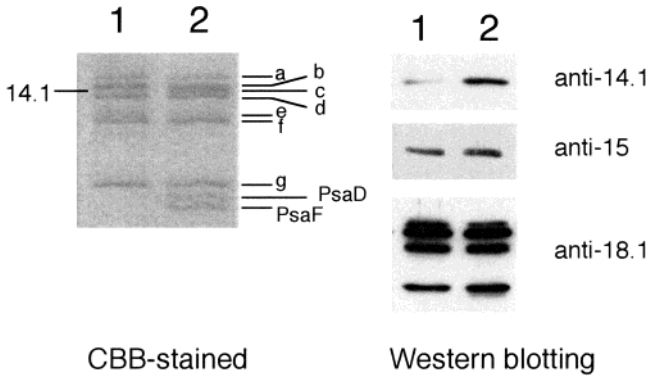

FIGURE 4: Comparison of the polypeptide profiles from wild-type and Δ*psaB* mutant strains. The purified LHCI from Δ*psaB* mutant cells (1) and the PSI−LHCI supercomplex from wild-type cells (2) are shown. Although seven distinctive Lhca polypeptides (a−g) were observed in the PSI−LHCI supercomplex, band c appears to be missing from the LHCI. Western blot analysis revealed that Lhca3 is significantly reduced in the LHCI.

Furthermore, as expected, neither PsaD nor PsaF was detected in LHCI from the Δ*psaB* strain, and band c, corresponding to Lhca3 (p14.1), was deficient or significantly reduced on the gel. This one-dimensional SDS−PAGE did not reveal any other differences between these two preparations. This was confirmed by the fact that Western blotting showed that p15 and p18.1, as well as several anti-p18.1 cross-reacting bands, which may correspond to bands a−f, were at essentially equal levels in the PSI−LHCI and LHCI preparations. However, as expected from the results in Figure 2, the amount of Lhca3 was significantly reduced in the LHCI but fully present in the PSI−LHCI supercomplex.

To determine in more detail which Lhca polypeptides are tightly associated with the PSI−LHCI supercomplex, we separated the polypeptides by 2DE and stained the gel with silver (Figure 5). To identify the Lhca polypeptides that do not copurify with the complex in the absence of PSI, the polypeptides of the LHCI isolated from Δ*psaB* were independently separated by 2DE, and the protein map was compared to the protein map from the PSI−LHCI supercomplex. Recent investigations of detergent-solubilized PSI−

Table 1: Genes of LHCI Polypeptides in *C. reinhardtii*

gene	protein	band on the gel
Lhca1	p22.1	g
Lhca2	p19	minor polypeptide
Lhca3	p14.1	c
Lhca4	p14	a
Lhca5	P15.1	d
Lhca6	p18.1	b
Lhca7	p15	e
Lhca8	p18	f
Lhca9	p22.2	minor polypeptide

LHCI supercomplex using 2DE coupled to Western blotting and MS/MS analysis (*11*, *17*) have identified the Lhca polypeptides present in individual 2DE spots and have shown that 2DE coordinates are reliable parameters for assigning protein identity. We therefore used these detailed 2DE maps for our current studies. In some cases, the identity of proteins in 2DE spots was confirmed by MS/MS analysis of tryptic peptides coupled with database searching (Table 2). In all cases, these results in Figure 5 confirmed previous analyses (*11*, *17*).

Comparison of the 2DE maps from PSI−LHCI and LHCI revealed that protein spots containing Lhca1 (p22.1; spots 2 and 29), Lhca7 (p15; spots 3, 4, 6−8, and 26), and Lhca8 (p18; spots 25 and 31) are enriched in the LHCI (Figure 5). In particular, spot 2, which is primarily composed of Lhca1 (p22.1), is the most intensely stained spot among the LHCI polypeptides on the 2DE gel. Spots 25 and 26, which are composed of only Lhca7 (p15) and Lhca8 (p18), respectively, are also enriched in the 2DE gel of the LHCI. In contrast to the spots containing the Lhca1, Lhca7, and Lhca8 proteins, the spots containing Lhca2 (p19; spot 8) and Lhca9 (p22.2; spot 1) are less intensely stained on the 2DE gel of the purified LHCI compared to those of the PSI−LHCI supercomplex. Spot 1, which is composed of only Lhca2-like polypeptide (p22.2), and spot 8, which is primarily composed of Lhca2 (p19), are present on the 2DE map of the Δ*psaB* thylakoids (see open circles in Figure 5a) and on the 2DE map of the PSI−LHCI supercomplex but not on the 2DE map of the LHCI (Figure 5). This indicates that these proteins are present in the thylakoid membrane but do not associate stably with the LHCI in the absence of PSI.

Spot 34 was detected on the 2DE gel of the PSI−LHCI supercomplex but not on the 2DE gel of the LHCI. The MS/MS analysis indicates that this spot corresponds to the α subunit of cytochrome b_{559}. Although the PSI−LHCI supercomplex is highly purified by sucrose gradient centrifugation and DEAE chromatography, the presence of other thylakoid-membrane proteins in this fraction is not completely excluded. The presence of this PSII−RC polypeptide with the PSI−LHCI supercomplex is thus probably an artifact of the purification procedure.

The protein spots containing Lhca5 (p15.1; spots 6−10), Lhca6 (p18.1; spots 7 and 9−11), and Lhca4 (p14; spots 7 and 33) are, for the most part, less intensely stained on the 2DE gel of the LHCI, although p14 (spot 33) may be slightly enriched in the LHCI. These Lhca polypeptides constitute minor components of the purified LHCI. In addition, Lhca3 (p14.1) is less abundant in the LHCI than in the PSI−LHCI supercomplex when the spot volumes were analyzed by Phoretix 2D software. This agrees with the immunoblots and the SDS−PAGE analyses (Figure 3).

Interestingly, a new protein spot appears on the 2DE gel of the purified LHCI (Figure 5). This 2DE spot is induced in thylakoids isolated from *C. reinhardtii* grown in iron-deficient media and was identified as an Lhca protein by Western blotting (*21*). Analysis of this 2DE spot with MS/MS suggests that this polypeptide is an N-terminal-processed form of Lhca3 (Stauber, E. J. and Hippler, M., unpublished). This is not surprising because Lhca3 is expected to be more susceptible to proteolytic degradation in the absence of PSI.

DISCUSSION

In the present paper, we used sucrose density gradient centrifugation and DEAE column chromatography to purify the PSI−LHCI supercomplex from wild-type *C. reinhardtii* and the LHCI the PSI-deficient *C. reinhardtii* mutant Δ*psaB*, and we compared the polypeptide composition of the two complexes. Relatively strong solubilization treatments are required for dissociation of LHCI from wild-type cells because of the tight association between the PSI core and LHCI. As a result, two types of LHCI, LHCI-680 and LHCI-705, are separated from wild-type *C. reinhardtii* (*3*). Although these LHCI subfractions emitted different low-temperature fluorescence emission maxima, the polypeptide composition was not distinguishable. Because the LHCI is synthesized normally in the PSI-deficient Δ*psaB* cells (*10*) but is not associated with the PSI complexes, it was easily purified under mild conditions. In addition, only one main type of LHCI was isolated from the mutant cells, probably as a result of these mild conditions, and we suggest that the two types of LHCI isolated in the former study correspond to different aggregation states caused by the detergent treatment (*3*). Thus, it appears that the LHCI isolated from the Δ*psaB* mutant maintains its structural and functional features to a higher extent than the complex isolated from the wild-type cells. Finally, on the basis of the apparent molecular mass of the LHCI on sucrose density gradients, we can conclude that the core of the LHCI from *C. reinhardtii* forms a stable multiprotein complex that is different from the apparent dimeric structures of LHCI from vascular plants.

The comparative analyses of the polypeptide composition of the PSI−LHCI supercomplex and the LHCI provided for us some new insight into the subunit structure of LHCI in *C. reinhardtii*. Western blotting of fractions from sucrose density gradients and DEAE column chromatography revealed that almost all of the Lhca polypeptides copurified with PSI polypeptides. The one-dimensional SDS−PAGE system optimized for separation of Lhca polypeptides resolved seven distinct polypeptides (corresponding to a−g) from the PSI−LHCI supercomplex (Figure 4). In addition, the 2DE system showed highly detailed polypeptide profiles of Lhca polypeptides as reported previously (*11*, *17*). The immunochemical results showed that most of Lhca3 (p14.1) dissociated from the oligomeric LHCI from Δ*psaB* cells, although this polypeptide was tightly associated with the PSI−LHCI supercomplex. Thus, the purified LHCI from the mutant contained a significantly reduced amount of Lhca3 (p14.1) (Figure 3). The 2D protein maps of the PSI−LHCI supercomplex and the LHCI indicated that, in the LHCI compared to the PSI−LHCI supercomplex, Lhca1 (p22.1), Lhca7 (p15), and Lhca8 (p18) are enriched, whereas Lhca2 (p19), Lhca3 (p14.1), and Lhca9 (p22.2) are diminished. This

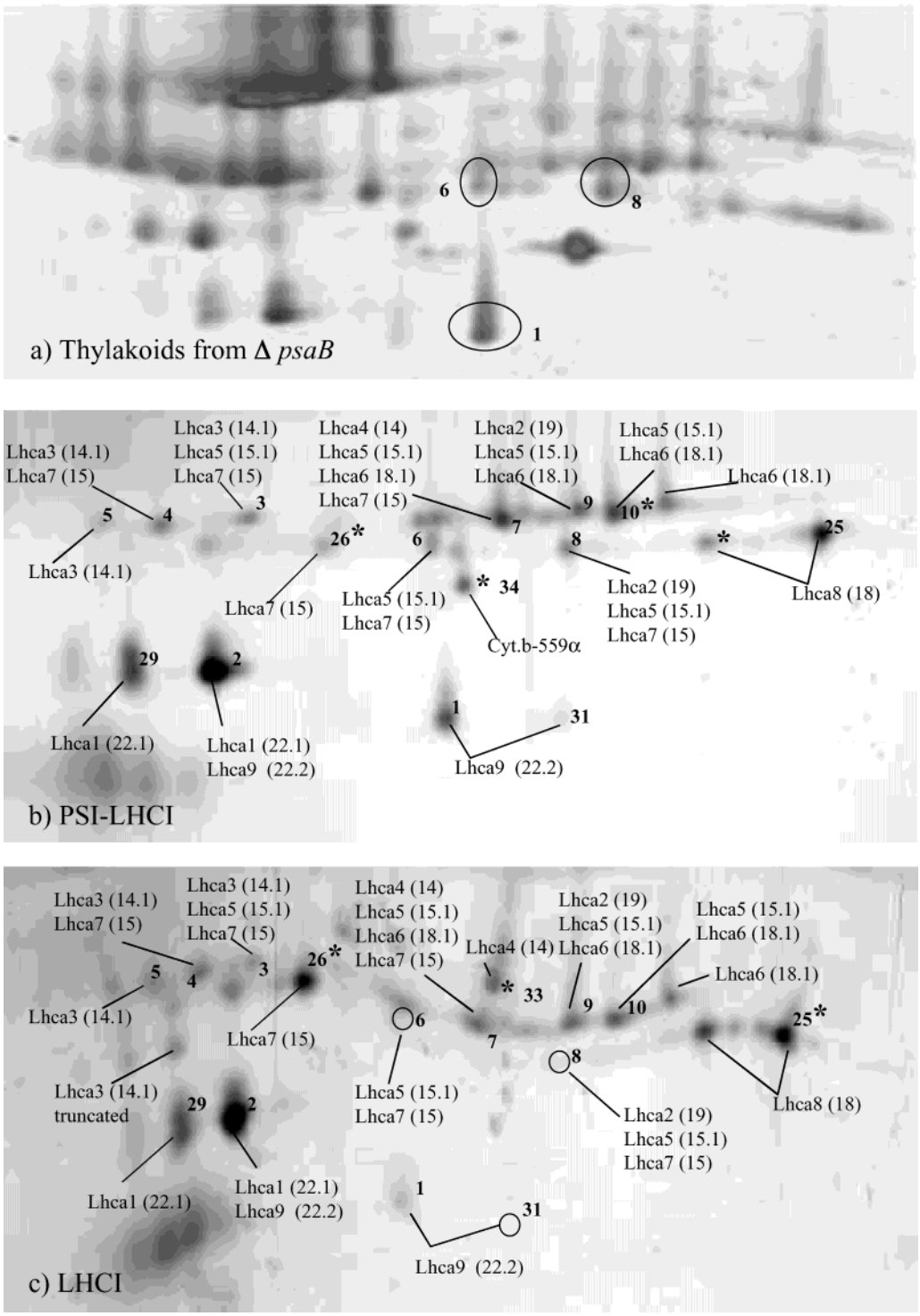

FIGURE 5: 2DE analysis of Lhca polypeptides. The thylakoids proteins from Δ*psaB* cells (a), PSI−LHCI supercomplex from wild-type cells (b), and LHCI from Δ*psaB* cells (c) were visualized by silver staining. The identity of the protein spots and labeling of Lhca polypeptides was inferred from the previous 2DE analysis of PSI particles or MS/MS analysis of thylakoids (*11*). Spots that were reanalyzed by MS/MS are indicated with an asterisk. Open circles in panel c show polypeptide spots that are lacking in the LHCI for the Δ*psaB* mutant but are present in the PSI−LHCI supercomplex for wild-type cells. Analysis of spot volumes from LHCI and PSI−LHCI maps resulted in the following ratios for PSI−LHCI/LHCI spots: 1:10.5, 2:0.85, 3:3.6, 4:2.3, 8:8.3, 9:0.9, 25:0.6, 26:0.2, and 29:0.8. Analysis of the spots was done using Phoretix 2D version 2004 (Build 1440.1) software using automatic spot picking and default values.

suggests that a majority of the Lhca2 (p19), Lhca3 (p14.1), and Lhca9 (p22.2) polypeptides in the thylakoids are weakly associated with the oligomeric LHCI or remain as a monomer. In either case, the presence of the PSI core complex is required for the stable binding of these three polypeptides to the LHCI. In addition, we propose that Lhca polypeptides, Lhca1 (p22.1), Lhca7 (p15), and Lhca8 (p18), together with the minor polypeptides, Lhca4 (p14) and Lhca6 (p18.1), form a stable multiprotein complex independent of the assembly of the PSI core complex in the thylakoid membrane.

The three-dimensional structure of the PSI−LHCI supercomplex from green plants has been recently examined by electron microscopy. This analysis indicates that, in contrast

Table 2: MS/MS Data for Selected Silver-Stained Spots[a]

complex	spot	protein	peptide	position	z	ΔM	X_{corr}
LHCI	25	Lhca8	YATGAGPVDNLAAHLK	211−226	2	0.7	4.21
		Lhca8	WYQQAELIHC[+57]R	68−78	2	1.0	3.39
		Lhca8	AGALNVPEWYDAGK	96−109	2	0.8	2.79
	26	Lhca7	NPGSQADGSFLGFtEEFK	141−158	2	1.1	5.52
		Lhca7	FFDPMGLSR	169−171	2	1.0	3.11
	33	Lhca4	WYAQAELMNAR	95−105	2	1.4	2.99
PSI−LHCI	10	Lhca5	NFGSVNEDPIFK	142−253	2	0.3	4.09
		Lhca5	LWAPGVVAPEYLK	34−46	2	−1.7	3.30
	25	Lhca8	TAMAGVAGILIPGLLTK	79−95	2	−0.2	3.24
		Lhca8	GTSELGYPGGPFDPLGLSK	162−180	2	0.8	3.18
		Lhca8	WYQQAELIHC[+57]R	68−78	2	−0.3	2.55
	26	Lhca7	VGLGFPEWYDAGK	95−107	2	−0.4	3.26
	34	Cytb559	PFSDILTSIR	8−17	2	1.0	3.59
		Cytb559	FNALEQVK	70−77	1	0.6	1.64

[a] The charge state (z) of the measured ion, as well as the calculated deviation (ΔM) of the experimentally determined mass from the theoretical average mass of the peptide, is given. The position of the peptide within the preprotein sequence is listed. Carbamidomethylation of cysteine (57 Da) residues is indicated where necessary. The cross-correlation factor (X_{corr}) calculated by the Sequest algorithm is listed in the far right column. All peptide sequences reported produced cross-correlation factors equal to or above 1.5, 2.25, or 3.5 for single-, double-, and triple-charged precursor ions, respectively.

to the trimeric form of the PSI core complex in cyanobacteria, the PSI−LHCI supercomplex of green plants is a monomer and that LHCI complexes consisting of 8−14 Lhca polypeptides form a half-ring structure that binds to one side of the PSI core complex (*6*, *7*). It appears that the oligomeric structure of the LHCI is located close to PsaK, PsaJ, PsaF, and PsaG, which possess one or more transmembrane helices, but is not close to PsaL, which is required for trimerization of the PSI core complex in cyanobacteria (*22*). Indeed, in agreement with the proposed structural model, interactions between PsaK and the LHCI as well as between PsaK/PsaG and the LHCI have been reported (*23*, *24*). However, how distinct Lhca polypeptides are organized into the oligomeric form of the LHCI is not currently clear. The proposed model also suggests that eight Lhca polypeptides form four dimers, while three additional Lhca polypeptides are monomers in the oligomeric LHCI structure (*7*). This heterogeneous localization of the Lhca polypeptides suggests different functions of each Lhca polypeptide in the oligomeric LHCI.

Recent determination of the crystal structure of the PSI−LHCI supercomplex from a higher plant has revealed that the LHCI of 150 kDa consists of only four Lhca polypeptides (*9*). In contrast, the LHCI from *C. reinhardtii* consists of seven major Lhca polypeptides, and its size was estimated to be 300−400 kDa. In fact, the particle size of the PSI−LHCI supercomplex from *C. reinhardtii* estimated by electron microscopy and image analysis is significantly larger than that of a higher plant (*6*).

Although the LHCI purified from Δ*psaB* cells forms an oligomeric structure, it is not known whether it retains the half-ring structure in the absence of the PSI core complex. The remarkable decrease in Lhca2, Lhca3, and Lhca9 in the purified LHCI indicates that there is no significant involvement of these three polypeptides in the oligomerization of the other Lhca polypeptides. This suggests that these three Lhca polypeptides might be located in an interface between the oligomeric structure of the LHCI and the PSI core complex and that their association with the LHCI is stabilized by the presence of the PSI core complex. This intimate structural interaction between these Lhca polypeptides and the PSI core complex may suggest a functional role in the transfer of light energy absorbed by the LHCI to the PSI core complex. Lhca3 (p14.1) and Lhca1 (p22.1) are relatively well-conserved in *C. reinhardtii* and higher plants and are classified as type III and type I proteins, respectively, according to phylogenic analyses (*25*). These two polypeptides are reminiscent of the minor light-harvesting complexes of PSII, CP24, CP26, and CP29, which are located between the PSII core complex and the major LHCII. These three complexes are involved in excitation energy transfer from the major LHCII to the PSII core complex. Interestingly, except for Lhca1 and Lhca3, the Lhca proteins are rather variable among green algae and higher plants. Together, Lhca3, as well as Lhca2, Lhca9, and probably Lhca1, could be directly bound to the PSI core complex and thus could participate in transferring excitation energy from a more peripheral LHCI consisting of Lhca4, Lhca5, Lhca6, Lhca7, and Lhca8 to the PSI core complex.

In conclusion, our results support the concept that, for the PSI−LHCI supercomplex of *C. reinhardtii*, the PSI complex and LHCI first assemble independently and then integrate into the thylakoid membrane (*26*). The integration of the two complexes appears to allow the stable association of the Lhca2, Lhca3, and Lhca9 polypeptides to the LHCI. In addition, the biochemical properties suggest that the LHCI of *C. reinhardtii* is approximately two times larger than that of a higher plant.

ACKNOWLEDGMENT

Antibodies raised against D1 and PSI polypeptides were kindly provided by Drs. M. Ikeuchi (University of Tokyo) and J.-D. Rochaix (University of Geneva), respectively. The *psaB*-deficient mutant strain was kindly provided by Dr. K. Redding (University of Alabama).

REFERENCES

1. Mullet, J. E., Burke, J. J., and Arntzen, C. J. (1980) Chlorophyll proteins of photosystem I, *Plant Physiol. 65*, 814−822.
2. Eshaghi, S., Andersson, B., and Barber, J. (1999) Isolation of a highly active PSII−LHCII supercomplex from thylakoid membranes by a direct method, *FEBS Lett. 446*, 23−26.
3. Bassi, R., Soen, S. Y., Frank, G., Zuber, H., and Rochaix, J. D. (1992) Characterization of chlorophyll a/b proteins of photosystem I from *Chlamydomonas reinhardtii*, *J. Biol. Chem. 267*, 25714−25721.

4. Lam, E., Ortiz, W., and Malkin, R. (1984) Chlorophyll a/b proteins of Photosystem I, *FEBS Lett. 168*, 10−14.
5. Boekema, E. J., Jensen, P. E., Schlodder, E., van Breemen, J. F., van Roon, H., Scheller, H. V., and Dekker, J. P. (2001) Green plant photosystem I binds light-harvesting complex I on one side of the complex, *Biochemistry 40*, 1029−1036.
6. Germano, M., Yakushevska, A. E., Keegstra, W., van Gorkom, H. J., Dekker, J. P., and Boekema, E. J. (2002) Supramolecular organization of photosystem I and light-harvesting complex I in *Chlamydomonas reinhardtii*, *FEBS Lett. 525*, 121−125.
7. Kargul, J., Nield, J., and Barber, J. (2003) Three-dimensional reconstruction of a light-harvesting complex I−photosystem I (LHCI−PSI) supercomplex from the green alga *Chlamydomonas reinhardtii*. Insights into light harvesting for PSI, *J. Biol. Chem. 278*, 16135−16141.
8. Castelletti, S., Morosinotto, T., Robert, B., Caffarri, S., Bassi, R., and Croce, R. (2003) Recombinant Lhca2 and Lhca3 subunits of the photosystem I antenna system, *Biochemistry 42*, 4226−4234.
9. Ben-Shem, A., Frolow, F., and Nelson, N. (2003) Crystal structure of plant photosystem I, *Nature 426*, 630−635.
10. Wollman, F. A., and Bennoun, P. (1982) A new chlorophyll−protein complex related to photosystem I in *Chlamydomonas reinhardtii*, *Biochim. Biophys. Acta 680*, 352−360.
11. Stauber, E. J., Fink, A., Markert, C., Kruse, O., Johanningmeier, U., and Hippler, M. (2003) Proteomics of *Chlamydomonas reinhardtii* Light-Harvesting Proteins, *Eukaryotic Cell 2*, 978−994.
12. Chua, N.-H., and Bennoun, P. (1975) Thylakoid Membrane Polypeptides of *Chlamydomonas reinhardtii*: Wild-Type and Mutant Strains Deficient in Photosystem II Reaction Center, *Proc. Natl. Acad. Soc. U.S.A. 72*, 2175−2179.
13. Takahashi, Y., Matsumoto, H., Goldschmidt-Clermont, M., and Rochaix, J. D. (1994) Directed disruption of the *Chlamydomonas* chloroplast psbK gene destabilizes the photosystem II reaction center complex, *Plant Mol. Biol. 24*, 779−788.
14. Porra, R. J., Thompson, W. A., and Kriedemann, P. E. (1989) Determination of accurate extinction coefficients and simultaneous equations for assaying chlorophylls a and b extracted with four different solvents: verification of the cocentration of chlorophyll standards by atomic absorption spectroscopy, *Biochim. Biophys. Acta 975*, 384−394.
15. Takahashi, Y., Goldschmidt-Clermont, M., Soen, S. Y., Franén, L. G., and Rochaix, J.-D. (1991) Directed chloroplast transformation in *Chlamydomonas reinhardtii*: insertional inactivation of the *psaC* gene encoding the iron sulfur protein destabilizes photosystem I, *EMBO J. 10*, 2033−2040.
16. Fling, S. P., and Gregerson, D. S. (1986) Peptide and protein molecular weight determination by electrophoresis using a high-molarity Tris buffer system without urea, *Anal Biochem. 155*, 83−88.
17. Hippler, M., Klein, J., Fink, A., Allinger, T., and Hoerth, P. (2001) Towards functional proteomics of membrane protein complexes: analysis of thylakoid membranes from *Chlamydomonas reinhardtii*, *Plant J. 28*, 595−606.
18. Sugimoto, I., and Takahashi, Y. (2003) Evidence that the PsbK polypeptide is associated with the photosystem II core antenna complex CP43, *J. Biol. Chem. 278*, 45004−45010.
19. Redding, K., MacMillan, F., Leibl, W., Brettel, K., Hanley, J., Rutherford, A. W., Breton, J., and Rochaix, J. D. (1998) A systematic survey of conserved histidines in the core subunits of Photosystem I by site-directed mutagenesis reveals the likely axial ligands of P700, *EMBO J. 17*, 50−60.
20. Tokutsu, R., Teramoto, H., Takahashi, Y., Ono, T. A., and Minagawa, J. (2004) The Light-Harvesting Complex of Photosystem I in *Chlamydomonas reinhardtii*: Protein Composition, Gene Structures and Phylogenic Implications, *Plant Cell Physiol. 45*, 138−145.
21. Moseley, J. L., Allinger, T., Herzog, S., Hoerth, P., Wehinger, E., Merchant, S., and Hippler, M. (2002) Adaptation to Fe-deficiency requires remodeling of the photosynthetic apparatus, *EMBO J. 21*, 6709−6720.
22. Zouni, A., Witt, H. T., Kern, J., Fromme, P., Krauss, N., Saenger, W., and Orth, P. (2001) Crystal structure of photosystem II from *Synechococcus elongatus* at 3.8-Å resolution, *Nature 409*, 739−743.
23. Jensen, P. E., Gilpin, M., Knoetzel, J., and Scheller, H. V. (2000) The PSI-K subunit of photosystem I is involved in the interaction between light-harvesting complex I and the photosystem I reaction center core, *J. Biol. Chem. 275*, 24701−24708.
24. Jensen, P. E., Rosgaard, L., Knoetzel, J., and Scheller, H. V. (2002) Photosystem I activity is increased in the absence of the PSI-G subunit, *J. Biol. Chem. 277*, 2798−2803.
25. Teramoto, H., Ono, T., and Minagawa, J. (2001) Identification of Lhcb gene family encoding the light-harvesting chlorophyll-a/b proteins of photosystem II in *Chlamydomonas reinhardtii*, *Plant Cell Physiol. 42*, 849−856.
26. Hippler, M., Rimbault, B., and Takahashi, Y. (2002) Photosynthetic complexc assembly in C*hlamydomonas reinhardtii*, *Protistologica 153*, 197−220.

BI035988Z

Manuscript 3

Stefanie Storf, Einar J. Stauber, Michael Hippler, and Volkmar H.R. Schmid (2004) Proteomic analysis of the photosystem I light-harvesting antenna in tomato (*Lycopersicon esculentum*). **Biochemistry** 43, 9214-9224.

Proteomic Analysis of the Photosystem I Light-Harvesting Antenna in Tomato (*Lycopersicon esculentum*)†

Stefanie Storf,‡ Einar J. Stauber,§ Michael Hippler,*,|| and Volkmar H. R. Schmid*,‡

Department of Biology, University of Pennsylvania, Philadelphia, Pennsylvania 19104, Institut für Allgemeine Botanik, Johannes Gutenberg-Universität Mainz, Müllerweg 6, 55099 Mainz, Germany, and Lehrstuhl für Pflanzenphysiologie, Friedrich Schiller-Universität Jena, Dornburger Strasse 159, 07743 Jena, Germany

Received January 25, 2004; Revised Manuscript Received May 17, 2004

ABSTRACT: Until now, more genes of the light-harvesting antenna of higher-plant photosystem I (PSI) than proteins have been described. To improve our understanding of the composition of light-harvesting complex I (LHCI) of tomato (*Lycopersicon esculentum*), we combined one- and two-dimensional (1-D and 2-D, respectively) gel electrophoresis with immunoblotting and tandem mass spectrometry (MS/MS). Separation of PSI with high-resolution 1-D gels allowed separation of five bands attributed to proteins of LHCI. Immunoblotting with monospecific antibodies and MS/MS analysis enabled the correct assignment of the four prominent bands to light-harvesting proteins Lhca1−4. The fifth band was recognized by only the Lhca1 antibody. Immunodetection as well as mass spectrometric analysis revealed that these protein bands contain not only the eponymous protein but also other Lhca proteins, indicating a heterogeneous protein composition of Lhca bands. Additionally, highly sensitive MS/MS allowed detection of a second Lhca4 isoform and of Lhca5. These proteins had not been described before on the protein level in higher plants. Two-dimensional gel electrophoresis revealed an even more diverse composition of individual Lhca proteins than was apparent from 1-D gels. For each of the four prominent Lhca proteins, four to five isoforms with different isoelectric points could be identified. In the case of Lhca1, Lhca4, and Lhca3, additional isoforms with slightly differing molecular masses were identified. Thus, we were able to detect four to ten isoforms of each individual Lhca protein in PSI. Reasons for the origin of Lhca heterogeneity are discussed. The observed variety of Lhca proteins and their isoforms is of particular interest in the context of the recently published crystal structure of photosystem I from pea, which showed the presence of only four Lhca proteins per photosystem I. These findings indicate that several populations of photosystem I that differ in their Lhca composition may exist.

The two photosystems (PS)[1] of the photosynthetic apparatus of higher plants carry out the reactions that are responsible for the conversion of solar radiation into chemically fixed energy. In both PS, a central core complex is surrounded by a light-harvesting antenna, which is composed of several light-harvesting complexes (LHCs). The main function of LHCs is collection of solar radiation and transfer of exitation energy to the central core, thereby enlarging the absorption cross section of the PS. This in turn leads to a concomitant increase in photosynthetic performance. In addition, the LHCs can also function in attenuation of the excitation energy transmitted to the core complexes of the PS under high-light conditions. This can be achieved either by translocation of a subpopulation of LHCII from PSII to PSI (*1*) or by dissipation of excess excitation energy via zeaxanthin formed in the xanthophyll cycle (*2*, *3*).

The light-harvesting antenna of PSII is composed of six different apoproteins arranged in four LHCs: LHCII (Lhcb1−3), CP29 (Lhcb4), CP26 (Lhcb5), and CP24 (Lhcb6) (*4*, *5*). Until now, most biochemical analyses of PSI in various plants have identifed four different LHCI proteins (Lhca1−4) with molecular masses determined to be between 20 and 25 kDa by fully denaturing gel electrophoresis (*6*). By gentle separation of mildly solubilized PSI, two different subfractions of LHCI, named LHCI-680 and LHCI-730 (*7*), could be identified. LHCI-730 is composed of Lhca1 and Lhca4 (*7*, *8*) and exists in a heterodimeric state (*9*, *10*). The nature of the oligomerization behavior of Lhca2 and Lhca3 that form LHCI-680 is not clear yet. It has been reported that they also form dimers (*11*). Considering that Lhca2 comigrates (*12*, *13*) and coelutes (*14*) with the LHCI-730 proteins Lhca1 and Lhca4 and that a chemical cross-linking study supports a dimeric state for Lhca2 and Lhca3 (*9*), a homodimeric state of the LHCI-680 proteins is the most probable scenario. However, until now, reconstitution experiments with Lhca2 and Lhca3 have failed to produce dimers of Lhca2 and/or Lhca3 (*15*, *16*). For a long period, it was

† This project was supported by Grant "Nachwuchsgruppe Pflanzenphysiologie" from the federal state of Thüringen (to M.H.) and Grants Schm 1203/2-3 and 1203/2-4 (to V.H.R.S.) from the Deutsche Forschungsgemeinschaft.

* To whom correspondence should be addressed. M.H.: phone, 001-215-898-4974; fax, 001-215-898-8780; e-mail, mhippler@sas.upenn.edu. V.H.R.S.: phone, 0049-6131-3924203; fax, 0049-6131-3923787; e-mail, vschmid@mail.uni-mainz.de.

|| University of Pennsylvania.

‡ Johannes Gutenberg-Universität Mainz.

§ Friedrich Schiller-Universität Jena.

[1] Abbreviations: 1-D and 2-D, one- and two-dimensional protein separation, respectively; Lhca, apoprotein of a light-harvesting complex of photosystem I; *lhca*, gene encoding Lhca; LHC, light-harvesting complex; MS/MS, tandem mass spectrometry; PS, photosystem.

10.1021/bi0498196 CCC: $27.50
Published on Web 06/26/2004

assumed that six to eight Lhca proteins (two copies of each protein) surround the core of PSI (*17*, *18*). However, the recently published 4.4 Å crystal structure of PSI from pea revealed the presence of only four Lhca proteins per PSI (*19*).

Because of the pioneering work that has been done to identify genes encoding LHCI proteins in tomato (*Lycopersicon esculentum*), it can be considered a model plant for studying LHCI protein composition (*20*). Moreover, more than 155 000 EST entries available through The Institute For Genomic Research (TIGR) website (http://www.tigr.org/tdb/tgi/lgi) provide an extensive resource of nucleotide sequence information for investigations of tomato LHC proteins. Furthermore, the adequacy of ESTs for the investigation of LHCI genes and proteins was demonstrated by previous studies in which the complete nucleotide sequence for six *lhca* genes in *Arabidopsis thaliana* (*21*) and nine *Chlamydomonas reinhardtii* Lhca proteins (*22*) was fully documented by EST information. The first two *lhca* genes (*cab6a* and *cab6b*) which were identified in tomato encode two Lhca1 proteins that have a molecular mass of ~ 22 kDa (*23*, *24*). In the years following this discovery, genes which encode Lhca2 (~23 kDa; cab7; *25*), Lhca3 (~25 kDa; cab8; *26*), and Lhca4 (~22 kDa; cab11 and cab12; *27*) were identified in tomato. In *A. thaliana*, two new genes (*lhca5* and *lhca6*) that encode additional putative LHCI proteins have been identified by database analysis (*21*). However, the corresponding proteins have not yet been detected in higher plants. The Lhca5 gene product is the most similar to Lhca4 when the sequences of putative transmembrane helices are compared. In contrast, the Lhca6 gene product is highly homologous to Lhca2 and can therefore be presumably considered to be an additional Lhca2 isoform. The failure to detect these gene products on the protein level in higher plants until now may have been a consequence of their low expression level (*21*). The inability to detect proteins encoded by *cab6b* (*24*) and *cab12* (*27*) from tomato for a long period may also be explained this way. Only recently, refined analytical procedures have allowed further dissection of the PSI light-harvesting system of tomato. By combining HPLC separation of solubilized PSI with electrospray ionization mass spectrometric (ESI-MS) analyses of eluted proteins, Zolla et al. (*28*) were able to detect gene products of *cab6a* and *cab6b*. In this study, additional Lhca2 proteins could be detected. Another investigation of the tomato LHCI antenna composition using SDS−PAGE with high resolution in the LHCI protein region revealed the presence of a fifth band in the region of LHCI protein bands. The relevant protein(s) copurifies with LHCI-730 (*15*). Due to (i) the availability of monospecific antibodies raised against short sequences of individual Lhca proteins, (ii) the improvement in 2-D gel electrophoresis of transmembrane proteins (*29*), and (iii) proteomic approaches facilitated by the combination of extensive sequence information with tandem mass spectrometry (MS/MS), further dissection of the LHCI antenna of tomato appears to be feasible.

In this study, we applied all of these analytical tools to the LHCI antenna of tomato for the first time. In our first approach, we used high-resolution 1-D gel electrophoresis in combination with immunoblotting using monospecific antibodies against Lhca1−4. Further characterization of the resolved protein bands was achieved by proteolytic digestion of excised bands followed by MS/MS. Subsequently, PSI was separated by 2-D gel electrophoresis with isoelectric focusing (IEF) in the first dimension and SDS−PAGE in the second dimension. Characterization by immunoblotting and MS/MS measurements allowed resolution of various isoforms of Lhca proteins and revealed for the first time the very diverse composition of the PSI light-harvesting system in higher plants.

EXPERIMENTAL PROCEDURES

Isolation of Thylakoids and Photosystem I. Thylakoids were isolated according to the methods described in ref *30* from tomato plants (*L. esculentum*) that were grown in a greenhouse under a 16 h−8 h light−dark regime and at a light intensity of ~120 μmol of photons m^{-2} s^{-1} supplied by fluorescent tubes (L58W/11-860 LumiluxPlusEco, Osram, München, Germany). The PSI holocomplex and LHCI-730 were isolated according to the methods described in ref *15* and stored at −70 °C in 30% (w/v) sucrose, 10 mM Tricine/NaOH (pH 7.8), and 1 mM EDTA/NaOH (pH 7.8) at a chlorophyll (Chl) concentration of 1.5−2 mg/mL. The Chl concentration was determined using acetone as a solvent and the equations of ref *31*.

1-D Gel Electrophoresis. Polyacrylamide gradient gels were used for improved separation of LHCI proteins. The resolving gel contained an acrylamide gradient of 14 to 20% (w/v) and 0.375 M Tris-HCl (pH 8.8). Stacking gels had a uniform acrylamide concentration of 4.5% and contained 0.13 M Tris-HCl (pH 6.8). PSI samples were mixed with 2 volumes of denaturing solution [5% (w/v) LDS, 180 mM DTT, 70 mM Tris-HCl (pH 8.4), and 0.666 M sucrose] followed by incubation at 100 °C for 1 min. Aliquots equivalent to 15 μg of Chl were applied per lane. Electrophoresis was conducted with 2× concentrated Laemmli running buffer [50 mM Tris, 384 mM glycine, and 0.1% (w/v) SDS (*32*)] supplemented with 1 mM EDTA/NaOH (pH 7.8) in a Maxigel electrophoresis unit (Biometra, Göttingen, Germany). Gels were run overnight for at least 18 h at 15 mA per gel. Afterward, proteins were either stained with Coomassie Brilliant Blue or transferred onto nitrocellulose. Analysis of protein phosphorylation was carried out with the Pro-Q diamond phosphoprotein gel stain (Molecular Probes, Leiden, The Netherlands) according to the guidelines of the manufacturer. Stained gels and immunodecorated blots were documented with an Epson GT 7000 flat bed scanner.

2-D Gel Electrophoresis. For IEF separation in the first dimension, proteins were precipitated to remove pigments and lipids according to the methods described in ref *33*. Usually, an aliquot of PSI equivalent to 20 μg of Chl was diluted with distilled water to a final volume of 100 μL. For detection of Lhca2 in 2-D spots by MS/MS, larger aliquots equivalent to 100 μg of Chl had to be used. Protein precipitation, lyophilization, and solubilization were carried out as described in ref *29*. The IEF was performed in an IPGphor apparatus using Immobiline DryStrips (Amersham Pharmacia Biotech, Freiburg, Germany) with a linear pH range of 3−10 or 4−7 following the procedure described in ref *29*. Following IEF, the cysteine residues of the proteins were reduced and carbamidomethylated by incubation in two different equilibration buffers as described in ref *29*.

Afterward, the strips were washed briefly in water, loaded onto the second-dimension SDS gel, and covered with 0.5%

agarose. The second-dimension SDS gels contained 13% polyacrylamide, 0.4% piperazine diacrylamide, 0.357 M Tris-HCl (pH 8.8), and 0.025% (w/v) $Na_2S_2O_3$ and were run in a Bio-Rad (München, Germany) multicell apparatus at 8 °C and 30 mA per gel until the bromophenol blue front reached the end of the gel. Gels were either stained with coomassie or silver or blotted onto nitrocellulose.

Immunoblot Analysis. Western Blot analysis was conducted as described in ref *29* with the following modifications. After electrotransfer, the entire band/spot profile of the membrane was visualized with Ponceau-S which allowed later alignment of immunostained bands with the entire band pattern. The primary antibodies used for detection of Lhca1, Lhca3, and Lhca4 were purchased from AgriSera (Vännäs, Sweden). The Lhca2 antibody was a kind gift of L. A. Staehelin (University of Colorado, Boulder, CO) and is described in ref *34*. The antibodies were used at dilutions of 1:2000 (Lhca1), 1:300 (Lhca2), 1:500 (Lhca3), and 1:1000 (Lhca4). Anti-rabbit IgG conjugates with either horseradish peroxidase or alkaline phosphatase were used as the secondary antibody at a dilution of 1:10000 or 1:2500, respectively. Bound antibodies were detected either by enhanced chemiluminescence with the ECL kit of Amersham or by nitro blue tetrazolium and 5-bromo-4-chloro-3-indolyl phosphate according to the guidelines of the suppliers.

Liquid Chromatography−Mass Spectrometry. Samples for tandem mass spectrometry were prepared by tryptic in-gel hydrolysis of proteins in excised bands/spots essentially as described in ref *35*, with the exception of 2-D spots C−E (from the gel shown in Figure 4), for which the concentration of the trypsin solution was increased to 0.125 μg/μL. In addition, these spots were kept for 1 h on ice with the trypsin solution and were gently agitated using a rotary table shaker. The remainder of the procedure was unchanged. Prior to tryptic digestion, silver-stained protein spots were first destained by incubating the gel piece in a 30 mM $K_3Fe(CN)_6$/100 mM $Na_2S_2O_3$ (1:1, v/v) mixture for 8 min. Double-distilled water and HPLC-grade solvents were used throughout the procedure. The lyophilized samples were stored at −80 °C until analysis was carried out. For MS/MS analysis, the dried samples were diluted in 10 μL of buffer A [0.1% (v/v) formic acid in 5% (v/v) acetonitrile and 95% (v/v) water] and centrifuged for 5 min at 12000*g*. An aliquot of the supernatant (9 μL) was transferred into an autosampling vial. Analyte sampling and chromatography as well as production and acquisition of MS/MS data were performed on-line using fully automated instrumentation as described in ref *22*.

Bioinformatic Data Analysis. Computational analyses of MS/MS data were performed with the Finnigan Sequest/Turbo Sequest software (revision 2.0, ThermoQuest, San Jose, CA) using the parameters described in ref *22*. The databases that were used were as follows: one genomic database containing all tomato DNA sequences found in the NCBI (nr)-nucleotide database, one database containing all tomato LHC protein sequences present in the NCBI (nr)-protein database, and one small EST data bank containing tomato ESTs found by searching the NCBI EST database with the Lhca5 cDNA sequence reported for *A. thaliana* (*21*; GenBank accession number AF134121). The databases were also processed to detect the presence of acetylation (+42 Da for peptide N-termini or lysine residues) and carbamylation (+43 Da for N-termini or arginine or lysine residues) from the MS/MS data from the 2-D gel spots. Cysteine modification by carbamidomethylation (+57 Da) was also attributed. To search for N-terminally processed protein forms, Sequest analyses were performed by choosing the option "no enzyme" for the *in-silico* digestion of a database containing all tomato LHC deduced protein sequences.

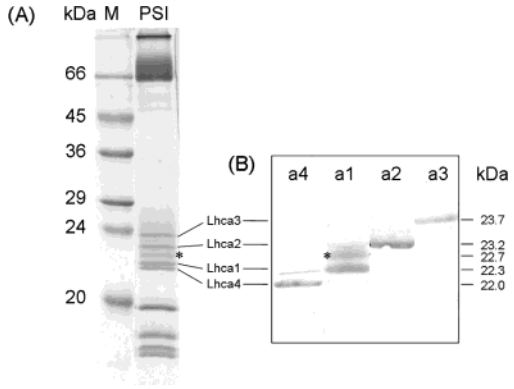

FIGURE 1: Protein composition of the PSI holocomplex of tomato. In panel A, a fully denaturing gel stained with Coomassie Blue is shown. Lhca1−4 bands and a fifth protein band in the LHCI mass range are marked. M represents the molecular mass standard. In panel B, immunoblots of proteins of the PSI holocomplex separated by SDS−PAGE as in panel A are shown. Blots were probed with antibodies against LHCI apoproteins Lhca1 (a1), Lhca2 (a2), Lhca3 (a3), and Lhca4 (a4).

BLAST searches were carried out against the NCBI databases (both genomic and EST) with the net-based blast program available at http://www.ncbi.nlm.nih.gov:80/BLAST using the default values. Alignments of peptide sequences derived from MS/MS data with complete protein sequences and alignment of the amino acid sequences of different Lhca proteins with each other were performed with the net-based align program at the GENESTREAM network server IGH (Montpellier, France, http://www2.igh.cnrs.fr/bin/align-guess.cgi) using the default values. Figure 3 was made on basis of these alignments using the GeneDoc program available at http://www.psc.edu/biomed/genedoc. Translation of cDNA and EST sequences into amino acid sequences and determination of theoretical molecular masses and isoelectric points of the Lhca proteins were carried out with the corresponding net-based tools at http://www.expasy.org/tools/.

RESULTS

Recently, a fifth protein band in the molecular mass range of LHCI proteins was resolved by SDS−PAGE for both the PSI holocomplex and LHCI-730 (*15*). By using long gels with an acrylamide gradient from 14 to 20% in the resolving gel and 2× Laemmli electrophoresis buffer, we could further improve the separation of protein bands in the LHCI region. As shown in Figure 1A, this procedure allowed clear resolution of four intensely stained bands with apparent molecular masses of ∼22.0, ∼22.3, ∼23.2, and ∼23.7 kDa. On the basis of their molecular mass, they were tentatively assigned to Lhca4 (22.0 kDa), Lhca1 (22.3 kDa), Lhca2 (23.2 kDa), and Lhca3 (23.7 kDa). In addition, a less intensely stained fifth band with a molecular mass of ∼22.7 kDa was clearly resolved (marked with an asterisk in Figure 1).

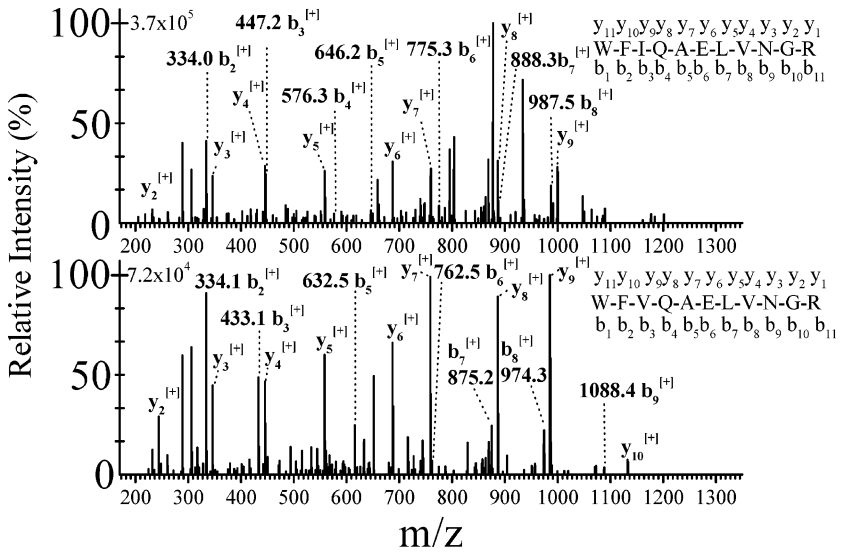

FIGURE 2: MS/MS spectra of tryptic peptide ions at *m*/*z* 666.7 ([2H$^+$]) (top graph) and *m*/*z* 660.2 ([2H$^+$]) (bottom graph) that are characteristic of the two different Lhca4 proteins (cab11 and cab12). The presence of isoleucine (cab11) rather than valine (cab12) at the third position of the peptide is reflected in a mass difference of 13.1 Da between ions of the b-series from the two spectra, beginning with the b_3 ion. Ions of the b-series (containing the N-terminus of the peptide) and y-series (containing the C-terminus of the peptide) are labeled. The amino acid sequences retrieved by the Sequest software are printed beside the corresponding spectra.

To ensure assignment of the protein bands to LHCI apoproteins already described for tomato (Lhca1−4), immunoblot analyses were performed. Proteins of the PSI holocomplex were separated by 1-D gel electrophoresis as described above, transferred onto nitrocellulose membranes, and probed with antibodies raised against short peptide sequences of the individual Lhca proteins. The monospecificity of the antibodies was tested with individual Lhca proteins obtained by overexpression of tomato Lhca genes in *Escherichia coli* (data not shown). Immunodetection using antibodies directed against Lhca2 and Lhca3 confirmed the previous assignment based on the band pattern on coomassie-stained gels. The Lhca3 antibody reacted with the band at 23.7 kDa and the Lhca2 antibody with the band resolved at 23.2 kDa (Figure 1B). In contrast, Lhca1 and Lhca4 antibodies recognized three and two distinct bands, respectively. The Lhca4 antibody cross reacted strongly with the band with an M_r of 22.0 kDa. Additionally, the Lhca4 antibody recognized the lower part of the band at 22.3 kDa, which was the main target of the Lhca1 antibody. The Lhca1 antibody also reacted strongly with the fifth band, which had not been identified until now (asterisk in Figure 1), and a weak reaction was observed with the 23.2 kDa band. These results suggest a heterogenic protein composition of the "Lhca1" and "Lhca2" band.

To examine further the protein composition of these bands, PSI and LHCI-730 were separated in high-resolution gels as described above. Following coomassie staining, bands were excised and digested with trypsin, and the tryptic peptides were subjected to liquid chromatography and MS/MS. Table 1 summarizes the results of these analyses. It is of note that more than one protein could be detected in all five LHCI bands.

In the 22.0 kDa band that was recognized by only the Lhca4 antibody, peptides specific for products of two different Lhca4 genes (*cab11* and *cab12*; *25*) were detected (Figure 2). Thus, the specific amino acid sequence information from highly sensitive MS/MS measurements enabled detection of the *cab12* gene product for the first time on the protein level. As a consequence of the very high level of amino acid sequence identity (91%) of the products of *cab11* and *cab12*, several additional peptides were found in the 22.0 kDa band that are common to both of these Lhca4 isoforms. In addition to these Lhca4 fragments, one peptide specific for Lhca1 was found.

In the 22.3 kDa band that strongly reacted with the Lhca1 antibody, several peptides specific for gene products of *cab6a* (*23*) and *cab6b* (*24*) were found. Also, single peptides specific for proteins derived from the two Lhca4 genes described above (*cab11* and *cab12*) were detected, which confirms immunoblot analyses showing comigration of Lhca4 with Lhca1 in the 22.3 kDa band. Two tryptic peptides (WYVQAELVHAR and DLPVWYEAGATK) identified from the MS/MS data matched the Lhca5 sequence from *A. thaliana*, but did not match any tomato protein retrieved from the NCBI databases. To determine if the MS/MS data could be used to identify tomato homologues of Lhca5 or Lhca6 from *A. thaliana*, BLAST searches were carried out using the tomato EST database (Cornell University, Ithaca, NY) and the cDNA sequences of Lhca5 and Lhca6 from *A. thaliana* (GenBank accession numbers AF134121 and U03395, respectively; *21*). Two EST clones (GenBank accession numbers AW041324 and AI778223) that share a very high level of nucleotide sequence identity with large sections of the *A. thaliana lhca*5 sequence were found. These two partially overlapping EST sequences were joined together, and the resulting nucleotide sequence was translated. Alignment of the obtained amino acid sequence with the Lhca5 sequence of *A. thaliana* demonstrates a very high level of sequence identity (Figure 3). The level of identity for the precursor protein is 68.8% and increases to 77.9% for the region that corresponds to the mature protein of *A. thaliana* as suggested by ref *21*. The two tryptic peptides that were identified within the Lhca5 amino acid sequence from *A. thaliana* are also present in the tomato protein sequence (Figure 3).

The additional band at 22.7 kDa resolved by high-resolution electrophoresis of PSI and LHCI-730 also contains

Table 1: Mass Spectrometric Identification of Proteins in the Bands Resolved in the Molecular Mass Range of LHCI Proteins following Separation of PSI[1] or LHCI-730[2] in Denaturing 1-D SDS Gels[a]

band[b]	protein[c]	peptide[d]	position[e]	ref[e]	*z*	Δ*M*	X_{corr}
Lhca4[1]	Lhca1 (*cab6a*/*6b*)	KYPGGAFDPLGYSK	168−180	P12360	2	−1.0	3.81
	Lhca4 (*cab11*/*12*)	WQDIKNPGSVNQDPIFK		S14305/6	3	0.4	4.66
		NPGSVNQDPIFK		S14305/6	2	−0.5	4.13
		NPGSVNQDPIFK		S14305/6	1	0.0	3.06
	Lhca4 (*cab11*)	WFIQAELVNGR	90−100	S14305	2	−0.7	4.07
	Lhca4 (*cab12*)	WFVQAELVNGR	89−99	S14306	2	0.2	2.33
Lhca1[1]	Lhca1 (*cab6a*/*6b*)	WAMLAVPGIIVPEALGLGNWVK	94−115	P12360	3	0.4	5.95
		PSYLDGSAPGDFGFDPLGLGEVPANLER	56−83	P12360	2	0.4	4.96
		YPGGAFDPLGYSKDPAKFEELK	168−189	P12360	3	0.4	4.41
		YPGGAFDPLGYSK	168−180	P12360	2	−0.1	4.30
		KYPGGAFDPLGYSK	167−180	P12360	3	−0.4	3.59
		DPAKFEELK	181−189	P12360	1	0.0	1.72
	Lhca4 (*cab11*/*12*)	NPGSVNQDPIFK		S14305/6	2	0.4	4.15
		WYDAGK		S14305/6	1	0.4	1.85
	Lhca4 (*cab11*)	WFIQAELVNGR	90−100	S14305	2	0.0	3.46
	Lhca4 (*cab12*)	WFVQAELVNGR	89−99	S14306	2	0.0	4.50
	Lhca5	WYVQAELVHAR	90−101		2	0.8	3.52
		WYVQAELVHAR	90−101		3	−0.2	3.45
		DLPVWYEAGATK	123−134		2	−0.8	3.04
new ∗[1]	Lhca1 (*cab6a*/*6b*)	YPGGAFDPLGYSK	168−180	P12360	2	0.2	4.06
		KYPGGAFDPLGYSK	167−180	P12360	2	0.0	3.37
		WAMLAVPGIIVPEALGLGNWVK	94−115	P12360	2	−0.4	3.51
		DPAKFEELK	181−189	P12360	1	0.6	2.06
		FEELK	185−189	P12360	1	0.2	1.56
	Lhca3 (*cab8*)	WLAYGEVINGR	95−105	P27522	2	0.5	3.43
		GLGGSGDPAYPGGPLFNPLGFGK	191−213	P27522	2	0.6	3.37
	Lhca4 (*cab11*/*12*)	WQDIKNPGSVNQDPIFK		S14305/6	2	0.3	3.85
		NPGSVNQDPIFK		S14305/6	2	−0.9	3.25
		NPGSVNQDPIFK		S14305/6	1	0.9	2.37
		WYDAGK		S14305/6	1	0.0	1.75
	Lhca4 (*cab11*)	WFIQAELVNGR	90−100	S14305	2	0.1	3.98
	Lhca4 (*cab12*)	WFVQAELVNGR	89−99	S14306	2	0.3	4.43
	Lhca5	DLPVWYEAGATK	123−134		2	0.5	3.98
new ∗[2]	Lhca1 (*cab6a*/*6b*)	WAM[#]LAVPGIIVPEALGLGNWVK[f]	94−115	P12360	3	0.4	4.91
		WAMLAVPGIIVPEALGLGNWVK	94−115	P12360	2	0.2	4.12
		KYPGGAFDPLGYSK	167−180	P12360	3	0.2	3.90
		YPGGAFDPLGYSK	168−180	P12360	2	0.0	3.54
	Lhca4 (*cab11*/*12*)	NPGSVNQDPIFK		S13405/6	2	0.1	3.81
		WQDIKNPGSVNQDPIFK		S13405/6	3	0.4	4.37
		WYDAGK		S13405/6	1	0.1	2.03
	Lhca4 (*cab11*)	WFIQAELVNGR	90−100	S13405	2	−0.7	3.59
	Lhca4 (*cab12*)	WFVQAEVNGR	89−99	S13406	2	0.2	4.14
	Lhca5	DLPVWYEAGATKFNF	123−137		2	0.1	3.16
Lhca2[1]	Lhca1 (*cab6a*/*6b*)	KYPGGAFDPLGYSK	167−180	P12360	3	−0.7	3.66
		KYPGGAFDPLGYSK	167−180	P12360	2	0.8	2.76
	Lhca2 (*cab7*)	WAMLGAAGIFIPELLTK	113−129	P10708	2	0.8	3.94
		LTGTDVGYPGGLWFDPLGWGSGSPAK	189−214	P10708	2	−0.1	3.89
		WADIIK	169−174	P10708	1	0.2	1.51
	Lhca3 (*cab8*)	FAMLGAAGAIAPEILGK	106−122	P27522	2	0.9	3.26
	Lhca4 (*cab11*)	WFIQAELVNGR	90−100	S13405	2	0.7	3.57
	Lhca5	DLPVWYEAGATK	123−134		2	−0.4	3.65
Lhca3[1]	Lhca1 (*cab6a*/*6b*)	YPGGAFDPLGYSK	168−180	P12360	2	0.0	4.71
	Lhca2 (*cab7*)	LTGTDVGYPGGLWFDPLGWGSGSPAK	189−214	P10708	2	0.4	4.07
	Lhca3 (*cab8*)	FAMLGAAGAIAPEILGK	106−122	P27522	3	−0.8	4.33
		FAMLGAAGAIAPEILGK	106−122	P27522	2	−0.1	2.35
		GLGGSGDPAYPGGPLFNPLGFGKDEK	191−216	P27522	3	0.5	4.27
		GLGGSGDPAYPGGPLFNPLGFGK	191−213	P27522	2	0.0	3.76
		WLAYGEVINGR	95−105	P27522	2	1.1	3.35
		FQDWAKPGSMGK	171−182	P27522	2	0.1	2.93
	CP22	SALGLSEGGPLFGFTK	188−203	P54773	2	−0.6	4.63
		FVDDPTPPTGLEK	165−177	P54773	2	0.0	3.87

[a] The charge state of the measured ion (*z*), the deviation of the experimentally determined mass from the theoretical average mass of the peptide (Δ*M* in daltons; ± means that the calculated mass is larger or smaller than the measured mass), and the cross-correlation factor calculated by the Sequest algorithm (X_{corr}) are listed. [b] Labeling of the bands according to immunoblot assignment as in Figure 1B. [c] Proteins detected by MS/MS in proteolytically digested gel bands. The names of proteins and genes (in parentheses) are given. [d] Peptides found by a database search done with MS/MS data. [e] Position of the identified peptide in the protein sequence retrieved from the given data bank. The GenBank accession numbers are given. For peptides that match both Lhca4 isoforms (*cab11*/*12*), no peptide position is given as it differs in both isoforms. Positions of identified Lhca5 peptides are given for the precursor sequence shown in Figure 3. [f] Oxidation of methionine indicated.

peptides characteristic for several Lhca proteins. One of these is a peptide specific for Lhca5. In addition, numerous peptides of Lhca1 and the two isoforms of Lhca4 are present in this band. The occurrence of Lhca1 was expected from

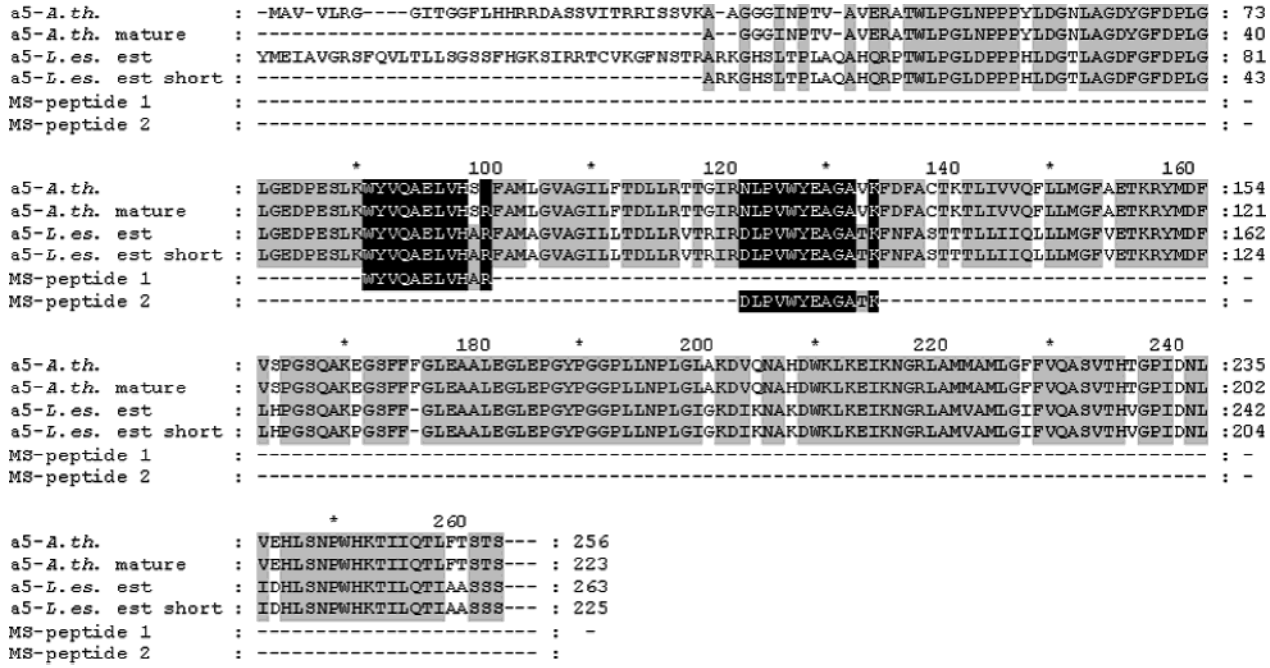

FIGURE 3: Alignment of the amino acid sequence of Lhca5 of *A. thaliana* (*21*; GenBank accession number AF134121), the reconstructed amino acid sequence of Lhca5 of *L. esculentum*, and Lhca5 peptides identified by MS/MS. The protein sequence of the Lhca5 protein of tomato was obtained by overlapping the EST clones (GenBank accession numbers AW041324 and AI778223) (see the text for further details).

the immunoblot analyses with the Lhca1 antibody. Finally, two Lhca3 peptides were detected also. These peptides were observed for only the band from the PSI holocomplex, but not for that from LHCI-730. This finding indicates that these two Lhca3 peptides are contaminations caused by smearing of Lhca3, which is found mainly in the 23.7 kDa band, as was demonstrated by immunodetection.

Surprisingly, fragments of all Lhca proteins could be detected in the 23.2 kDa band, which was specifically recognized by the Lhca2 antibody. However, only for Lhca2 were three different peptides found indicating its enrichment in this band in comparison with other bands. Additionally, single peptides of Lhca1, Lhca3, the *cab11* gene product, and Lhca5 could be detected.

The Lhca1 and Lhca2 proteins each could be identified by one peptide in the uppermost band at 23.7 kDa. In contrast, five different peptides characteristic of Lhca3 were found. This indicates the dominance of Lhca3 in this band in concurrence with the immunoblots. Interestingly, two additional peptides that matched CP22 of photosystem II were identified. Since no LHCII proteins could be detected, this may indicate weak contamination of the PSI preparation with PSII cores. In summary, highly sensitive MS/MS demonstrated that bands resolved by 1-D gel electrophoresis usually contain more than only one protein and thus confirms the results obtained with immunoblots.

To learn more about the heterogeneity of LHCI proteins, we used 2-D gel electrophoresis as described in ref *29* to separate PSI. Spots from 2-D gels were identified again by either immunoblot analyses or MS/MS. The top panel of Figure 4A shows a complete 2-D gel of PSI proteins stained with silver. Enrichment of neutral to slightly acidic proteins of the PSI core in the top right part and of LHCI proteins at more acidic pH in the middle section of the gel is clearly visible. In the bottom panel of Figure 4A, the typical resolution of the LHCI region is shown in more detail. Depending on the staining intensity, the individual horizontal spot rows consist of four to five spots for each Lhca protein. The assignment of the spots in Figure 4A is based on immunoblots like those shown in Figure 4B. All spots in silver-stained gels assigned to Lhca3, Lhca2, and Lhca1 on the basis of apparent molecular mass were recognized by antibodies raised against the respective protein. By contrast, due to the weak reaction of the Lhca4 antibody with Lhca4, only the Lhca4 spots that were stained most intensely by silver were detected. It is conspicuous that each Lhca protein forms one or two spot row(s) with proteins of the same molecular mass, but with different isoelectric points, indicative of protein isoforms with different isoelectric points. The row recognized by the Lhca2 antibody has the most acidic isoelectric points. The ones detected by the Lhca3 antibody exhibit the least acidic pI, and those of Lhca1 and Lhca4 are intermediate. This corresponds well with the theoretical pI values calculated for the different Lhca proteins. In addition to the heterogeneity regarding isoelectric points, Lhca3, Lhca1, and Lhca4 show a heterogeneity in molecular mass as is visible from detection of two spot rows by immunoblotting of these proteins (Figure 4B).

To gain specific amino acid sequence information from the proteins comprising individual spots resolved by 2-D gel electrophoresis, prominent spots were excised from gels, digested with trypsin, and analyzed by MS/MS. Table 2 summarizes the data from these analyses, and the assignment of the Lhca proteins to different spots is depicted in Figure 4C. In the spots recognized by the Lhca3 antibody, which have the same isoelectric point (pI ~6) but migrate at different molecular mass, only peptides corresponding to Lhca3 (labeled A and B in Figure 4C) were identified. By contrast, with the exception of spot C, all other spots that

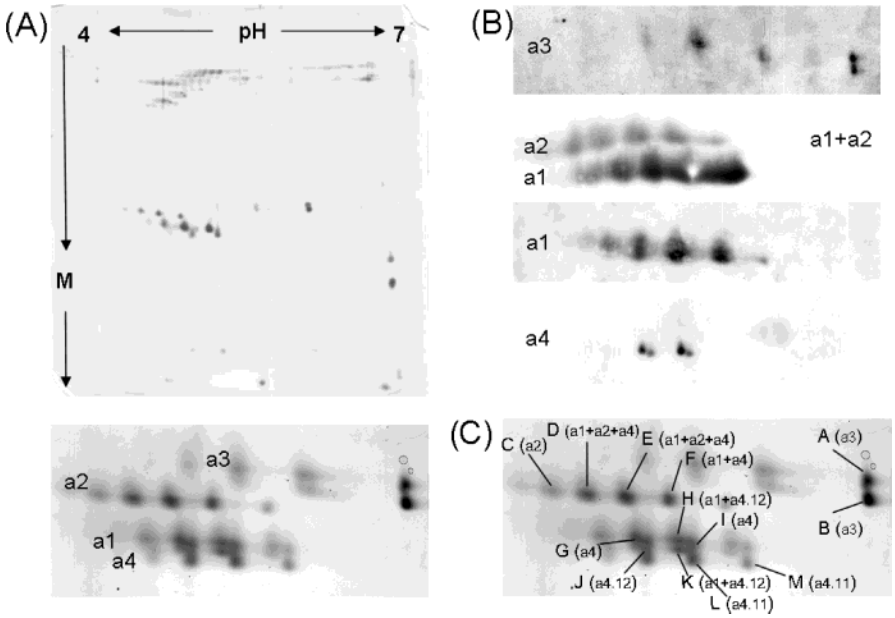

FIGURE 4: Protein maps of the PSI holocomplex obtained by 2-D gel electrophoresis using isoelectric focusing in the first and fully denaturing SDS−PAGE in the second dimension. In the top portion of panel A, the whole 2-D map stained with silver is shown. The bottom panel depicts the LHCI region at a higher magnification. The assignment of the different spot rows to the LHCI proteins was carried out according to the immunoblots shown in panel B. Depicted are immunoblots, which were developed with antibodies raised against the four different LHCI apoproteins (Lhca1−4) as indicated. Identification of Lhca1, Lhca3, and Lhca4 was achieved via incubation with a single antibody (a1, a3, and a4), whereas immunodetection of Lhca2 occurred simultaneously with that of Lhca1 to illustrate the relative position of the two spot rows. M is the molecular mass; a1−a4 are Lhca1−4, respectively. (C) Protein map of the molecular mass region of LHCI with Lhca spots identified by mass spectrometry as indicated: a1, Lhca1; a3, Lhca3; a4.11, Lhca4 derived from *cab11*; a4.12, Lhca4 derived from *cab12*; a4, Lhca4 derived from *cab11* or *cab12*.

were analyzed contained at least one of the Lhca4 isoforms. Spots L and M with higher pI contained the *cab11* gene product, whereas in the spots H, J, and K with a lower pI the *cab12* gene product was found. In spots D−G and I, peptides characteristic of Lhca4 were found that are common to both *cab11* and *cab12*. In spots D−F, H, and K, the Lhca1 protein (*cab6a/cab6b*) was also detected. Peptides identifying Lhca2 could be detected in spots C−E only after the amount of protein loaded on the gels and the trypsin concentration used for digestion were increased (see Experimental Procedures).

One possible explanation for the different electrophoretic forms of each Lhca protein could be that the proteins are phosphorylated to different degrees as suggested from a study with barley and antibodies that recognize phosphorylated proteins (*36*). To examine phosphorylation of Lhca proteins in tomato, proteins of PSI and thylakoids were separated in a 1-D gel. Subsequent detection of phosphorylated proteins revealed strong staining of phosphoproteins of photosystem II (e.g., Lhcb2, D1, and CP43), but not of Lhca proteins (data not shown). This shows that there is no significant phosphorylation of Lhca proteins, which could explain the electrophoretic behavior observed by 2-D electrophoresis.

DISCUSSION

Using high-resolution 1-D and 2-D gel electrophoresis in combination with immunoblotting and tandem mass spectrometry, our data yield a highly diverse protein composition of the PSI light-harvesting antenna of tomato. The data revealing this great diversity of Lhca proteins are summarized in Figure 5, which shows a 2-D map of the LHCI mass region. The assignment of individual spots to individual Lhca proteins is based on molecular mass determination, immunoblotting, and MS/MS analysis. Highly sensitive MS/MS additionally allowed detection of Lhca5 and of two different isoforms of Lhca4 for the first time on the protein level in a higher plant.

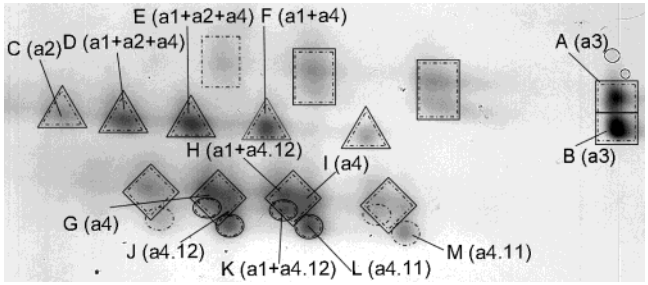

FIGURE 5: 2-D map summarizing the Lhca proteins of photosystem I. Identification of Lhca proteins is based on molecular mass determination of silver-stained gels (-•-), immunoblotting (—), and mass spectrometry (indicated with letters) of Lhca3 (rectangles), Lhca2 (triangles), Lhca1 (squares), and Lhca4 (ellipsoids).

Heterogeneity of the PSI Light-Harvesting Antenna. High-resolution SDS−PAGE resolved five bands in the molecular mass range of light-harvesting proteins (Figure 1A). Four of these bands are stained strongly by coomassie and are assigned to the well-known Lhca1−4 proteins. In addition, this gel system allowed resolution of a fifth band, which until now has been described for only barley (*13*) and tomato (*15*). From 1-D gels and immunoblotting with monospecific antibodies, it is obvious that the four bands attributed to Lhca1−4 do not contain only the eponymous proteins. The Lhca4 antibody reacted with the Lhca4 band and additionally with the band usually assigned to Lhca1. The reactivity of the Lhca1 antibody with the Lhca2 band indicated a heterogeneous protein composition of this band as well. This heterogeneity in molecular mass observed for Lhca4 and

Table 2: Protein Composition of Spots Resolved by 2-D Gels of PSI As Determined by MS/MS[a]

2-D spot[b]	protein[c]	peptide[d]	position[e]	ref[e]	*z*	Δ*M*	X_{corr}
A	Lhca3 (*cab8*)	WLAYGEVINGR	95−105	P27522	2	−0.5	2.94
		FAMLGAAGAIAPEILGK	106−122	P27522	2	−0.9	2.67
B	Lhca3 (*cab8*)	GLGGSGDPAYPGGPLFNPLGFGK	191−213	P27522	2	1.3	4.21
		WLAYGEVINGR	95−105	P27522	2	0.9	3.70
		FAMLGAAGAIAPEILGK	106−122	P27522	2	1.3	2.98
		FQDWAKPGSMGK	171−182	P27522	2	0.9	3.25
C	Lhca2 (*cab7*)	PGC#VNTDPIFPNNK[f]	175−188	P10708	2	0.1	2.52
D	Lhca2 (*cab7*)	PGC#VNTDPIFPNNK[f]	175−188	P10708	2	−1.2	2.62
	Lhca1 (*cab6a*/*6b*)	KYPGGAFDPLGYSK	167−180	P12360	2	−0.4	2.49
		YKESELIHC#R[f]	84−93	P12360	2	−0.2	2.35
	Lhca4 (*cab11*/*12*)	NPGSVNQDPIFK		S14305/6	2	0.4	2.85
E	Lhca1 (*cab6a*/*6b*)	YPGGAFDPLGYSK	168−180	P12360	2	0.9	4.63
		KYPGGAFDPLGYSK	167−180	P12360	2	1.1	3.93
	Lhca2	WADIIKPGC#VNTDPIFPNNK[f]	169−188	P10708	3	2.2	5.05
		WAM*LGAAGIFIPELLTK[g]	113−129	P10708	2	1.3	4.20
		W§AMLGAAGIFIPELLTK[h]	113−129	P10708	2	1.3	4.19
	Lhca4 (*cab11*/*12*)	NPGSVNQDPIFK		S14305/6	2	0.8	3.68
F	Lhca1 (*cab6a*/*6b*)	KYPGGAFDPLGYSK	167−180	P12360	2	0.0	3.20
		YPGGAFDPLGYSK	168−180	P12360	2	−1.2	3.06
	Lhca4 (*cab11*/*12*)	NPGSVNQDPIFK		S14305/6	2	−1.2	3.40
G	Lhca4 (*cab11*/*12*)	NPGSVNQDPIFK		S14305/6	2	−0.9	3.61
H	Lhca1 (*cab6a*/*6b*)	YPGGAFDPLGYSK	168−180	P12360	2	−0.5	3.74
		KYPGGAFDPLGYSK	167−180	P12360	3	1.2	4.20
	Lhca4 (*cab11*/*12*)	NPGSVNQDPIFK		S14305/6	2	0.7	3.69
		WQDIKNPGSVNQDPIFK	157−173	S14305/6	3	1.2	3.83
	Lhca4 (*cab12*)	WFVQAELVNGR	89−99	S14306	2	0.0	3.94
I	Lhca4 (*cab11*/*12*)	NPGSVNQDPIFK		S14305/6	2	0.0	2.79
J	Lhca4 (*cab11*/*12*)	NPGSVNQDPIFK		S14305/6	2	0.2	3.98
	Lhca4 (*cab12*)	WFVQAELVNGR	89−99	S14306	2	0.1	3.69
K	Lhca1 (*cab6a*/*6b*)	YPGGAFDPLGYSK	168−180	P12360	2	0.1	2.68
	Lhca4 (*cab11*/*12*)	NPGSVNQDPIFK		S14305/6	2	0.3	3.81
		WQDIKNPGSVNQDPIFK		S14305/6	3	1.2	4.80
	Lhca4 (*cab12*)	WFVQAELVNGR	89−99	S14306	2	0.8	3.98
L	Lhca4 (*cab11*/*12*)	NPGSVNQDPIFK		S14305/6	2	0.8	4.03
		WQDIKNPGSVNQDPIFK		S14305/6	3	1.2	5.37
	Lhca4 (*cab11*)	C#GYPGGIFNPLNFAPTEEAK[f]	182−201	S14305	2	0.9	4.55
M	Lhca4 (*cab11*/*12*)	NPGSVNQDPIFK		S14305/6	2	0.8	3.74
		WQDIKNPGSVNQDPIFK		S14305/6	3	1.4	3.60
	Lhca4 (*cab11*)	C#GYPGGIFNPLNFAPTEEAK[f]	182−201	S14305	2	1.4	4.90
		WFIQAELVNGR	90−100	S14305	2	0.8	4.70

[a] Spots were excised from gels, proteolytically hydrolyzed, and analyzed by tandem mass spectrometry. For further details, see footnote a of Table 1. [b] The labeling of the spots is according to Figure 4C. [c] Proteins identified in the 2-D spots by MS/MS. [d] Peptides found by matching the MS data with tryptic peptides derived from proteins in tomato databases. [e] Position of the identified peptide within the protein sequence retrieved from the given data bank. The GenBank accession numbers are given. For peptides that match both Lhca4 isoforms (*cab11*/*12*), no peptide position is given as it differs in both isoforms. [f] Carbamidomethylation of cysteine indicated (+57 Da). [g] Oxidation of methionine indicated (+16 Da). [h] Keto, amino, or hydroxy modification of tryptophan indicated (+16 Da).

Lhca1 also could be detected by 2-D electrophoresis and subsequent immunodetection. Two-dimensional protein maps indicate that Lhca3 also exists in two isoforms with differing molecular masses. Due to the absence of a stacking gel in the second-dimension gel, the separation distance is longer than in 1-D gels. Therefore, separation of two differently migrating Lhca3 isoforms solely in 2-D and not in 1-D gels may be the result of a better resolution at this molecular mass in the second-dimension gel. Only Lhca2 did not show a heterogeneous behavior regarding electrophoretic mobility in 1-D or 2-D gels as judged from immunoblot analyses. MS/MS analyses, which are more sensitive, confirmed these results (Tables 1 and 2). The immunoblots and MS/MS data demonstrate that the light-harvesting antenna of PSI is very heterogeneous, and that the assignment of the four bands obtained by standard 1-D gel electrophoresis to individual proteins is an oversimplification. Therefore, quantification of individual Lhca proteins that relies on the staining intensity of these individual bands can be erroneous. In addition, our MS/MS analyses of trypsin-digested spots demonstrate the superior resolution of 2-D gels versus 1-D gels. In the majority of analyzed spots of 2-D gels, only one Lhca protein could be detected. From this observation, it can be concluded that minor constituents comigrating with the dominating protein in a band in 1-D gels are separated in 2-D gels as a consequence of the different pIs and escape detection in 2-D gels.

Isoforms with different masses have already been reported for various proteins of PSII (*37*, *38*) and the PSI core complex (*39*). Additionally, isoforms of individual Lhca proteins were observed by using different technical approaches. Using a combination of weakly and fully denaturing SDS gel electrophoresis in the first and second dimension, respectively, two Lhca3 proteins with slightly different electrophoretic mobility were observed in spinach PSI (*12*). Additionally, the same authors sometimes observed an additional band in 1-D gels with an electrophoretic migration similar to that of Lhca2. By HPLC separation coupled with ESI-MS it was possible to identify Lhca2 isoforms in PSI of tomato (*28*). In addition, two Lhca1 isoforms encoded by

cab6a (*23*) and *cab6b* (*24*) could be detected with this approach. We were not able to detect peptides specific for products of *cab6a* or *cab6b* or for Lhca2 isoforms. This failure can be explained by the different methodical approaches used in this study and in ref *28*. In contrast to the latter study in which entire proteins were analyzed, we employed tryptic protein fragments for detection and identification of proteins. The two Lhca1 isoforms differ by only three amino acids. Therefore, the most probable explanation is that proteolytic fragments specific for single isoforms have not been detected. For Lhca2, it is conspicuous that MS analyses of bands of 1-D gels resulted in the detection of only a few peptides (Table 1). It is also surprising that in 2-D gels only in spots C−E were Lhca2 peptides found by MS (Table 2), although spot F clearly contains Lhca2 as could be demonstrated by immunoblotting (Figure 4B). This could be due to poor extraction of Lhca2 tryptic peptides from a polyacrylamide matrix and/or to poor electrospray ionization efficiencies of these peptides. Such an interpretation is consistent with the mass spectrometric analysis of tryptic peptides of the Lhca2 1-D band, which resulted in the identification of only three peptides, whereas for the 1-D bands of Lhca1, Lhca3, and Lhca4 (*cab11* and *cab12*), six, five, and four peptides, respectively, were recognized (Table 1).

Due to the use of the 2-D gel electrophoresis procedure recently developed for the separation of membrane proteins (*29*), we could also demonstrate several isoelectric points for individual Lhca proteins (Figure 4). This technique allowed resolution of four to five isoforms with different pI values for Lhca1−4. The 2-D protein maps show that Lhca3 is the least acidic Lhca protein whereas Lhca2 is the most acidic one, which is consistent with the theoretical pI values of 5.95 (Lhca3), 5.22 (Lhca1; *cab6a* and *cab6b*), and 4.99 (Lhca2) as calculated from the amino acid sequence. The resolving power of this 2-D gel electrophoresis, in combination with the specific amino acid sequence tags generated by MS/MS, allowed the resolution and identification of the two Lhca4 isoforms derived from *cab11* and *cab12* genes (*27*). The product of *cab12* possessing a theoretical pI of 5.15 could be clearly separated from the *cab11* product with a pI of 5.34 (Figure 4C and Table 2), and in this way, its first detection on the protein level was facilitated.

Detection of four to five isoforms resolved at different isoelectric points for each of the prominent Lhca proteins raises the question about the origin of these charge differences. One possible explanation are posttranslational modifications. Various proteins of PSII could be isolated in a phosphorylated form (*38*, *40*). However, with regard to LHCI proteins, it is not clear whether phosphorylation occurs. ^{32}P labeling of plant material followed by gel electrophoresis and autoradiography did not prove phosphorylation of LHCI proteins under conditions in which the various PSII proteins are phosphorylated (*41*, *42*). These results are in contrast to an immunoblot study performed with anti-phosphothreonine and anti-phosphoserine antibodies (*36*). Both antibodies cross reacted with all Lhca proteins that were tested (Lhca1−4), indicating phosphorylation at various sites in all proteins. Such extensive phosphorylation at different sites of one protein could explain a heterogeneity in pI as was observed in this study. However, in addition to shifts in pI, phosphorylation may also cause shifts in electrophoretic mobility as was observed for phosphorylated PSII proteins, e.g., D1 and CP29 (*43*, *44*). To test whether the Lhca proteins of tomato are phosphorylated to an extent that would explain the spot pattern obtained by 2-D gels, we subjected PSI proteins to 1-D electrophoresis and phosphoprotein staining. However, we could not detect significant phosphorylation, which would support the idea that phosphorylation causes the heterogeneity of individual Lhca proteins. Another explanation for the heterogeneity in molecular mass observed for Lhca4, Lhca1, and Lhca3 may result from different processing of individual Lhca precursor proteins. Processing of LHC proteins at different sites has been reported in higher plants (*39*, *45*, *46*) and the green alga *C. reinhardtii* (*22*). Because the size differences observed in these investigations are comparable to those detected by us, differential processing may also be germane to the distinct electrophoretic behavior found for Lhca proteins of tomato. In addition to posttranslational modifications such as phosphorylation, acetylation or modification of the peptide amino terminus or the side chains of lysine or arginine by isocyanic acid (carbamylation) could be an explanation for the different Lhca isoforms. We specifically searched the MS/MS data of all Lhca proteins for protein carbamylation and acetylation. We also aimed to identify differentially N-terminally processed Lhca proteins by searching the MS/MS data for such processing events (see Experimental Procedures). However, no carbamylation or acetylation was detected, nor was it possible to determine the identity of any differentially N-terminally processed proteins. However, the existence of such modifications cannot be ruled out by the applied MS/MS procedure since only between 17% (*cab12*) and 36% (Lhca1) of the entire proteins were covered in the 1-D gel bands and even less in the spots of 2-D gels (Tables 1 and 2). Additionally, no peptides were detected that derive from the N-terminus, which is especially predestined to differential processing and protein modifications. Therefore, we are left with the speculation that the distinct Lhca isoforms are caused by posttranslational modifications, protein processing, or even charge heterogeneity that occur in the protein segments, which have not been detected. Further proteomic analyses using other proteases for in-gel digestion may be suitable for clarifying the origin of the distinct electrophoretic behavior. Additionally, plants grown under different environmental conditions (e.g., high light, low temperature, and nutrient deficiency) hold promise for providing insight into the physiological significance of these isoforms.

Detection of Lhca5 on the Protein Level in a Higher Plant. Our approach allowed not only identification of Lhca4 isoforms (gene products of *cab11* and *cab12*) but also detection of Lhca5, a protein that was not yet identified on the protein level in higher plants. The *lhca*5 gene has a low expression level and was first described for *A. thaliana* (*21*). Very recently, a detailed MS/MS analysis indicated its presence in the green alga *C. reinhardtii* (*22*). In the study presented here, combining electrophoresis and MS/MS with bioinformatic analyses, we were able to demonstrate the presence of Lhca5 on the protein level in a higher plant (Table 1). A contig (TC116242) resulting in a protein with the same amino acid sequence as in Figure 3 that lacks the final five amino acids (AASSS) can be found at The Institute for Genomic Research (TIGR) tomato gene index (http://www.tigr.org/tdb/tgi/lgi). This confirms the sequence of the reconstructed Lhca5.

As a consequence of the presence of Lhca5 in bands with apparent molecular masses of 22.3, 22.7, and 23.2 kDa, it appears that this protein also occurs in different isoforms. This corresponds to the observation in *C. reinhardtii* in which two different isoforms of Lhca5 have been found (*22*). On the basis of the molecular masses, one can speculate about the processing site at which the protein is cleaved during maturation. For *A. thaliana*, it was suggested that the mature protein starts with the sequence AAGGGIN..., which corresponds to a protein of 24.1 kDa (*21*). By using the net-based ChloroP software (at http://www.cbs.dtu.dk/services/ChloroP/), we obtained the same processing site for tomato Lhca5. Thus, if one assumes that the mature tomato Lhca5 starts with the sequence ARKGHS... (Figure 3), a protein of 24.5 kDa is obtained, which does not correspond to the observed molecular masses. Recent analyses demonstrated that the predictions of the ChloroP software are only reliable for soluble proteins and not for membrane proteins (*47*), which may also apply for Lhca5. Therefore, we calculated the molecular masses for shortened versions of Lhca5. Given the same N-terminus for tomato as suggested for *A. thaliana* (*21*), removal of 12, 16, and 19 amino acids from the N-terminus of tomato Lhca5 would result in proteins of 23.2, 22.7, and 22.3 kDa, respectively, which would fit to the molecular masses obtained by 1-D SDS−PAGE. Therefore, we assume that mature Lhca5 of tomato starts with one of the following three amino acid sequences: LPGLDP (minus 19 amino acids), PTWLPG (minus 16 amino acids), and AHQRPT (minus 12 amino acids). Due to the presence of Lhca5 in LHCI-730, it may interact with either Lhca1 or Lhca4. It will be interesting to perform dimerization experiments as described in ref *48* with Lhca5 and other Lhca proteins to elucidate the dimer formation capability of this protein.

Significance of LHCI Heterogeneity for PSI Composition. Depending on the staining intensity and resolution of 1-D and 2-D gels, we were able to resolve five different Lhca proteins occurring in several isoforms. This variety of Lhca proteins found in the present work and by Zolla and coworkers (*28*) for Lhca2 is surprising considering that according to the recently published crystal structure of PSI from pea (*19*) and single-particle analyses of PSI from spinach (*18*) isolated PSI complexes of higher plants contain between four and eight Lhca proteins per PSI core complex. The detected variety indicates the existence of different populations of PSI in higher plants, which differ in their Lhca protein composition. In fact, using phase partitioning, the existence of two different PSI populations (PSI_α and PSI_β) was demonstrated (*49*). Immunoblot analyses showed that PSI_α located in the inner parts of grana thylakoids possesses a smaller Lhca antenna than PSI_β localized in stroma thylakoids (*50*). In addition, it was shown recently that high levels of light resulted in a selective reduction of Lhca4 and Lhca1 (*51*). Finally, it can be inferred from analyses of mutants of barley and *A. thaliana* that PSI complexes with a varying complement of antenna proteins exist (*52*−*54*). All these examples show that PSI with varying Lhca composition occurs depending on the location in the thylakoid membrane, physiological state, and genotype. Our results imply that even under normal growth conditions several PSI populations differing in their Lhca protein composition are present. Therefore, it will be interesting to analyze plants grown under different environmental conditions with regard to up- or downregulation of individual Lhca proteins and their isoforms. This will shed light on the physiological significance of Lhca heterogeneity and the existence of PSI with different Lhca compositions.

NOTE ADDED AFTER ASAP POSTING

After being posted on the Web on 06/26/04, this paper was altered (subscript Greek characters in last paragraph of Discussion). The correct version was posted 06/29/04.

ACKNOWLEDGMENT

We thank Prof. L. A. Staehelin (Department of Molecular, Cellular and Developmental Biology, University of Colorado) for the kind gift of Lhca2 antibody and Christine Markert (Lehrstuhl für Pflanzenphysiologie, Friedrich Schiller-Universität Jena) for help with MS measurements.

REFERENCES

1. Haldrup, A., Jensen, P. E., Lunde, C., and Scheller, H. V. (2001) Balance of power: a view of the mechanism of photosynthetic state transitions, *Trends Plant Sci. 6*, 301−305.
2. Demmig-Adams, B. (1990) Carotenoid and photoprotection in plants: A role for the xanthophyll zeaxanthin, *Biochim. Biophys. Acta 1020*, 1−24.
3. Yamamoto, H., and Bassi, R. (1996) Carotenoids: Localization and Function, in *Oxygenic Photosynthesis: The Light Reactions* (Ort, D. R., and Yocum, C. F., Eds.) pp 507−521, Kluwer Academic Publishers, Dordrecht, The Netherlands.
4. Peter, G. F., and Thornber, J. P. (1991*)* Biochemical composition and organization of higher plant photosystem II light-harvesting pigment−proteins, *J. Biol. Chem. 266*, 16745−16754.
5. Bassi, R., Pineau, B., Dainese, P., and Marquardt, J. (1993) Carotenoid-binding proteins of photosystem II, *Eur. J. Biochem. 21*, 297−303.
6. Haworth, P., Watson, J. L., and Arntzen, C. J. (1983) The detection, isolation, and characterization of a light-harvesting complex which is specifically associated with photosystem I, *Biochim. Biophys. Acta 724*, 151−158.
7. Lam, E., Ortiz, W., and Malkin, R. (1984) Chlorophyll a/b proteins of photosystem I, *FEBS Lett. 168*, 10−14.
8. Bassi, R., Machold, O., and Simpson, D. (1985) Chlorophyll-proteins of two photosystem I preparations from maize, *Carlsberg Res. Commun. 50*, 145−162.
9. Jansson, S., Andersen, B., and Scheller, H. V. (1996) Nearest-neighbor analysis of higher-plant photosystem I holocomplex, *Plant Physiol. 112*, 409−420.
10. Schmid, V. H. R., Cammarata, K. V., Bruns, B. U., and Schmidt, G. W. (1997) In vitro reconstitution of the photosystem I light harvesting complex LHCI-730: heterodimerization is required for antenna pigment organization, *Proc. Natl. Acad. Sci. U.S.A. 94*, 7667−7672.
11. Croce, R., Morosinotto, T., Castelletti, S., Breton, J., and Bassi, R. (2002) The Lhca antenna complexes of higher plant photosystem I, *Biochim. Biophys. Acta 1556*, 29−40.
12. Ikeuchi, M., Hirano, A., and Inoue, Y. (1991) Correspondence of apoproteins of light-harvesting chlorophyll a/b complexes associated with photosystem I to cab genes: evidence for a novel type IV apoprotein, *Plant Cell Physiol. 32*, 103−112.
13. Knoetzel, J., Svendsen, I., and Simpson, D. J. (1992) Identification of the photosystem-I antenna polypeptides in barley: isolation of 3 pigment-binding antenna complexes, *Eur. J. Biochem. 206*, 209−215.
14. Tjus, S. E., Roobol-Boza, M., Palsson, L. O., and Andersson, B. (1995) Rapid isolation of photosystem I chlorophyll-binding proteins by anion exchange perfusion chromatography, *Photosynth. Res. 45*, 41−49.
15. Schmid, V. H. R., Potthast, S., Wiener, M., Bergauer, V., Paulsen, H., and Storf, S. (2002) Pigment Binding of Photosystem I Light-harvesting Proteins, *J. Biol. Chem. 277*, 37307−37314.

16. Castelletti, S., Morosinotto, T., Robert, B., Caffarri, S., Bassi, R., and Croce, R. (2003) Recombinant Lhca2 and Lhca3 Subunits of the Photosystem I Antenna System, *Biochemistry 42*, 4226−4234.
17. Boekema, E. J., Wynn, R. M., and Malkin, R. (1990) The structure of spinach photosystem I studied by electron microscopy, *Biochim. Biophys. Acta 1017*, 49−56.
18. Boekema, E. J., Jensen, P. E., Schlodder, E., van Breemen, J. F. L., van Roon, H., Scheller, H. V., and Dekker, J. P. (2001) Green plant photosystem I binds light-harvesting complex I on one side of the complex, *Biochemistry 40*, 1029−1036.
19. Ben-Shem, A., Frolow, F., and Nelson, N. (2003) Crystal structure of plant photosystem I, *Nature 426*, 630−635.
20. Pichersky, E., and Jansson, S. (1996) The light-harvesting chlorophyll a/b-binding polypeptides and their genes in angiosperm and gymnosperm species, in *Oxygenic Photosynthesis: The Light Reactions* (Ort, D. R., and Yocum, C. F., Eds.) pp 507−521, Kluwer Academic Publishers, Dordrecht, The Netherlands.
21. Jansson, S. (1999) A guide to the Lhc genes and their relatives in *Arabidopsis*, *Trends Plant Sci. 4*, 236−240.
22. Stauber, E. J., Fink, A., Markert, C., Kruse, O., Johanningmeier, U., and Hippler, M. (2003) Proteomics of *Chlamydomonas reinhardtii* light-harvesting proteins, *Eukaryotic Cell 2*, 978−994.
23. Hoffman, N. E., Pichersky, E., Malik, V. S., Castresana, C., Ko, K., Darr, S. C., and Cashmore, A. R. (1987) The nucleotide sequence of a tomato cDNA clone encoding a photosystem I protein with homology to photosystem II chlorophyll a/b-binding polypeptides, *Proc. Natl. Acad. Sci. U.S.A. 84*, 8844−8848.
24. Pichersky, E., Hoffman, N. E., Bernatzky, R., Piechulla, B., Tanksley, S. D., and Cashmore, A. R. (1987) Molecular characterization and genetic mapping of DNA sequences encoding type I chlorophyll *a*/*b*-binding polypeptide of photosystem I in *Lycopersicon esculentum* (tomato), *Plant Mol. Biol. 9*, 205−216.
25. Pichersky, E., Tanksley, S. D., Piechulla, B., Stayton, M. M., and Dunsmuir, P. (1988) Nucleotide sequence and chromosomal location of cab-7, the tomato gene encoding the type II chlorophyll a/b-binding polypeptide of photosystem I, *Plant Mol. Biol. 11*, 69−71.
26. Pichersky, E., Brock, T. G., Nguyen, D., Hoffman, N. E., Piechulla, B., Tanksley, S. D., and Green, B. R. (1989) A new member of the cab gene family: structure, expression and chromosomal location of cab-8, the tomato gene encoding the type III chlorophyll a/b-binding polypeptide of photosystem I, *Plant Mol. Biol. 12*, 257−270.
27. Schwartz, E., Shen, D., Aebersold, R., McGrath, J. M., Pichersky, E., and Green, B. R. (1991) Nucleotide sequence and chromosomal location of cab11 and cab12, the genes for the fourth polypeptide of the photosystem I light-harvesting antenna (LHCI), *FEBS Lett. 280*, 229−234.
28. Zolla, L., Rinalducci, S., Timperio, A. M., and Huber, C. G. (2002) Proteomics of Light-Harvesting Proteins in Different Plant Species. Analysis and Comparison by Liquid Chromatography-Electrospray Ionization Mass Spectrometry. Photosystem I, *Plant Physiol. 130*, 1938−1950.
29. Hippler, M., Klein, J., Fink, A., Allinger, T., and Hoerth, P. (2001) Towards functional proteomics of membrane protein complexes: analysis of thylakoid membranes from *Chlamydomonas reinhardtii*, *Plant J. 28*, 595−606.
30. Paulsen, H., and Schmid, V. H. R. (2002) Analysis and Reconstitution of Chlorophyll-Proteins, in *Heme, Chlorophyll and Bilins: Methods and Protocols* (Smith, A. G., and Witty, M., Eds.) pp 235−253, Humana Press, Totowa, NJ.
31. Porra, R. J., Thompson, W. A., and Kriedemann, P. E. (1989) Determination of accurate extinction coefficients and simultaneous equations for assaying chlorophylls a and b extracted with four different solvents: verification of the concentration of chlorophyll standards by atomic absorption spectroscopy, *Biochim. Biophys. Acta 975*, 384−394.
32. Laemmli, U. K. (1970) Cleavage of structural proteins during the assembly of the head of bacteriophage T4, *Nature 227*, 680−685.
33. Wessel, D., and Fluegge, U. I. (1984) A method for the quantitative recovery of protein in dilute solution in the presence of detergents and lipids, *Anal. Biochem. 138*, 141−143.
34. Sigrist, M., and Staehelin, L. A. (1994) Appearance of type 1, 2, and 3 light-harvesting complex II and light-harvesting complex I proteins during light-induced greening of barley (*Hordeum vulgare*) etioplasts, *Plant Physiol. 104*, 135−145.
35. Mortz, E., Vorm, O., Mann, M., and Roepstorff, P. (1994) Identification of proteins in polyacrylamide gels by mass spectrometric peptide mapping combined with database search, *Biol. Mass Spectrom. 23*, 249−261.
36. Knoetzel, J., Meyer, D. U., and Grimme, L. H. (1998) Phosphorylated Photosystem I antenna proteins in Barley, in *Photosynthesis: from Light to Biosphere* (Mathis, P., Ed.) Vol. 1, pp 131−134, Kluwer Academic Publishers, Dordrecht, The Netherlands.
37. Huber, C. G., Timperio, A.-M., and Zolla, L. (2001) Isoforms of Photosystem II Antenna Proteins in Different Plant Species Revealed by Liquid Chromatography-Electrospray Ionization Mass Spectrometry, *J. Biol. Chem. 276*, 45755−45761.
38. Gómez, S. M., Nishio, J. N., Faull, K. F., and Whitelegge, J. P. (2002) The Chloroplast Grana Proteome Defined by Intact Mass Measurements from Liquid Chromatography Mass Spectrometry, *Mol. Cell. Proteomics 1*, 46−59.
39. Obokata, J., Mikami, K., Hayashida, N., Nakamura, M., and Sugiura, M. (1993*)* Molecular Heterogeneity of Photosystem I, *Plant Physiol. 102*, 1259−1267.
40. Bennett, J. (1991) Protein phosphorylation in green plant chloroplasts, *Annu. Rev. Plant Physiol. Plant Mol. Biol. 42*, 281−311.
41. Dunahay, T. G., Schuster, G., and Staehelin, L. A. (1987) Phosphorylation of spinach chlorophyll-protein complexes, *FEBS Lett. 215*, 25−30.
42. Bassi, R., Giacometti, G. M., and Simpson, D. J. (1988) Changes in the organization of stroma membranes induced by in vivo state 1−state 2 transition, *Biochim. Biophys. Acta 935*, 152−165.
43. Elich, T. D., Edelman, M., and Mattoo, A. K. (1992) Identification, characterization, and resolution of the in vivo phosphorylated form of the photosystem II reaction center protein, *J. Biol. Chem. 267*, 3523−3529.
44. Bergantino, E., Sandona, D., Cugini, D., and Bassi, R. (1998) The photosystem II subunit CP29 can be phosphorylated in both C3 and C4 plants as suggested by sequence analysis, *Plant Mol. Biol. 36*, 11−22.
45. Clark, S. E., Abad, M. S., and Lamppa, G. K. (1989) Mutations at the transit peptide-mature protein junction separate two cleavage events during chloroplast import of the chlorophyll a/b-binding protein, *J. Biol. Chem. 264*, 17544−17550.
46. Pichersky, E., Hoffman, N. E., Malik, V. S., Bernatzky, R., Szabo, L., and Cashmore, A. R. (1987) The tomato Cab-4 and Cab-5 genes encode a second type of CAB polypeptides localized in photosystem II, *Plant Mol. Biol. 9*, 109−120.
47. Gómez, S. M., Bil', K. Y., Aguilera, R., Nishio, J. N., Faull, K. F., and Whitelegge, J. P. (2003) Transit peptide cleavage sites of integral thylakoid membrane proteins, *Mol. Cell. Proteomics 2*, 1068−1085.
48. Schmid, V. H. R., Paulsen, H., and Rupprecht, J. (2002) Identification of N- and C-terminal amino acids of Lhca1 and Lhca4 required for formation of the heterodimeric peripheral photosystem I antenna LHCI-730, *Biochemistry 41*, 9126−9131.
49. Svensson, P., Andreasson, E., and Albertsson, P.-A. (1991) Heterogeneity among photosystem I, *Biochim. Biophys. Acta 1060*, 45−50.
50. Jansson, S., Stefansson, H., Nyström, U., Gustafsson, P., and Albertsson, P.-A. (1997) Antenna protein composition of PS I and PS II in thylakoid subdomains, *Biochim. Biophys. Acta 1320*, 297−309.
51. Bailey, S., Walters, R. G., Jansson, S., and Horton, P. (2001) Acclimation of *Arabidopsis thaliana* to the light environment: the existence of separate low light and high light responses, *Planta 213*, 794−801.
52. Bossmann, B., Knoetzel, J., and Jansson, S. (1997) Screening of chlorina mutants of barley (*Hordeum vulgare* L.) with antibodies against light-harvesting proteins of PSI and PSII: absence of specific antenna proteins, *Photosynth. Res. 52*, 127−136.
53. Ganeteg, U., Strand, A., Gustafsson, P., and Jansson, S. (2001) The Properties of the Chlorophyll *a*/*b*-Binding Proteins Lhca2 and Lhca3 Studied in Vivo Using Antisense Inhibition, *Plant Physiol. 127*, 150−158.
54. Zhang, H., Goodman, H. M., and Jansson, S. (1997) Antisense inhibition of the Photosystem I Antenna Protein Lhca4 in *Arabidopsis thaliana*, *Plant Physiol. 11*, 1525−1531.

BI0498196

Manuscript 4

Bianca Naumann*, Einar J. Stauber*, Andreas Busch, Frederik Sommer, and Michael Hippler (2005) N-terminal processing of Lhca3 is a key step in remodeling of the photosystem I-Light-harvesting complex under iron deficiency in *Chlamydomonas reinhardtii*. **Journal of Biological Chemistry** 280, 20431-20441, * Both authors contributed equally.

THE JOURNAL OF BIOLOGICAL CHEMISTRY
Vol. 280, No. 21, Issue of May 27, pp. 20431–20441, 2005
Printed in U.S.A.

N-terminal Processing of Lhca3 Is a Key Step in Remodeling of the Photosystem I-Light-harvesting Complex Under Iron Deficiency in *Chlamydomonas reinhardtii**

Received for publication, December 22, 2004, and in revised form, March 11, 2005
Published, JBC Papers in Press, March 17, 2005, DOI 10.1074/jbc.M414486200

Bianca Naumann‡§, Einar J. Stauber§¶, Andreas Busch‡, Frederik Sommer‡, and Michael Hippler‡¶‖

From the ‡Plant Science Institute, Department of Biology, University of Pennsylvania, Philadelphia, Pennsylvania 19104 and ¶Lehrstuhl für Pflanzenphysiologie, Friedrich-Schiller-Universität Jena, Dornburger Strasse 159, 07743 Jena, Germany

Iron deficiency induces a remodeling of the photosynthetic apparatus in *Chlamydomonas reinhardtii*. In this study we showed that a key mechanistic event in the remodeling process of photosystem I (PSI) and its associated light-harvesting proteins (LHCI) is the N-terminal processing of Lhca3. N-terminal processing of Lhca3 is documented independently by two-dimensional gel electrophoresis and tandem mass spectrometric (MS/MS) analysis as well as by quantitative comparative MS/MS peptide profiling using isotopic labeling of proteins. Dynamic remodeling of the LHCI complex under iron deficiency is further exemplified by depletion of Lhca5 and up-regulation of Lhca4 and Lhca9 polypeptides in respect to photosystem I. Most importantly, the induction of N-terminal processing of Lhca3 by progression of iron deficiency correlates with the functional drop in excitation energy transfer efficiency between LHCI and PSI as assessed by low temperature fluorescence emission spectroscopy. Using an RNA interference (RNAi) strategy, we showed that the truncated form of Lhca3 is essential for the structural stability of LHCI. Depletion of Lhca3 by RNAi strongly impacted the efficiency of excitation energy transfer between PSI and LHCI, as is the case for iron deficiency. However, in contrast to iron deficiency, comparative MS/MS peptide profiling using isotopic labeling of proteins demonstrated that RNAi depletion of Lhca3 caused strong reduction of almost all Lhca proteins in isolated PSI particles.

The viability of a photosynthetic organism is dependent on its ability to regulate the structure and function of its photosynthetic apparatus in anticipation of or in response to external factors such as light quality and nutrient availability. Iron is a cofactor in many essential biological redox reactions, including respiration and photosynthesis, and its scarcity leads to chlorosis (chlorophyll deficiency) in photosynthetic organisms, which is connected to degradation and rearrangement of the photosynthetic machinery (1–4). The global impact of iron deficiency on photosynthetic productivity has been shown in vast ocean regions that are severely limited in iron (5). On the molecular level, photosystem (PS)[1] I is a prime target of iron deficiency, probably because of its high iron content (12 iron per PSI). In the green alga *Chlamydomonas reinhardtii* iron deficiency leads not only to a pronounced degradation of PSI but also to a remodeling of the PSI-associated light-harvesting antenna (LHCI), which proceeds severe iron deficiency (4). These structural changes decrease the functional efficiency of excitation energy transfer between LHCI and PSI and minimize photo-oxidative stress to the thylakoid membrane. Cyanobacteria also respond to iron deficiency by degradation of light-harvesting phycobilisomes (6). Additionally, cyanobacteria express the "iron stress-induced" gene *isiA*. The IsiA protein has significant sequence similarity with CP43, a chlorophyll *a*-binding protein of photosystem II (PSII (7, 8)) and forms a ring of 18 molecules around a PSI trimeric reaction center, as shown by electron microscopy (9, 10).

These results highlight the adaptive nature of the response to iron deficiency that is directed toward optimizing the photosynthetic architecture to the conditions in which iron is a limiting cofactor. In *Chlamydomonas*, neither the molecular mechanisms underlying the remodeling of LHCI nor its structural and functional characteristics have been investigated. It is of note that the LHCI composition of *Chlamydomonas* is complex and consists of nine distinct subunits (11). In this study we combined low temperature fluorescence spectroscopy, reverse genetics, and comparative quantitative proteomics to correlate the efficiency of excitation energy transfer with dynamic alterations of LHCI. We established an approach that is based on differential isotopic labeling of proteins in *Chlamydomonas* by isotopically labeled arginine and mass spectrometric quantitative analysis of labeled and unlabeled peptides.

Mass spectrometry has become a powerful tool for quantitative proteomics, because it allows sensitive, fast, and specific identification of proteins from complex mixtures (12–14). Comparative analysis of a protein between experimental and control samples can be used to monitor its relative changes in abundance under these two conditions. Comparing the relative amount of many proteins in parallel in this manner enables a quantitative overview of the dynamically altered proteome, in our case the remodeled photosynthetic apparatus. To distinguish proteins from control and experimental conditions, differential isotopic labeling strategies can be

* The costs of publication of this article were defrayed in part by the payment of page charges. This article must therefore be hereby marked "*advertisement*" in accordance with 18 U.S.C. Section 1734 solely to indicate this fact.

§ Both authors contributed equally to this work.

‖ Supported by the Deutsche Forschungsgemeinschaft and the Research Foundation of the University of Pennsylvania. To whom correspondence should be addressed. Tel.: 215-898-4974; Fax: 215-898-8780; E-mail: mhippler@sas.upenn.edu.

[1] The abbreviations used are: PS, photosystem; LC-MS/MS, liquid chromatography and tandem mass spectrometry; RNAi, RNA interference; LHCI, light-harvesting complex; EST, expressed sequence tag.

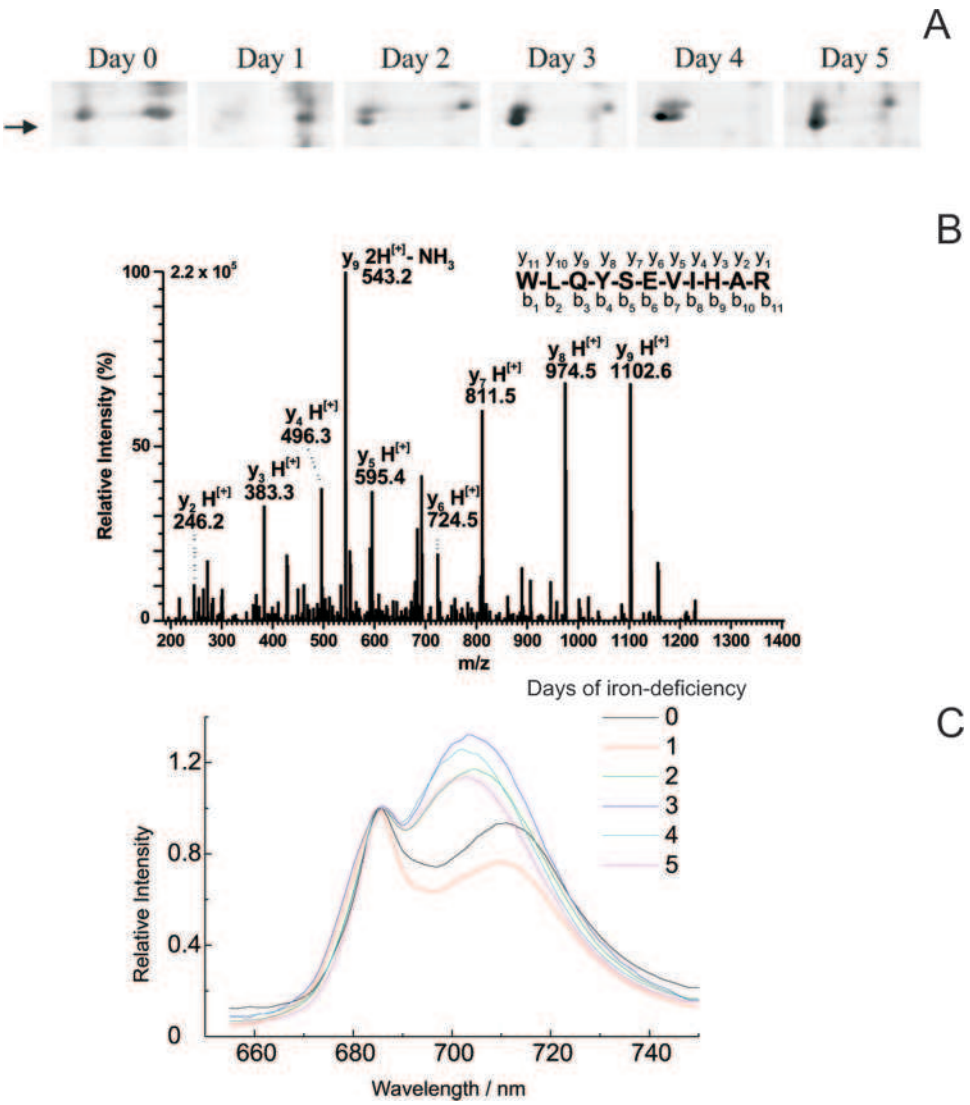

FIG. 1. **Induction of N-terminal processing of Lhca3 with the onset of iron deficiency correlates with the drop in efficiency in excitation energy transfer between LHCI and PSI.** *A*, analysis of thylakoid membranes isolated from *Chlamydomonas* cells grown for 0–5 days in iron deficiency revealed the induction of a new Lhca polypeptide, see *arrow* (adapted from Ref. 4). *B*, MS/MS analysis of this polypeptide identifies it as Lhca3. *C*, low temperature fluorescence emission spectroscopy of *Chlamydomonas* cells grown for 0–5 days in iron deficiency.

employed. Tagging of protein mixtures is either achieved by cross-linking proteins isolated from cells grown under different conditions with isotopically labeled and unlabeled chemical probes (15) or metabolic labeling with stable isotopes by growing cells in isotopically enriched media (16, 17). After tagging the protein or cells, pools are mixed, digested with enzymes, and quantified by liquid chromatography and tandem mass spectrometry (LC-MS/MS). A key assumption for both processes is that isotopically labeled and native peptides will behave similarly because the quantification is based on intensities or peak areas of both forms of the same peptide as measured in the mass spectrometer.

The green unicellular alga *C. reinhardtii* has emerged as a eukaryotic model system for the investigation of fundamental molecular processes in cell biology (18), and especially for the study of chloroplast-based oxygenic photosynthesis (19, 20). The availability of a draft genome sequence, including over 200,000 ESTs (21), allows application of genomic and proteomic methodologies (22). Quantitative approaches that are applicable on the proteomic scale, such as the one used in this study, will aid in the characterization of dynamic changes because of different physiological conditions or distinct genetic backgrounds.

MATERIALS AND METHODS

Strains and Cultures—The cell wall-less strain CC124 [CW15] or the arginine auxotrophic strain CC424 was used for all experiments. For all quantitative experiments using LC-MS/MS, strain CC424 was used. This strain was kindly provided by the *Chlamydomonas* culture collection (for information see the website www.chlamy.org). Cells were grown in the presence of either normal or isotopically labeled $^{13}C_6$-L-arginine (Cambridge Isotope Laboratories, Andover, MA). Arginine concentrations were 50 μg/ml (23). Cell culture and transfer of cells from iron-sufficient to iron-deficient media were carried out essentially as described (4).

Plasmid Construction—For generation of the inverted repeat Lhca3 construct, a short 216-bp fragment corresponding to the 3′-untranslated region of Lhca3 was amplified with PCR by using the EST clone AV387462 (www.kazusa.or.jp/en/plant/chlamy/EST/) (24) as template and the primers LH-FORS-P (aaaactgcaggctccagtcagc, underlined PstI) and LH-REV-E (atcgaattcggccgcagccacgac, underlined EcoRI) adding EcoRI and PstI restriction sites. A longer 316-bp fragment additionally contained 100 bp from the adjacent coding sequence that function as spacer in the inverted repeat construct and was amplified by using the primers LH-FORL-P (aaaactgcagtgtgatgaccggcaaag, underlined PstI) and LH-REV-E (atcgaattcggccgcagccacgac, underlined EcoRI). Both fragments were cloned in the antisense direction by using the vector pBluescript SK. The resulting inverted repeat cassette was excised with EcoRI and cloned in the unique EcoRI site of the Maa7/X inverted repeat construct that was kindly provided by H. Cerutti (see Ref. 25).

Nuclear Transformation and Selection—Nuclear transformation of *Chlamydomonas* was carried out by using a helium-driven PDS-1000/He particle gun (Bio-Rad) with 1100 pounds/square inch rupture discs (Bio-Rad). M10 tungsten particles (Bio-Rad) were coated with 2 μg of DNA of the IRMaa7/IRLhca3 construct, washed three times with 500 μl of absolute ethanol, and resuspended in 25 μl of absolute ethanol; 7 μl of the suspension were used for one transformation. Wild-type cells were grown at 25 °C and 50 μE m^{-2} s^{-1} in liquid TAP medium, and 4 × 10^7 cells were dispersed per TAP plate containing 1.5 mM L-tryptophan, 5 μg/ml paromomycin, and 5–10 μM 5-fluoroindole. The transformed cells were incubated at 25 °C and 3 μE m^{-2} s^{-1} for 1–2 weeks. The appearing transformants were transferred on fresh TAP plates containing L-tryptophan, paromomycin, and 5-fluoroindole and used for further investigations.

Isolation of Intact Chloroplasts—Cells were harvested by centrifugation (4 °C and 3,500 × *g*) and resuspended to a concentration of ~7 × 10^7 cells/ml in buffer with 0.3 M sucrose, 25 mM HEPES, and 0.5 mM $MgCl_2$. Cells were disrupted in a self-made nebulizing chamber by nebulizing the cell suspension against a ceramic ball with N_2 gas at a pressure of ~15 pounds/square inch. Intact chloroplasts were harvested using Percoll cushions of 80, 60, and 40% (v/v). Thylakoid membranes were isolated as described previously (26) from broken chloroplasts.

Isolation of PSI—Enrichment of PSI from thylakoids solubilized in *n*-dodecyl β-D-maltoside using sucrose gradient centrifugation was done as described previously (27).

Protein Analysis—Protein concentrations were determined using the Bradford assay (28). Differentially labeled samples (^{12}C and ^{13}C) were combined on an equal protein basis. Proteins were separated on 13% gels by SDS-PAGE (29, 30).

Immunodetection and LC-MS/MS Analyses of Proteins—Immunodetection was carried out as described previously (31). Antibodies directed against PsaD were produced using the following two peptides for immunization of rabbits: peptide 1, EAEAAPAAAKKAAEK; peptide 2, EAKKEQIFEMPTGGAA. Antibody production was managed by Eurogentec (Belgium). The antibodies were used in a 1:1000 dilution. The other antibodies used have been described before (4). In-gel tryptic digestion was carried out essentially as described previously (31), with acetonitrile as the organic phase. Autosampling and chromatography were done essentially as described previously (11). The following changes were made. Samples were first injected onto a μ-Precolumn (PepMap™ C18, 5 μm, 100 Å, 300 μm inner diameter × 5 mm; LC-Packings, Sunnyvale, CA) and washed for 4 min at a flow rate of 0.25 μl/min with the aqueous phase by a nano-column switching device (Switchos, LC-Packings) that directed the flow to the analytical column. A fused silica needle with 8-μm aperture (FS360-75-8-N-5-C12; New Objective, Woburn, MA) was used for ionization of peptides. Mass spectra were measured with an LCQ Deca XP Plus ion trap mass spectrometer (Thermo Electron, San Jose, CA). Acquisition of mass spectra and sequence identification using Sequest software (Thermo Electron, San Jose, California) were done as described previously (11). The presence of the $^{13}C_6$-Arg label was taken into account (+6 Da). For quantitative analysis, doubly charged sister peptides were chosen. Tandem mass spectra were gathered within a *m/z* range so that both sister peptides would be fragmented concurrently. A wide enough range (7–10 *m/z*) was chosen so that all isotope peaks were acquired. This was important because we observed a broadening of the isotope profile for the ^{13}C-labeled samples, which was probably because of metabolism of $^{13}C_6$-Arg and incorporation of ^{13}C into other amino acids. Peak areas for the LC-MS/MS elution profiles of ^{12}C- and ^{13}C-labeled singly or doubly charged y ions were then determined using Qualbrowser software (Thermo Electron, San Jose, CA). The abundance ratios were calculated from the peak areas. Ratios were calculated for all identified y ion pairs, and the mean ± S.D. was calculated. Because ratios calculated from the LC-MS/MS data differed from those observed from immunoblot analyses, the peak areas from the LC-MS/MS analyses were normalized to the immunoblot signals for Lhca3, PsaD, and CF1.

Fluorescence Emission Analysis—Low temperature fluorescence emission spectra were recorded on whole cells with a Fluorolog-3 (Horiba, Jobin Yvon Inc., Edison, NJ) spectrofluorometer. Data were normalized to the emission peak at 685 nm.

RESULTS

Identification of a New Lhca Protein by Two-dimensional Gel Electrophoresis and MS/MS—In a recent investigation, immunoblotting in combination with two-dimensional gel electrophoresis was used to detect a new light-harvesting complex protein that is specific for iron-deficient growth conditions (4).

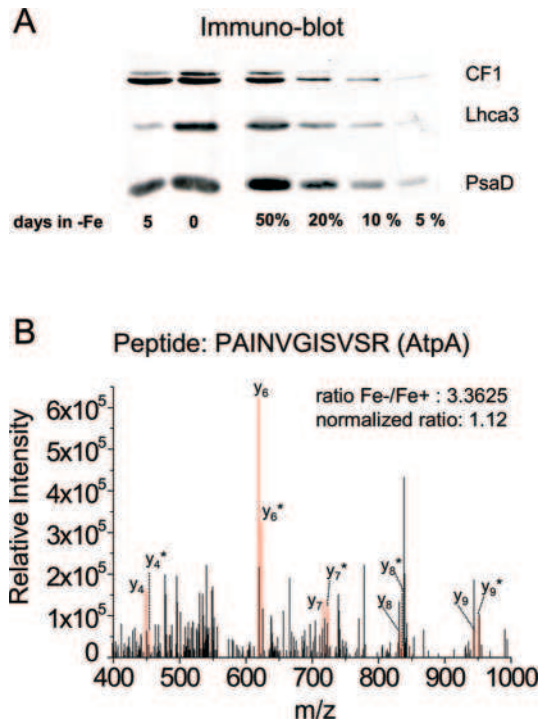

FIG. 2. **We performed quantitative immunoblot analysis of thylakoid membranes isolated from iron-sufficient and 5-day iron-deficient cells using anti-Lhca3, anti-PsaD, and anti-CF1 antibodies.** *A*, the abundance of CF1 remained stable after 5 days in iron deficiency, whereas the abundance of Lhca3 and PsaD are reduced to about 10–20 and 50%, respectively, as compared with iron-sufficient conditions at day 0. *B*, differentially isotopically labeled thylakoid membranes were fractionated by SDS-PAGE, and a protein band corresponding to AtpA was excised and digested with trypsin, and peptides were analyzed by LC-MS/MS. In the MS/MS fragmentation spectrum of the doubly charged peptide ion PAINVGISVSR (*m/z* 556.83) (chloroplast AtpA), labeled (*Fe+*) and unlabeled (*Fe−*), sister fragment ions can be detected. The labeled (marked *) y-type ions are 6 Da heavier in respect to the unlabeled y-type ions. For each y-type ion pair, the elution profiles were reconstructed and respective peak areas calculated. By dividing peak areas of sister ions, the relative abundance between iron-sufficient and -deficient conditions can be calculated. Calculation of the ratios in Fe−/Fe+ conditions of four y-type ion pairs resulted in a mean value of about 3.36. Western blot data, however, showed that the relative abundance of the ATP synthase does not change between iron-sufficient and -deficient conditions. Therefore, we normalized the quantitative mass spectrometric data and divided the ratio obtained from Fe−/Fe+ conditions by a factor of 3. This normalization is applied to all comparative quantitative mass spectrometric data.

The protein spot containing this novel Lhca protein had been shown to increase in abundance during the adaptation to iron-deficient growth conditions in thylakoid membrane preparations (Fig. 1*A*). Analysis of a tryptic digest of this spot by MS/MS identified the protein as Lhca3 based on the fragmentation pattern of the two doubly charged ions, *m/z* 701.8 and 1015.8, that were matched with the Lhca3 peptide sequences WLQYSEVIHAR and GSGDAAYPGGPFFNLFNLGGK, respectively, using Sequest software. The fragmentation pattern of the peptide with a *m/z* 701.8 is shown in Fig. 1*B*.

The New Lhca3 Protein Is a Result of N-terminal Processing—Immunodetection of a higher molecular weight form of Lhca3 using an antibody specific for its N terminus (anti-14.1 (31)) showed that this form nearly completely disappeared in thylakoids isolated from iron-deficient growth conditions (4) (Fig. 2*A*). Because the lower molecular weight form of Lhca3 was no longer detected by the N-terminal specific antibody, it must be the product of a processing event at the N terminus of the protein. The protein spot corresponding to the processed form of Lhca3

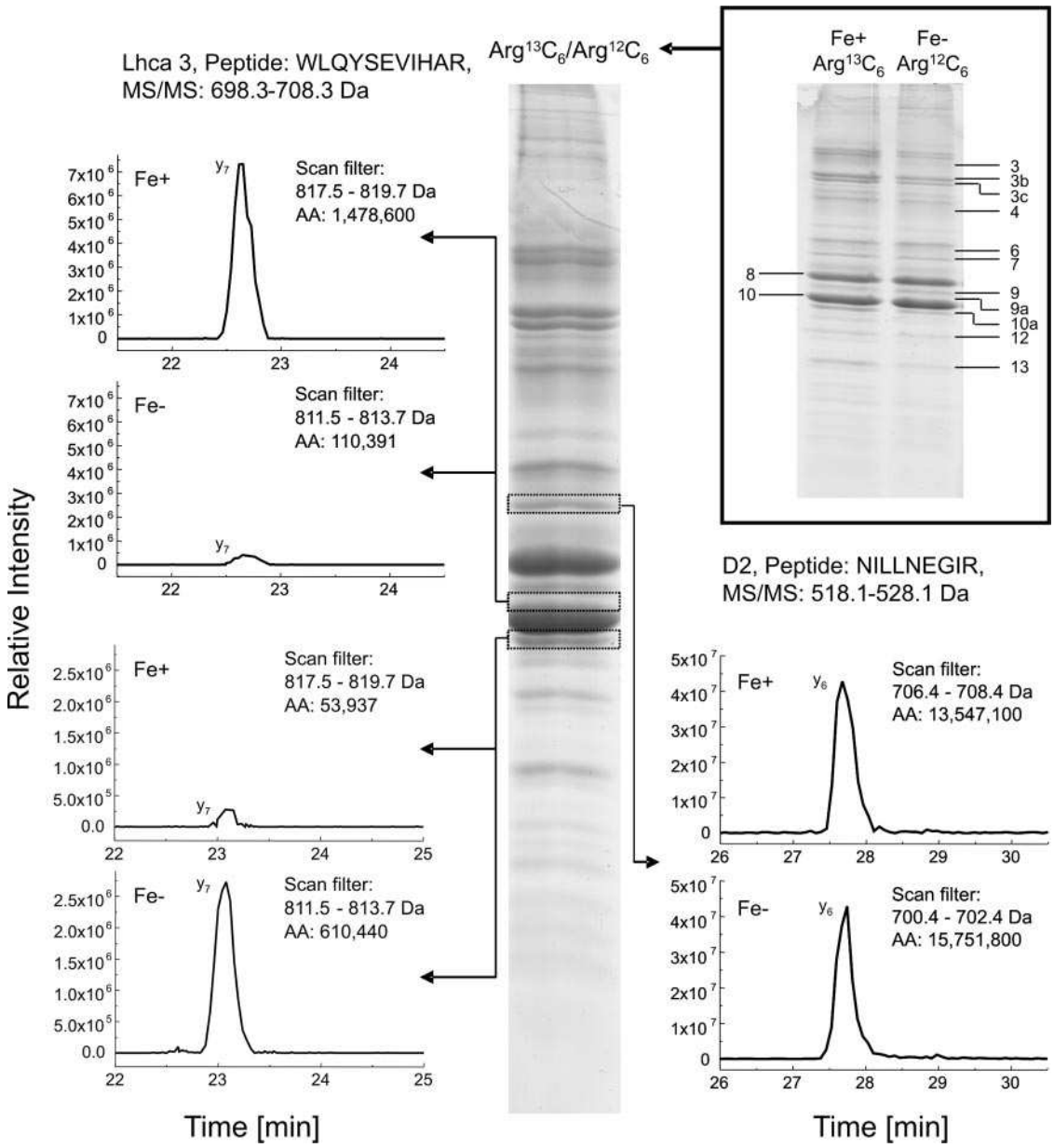

FIG. 3. **Comparative quantitative mass spectrometric peptide profiling using isotopic labeling of proteins demonstrates proteolytic processing of Lhca3.** Thylakoids isolated from $^{13}C_6$-Arg-labeled cells (+*Fe*) and $^{12}C_6$-Arg cells (5 days −*Fe*) were mixed on equal protein basis and separated by SDS-PAGE. Protein bands corresponding to the position of the mature Lhca3 proteins and the putative processed form were excised, and the proteins were digested with trypsin and analyzed by LC-MS/MS. Pairs of $^{13}C_6$-Arg- and $^{12}C_6$-Arg-labeled sister peptide ions were measured in the same MS/MS spectrum by choosing a respective parent ion for collision-induced fragmentation and a mass window of ± 5 Da. Resolution of the y_7 H^+ ion derived from the MS/MS fragmentation of a doubly charged Lhca3 peptide ion WLQYSEVIHAR[$2H^+$] using the data filter 817.5–819.7 ($^{13}C_6$-Arg/Fe(+)) and 811.5–813.7 ($^{12}C_6$-Arg/Fe(−)) shows that the Fe(+) peptide is present in the higher molecular weight band in iron-sufficient conditions but absent from the lower molecular weight band, whereas the reverse is true for the Fe(−) peptide, demonstrating that only the processed form of Lhca3 is present under iron-deficient conditions. Resolution of the doubly charged y ions of the D2 peptide NILLNEGIR shows nearly equal protein loading of the thylakoids isolated from iron-sufficient and -deficient conditions.

has an isoelectric point (pI) of about 5.0 and is slightly more acidic as compared with the mature protein (pI 5.1) (4). Calculation of its molecular mass from SDS-PAGE analysis, using known masses for Lhca1, Lhca3, Lhca4, Lhca5, and PsaF yielded a value of about 23,800 Da. Molecular masses and pI of processed forms, assuming putative processing events within the N-terminal part, were calculated by using the computation pI/MW tool on the Expasy website (us.expasy.org/tools/pi_tool.html). This analysis revealed that processing between DR (closest to the N terminus, between positions 9 and 10) and DG (most distant from N terminus, positions 27 and 28) defined the region where processing occurs, because only processing in-between these sites would produce a product having a pI value more acidic as compared with the mature protein and an appropriate molecular mass in respect to the mass estimated for the processed form. By taking the molecular mass, the fact that the first 15 N-terminal amino acids were used for immunization (EEKSIAKVDRSKDQL), and the pI of the processed form into account, we suggested that the novel N terminus starts at amino acid 16 (YVGASQ . . .) or amino acid 17 (VGASQ . . .).

N-terminal Processing of Lhca3 Correlates with the Impaired Efficiency of Excitation Energy Transfer from LHCI to PSI—Adaptation of *Chlamydomonas* to iron deficiency leads to a decreased efficiency of excitation energy transfer between LHCI and PSI (4). To determine whether the impact on efficiency correlates with induction of the N-terminal processing of

TABLE I

Relative abundance of proteins from the LHCI and the PSI core complex, the LHCII and the PSII core complex, and proteins from the ATP synthase (Fig. 3) isolated from thylakoids from cells grown in iron-deficient and iron-sufficient conditions, respectively

$^{13}C_6$-Arg-labeled cells (+Fe) and $^{12}C_6$-Arg cells (5 days −Fe) are shown.

Protein	Peptide	Band	Ratio Fe−/Fe+[a]	S.D.[b]	*n*
Lhca1	FTESEVIHGR	12	0.39	0.08	7
Lhca3	WLQYSEVIHAR	9a	0.02	0.01	8
Lhca3	WLQYSEVIHAR	10	0.17	0.05	6
Lhca3 N-terminal processed	WLQYSEVIHAR	10a	10.96	5.26	6
Lhca4	WYAQAELMNAR	9	1.13	0.26	4
Lhca5	QSELQHAR	9a	0.03	0.03	3
Lhca7	FFDPMGLSR	11	0.31	0.26	4
	WYVQAELVHGR	11	<0.01	<0.01	3
	Average of two peptides		0.15	0.22	
Lhca8	WYQQAELIHCR	11	0.07	0.03	2
Lhca9	GALAGDNGFDPLGLGQDEGR	12	1.69	0.67	8
PsaA	DYDPTNNYNNLLDR	3	0.45	0.14	4
PsaB	DKPVALSIVQAR	3	0.34	0.03	3
	FSQGLAQDPTTR	3	0.59	0.33	3
	Average of two peptides		0.47	0.15	
PsaD	EQIFEMPTGGAAIMR	13	0.55	0.20	4
PsaF	EENITVSPR	13	0.38	0.00	3
Lhcbm1–10	ELELIHAR	10	0.90	0.19	9
D1	VLNTWADIINR	6	0.63	0.12	4
	FGQEEETYNIVAAHGYFGR	6	0.82	0.31	4
	Average of two peptides		0.72	0.13	
D2	NILLNEGIR	7	0.83	0.09	3
	AFNPTQAEETYSMVTANR	7	1.26	0.35	4
	AYDFVSQEIR	7	1.02	0.52	3
	Average of three peptides		1.04	0.21	
CP43	SPTGEIIFGGETMR	4	1.08	0.21	4
	LKNDIQPWQER	4	1.17	0.09	4
	DQETTGFAWWSGNAR	4	0.76	0.16	4
	Average of three peptides		1.01	0.22	
AtpA	AIESPAPGIVAR	3b	1.63	0.35	4
	EAYPGDVFYLHSR	3b	0.91	0.24	4
	PAINVGISVSR	3b	1.12	0.65	4
	Average of three peptides		1.22	0.37	
AtpB	DVNKQDVLFFINDNIFR	3c	1.01	0.36	4
	FVQAGAEVSALLGR	3c	1.01	0.15	4
	Average of two peptides		1.01	0.00	

[a] Ratios were normalized with immunoblot data (Fig. 2).

[b] S.D. was calculated for different y ions, and for some peptides y-type ions from up to five independent measurements are presented.

Lhca3, we measured low temperature fluorescence emission spectra from *Chlamydomonas* cells that were grown under iron-sufficient conditions and then shifted to iron-deficient growth conditions for 1–5 days (Fig. 1*C*). Fluorescence peaks at 685 and 711 nm obtained with whole cells grown under iron-sufficient conditions are characteristic of LHCII attached to PSII and LHCI attached to PSI, respectively (32). In the absence of PSI or in case of functional impairment of excitation energy transfer between LHCI and PSI, the LHCI fluorescence emission is shifted toward 700–705 nm (32, 33). Most interestingly, the low temperature fluorescence emission maximum from iron-replete cells at 711 nm changes to 704 nm after 2 days in iron deficiency (Fig. 1*C*). Concomitant with the "blue shift" is an increase of the fluorescence emission as normalized to emission at 685 nm, indicating that excitation energy transfer between LHCI and PSI was strongly impaired. In the subsequent days, the fluorescence emission maximum remained "blue-shifted," and the extent of fluorescence decreased toward day 5. A significant portion of the processed product of Lhca3 was already detectable after 2 days (Fig. 1*A*) and thus correlated with the drop in efficiency of excitation energy transfer between LHCI and PSI. In order to monitor the dynamic adaptation to iron deficiency, with a particular emphasis on the LHCI protein composition, we employed comparative quantitative proteomics.

The Lhca Proteins Are Affected to Varying Degrees by Iron Deficiency—We took advantage of arginine auxotrophic *Chlamydomonas* cells, which were grown in the presence of L-Arg in iron-replete conditions and transferred for 5 days to iron-deficient conditions. In parallel, the auxotrophic cells were grown under iron-sufficient conditions in the presence of isotopically labeled L-Arg, harboring six ^{13}C atoms. Chloroplasts were isolated from both conditions and separated into thylakoid and envelope membranes and stroma proteins. Thylakoid samples were mixed on an equal protein basis and separated by SDS-PAGE (Fig. 3). Protein bands as indicated in Fig. 3 were excised, digested with trypsin, and analyzed by LC-MS/MS. In a first round of analyses, sequence identity and the presence of an Arg residue in the tryptic peptide was established by using the Sequest algorithm. In a second round of analyses, Arg-containing peptides were analyzed quantitatively. The selected peptide ion pairs ($^{12}C_6$-Arg/$^{13}C_6$-Arg) were fragmented concurrently (Fig. 2*B*). In the MS/MS spectrum, singly charged y ions can be distinguished by a mass difference of 6 or 3 Da in the case of doubly charged ions. These different y ions originating from the sister peptide ions were used for quantification by comparing the total ion count peak area of respective labeled and unlabeled fragment sister ions (Table I). Quantification using fragment ions rather than parent ions reduced background signals from unrelated peptide ions significantly, and in most cases nearly completely. The abundance of the peptides was based on the peak areas for several fragment ions. We also performed quantitative immunoblot analysis of thylakoid membranes isolated from iron-sufficient and 5-day iron-deficient cells using anti-Lhca3, anti-PsaD, and anti-CF1 antibodies (Fig. 2*A*). These analyses showed that the mature forms of Lhca3 and PsaD were down to 5–10% and 20–50%, respectively, whereas the ATPase was unaffected as reported before

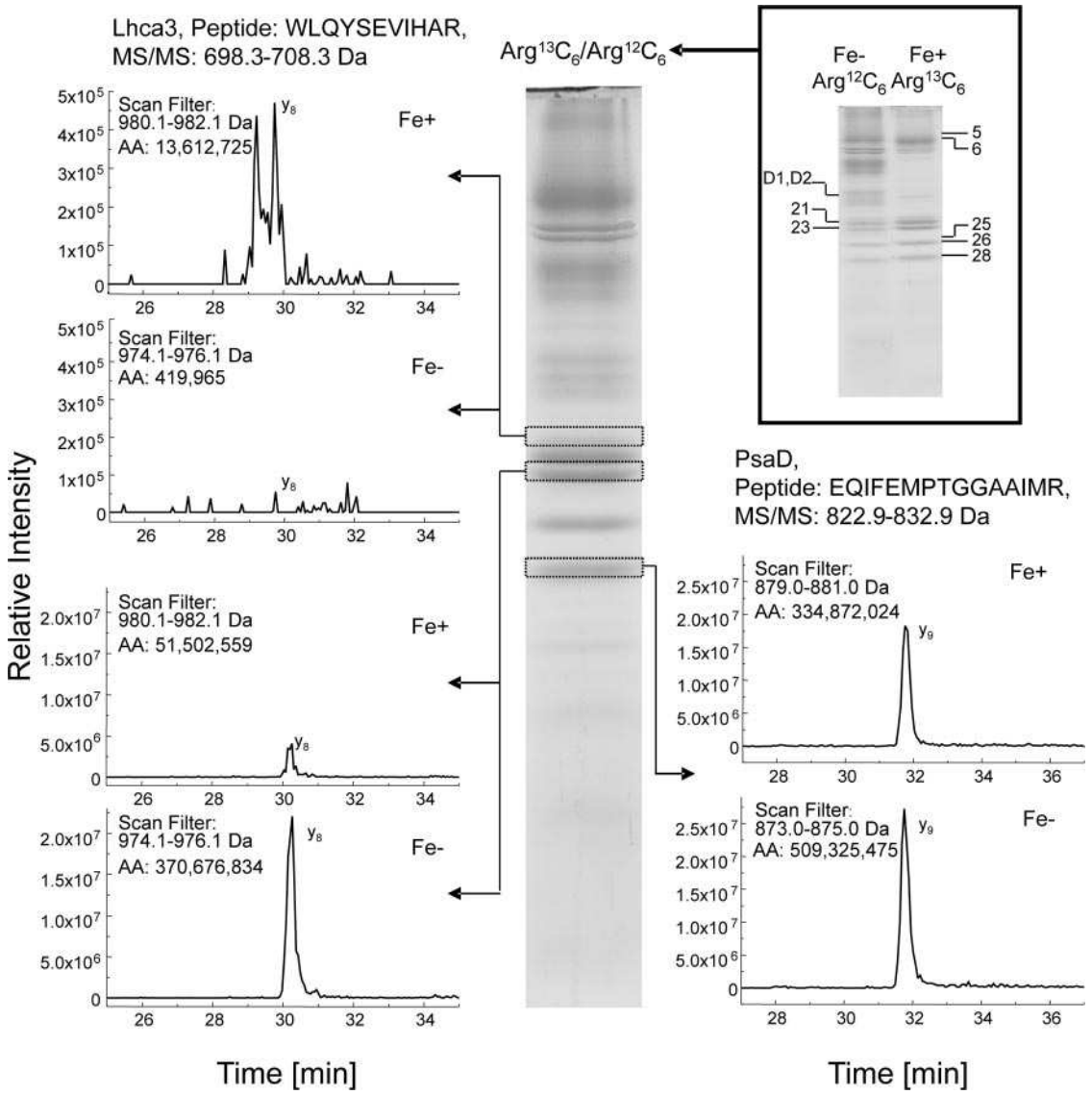

FIG. 4. **Quantitative mass spectrometric peptide profiling reveals that the processed form of Lhca3 remains stably associated with PSI under iron deficiency.** Quantitative analysis was performed as described in Fig. 2.

(4). More importantly, we used these immunoblot data to normalize the LC-MS/MS data for isotopically labeled peptides. By using the comparative quantitative assay, we investigated the N-terminal processing of Lhca3 (Fig. 3). Resolution of a singly charged y_7 ion, derived from the MS/MS fragmentation of the Lhca3 peptide ion WLQYSEVIHAR[$2H^+$], using the *m/z* filters 817.5–819.7 (for the labeled ion) and 811.5–813.7 (for the unlabeled ion), showed that the labeled peptide was present in the higher molecular weight band in iron-sufficient conditions but was absent from the lower molecular weight band, whereas the reverse is true for the unlabeled peptide. These data demonstrated that the processed form of Lhca3 was dominant under iron-deficient conditions, whereas the mature form was largely diminished under the same conditions. Resolution of the doubly charged y_6 fragment ion from the MS/MS fragmentation of the peptide NILLNEGIR[$2H^+$], originating from the PSII core subunit D2, showed nearly equal protein loading of the thylakoids isolated from iron-sufficient and -deficient conditions. Analysis of other y-type ions resulting from fragmentation of the Lhca3 or D2 peptide ions showed the same results (Table I). Consistent with the data for D2, analysis of CP43 peptides ions clearly indicated that PSII was not affected after 5 days of iron deficiency; however, the levels of D1 were slightly decreased with respect to iron-sufficient conditions. The ATPase subunits (AtpA and AtpB), as well as the major light-harvesting complex proteins Lhcbm (Table I) (all of which were used as loading controls), do not change significantly between iron-replete and -deficient conditions. Analysis of the PSI subunits PsaA, PsaB, PsaD, and PsaF showed that after 5 days in iron deficiency the PSI complex was down to about 45% with respect to iron-replete conditions (Table I). The impact of iron deficiency on LCHI was more dramatic. Besides the N-terminal processing of Lhca3, Lhca5 almost completely disappeared, and the amounts of Lhca1, Lhca7, and Lhca8 were reduced, whereas the Lhca4 and Lhca9 polypeptides were induced under iron-deficient conditions in respect to PSI (Table I). We confirmed the down-regulation of Lhca5 by immunoblotting using Lhca5-specific antibodies (31) (data not shown). We also detected peptides of Lhca2 and Lhca6 by MS/MS, but did not obtain adequate resolution of fragment ions for quantification.

The N-terminal Processed Form of Lhca3 Remains with the PSI Complex When Isolated from Iron-deficient Conditions—To evaluate whether the processed form of Lhca3 remained with PSI after the onset of iron deficiency and to define the LHCI composition under these conditions, we isolated PSI particles from arginine auxotrophic cells that were grown for 5 days

TABLE II
Relative abundance of proteins from LHCI and PSI core complex isolated from purified PSI from cells grown either under iron-deficient or -sufficient conditions (for some peptides, y-type ions from up to five independent measurements are presented)
$^{13}C_6$-Arg-labeled cells (+Fe) and $^{12}C_6$-Arg cells (5 days −Fe) are shown.

Protein	Peptide	Band	Ratio Fe−/Fe+	S.D.	*n*
Lhca1	FTESEVIHGR	26	0.62	0.04	3
Lhca3	WLQYSEVIHAR	21	0.20	0.16	7
Lhca3 N-terminal processed	WLQYSEVIHAR	23	8.05	2.33	7
Lhca4	WYAQAEILMNAR	21	1.27	0.52	9
Lhca5	QSELQHAR	21	0.13	0.07	6
Lhca7	WYVQAELVHGR	23	0.72	0.15	8
Lhca8	WYQQAELIHCR	23	0.66	0.34	12
Lhca9	GALAGDNGFDPLGLGQDEGR	25,26	1.45	0.45	22
PsaA	DYDPTNNYNNLLDR	6	1.30	0.81	4
	EIPLPHDLLLNR	6	2.79	0.64	10
	Average of two peptides		2.05	1.05	
PsaB	DKPVALSIVQAR	5,6	1.33	0.65	8
PsaD	EQIFEMPTGGAAIMR	28	1.73	0.45	19
PsaF	LAWQGAGWPLAAVQELQR	28	1.38	0.33	8

under iron deficiency in the presence of $^{12}C_6$-Arg. In parallel, we isolated PSI particles from cells of the same strain that were grown under iron-sufficient conditions in the presence of $^{13}C_6$-Arg. In contrast to iron-sufficient conditions, PSI particles from iron-deficient conditions migrated at lower sucrose density after sucrose density centrifugation together with PSII particles (confirmed by mass spectrometric analyses, see the presence of D1 and D2 PSII core subunits in iron-deficient PSI preparation in Fig. 4). PSI particles isolated from iron-deficient conditions had a higher chlorophyll *a*/*b* ratio (9.3) as compared with iron-sufficient particles (5.5). PSI particles from both fractions were mixed on an equal protein basis and fractionated by SDS-PAGE. Protein bands corresponding to the mature and processed form of Lhca3 were excised from the gel and digested in-gel with trypsin. The corresponding peptides were analyzed by LC-MS/MS. Resolution of the y_8 H^+ ion, from Lhca3 peptide ion WLQYSEVIHAR[2H$^+$], showed that the $^{13}C_6$-Arg/Fe+ peptide is present in the higher molecular weight band in iron-sufficient conditions but absent from the lower molecular weight band, whereas the contrary was true for the $^{12}C_6$-Arg/Fe− peptide. These data demonstrated that the processed form of Lhca3 can be isolated with the PSI complex under iron-deficient conditions. In contrast the mature form of Lhca3 was significantly reduced under the same conditions as expected from the results obtained with thylakoids. The PSI core subunits isolated from iron-deficient conditions were slightly enriched compared with the PSI core complex isolated under iron-sufficient samples. Analysis of the PSI subunits PsaA, PsaB, PsaD, and PsaF showed that the PSI core complex from iron-deficient conditions was about 1.6-fold more abundant than the one isolated from iron-sufficient conditions (Table II). The antenna proteins Lhca1, Lhca7, and Lhca8 were equally reduced with respect to iron-sufficient conditions. On the contrary, levels of Lhca4 and Lhca9 were significantly increased, which is consistent with the results obtained with whole thylakoids (Tables I and II). We did not obtain quantitative data for Lhca2 and Lhca6. When the relative abundance of Lhca polypeptides *versus* PSI subunits was calculated from ratios obtained from iron-deficient and iron-sufficient thylakoids and isolated PSI particles (Tables I and II), Lhca1 decreased from 0.86 in thylakoids to 0.38 in purified particles; the mature form of Lhca3 increased from 0.04 to 0.12; Lhca4 decreased from 2.53 to 0.79; Lhca5 remained low; Lhca7 slightly increased from 0.34 to 0.44; Lhca8 increased from 0.15–0.40, and Lhca9 decreased from 3.78 to 0.89 (Table III). The relative loss of Lhca1, Lhca4, and Lhca9 in PSI particles *versus* thylakoids could be explained by the fact that these proteins were lost during the purification procedure. Nevertheless, it is interesting to note that the relative abundance of Lhca1, Lhca7, and Lhca8 are the same and that Lhca4 and Lhca9 proteins are 2–3-fold higher as compared with the other three polypeptides per iron-deficient PSI. The same holds true for the processed form of Lhca3 that is significantly enriched in PSI particles isolated from iron-deficient conditions. The functional implication of the N-terminal processing of Lhca3 on the remodeling process of PSI-LHCI was further tested by depletion of Lhca3 using an RNAi strategy.

TABLE III
Differential ratios for LCHI proteins and the PSI core during iron deficiency adaptation
Data are taken from Tables I and II.

Protein	Ratio subunit/PSI core	
	Thylakoids	Purified PSI particles
Lhca1	0.9	0.40
Lhca3	0.04	0.10
Lhca3 N-terminal processed	24.5	5.00
Lhca4	2.50	0.80
Lhca5	0.07	0.08
Lhca7	0.34	0.45
Lhca8	0.15	0.40
Lhca9	3.8	0.90

Suppression of Lhca3 by RNAi Technology Impairs Excitation Energy Transfer between LHCI and PSI and Abolishes Binding between LHCI and PSI—Using a tandem inverted repeat system for selection of effective transgenic RNAi strains in *Chlamydomonas* (25), we generated mutant strains with significantly reduced levels of Lhca3 protein expression. For construction of the RNAi expression cassette, we used 216 bp of the 3′-untranslated region of the *lhca3* gene. Low temperature fluorescence emission spectroscopy (Fig. 5*A*) using whole cells of a strain that contained less than 10% of Lhca3, as assessed by immunoblot analysis (see Fig. 5*B*), showed a blue-shifted fluorescence emission maximum at 704 nm and exhibited a higher level of maximal fluorescence as compared with wild type. These observed changes in the low temperature fluorescence spectrum between the Lhca3-depleted mutant and wild type were very similar to spectral changes obtained with iron-deficient wild-type cells (Fig. 1), indicating that in terms of excitation energy transfer, LHCI and PSI are largely disconnected in the absence of Lhca3. Solubilization of Lhca3-depleted thylakoid membranes with detergent and fractionation by sucrose density centrifugation resulted, in contrast to wild type, in PSI particles that contained different amounts of Lhca3 with respect to the PSI core (as assessed by PsaD immunoblot analysis, see Fig. 5*C*). The lower sucrose density

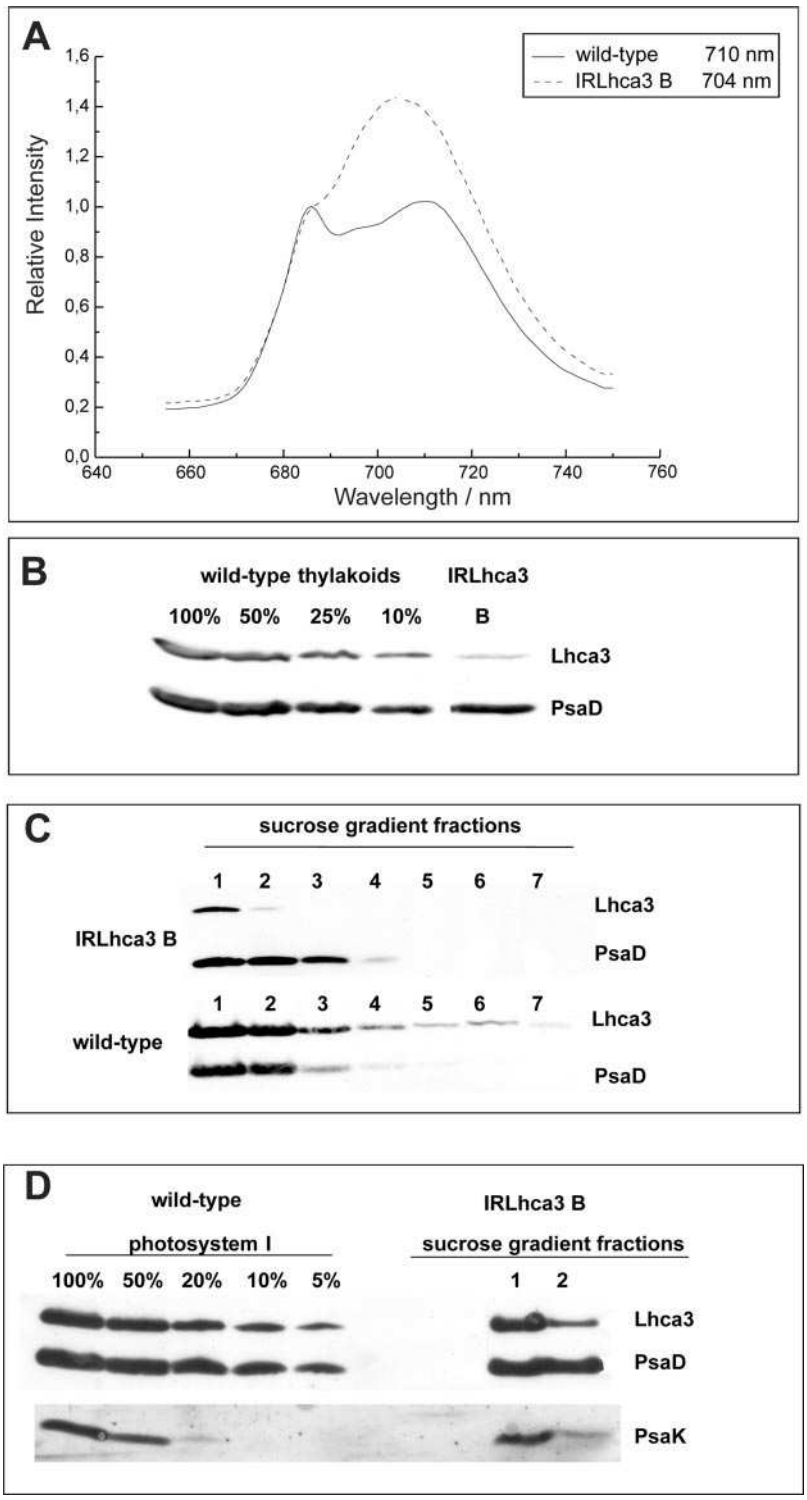

FIG. 5. **Suppression of Lhca3 by RNAi technology impairs excitation energy transfer between LHCI and PSI and impacts binding between LHCI and PSI.** *A*, for low temperature fluorescence emission spectra of whole cells at 77 K, cells were suspended in 60% glycerol, 10 mM HEPES, pH 7.5, on the basis of equal chlorophyll (20 μg/ml); *B–D*, SDS-PAGE separation according to Laemmli (29) (*B* and *C*) and Schaegger and von Jagow (30) (*D*) followed by Western blot analysis using anti-Lhca3, anti-PsaD or PsaK antibodies. *B*, for immunodetection of Lhca3 and PsaD in isolated thylakoids, the samples were loaded on the basis of equal chlorophyll (5 μg). *C*, for immunodetection of Lhca3 and PsaD in sucrose gradient fractions after solubilization of thylakoids with detergent and sucrose density centrifugation, the gradient was fractionated from the bottom to the top starting under the band corresponding to PSI-LHCI; the samples were loaded on the basis of equal volume (40 μl). *D*, for immunodetection of Lhca3, PsaD, and PsaK, dilution series of wild-type PSI was generated to estimate the remaining levels of Lhca3 and PsaK in the sucrose gradient fractions; the samples were loaded on the basis of equal protein (20 μg).

fraction 1 contained about 40% and the lighter sucrose fraction 2 less than 10% of the wild-type Lhca3 levels (Fig. 5*C*). Most interestingly, PSI particles that are strongly depleted in Lhca3 (fraction 2) were also depleted in PsaK (Fig. 5*D*). To assess the LHCI polypeptide composition of the Lhca3-depleted cells with respect to wild type, we isolated thylakoids and PSI particles. The isolated membranes and particles were mixed on a equal protein concentration with corresponding material isolated from wild-type cells grown in the presence of isotopically labeled arginine and separated by SDS-PAGE. Protein bands containing LHCI and PSI polypeptides were excised, digested with trypsin, and analyzed by LC-MS/MS for quantitative peptide profiling. By using this technique, we were able to generate comparative quantitative data for PsaA and PsaB as well as Lhca1, Lhca3, Lhca4, Lhca5, Lhca7, Lhca8, and Lhca9 polypeptides (Tables IV and V). In thylakoid membranes, the Lhca subunit to PSI core ratios were about 1 and 0.9 for Lhca7 and Lha5, respectively, slightly decreased for Lhca1 and Lhca4, increased for Lhca9, and strongly diminished for Lhca3, as expected from the immunoblot results (Fig. 5*B*). These data showed that stable accumulation of Lhca1, Lhca4, Lhca5, Lhca7, Lhca8, and Lhca9 in thylakoids was not severely affected by the absence of Lhca3. The relative Lhca3 polypeptide to PSI core content in isolated Lhca3-depleted *versus* wild-type

TABLE IV

Relative abundance of proteins from the LHCI and the PSI core complex isolated from thylakoids and isolated PSI particles from wild type cells ($^{13}C_6$-Arg-labeled cells) and cells of an Lhca3-depleted RNAi strain (strain B, Fig. 5, $^{12}C_6$-Arg cells)

Protein	Peptide	Ratio IRLhca3/WT	S.D.	*n*
Thylakoids				
Lhca1	FTESEVIHGR	0.59	0.14	9
Lhca3	WLQYSEVIHAR	0.14	0.03	7
Lhca4	WYAQAELMNAR	0.58	0.26	4
Lhca5	QSELQHAR	0.91	0.36	3
Lhca7	FFDPMGLSR	1.37	0.64	4
	WYVQAELVHGR	0.62	0.44	14
	Average of two peptides	1.00	0.53	
Lhca9	GALAGDNGFDPLGLGQDEGR	2.49	0.79	15
PsaA	EIPLPHDLLLNR	1.95	0.48	5
	EILEAHR	0.75	0.50	5
	Average of two peptides	1.35	0.84	
PsaB	FSQGLAQDPTTR	0.83	0.25	8
PSI particles, fraction 1				
Lhca1	FTESEVIHGR	0.96	0.21	9
Lhca3	WLQYSEVIHAR	0.71	0.22	7
Lhca4	WYAQAELMNAR	0.41	0.13	6
Lhca7	FFDPMGLSR	0.71	0.41	4
	WYVQAELVHGR	0.53	0.21	4
	Average of two peptides	0.62	0.13	
Lhca9	GALAGDNGFDPLGLGQDEGR	4.34	1.75	15
PsaA	EIPLPHDLLLNR	2.66	1.01	6
PsaB	FSQGLAQDPTTR	1.81	0.92	10
PSI particles, fraction 2				
hca1	FTESEVIHGR	0.33	0.12	16
Lhca3	WLQYSEVIHAR	0.15	0.04	13
Lhca4	WYAQAELMNAR	0.39	0.16	3
Lhca5	QSELQHAR	0.60	0.09	3
Lhca7	WYVQAELVHGR	0.20	0.10	8
Lhca8	WYQQAELIHCR	0.37	0.27	3
Lhca9	GALAGDNGFDPLGLGQDEGR	1.22	0.36	10
PsaA	EIPLPHDLLLNR	1.60	0.21	3
	DYDPTNNYNNLLDR	2.73	0.95	5
	Average of two peptides	2.17	0.53	

TABLE V

Differential ratios for LCHI proteins and the PSI core derived from thylakoids and isolated PSI particles from wild type cells and cells of an Lhca3-depleted RNAi strain (strain B, Fig. 5)

Data are taken from Table IV.

Protein	Ratio subunit/PSI core		
	Thylakoids	PSI particles, fraction 1	PSI particles, fraction 2
Lhca1	0.59	0.44	0.15
Lhca3	0.14	0.32	0.07
Lhca4	0.58	0.19	0.18
Lhca5	0.91		0.28
Lhca7	1.00	0.28	0.09
Lhca8			0.17
Lhca9	2.49	1.97	0.56

PSI declined to 0.3 and 0.07 in sucrose gradient fractions 1 and 2 (Fig. 5*C*), respectively. Strong depletion of Lhca3 (fraction 2) suppressed the accumulation of Lhca1, Lhca4, Lhca5, Lhca7, and Lhca8 with PSI below 30% in respect to wild type, suggesting that their binding to PSI was destabilized in the absence of Lhca3 (Fig. 6). In contrast, the ratio of Lhca9 to PSI appeared to be less affected by Lhca3 protein levels, indicating that Lhca9 binding to PSI might be more independent of Lhca3.

DISCUSSION

Adaptation to iron deficiency requires remodeling of the photosynthetic apparatus in *Chlamydomonas* (4). Our study reveals that a key mechanistic event of the remodeling process that affects PSI and its associated LHCI complex is the N-terminal processing of Lhca3. The induction of N-terminal processing of Lhca3 by progression of iron deficiency has been shown independently by 2-DE and mass spectrometric analysis and quantitative MS/MS peptide profiling using isotopic labeling of proteins. We further demonstrate that the remodeling of the LHCI complex under iron deficiency involves up-regulation of Lhca4 and Lhca9 polypeptides and down-regulation of Lhca5 in respect to PSI, which implies specific functional roles for these proteins. More importantly, the induction of N-terminal processing of Lhca3 by progression of iron deficiency correlates with the functional drop of excitation energy transfer efficiency between LHCI and PSI as assessed by low temperature fluorescence emission spectroscopy (Fig. 1). Most interestingly, depletion of Lhca3 by an RNAi approach also strongly impacts the efficiency of excitation energy transfer between PSI and LHCI (Fig. 5). However, in contrast to iron deficiency, depletion of Lhca3 abolishes stable binding of most Lhca proteins to PSI.

The recent crystal structure of PSI to 4.4 Å resolution from *Pisum sativum* (34) indicates that LHCI of higher plants forms a crescent structure that associates with the reaction center primarily through interactions between Lhca1 and the PsaG pole of PSI as well as through weaker interactions (mostly on the stromal side) between Lhca3 and the PsaK pole. The partners participating in the weaker of the interactions (PsaK/Lhca3) are primarily affected during iron deficiency in *Chlamydomonas* (4). N-terminal processing of Lhca3 could initiate the remodeling process and may also readily impair the excitation energy transfer between the antenna and the reaction center. In vascular plants as well as in *Chlamydomonas*, the major contributor to far red fluorescence is the LHCI complex, which contains chlorophylls that absorb at 710 nm and emit at 730 nm in vascular plants (~710 nm in *Chlamydomonas* (32, 33, 35)). These low energy forms have a large impact on energy transfer, and most of the excitation energy passes through them, via thermal activation to bulk chlorophylls, on the way to P700 (36, 37). Thermal transfer of energy may occur at the Lhca3/PsaK pole through the densely packed chlorophylls that are visible there in the crystal structure. The structural

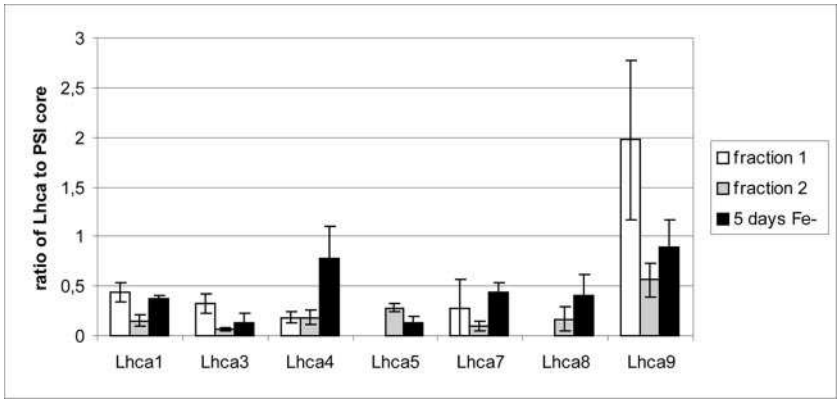

FIG. 6. **Ratio of Lhca polypeptide to PSI core in PSI particles isolated from cells grown for 5 days under iron deficiency and from an Lhca3-depleted strain (fractions 1 and 2, Fig. 5*C*) as revealed by comparative quantitative peptide profiling (data from Tables III and V).**

changes that occur may hamper this energy transfer. In vascular plants, Lhca3 contributes significantly to the most far red emissions (38, 39). In *Chlamydomonas* depletion of Lhca3 also causes a blue shift of the maximal low temperature fluorescence emission. However, in contrast to vascular plants (40), we show here that Lhca3 appears to be required for stable binding of Lhca1, Lhca4, Lhca5, Lhca7, and Lhca8 to PSI. Therefore, the fluorescence emission in the Lhca3-depleted strain may originate mainly from unassembled LHCI as observed in a PSI-deficient mutant (33). In light of the pea PSI crystal structure (34), it is surprising that depletion of Lhca3 has such a strong impact on binding of Lhca polypeptides to PSI. However, in contrast to vascular plants, LHCI can be isolated in the absence of PSI as a stable oligomeric complex from *Chlamydomonas* (33). Most interestingly Lhca2, Lhca3, and Lhca9 are not required for the stable oligomeric structure of the LHCI complex (33). It was suggested that association of these polypeptides with the LHCI complex is stabilized by the presence of the PSI core complex and/or promote formation of the PSI·LHCI complex. In line with this, we propose that Lhca3 functions as a linker to support formation of the PSI·LHCI supercomplex in *Chlamydomonas*.

It is interesting to note that binding of Lhca9 to PSI is less dependent on Lhca3. Lhca9 even seems to be induced by the absence of Lhca3, a behavior that has been also observed for Lhca5 in the absence of Lhca4 in *Arabidopsis* (41). As Lhca5 from *Arabidopsis*, Lhca9 from *Chlamydomonas* is, with respect to the other Lhca polypeptides, a rather low abundant protein (11). In contrast to Lhca3-depleted PSI particles, the levels of Lhca1, Lhca4, Lhca7, and Lhca8 are higher in the iron-deficient particles and do not correlate with levels of mature Lhca3. This indicates that the presence of the processed form of Lhca3 is sufficient to promote more stable binding between these Lhca polypeptides and PSI, which seems to be particularly important for the elevated accumulation of Lhca4 under iron deficiency. On the contrary, the level of Lhca5 to PSI ratio is lower under iron deficiency as compared with the ratio in Lhca3-depleted PSI particles, pointing to additional regulatory mechanisms that affect levels of Lhca5 accumulation under iron deficiency.

The fact that the processed form of Lhca3 remains with PSI is an important finding, because it strongly suggests that the processing of Lhca3 occurs at the level of the functionally assembled LHCI·PSI complex, which in turn implicates that the N-terminal processing of Lhca3 is a regulatory process that is catalyzed by a site-specific protease. It was shown recently (42) that de-epoxidation of violaxanthin to zeaxanthin is specifically associated with Lhca3. It was postulated that this conversion may function in scavenging reactive oxygen species. Therefore, the processed form of Lhca3 might stay with the PSI complex to fulfill this function.

From the crystal structure, the helix nearest the N terminus (helix B) of Lhca3 appears to project into the stroma and away from any other proteins present in the structure. Sequence alignments indicate that this unusually long helix B has been conserved throughout evolution (not shown). The excised N-terminal epitope contains eight charged amino acids, which likely serves as an electrostatic protein-protein interaction module for additional Lhca present in the *Chlamydomonas* PSI·LHCI supercomplex. Removal of this N-terminal domain could likely alter protein-protein interactions within LHCI, which thereby facilitates remodeling of the complex.

Besides, N-terminal processing of Lhca3, the down-regulation of Lhca5 and the up-regulation of Lhca4 and Lhca9 on protein levels in respect to PSI, are also major changes induced by iron deficiency. Lhca4 and Lhca5 are close homologues (11). It is tempting to speculate that the increase in Lhca4 and/or Lhca9 compensates for the loss of Lhca5 under iron deficiency. This may implicate that Lhca4 and Lhca9 are different in function with respect to Lhca5. Both proteins could be more efficient in energy dissipation than in light-harvesting, a hypothesis that can be tested in the future. It is interesting to note that both Lhca4 and Lhca9, but not Lhca5, possess an asparagine rather than a histidine residue at chlorophyll position *a5*. The presence of an asparagine residue at this position has been shown to be responsible for far red fluorescence in higher plants (39). Providing that there are no bulk chlorophylls connecting Lhca4 and Lhca9 and PSI, these proteins may act as sinks for dissipation of light energy.

In summary, we suggest that the N-terminal processing of Lhca3 induces a conformational change that triggers (i) the remodeling of LHCI and (ii) a decrease in the efficiency of excitation energy transfer from the antenna to the PSI reaction center. By comparing iron-deficient cells with those depleted in Lhca3 by using RNAi, we demonstrate here that the truncated form of Lhca3 must act as a keystone to stabilize the interaction of LHCI with PSI because lack of Lhca3 abolishes the interactions of other Lhca with PSI. Under this scenario, truncation of Lhca3 alters the structure of LHCI, and concurrently modulates the functional interaction of LHCI with PSI but does not abolish the physical link between LHCI and PSI. We also speculate that the loss of PsaK because of the onset of iron deficiency (4, 43) may be responsible for the enhanced susceptibility of Lhca3 to proteolytic processing, which in turn initiates the entire process. The comparative quantitative proteomic approach using isotopic labeling of proteins by labeled arginine has proven to be a very valuable tool. It is foreseeable that this approach will be attractive for studies in *Chlamydomonas* where physiological changes are related to dynamic comparative alterations in the proteome.

Acknowledgment—We are grateful to Monica Zhang for help with the isolation of iron-deficient PSI particles.

REFERENCES

1. Spiller, S., and Terry, N. (1980) *Plant Physiol.* **65,** 121–125
2. Terry, N. (1980) *Plant Physiol.* **65,** 114–120
3. Straus, N. A. (1994) in *The Molecular Biology of Cyanobacteria* (Bryant, D. A., ed) Kluwer Academic Publishers Group, Dordrecht, The Netherlands
4. Moseley, J. L., Allinger, T., Herzog, S., Hoerth, P., Wehinger, E., Merchant, S., and Hippler, M. (2002) *EMBO J.* **21,** 6709–6720
5. Behrenfeld, M. J., and Kolber, Z. S. (1999) *Science* **283,** 840–843
6. Guikema, J. A., and. Sherman, L. A. (1983) *Plant Physiol.* **74,** 90–95
7. Laudenbach, D. E., and Straus, N. A. (1988) *J. Bacteriol.* **170,** 5018–5026
8. Burnap, R. L., Troyan, T., and Sherman, L. A. (1993) *Plant Physiol.* **103,** 893–902
9. Boekema, E. J., Hifney, A., Yakushevska, A. E., Piotrowski, M., Keegstra, W., Berry, S., Michel, K. P., Pistorius, E. K., and Kruip, J. (2001) *Nature* **412,** 745–748
10. Bibby, T. S., Nield, J., and Barber, J. (2001) *Nature* **412,** 743–745
11. Stauber, E. J., Fink, A., Markert, C., Kruse, O., Johanningmeier, U., and Hippler, M. (2003) *Eukaryot. Cell* **2,** 978–994
12. Ranish, J. F., Yi, E. C., Leslie, D. M., Purvine, S. O., Goodlett, D. R., Eng, J., and Aebersold, R. (2003) *Nat. Genet.* **33,** 349–355
13. Steen, H., and Pandey, A. (2002) *Trends Biotechnol.* **20,** 361–364
14. Regnier, F. E., Riggs, L., Zhang, R., Xiong, L., Liu, P., Chakraborty, A., Seeley, E., Sioma, C., and Thompson, R. A. (2002) *J. Mass Spectrom.* **37,** 133–145
15. Gygi, S. P., Rist, B., Gerber, S. A., Turecek, F., Gelb, M. H., and Aebersold, R. (1999) *Nat. Biotechnol.* **17,** 994–999
16. Ong, S. E., Blagoev, B., Kratchmarova, I., Kristensen, D. B., Steen, H., Pandey, A., and Mann, M. (2002) *Mol. Cell. Proteomics* **1,** 376–386
17. Oda, Y., Huang, K., Cross, F., Cowburn, D., and Chait, B. (1999) *Proc. Natl. Acad. Sci. U. S. A.* **96,** 6591–6596
18. Harris, E. H. (2001) *Annu. Rev. Plant Physiol. Plant Mol. Biol.* **52,** 363–406
19. Hippler, M., Rimbault, B., and Takahashi, Y. (2002) *Protist* **153,** 197–220
20. Rochaix, J. D. (2002) *FEBS Lett.* **529,** 34–38
21. Shrager, J., Hauser, C., Chang, C. W., Harris, E. H., Davies, J., McDermott, J., Tamse, R., Zhang, Z., and Grossman, A. R. (2003) *Plant Physiol.* **131,** 401–408
22. Stauber, E. J., and Hippler, M. (2004) *Plant Physiol. Biochem.* **42,** 989–1001
23. Yamaguchi, K., Prieto, S., Beligni, M. V., Haynes, P. A., McDonald, W. H., Yates, J. R., III, and Mayfield, S. P. (2002) *Plant Cell* **14,** 2957–2974
24. Asamizu, E., Nakamura, Y., Sato, S., Fukuzawa, H., and Tabata, S. (1999) *DNA Res.* **6,** 369–373
25. Rohr, J., Sarkar, N., Balenger, S., Jeong, B. R., and Cerutti, H. (2004) *Plant J.* **40,** 611–621
26. Chua, N. H., and Bennoun, P. (1975) *Proc. Natl. Acad. Sci. U. S. A.* **72,** 2175–2179
27. Hippler, M., Drepper, F., Farah, J., and Rochaix, J. D. (1997) *Biochemistry* **36,** 6343–6349
28. Bradford, M. M. (1976) *Anal. Biochem.* **72,** 248–254
29. Laemmli, U. K. (1970) *Nature* **227,** 680–685
30. Schagger, H., and von Jagow, G. (1987) *Anal. Biochem.* **166,** 368–379
31. Hippler, M., Klein, J., Fink, A., Allinger, T., and Hoerth, P. (2001) *Plant J.* **28,** 595–606
32. Wollman, F.-A., and Bennoun, P. (1982) *Biochim. Biophys. Acta* **680,** 352–360
33. Takahashi, Y., Yasui, T. A., Stauber, E. J., and Hippler, M. (2004) *Biochemistry* **43,** 7816–7823
34. Ben-Shem, A., Frolow, F., and Nelson, N. (2003) *Nature* **426,** 630–635
35. Bassi, R., Soen, S. Y., Frank, G., Zuber, H., and Rochaix, J. D. (1992) *J. Biol. Chem.* **267,** 25714–25721
36. Croce, R., Zucchelli, G., Garlaschi, F. M., and Jennings, R. C. (1998) *Biochemistry* **37,** 17355–17360
37. Jennings, R. C., Zucchelli, G., Croce, R., and Garlaschi, F. M. (2003) *Biochim. Biophys. Acta* **1557,** 91–98
38. Schmid, V. H., Potthast, S., Wiener, M., Bergauer, V., Paulsen, H., and Storf, S. (2002) *J. Biol. Chem.* **277,** 37307–37314
39. Morosinotto, T., Breton, J., Bassi, R., and Croce, R. (2003) *J. Biol. Chem.* **278,** 49223–49229
40. Ganeteg, U., Strand, A., Gustafsson, P., and Jansson, S. (2001) *Plant Physiol.* **127,** 150–158
41. Ganeteg, U., Klimmek, F., and Jansson, S. (2004) *Plant Mol. Biol.* **54,** 641–651
42. Wehner, A., Storf, S., Jahns, P., and Schmid, V. H. (2004) *J. Biol. Chem.* **279,** 26823–26829
43. Nield, J., Redding, K., and Hippler, M. (2004) *Eukaryot. Cell* **3,** 1370–1380

Manuscript 5

Einar J. Stauber, Andreas Busch, Bianca Naumann, Aleš Svatoš, and Michael Hippler (2007) Proteotypic profiling of LHCI from *Chlamydomonas reinhardtii* provides new insights into structure and function of the complex. **In preparation for Proteomics** .

Proteotypic profiling of LHCI from Chlamydomonas reinhardtii provides new insights into structure and function of the complex

Journal:	*PROTEOMICS*
Manuscript ID:	draft
Wiley - Manuscript type:	Research Article
Date Submitted by the Author:	n/a
Complete List of Authors:	Hippler, Michael; University of Münster, Institute of Plant Biochemistry and Biotechnology Stauber, Einar; Max Planck Institute for Chemical Ecology, Mass Spectrometry Group Busch, Andreas; Max Planck Institute for Chemical Ecology, Mass Spectrometry Group; University of Münster, Institute of Plant Biochemistry and Biotechnology Naumann, Bianca; University of Münster, Institute of Plant Biochemistry and Biotechnology Svato, Ale; Max Planck Institute for Chemical Ecology, Mass Spectrometry Group
Key Words:	Membrane proteins, quantitative analysis, Stable isotope labelling

Proteotypic profiling of LHCI from *Chlamydomonas reinhardtii* provides new insights into structure and function of the complex

Einar J. Stauber[*‡], Andreas Busch[†], Bianca Naumann[†], Aleš Svatoš[*], and Michael Hippler[†§]

[*]Mass Spectrometry Group, Max Planck Institute for Chemical Ecology, Hans-Knöll-Str. 8, D-07745 Jena, Germany; and [†]Institut für Biochemie und Biotechnologie der Pflanzen, Westfälische Wilhelms-Universität Münster Hindenburgplatz 55, 48143 Münster, Germany; [‡]current address: Institut für Pharmazeutische Biologie, Technische Universität Braunschweig, Mendelssohnstr. 1, 38106 Braunschweig, Germany

Running title: Insights into structure and function of LHCI

[§]To whom the correspondence should be addressed. Tel: ++49 (251) 8324790. Fax: ++49 (251) 8328371 E.mail: mhippler@uni-muenster.de

ABSTRACT

We used isotope dilution mass spectrometry to measure the stoichiometry of LHCI proteins with the PSI core complex in the green alga *Chlamydomonas reinhardtii*. Proteotypic peptides served as quantitative markers for each of the nine gene products (Lhca1 – Lhca9) and for PSI subunits. The quantitative data revealed that the LHCI antenna of *C. reinhardtii* possesses at least six subunits. It further demonstrated that the thylakoid LHCI population is heterogeneously composed and that several *lhca* gene products are not present in 1:1 stoichiometries with PSI. When compared with vascular plants, LHCI of *C. reinhardtii* possesses a lower proportion of proteins potentially contributing to far-red fluorescence emission. In general, the strategy presented is universally applicable for exploring subunit stoichiometries within the *C. reinhardtii* proteome.

1 Introduction

By using solar energy to oxidize water into molecular oxygen and produce reducing equivalents and ATP during the light reactions of oxygenic photosynthesis, plants and photosynthetic prokaryotes provide the biochemical foundation for most lifeforms on our planet. Photosystem I (PSI), an essential component of the photosynthetic machinery, is a multiprotein complex that spans the thylakoid membranes of the chloroplast. It harnesses light energy to drive transmembrane electron transfer from plastocyanin or cytochrome c_6 to ferredoxin which initiates photoreduction of $NADP^+ + H^+$ to NADPH. In eukaryotes it consists of at least 17 protein subunits that coordinate and determine the functional properties of ~170 chlorophyll molecules, 2 phylloquinones, numerous carotenoids as well as three 4Fe-4S clusters [1]. The PSI supercomplex can be subdivided into a PSI core and an acessory light harvesting complex (LHCI) which can function either to gather light to increase energy available for electron transport or to protect the photosynthetic apparatus by dissipating excess energy that would otherwise lead to the formation of destructive oxidizing compounds [2-6]. Therefore LHCI plays an important role in maintaining overall performance and homeostasis of the entire photosynthetic apparatus.

LHCI is composed of homologous transmembrane spanning proteins which share conserved pigment binding domains but which each have different spectral properties and likely distinct functions [6]. In vascular plants the complex is composed of four main proteins (Lhca1-Lhca4) and Lhca5 which is expressed at low levels [7, 8]. The crystal structures of *Pisum sativum* (pea) PSI-LHCI show that Lhca1-4 form a half crescent which attatches to PSI on the PSI-F/PSI-J side of the complex [9, 10]. Biochemical isolation of plant LHCI results in two fractions consisting of the Lhca1/Lhca4 and Lhca2/Lhca3 hetero-dimers [11]. Each of the Lhca proteins, and in particular Lhca3 and Lhca4, are characterized by low energy (red) chlorophylls with prominent long wavelength fluorescence emission. Mutagenesis studies

have identified conserved chlorophyll binding residues responsible for the low energy forms [12-15].

In the green alga *Chlamydomonas reinhardtii*, a model organism for the study of the photosynthetic apparatus, LHCI can be isolated as an oligomeric complex which contains several different Lhca proteins [16, 17]. Compared to vascular plants, the LHCI complex of *C. reinhardtii* is more complex. Biochemical studies showed that it is composed of between 10-18 proteins [18, 19] and with the availability of a genomic sequence it was possible to demonstrate that all nine genes encoding for LHCI proteins (*lhca1-lhca9*) are expressed on the protein level [20]. Low-resolution models from electron microscopy studies show that the main portion *C. reinhardtii* LHCI binds to the PSI-F/PSI-J side of PSI but that individual monomers likely associate with different surfaces of PSI [21-24]. Despite these advances, to date little is known about the stoichiometry of the *C. reinhardtii* Lhca proteins with PSI. Quantitative proteome analysis has most commonly been used to compare changes in a proteome by measuring the staining intensity of a gel-separated protein that has been stained using a dye, immunostain or a radioisotope [25]. By comparing the staining intensity of proteins of interest with standards it is also possible to determine the stoichiometry between different proteins with this technique. Using Coomassie staining, the stoichiometry of *Arabidopsis thaliana* Lhca1-Lhca4 with PSI was determined to be 1:1 from proteins that had been separated with 1D gel electrophorhesis [26], which is in agreement with the pea crystal structure [9, 10]. A limitation of a gel based approach for complex samples is that co-migration of proteins, a common occurrence even with 2DE [27], can limit accurate quantitation. A second drawback is that dye or immunostaining techniques are inherently limited in their quantitative reproducibility which results in coefficients of variation (CV) (relative standard deviation) ranging from between 20 and 30 % [28-30] which precludes the detection of small differences in abundance between two proteins. While difference gel electrophorhesis (DIGE) [31] and radiolabelling [25] can reduce the variation, they offer no

advantage for distinguishing co-migrating proteins that originate from the same sample. Because of its complexity *C. reinhardtii* LHCI components can not be adequately separated by gel electrophoresis for quantitation (for example Lhca1/9 likely differ from each other by only 7 Da while Lhca5/6 and Lhca7/8 respectively differ from one another by less than 100 Da) and we therefore sought an alternative approach.

Quantitation of peptides using isotope dilution mass spectrometry enables higher accuracy than gel based approaches with CVs ranging between 4 and 10 % [29, 32, 33]. Additionally, when using tandem mass spectrometry a very high degree of selectivity can be obtained [34, 35] which is essential when analyzing complex mixtures. Techniques for determining protein stoichometry from proteotypic peptides using synthetic isotopically labled peptides have been described [36-38]. In this study, we marked the entire proteome of *C. reinhardtii* using metabolic labelling [39, 40] and used synthetic LHCI peptides and isotope dilution mass spectrometry to gain deeper insight into stoichiometry and functional relationship between LHCI and PSI.

2 Materials and methods

2.1 Strains and cultures

The arginine auxotrophic strain CC425/424 was cultured as described in [40] with a light intensity of approximately 50 µmol photons $m^{-2}s^{-1}$ and cultures were agitated at 120 rpm with a rotary shaker. Three separate cell cultures were grown with densities of 5 x 10^6 cells/ml (culture 1), 3 x 10^6 cells/ml (culture 2) and 3x 10^6 cells/ml (culture 3). These cultures were then used for the isolation of three independent PSI-LHCI preparations (see Methods "PSI-LHCI isolation" below).

2.2 Synthetic Peptides

The peptides PSI-A 1 MTISTPEREAKKVKIAVDR, PSI-A 709 VAPAIQPRALSTITQGR, PSI-B 9 FSQGLAQDPTTRR, Lhca1_73 RFTESEVIHGR, Lhca3_86 WLQYSEVIHAR, Lhca4_85 WYAQAELMNAR, Lhca5_59 WYRQSELQHAR, Lhca7_159 GLENGYPGGRFFDPMGLSR, Lhca8_62 DPVALRWYQQAELIHCR, and Lhca9_126 RYQGFK were purchased from Eurogentec (Seraing, Belgium) with a reported purity of 95%. Peptides PSI-C 67 VYLGSESTR, Lhca2_125 RYEIYKK, Lhca6_69 ESELVHSR, and Lhca8_137 RWQDIRK were synthesized by Dr. Miroslova Blechová from the Institute of Organic Chemistry and Biochemistry of the Czech Academy of Sciences, Prague.

Stock solutions with a concentration of 0.5 – 0.8 mM were prepared in 1.00 ml of milli-Q filtered (Millipore, Bedford, MA, USA) and degassed water. Solid peptides were stored dessicated with P_2O_5 (phosphorous pentoxide) under an argon atmosphere in the dark and solubilized peptides were stored frozen.

2.3 PSI-LHCI Isolation.

Thylakoid membranes were prepared as described in [41] from the three different cell cultures described above (cultures 1-3) and used for the enrichment of three different PSI-LHCI preparations (referred to as prep 1-3 hereafter) as described previously [42]. PSI-LHCI prep 1 was further purified with a second round of sucrose gradient centrifugation. Chlorophyll concentrations were determined according to Porra *et al.*[43], resulting in a Chl a/b ratio of 5.1 for prep1, 5.4 for prep2 and 6.4 for prep3.

2.4 Enzymatic digestion

For each digest mixture, n-dodecyl-β-D-maltoside was at a concentration of 0.1 % (w/vol), NH_4HCO_3 (ammonioum hydrogen carbonate) was 50 mM, and peptides were at a level of 5.0 pmol per µg chlorophyll (~ 220 copies of chlorophyll per peptide molecule). Trypsin, which cleaves after lysyl and arginyl residues (TPCK treated, V511A, Promega, Madison, WI, USA), and endoproteinase Lys-C (*Lysobacter enzymogenes*), which cleaves exclusively after lysyl residues (Roche Applied Science, Penzberg, Germany), were used in the experiments. For all three preparations the reaction volume was about 100 µL. For prep 1, PSI-LHCI proteins corresponding to 10.0 µg of chlorophyll and 50.0 pmol of each peptide were incubated with 5 µg of trypsin overnight at 37°C followed by 2.5 µg trypsin with incubation at 42 °C for two hours. For prep 2, proteins corresponding to 40.0 µg of chlorophyll were incubated with 20 µg and then 20 µg of trypsin. For Lys-C proteolysis of prep 2, proteins corresponding to 10.0 µg of chlorophyll were incubated with 6 µg of enzyme using the recommended buffers overnight at 37°C followed by an additional 2 µg of enzyme for two hours at 37°C. For prep 3 proteins corresponding to 20 µg of chloropyll were incubated with

15 µg trypsin overnight, followed by 5 µg trypsin for two hours at 42°C. Reactions were stopped with 10 µl of 10 % (vol/vol) CHOOH (formic acid) in H_2O (water).

Peptides from prep 1 and 2 were recovered from the reaction mix by first binding them to Zorbax 300-SCX material (Agilent Technologies, Palo Alto, CA, USA) and then washing them with 0.1 % (vol/vol) CHOOH in 60:40 CH_3CN (acetonitrile)-H_2O, either with a batch method or in a self-packed column. After re-equilibrating the SCX material with 0.1% (vol/vol) CHOOH/H_2O, the peptides were eluted stepwise with NaCl or KCl in 0.1% (vol/vol) CHOOH/H_2O and then desalted with small spin columns as described in [20] using C18 Zip Tips (Millipore, Eschborn, Germany) that had been packed with additional POROS-R2 (Applied Biosystems, Foster City, CA, USA) and conditioned with 0.1% (vol/vol) CHOOH/H_2O. Prep 3 was desalted using prepacked C18 spin columns (Agilent Technologies, Palo Alto, CA, USA) and equilibrated with 0.1% (vol/vol) CHOOH/H_2O. The peptides were recovered by a 3 step gradient of Acetonitrile (10%, 30% and 75%) (CH_3CN) in 0.1% (vol/vol) CHOOH/H_2O

2.5 LC-MS/MS

Autosampling, HPLC, and MS were performed with an Agilent series 1100 HPLC system (Agilent Technologies, Palo Alto, CA, USA) and an LTQ linear ion trap mass spectrometer as described in [44]. The 10 µl/min primary flow was split with a handmade splitter as described for the Pepfinder Kit (Application note 321, Thermo Electron Corporation, San Jose, CA, USA) using a P885 microtee (Upchurch Scientific, Oak Harbor, WA, USA). A used Symmetry trapping column (0.18 I.D. × 23 mm, Waters, Millford, MA, USA) provided resistance for back pressure. Measurements for prep 3 were performed with an LC-MS essentially as described in [40] using an UltiMate ™ 3000 (Dionex Corporation, Sunnyvale, CA, USA) device for autosampling, column switching, and nano-HPLC.

Quantitation was based on MS/MS products of proteotypic ^{12}C and ^{13}C isotopomers. Parent ions were fragmented concurrently with at least a 2 Da window on either side of the ^{12}C and ^{13}C isotopic pattern using either the normal or "turbo" scanning rates. The window was wide enough to encompass the entire isotopic pattern of ^{13}C-labeled peptides which is due to metabolism of the $^{13}C_6$-arginine as we have previously noted [40].

Likewise, chromatographic peak areas were determined frome the complete distribution of light and heavy isotopomers using Qualbrowser software (Thermo Electron Corporation, San Jose, CA, USA). Multiple fragment ions were used for quantitation and we noticed some irregularities for fragment ions which had resulted from loss of water. The ratio of the peak areas ($^{13}C/^{12}C$) was used to determine the amount of native (^{13}C) peptide per µg of chlorophyll present in the PSI-LHCI preparation. Protein abundances were inferred from these values. For each preparation the mean and the standard deviation of the protein/chlorophyll ratios (prot/chl) (pmol protein/µg chlorophyll) from all detected arginine containing-ions for a peptide were calculated. In addition, the mean ratio (prot/chl) of a protein over all preparations was calculated. This was done by averaging the respective mean values from the different preparations. The standard deviation of the mean is represented as the combined standard deviation that was calculated by taking all arginine containing-ions, measured over all preparations, into account.

By normalizing the protein/chlorophyll ratios for each Lhca to the mean of the values for PSI-A, PSI-B, and PSI-C, the stoichiometry between each Lhca and PSI was determined. For the Lhca4 peptide WYAQAELMNAR methionyl oxidation was observed. To determine the amount of native (^{13}C) peptide the peak area of the reduced and the respective oxidized y-ion were added up. This combined area was then used to calculate the $^{13}C/^{12}C$ ratio of the y-ions.

3 RESULTS

Nine different gene products (Lhca1 – Lhca9) have been determined to constitute LHCI in *C. reinhardtii* [20]; however until now the stoichiometric composition of LHCI has not been directly addressed. In this study, we applied isotope dilution-mass spectrometry to quantitatively probe the LHCI complex (Figure 1).

3.1 Stoichiometry between LHCI and PSI

In this study, we purified three preparations of PSI-LHCI, which we refer to as prep 1-3 (see methods), from three independent *C. reinhardtii* cell cultures that had been metabolically labled with $^{13}C_6$-arginine as described previously [40]. Because previous analyses of the chlorophyll/P700 ratios indicate that about 215 chlorophyll molecules associate with the PSI-LHCI complex in *C. reinhardtii* [22, 42] each of the preparations were combined with synthetic peptides at a level of 5.0 pmol/µg chlorophyll, which corresponds to 223 molecules of chlorophyll per peptide copy. After enzymatic digestion and sample cleanup, LC-MS/MS chromatograms were measured for native (^{13}C) and synthetic (^{12}C) isotopomers (selected chromatograms shown in Figure 2). From the $^{13}C/^{12}C$ values derived from the chromatograms, prot/chl ratios from three independent preparations were calculated for each protein (Table 1).

For prep 2, prot/chl ratios were obtained from each Lhca protein (Table 1), which allowed an overview of the total size of LHCI. Figure 2 shows LC-MS/MS chromatograms for the PSI-A and PSI-C core peptides (upper panel) and for Lhca3, Lhca2, and Lhca9 (lower panel). From the prot/chl ratios (Table 1), we determined the stoichiometries between the Lhca and PSI by normalizing to the average of the values for PSI-A, PSI-B and PSI-C taking the mass spectrometric data from the three independent preparations into account (Figure 3).

For comparison and evaluation of the data stemming from the three independent samples, we calculated the combined mean and combined standard deviation. From the quantitative data obtained for the PSI core subunits, 189 ± 32 chlorophylls were calculated to be coordinated by PSI-LHCI (Table 1). This ratio is close to the expected number of 215 chlorophyll molecules associated with the PSI-LHCI complex in *C. reinhardtii* [22, 42], strongly indicating that incomplete proteolytic digestion of PSI core polypeptides can be excluded. Remarkably, the data for WLQYSEVIHAR indicated that Lhca3 is present at a stoichiometry of approximately 1.7:1 with PSI, indicating that a portion of the PSI-LHCI population has more than one copy of Lhca3 (Table 1, Figure 3). In contrast, Lhca2 (RYEIYK), (Lhca6 (ESEVHLSR), Lhca8 (DPVLAR, WQDIRK) and Lhca9 (RYQGFK) were present at levels of about 0.5:1 with PSI. Lhca5 (Lhca5 (Q(-NH3)SELQHAR) was of even lower abundance with respect to the PSI core and was found at a level of about 0.3 with PSI. Lhca1, Lhca4 and Lhca7 are closer to 1:1 with PSI as compared to Lhca3. A larger experimental error was associated WYAQAELMNAR (Lhca4) (Table I) due to differential amounts methionyl oxidation. The summarized data point towards 8.0 ± 1.4 Lhca subunits per PSI core (Table I), indicating that between six to nine Lhca subunits are present per PSI core in *C. reinhardtii*.

3.2 N-terminal modification of PsaA

Finally measurements from the synthetic peptide MTISTPEREAKKVKIAVDR, which begins the N-terminus of the predicted *C. reinhardtii* PSI-A amino acid sequence (Genebank acession number P12154), indicate that the N-terminus of the protein has been modified (Figure 4). Trypsin digestion of the synthetic peptide results in the formation of the two peptides MTISTPER and IAVDR. For the latter of the two sequences, which begins at position 15 of the predicted PSI-A sequence, both ^{12}C- and ^{13}C-isoforms of the peptide are detectable (Figure 4 and Table 1). The synthetic ^{12}C-peptide MTISTPER, which begins the

predicted N-terminus of PSI-A, as well as its methionyl oxidized counterpart M(Ox)TISTPER were identified, however the ^{13}C-isotopomers were completely missing. Analysis of the Lys-C digest (which cleaves only after lysyl residues) likewise showed that only the ^{12}C-isoforms of MTISTPEREAK and M(Ox)TISTPEREAK were present while the ^{13}C-isoforms were missing (data not shown).

4 Discussion

Using stable isotopes, we were able to directly address the stoichiometry of LHCI in *C. reinhardtii*. Overall, the Lhca fall into three general categories: (i) proteins present at a ratio of about 1:1 with the PSI core complex, (Lhca1, Lhca4, Lhca7); (ii) proteins present at substoichiometric levels with PSI (Lhca2, Lhca5, Lhca6, Lhca8 and Lhca9); and (iii) one protein that may be present at a ratio higher than 1 with PSI (Lhca3). The data indicate that PSI-LHCI contains between six to eight Lhca polypeptides per PSI core complex (Table I), which agrees with the larger size of *C. reinhardtii* LHCI as compared to vascular plant LHCI [21-24]. The pea PS-LHCI crystal structures reveal 56 chlorophyll molecules bound to LHCI and 168 chlorophyll molecules in the PSI-LHCI supercomplex [9, 10]. Assuming that the number of gap chlorophylls between PSI core and LHCI as well as the number of chlorophyll molecules bound to LHCI is conserved, about 30 chlorophyll molecules remain to be distributed, suggesting that likely two additional Lhca subunits are present in PSI-LHCI as compared to pea PSI-LHCI. In the case that the number of gap chlorophylls as well as the number of chlorophyll molecules bound to LHCI is not conserved more than six subunits could be envisioned. Interestingly the distinct Lhca polypeptides accumulate at different levels with PSI. The data clearly demonstrate that the population of *C. reinhardtii* PSI-LHCI is highly heterogeneous, a feature that might be important for regulating the excitation energy transfer between the peripheral antenna and PSI and allowing an instant response to changing environmental conditions.

A remarkable feature of PSI-LHCI is the presence of “red” chlorophylls which have energy states lower than those of P700 and arise from excitonic coupling between two or more chlorophylls [45]. Because they determine excitation energy transfer pathways and rates within PSI-LHCI [46, 47] and likely play an important role in photoprotection [5, 48] they are of critical functional importance for the entire photosynthetic apparatus. In plant

PSI-LHCI, most red chlorophylls are associated with LHCI of which Lhca3 and Lhca4 have the most red-shifted chlorophylls with low temperature fluorescence emission maxima at 725 an 732 nm respectively [49].

Extensive work has been done to identify the chromophores and interactions responsible for the red shifted emission in the Lhca proteins using mutated recombinant proteins and spectroscopic methods [12-15, 49]. Pigment-pigment interactions between chlorophylls at sites A5 and B5 (nomenclature according to Kühlbrandt *et al.* [50]) have been shown to give rise to the red-shifted forms of Lhca1-Lhca4 in *A. thaliana*. In Lhca3 and Lhca4, the two proteins with the most red-shifted forms, the ligand at site A5 is an asparagine (N) whereas Lhca1 and Lhca2 have a histidine (H) at this site. Substitution of histidine for asparagine at the A5 abolished the red-shifted emission for Lhca3 and Lhca4 while the (H)A5(N) mutation of Lhca1 resulted in an 11 nm shift toward the red [13].

An alignment of the Lhca sequences from *A. thaliana* and *C. reinhardti* (Figure 5) shows that *A. thaliana* Lhca3 and Lhca4 contain an asparigine at position A5 of helix B, a feature which is conserved among vascular plant Lhca3 and Lhca4 proteins. Lhca1-Lhca4 have been shown to be at a 1:1 stoichiometry with PSI in vascular plants from the crystal structures [9, 10] and a study based on quantitation of Coomassie binding [26] whereas Lhca5 is expressed at low levels [7, 8]. Together Lhca3 and Lhca4 constitute between 44 and 50% of LHCI (assuming that Lhca5 can be expressed at a stoichiometry of up to 0.5:1 with PSI). In contrast, *C. reinhardtii* has three proteins with an asparigine at the A5 site (Lhca2, Lhca4 and Lhca9). Notably *C. reinhardtii* Lhca3, which is a clear homolog of vascular plant Lhca3 [51] has a histidine rather than an asparagine at this A5 site. Our data indicate that *C. reinhardtii* Lhca4, which shares similarity with vascular plant Lhca4, is likely present at a 1:1 ratio with PSI, whereas Lhca2 and Lhca9 are both present at a ratio of slightly less than 0.5:1 with PSI. Together, these three proteins compose about 28% of the LHCI complex.

Other factors contributing to red fluorescence differentiate *C. reinhardtii* and vascular plants. Modelling studies suggest that a chlorophyll coordinated by a conserved histidine residue of helix C (Linker 2) in vascular plant Lhca4 [48, 52]. However, this histidine is not present in *C. reinhardtii* Lhca4, Lhca2 or Lhca9 which might lead to a less red-shifted low temperature fluorescence which is observed for the green alga.

Using time-resolved fluorescence spectroscopy to compare exciton decay transients from *A. thaliana* and *C. reinhardtii* Ihalainen and coworkers [46] found that for the slowest trapping phase (originating from red chlorophylls) the fluorescence lifetimes are shorter for *C. reinhardtii* than for *A. thaliana*. In addition, the slowest trapping phase has a lower contribution to the overall decay of the system. These differences between algal and vascular plant PSI-LHCI were also suggested in another study [53]. These results indicate that while the size of *C. reinhardtii* LHCI is approximately 1.5 to 2 times larger than *A. thaliana* LHCI, it has a lower proportion of far-red fluorescing chlorophylls which have low temperature fluorescence spectra with a less red-shifted emission maximum which is in agreement with the biochemical data that we have obtained here. Using time resolved absorption spectroscopy at 77K, Melkozernov and coworkers [54] identified two distinct red spectral pools which belong to low-energy pigments in LHCI that absorb at 687 nm and 697 nm. They interpreted the fluorescence absorption at 687 nm as being due to Lhca1 based on reports from our laboratory which indicated that Lhca1 may be present at a level of several copies per LHCI [19, 20]. The results presented here clarify this issue. Our previous findings were based on Coomassie staining from two dimensional gels, which already indicated a rather heterogeneous composition of LHCI with Lhca1 as a prominent subunit. Based on the results obtained by stable isotope dilution mass spectrometry, we propose that the absorption bands at 687 nm and 697 nm may be due to Lhca4 and the Lhca2 and Lhca9 pair which are close homologues.

In a study comparing the composition of LHCI isolated from a PSI-deficient mutant with wild-type *C. reinhardtii* PSI-LHCI particles, both Lhca2 and Lhca9 were found to require PSI for stable association into PSI-LHCI, which indicates that both are in direct contact with PSI [17]. These two proteins may account for the density observed on the surface of PSI-A between PSI-K and PSI-H, or on the surface of PSI-B between PSI-G and PSI-H by electron microscopy [2]. Based on site selective fluorescence measurements, Gibasiewicz an colleagues [55] identified a red pool composed of two to three chlorophyll pairs with absorbance centered at 700 nm. It was suggested that one of the pairs may be located at the periphery of PSI or at the interface between PSI and LHCI but not in oligomeric LHCI since it has less red shifted chlorophylls [17, 18, 22]. One possibility is that this red pair is coordinated by Lhca2/9 since these two proteins are not a part of oligomeric LHCI but seem to associate directly with PSI. The results presented here indicate that Lhca2 and Lhca9 are each associated with about every other copy of PSI. Both are found in a wide variety of green alga and were recently proposed to be green algal specific Lhca proteins [51].

Interestingly, Lhca1 and Lhca7 as well as its homologue Lhca8 were found to be enriched in LHCI from a PSI-deficient mutant as compared with PSI-LHCI (1.2-fold, 5.0-fold and 1.7-fold, respectively), whereas other LHCI were diminished or remained constant [17]. This indicates that both Lhca7 and Lhca8 are not in direct contact with PSI but are integral parts of LHCI.

The number of chlorophyll molecules per PSI complex were close to the expected value of 215, which indicates that proteolytic digestion proceeded to completion. In addition, we choose several peptides with internal cleavage sites to serve as controls for the progress of the proteolytic digest. Nevertheless, some of the LHCI proteins may not have completely cleaved; therefore the stoichiometries should be regarded as minimum values. Indeed, we obtained data for each of the Lhca product peptides (Table I) excluding WYR (Lhca5) and

WYQQAELIHCR (Lhca8) whose LC-MS/MS signals were too low to quantify. This may be due to the poor recovery of WYR during the peptide cleanup procedure and the formation of inter-peptide S-S bonds between cystinyl residues of WYQQAELIHCR. Although the PSI peptide ALSITQGR (PSI-A) was only detectable in the (^{12}C) form, both isotopomers of the adjacent peptide VAPAIQPR were found (Table I). ALSITQGR is part of transmembrane helix K, which is surrounded by other helices, and is therefore likely inaccessible to protease under non-denaturing conditions. On the other hand, VAPAIQPR is completely contained within the stromal loop –jk of PSIA, which is an exposed region.

Finally, we surmise that PSI-A has a modified N-terminus (Figure 4). The most likely modification would be *via* N-terminal methionine excision, but until now no evidence has shown that PSI-A undergoes this process [56]. The crystal structures of pea PSI-LHCI, show that the N-terminus of PSI-A is located on the stromal side in the cleft between PSI and Lhca2 and Lhca3 [9, 10]; however, since the structure begins at position 31 the question as to whether it functionally interacts with gap chlorophylls remains open.

In conclusion, our results provide deeper insight into structural and functional characteristics of *C. reinhardtii* LHCI. The stoichiometric data presented here provide an explanation for the fluorescence emission properties of the *C. reinhardtii* PSI-LHCI complex which possesses a lower proportion of red-shifted chlorophylls than the vascular plant complex. This is likely due to the lower proportion of Lhca proteins with strong chlorophyll coupling in the region of the A5-B5 chlorophylls. Interestingly, it has been shown that Lhca4 and Lhca9 are induced under iron-deficiency in *C. reinhardtii*, which would thereby increase the number of red chlorophylls per PSI-LHCI [40]. Since LHCI is uncoupled from PSI during iron deficiency, the fast energy transfer route through gap chlorophylls to the PSI core is severed (as is the case at low temperatures [54]) which decreases delivery of excitation energy to P700 while increasing delivery of exitation energy to non-light harvesting carotenoids which results in photoprotective energy loss [5]. In addition, our results suggest

that the population of PSI-LHCI in *C. reinhardtii* is heterogeneously composed with differing LHCI composition which implies heterogeneity in energy transfer routes within PSI-LHCI. The crystal structure of PSI-LHCI indicates that Lhca1 forms a fixed association with PSI through strong hydrophobic interactions with PSI-G, while the interactions of Lhca3 and PSI-K are more dynamic [10]. Biochemical [17, 40] and sequence alignment [57] data indicate that this is also likely the case in *C. reinhardtii* where Lhca1 and Lhca3 probably also form fixed and dynamic interactions, respectively, with PSI. However, clear orthologues to vascular plant Lhca2, Lhca4, and Lhca5 appear to be missing. Instead, these "types" of Lhca are represented by more than one protein with similarities to the vascular plant counterpart (Figure 5). This degeneracy may enable *C. reinhardtii* to modulate the structure and function of its LHCI complex in response to varying light and environmental conditions.

The approach established in this study also opens the door for the quantitation of subunit stoichiometries within any multi-protein complex in *C. reinhardtii* or any other organism that is auxotrophic for one or more amino acids.

Acknowledgments

The funding of this project by the Max Planck Society to A.S. and the DFG (HI 739/1-3; HI739/2-1) to M.H are gratefully acknowledged. The authors thank Emily Wheeler for editorial assistance.

5 References

[1] Nelson, N., Yocum, C., F., Structure and function of photosystems I and II. *Annu. Rev Plant. Biol.* 2006, 57, 521 - 565.

[2] Nield, J., Redding, K., Hippler M., Remodeling of light-harvesting protein complexes in *Chlamydomonas* in response to environmental changes. *Eukaryotic Cell* 2004, 3, 1370-1380.

[3] Melkozernov, A. N., Barber, J., and Blankenship, R. E., Light Harvesting in Photosystem I Supercomplexes. *Biochemistry* 2006, 45, 331-345.

[4] Ihalainen, J. A., D'Haene, S., Yeremenko, N., van Roon, H., Arteni, A. A., Boekema, E. J., van Grondelle, R., Matthijs, H. C., Dekker, J. P., Aggregates of the chlorophyll-binding protein isiA (CP43') dissipate energy in cyanobacteria. *Biochemistry* 2005, 44.

[5] Carbonera, D., Giancarlo, A., Morosinotto, T., Bassi, R., Quenching of chlorophyll triplet states by carotenoids in reconstituted Lhca4 subunit of peripheral light-harvesting complex of photosystem I. *Biochemistry* 2005, 44, 8337-8346.

[6] Jensen, P. E., Bassi, R., Boekema, E. J., Dekker, J. P., Jansson, S., Leister, D., Robinson, C., Vibe Scheller, H., Structure, function and regulation of plant photosystem I. *Biochim. Biophys. Acta* 2007, 1767, 335-352.

[7] Ganeteg, U., Klimmek, F., Jansson, S., Lhca5 - an LHC - type protein associated with photosystem I. *Plant Molecular Biology* 2004, 54, 641-651.

[8] Storf, S., Stauber, E. J., Hippler, M., Schmid, V. H. R., Proteomic analysis of phtosystem I light-harvesting antenna in tomato (*Lycopersicon esculentum*). *Biochemistry* 2004, 43, 9214-9224.

[9] Almuts, A., Omri, Drory, Nelson, N., The structure of a plant photosystem I supercomplex at 3.4 Å resolution. *Nature* 2007, 447, 50-63.

[10] Ben-Shem, A., Frolow, F., Nelson, N., Crystal structure of plant photosystem I. *Nature* 2003, 426, 630-635.

[11] Lam, E., Oritz, W., Malkin, R., Chlorophyll a/b proteins of photosystem I. *FEBS Lett* 1984, 525, 121-125.

[12] Morosinotto, T., Mozzo, M., Bassi, R., Croce, R., Pigment-pigment interactions in Lhca4 antenna complex of higher plants photosystem I. *J. Biol. Chem.* 2005, 280, 20612-20619.

[13] Morosinotto, T., Breton, J., Bassi, R., Croce, C., The nature of a chlorophyll ligand in Lhca proteins determines the far red fluorescence emission typical of photosystem I. *J. Biol. Chem.* 2003, 278, 49223-49229.

[14] Croce, R., Morosinotto, T., Ihalainen, J. A., Chojnicka, A., Breton, J.., Dekker, J. P., van Grondelle, R., Bassi, R., Origin of the 701-nm fluorescence emission of the Lhca2 subunit of higher plant photosystem I. *J. Biol. Chem.* 2004, 280, 48543-48549.

[15] Mozzo, M., Morosinotto, T., Bassi, R., Croce, R., Probing the structure of Lhca3 by mutation analysis. *Biochim. Biophys. Acta* 2006, 1757, 1607-1613.

[16] Wollman, F.-A., Bennoun, P., A new chlorophyll-protein complex related to photosystem I in *Chlamydomonas reinhardtii*. *Biochim. Biophys. Acta* 1982, 680, 352-360.

[17] Takahashi, Y., Yasui, T.-a., Stauber, E. J., Hippler, M., Comparison of the subunit compositions of the PSI-LHCI supercomplex and the LHCI in the green alga *Chlamydomonas reinhardtii*. *Biochemistry* 2004, 43, 7816-7823.

[18] Bassi, R., Soen, S., Y., Frank, G., Zuber, H., Rochaix, J., D., Characterization of chlorophyll a/b proteins of photosystem I from *Chlamydomonas reinhardtii*. *J. Biol. Chem.* 1992, 267, 25714-25721.

[19] Hippler, M., Klein, J., Fink, A., Allinger, T., Hoerth, P., Towards functional proteomics of membrane protein complexes: analysis of thylakoid membranes from *Chlamydomonas reinhardtii*. *Plant Journal* 2001, 28, 595-606.
[20] Stauber, E. J., Fink, A., Markert, K., Kruse, O., Johanningmeier, U., Hippler, M.,, Proteomics of *Chlamydomonas reinhardtii* light-harvesting proteins. *Eukaryotic Cell* 2003, 2, 978-994.
[21] Germano, M., Yakushevska, A. E., Keegstra, W., van Gorkom, J. J., Dekker, J. P., Boekema, E. J., Supramolecular organization of photosystem I and light harvesting complex I in *Chlamydomonas reinhardtii*. *FEBS Lett.* 2002, 525, 121-125.
[22] Kargul, J., Nield, J., Barber J., Three dimensional reconstruction of a light harvesting complex I photosystem I (LHCI-PSI) supercomplex from the green alga *Chlamydomonas reinhardtii*. *J. Biol. Chem.* 2003, 278, 16135-16141.
[23] Kargul, J., Turkina, M. V., Nield, J., Benson, S., Vener, A. V., Barber J., Light harvesting complex II protein CP29 binds to photosystem I of *Chlamydomonas reinhardtii* under state 2 conditions. *FEBS Journal* 2005, 272, 4797-4806.
[24] Dekker, J., P., Boekema, E., J., Supramolecular organization of thylakoid membrane proteins in green plants. *Biochim. Biophys. Acta* 2005, 1706, 12-39.
[25] Görg, A., Weiss, W., Dunn, M. J., Current two-dimensional electrophoresis technology for proteomics. *Proteomics* 2004, 4, 3665-3685.
[26] Ballottari, M., Govoni, C., Caffari, S., Morosinotto, T., Stoichiometry of LHCI antenna polypeptides and characterization of gap and linker pigments in higher plants Photosystem I. *Eur. J. Biochem.* 2004, 271, 4659 - 4665.
[27] Westbrook, J. A., Yan, J. X., Wait, R., Welson, S. Y., Dunn, M. J., Zooming-in on the proteome: very narrow-range immobilised pH gradients reveal more protein species and isoforms. *Electrophoresis* 2001, 22, 2865-2871.
[28] Koller, A., Wätzig, H., Precision and variance components in quantitative gel electrophoresis. *Electrophoresis* 2005, 26, 2470-2475.
[29] Uitto, P. M., Lance, B. K., Wood, G. R., Sherman, J., Baker, M. S., Molloy, M. P., Comparing SILAC and two-dimensional gel electrophoresis image analysis for profiling urokinase plasminogen activatior signaling in ovarian cancer cells. *J. Prot. Res.* 2007, In press.
[30] Ballottari, M., Dal´Òsto, L., Morosinotto, T., Bassi, R., Contrasting behaviour of higher plant photosystem I and II antenna systems during acclimation. *J. Biol. Chem.* 2007, 282, 8947-8958.
[31] Alban, A., Olu David, S., Bjorkesten, L., Andersson, C., Sloge, E., Lewis, S., Currie, I., A novel experimental design for comparative two-dimensional gel analysis: Two-dimensional difference gel electrophoresis incorporating a pooled internal standard. *Proteomics* 2003, 3, 36-44.
[32] Berna, M., Schmalz, C., Duffin, K., Mitchell, P., Chambers, M., Ackermann, B., Online immunoaffinity liquid chromatography/tandem mass spectrometry determination of a type II collagen peptide biomarker in rat urin: Investigation of the impact of collision-induced dissociation fluctuation on peptide quantitation. *Anal. Biochem.* 2006, 356, 235-243.
[33] Zhu, X., Desiderio, D., M., Peptide quantification by tandem mass spectrometry. *Mass Spectrom. Rev.* 1996, 15, 213-240.
[34] De Leenheer, A. P., Thienpont, L. M., Applications of isotope dilution-mass spectrometry in clinical chemistry, pharmacokinetics, and toxicology. *Mass Spectrom. Rev.* 1992, 11, 249-307.
[35] McLafferty, F., W., Bockhorr, F., M., Separation/identification system for complex mixtures using mass separation and mass spectral characterization. *Anal. Chem.* 1978, 50, 69-75.

[36] Barndridge, D. R., Dratz, E. A., Martin, T., Bonilla, L. E., Moran, L. B., Lindall, A., Absolute quantification of the G-protein coupled receptor rhodopsin by LC/MS/MS using proteolysis product peptides and synthetic peptide standards. *Analytical Chemistry* 2003, 75, 445 - 451.

[37] Gerber, S. A., Rush, J., Stemman, O., Kirschner, M. W., Gygi, S. P., Absolute quantification of proteins and phosphoproteins from cell lysates by tandem MS. *Proc. Natl. Acad. Sci. USA* 2003, 12, 6940-6945.

[38] Ong, S.-E., Mann, M., Mass Spectrometry-based proteomics turns quantitative. *Nature Chemical Biology* 2005, 1, 252-262.

[39] Ong, S.-E., Blagoev, B., Kratchmarova, I., Kristensen, D. B., Steen H., Pandey, A., Mann, M., Stable isotope labeling by amino acids in cell culture, SILAC, as a simple and accurate approach to expression proteomics. *Proteomics* 2002, 1, 376-386.

[40] Naumann, B., Stauber E. J., Busch, A., Sommer, F., Hippler, M., N-terminal processing of Lhca3 is a key step in remodelling of the photosystem-I-light-harvesting complex under iron deficiency in *Chlamydomonas reinhardtii*. *J. Biol. Chem.* 2005, 280, 20431-20441.

[41] Chua, N.-H., and Bennoun, P., Thylakoid membrane polypeptides of *Chlamydomonas reinhardtii*: wild-type and mutant strains deficient in photosystem II reaction center. *Proc. Natl. Sci. USA* 1975, 72, 2175-2179.

[42] Hippler, M., Drepper, F., Farah, J. and Rochaix, J. D., Fast electron transfer from cytochrome c6 and plastocyanin to photosystem I of Chlamydomonas reinhardtii requires PsaF. *Biochemistry* 1997, 36, 6343-9.

[43] Porra, R. J., Thompson, W. A., Kreidemann, P. E., Determination of accurate extinction coefficients and simultaneous equations for assaying chlorophylls a and b extracted with four different solvents: verification of the concentration of chlorophyll standards by atomic absorption spectroscopy. *Biochim. Biophys. acta* 1989, 975, 384-394.

[44] Muck, A., Ibanez, A. J., Stauber, E. J., Mansourova, M. and Svatos, A., Atmospheric molding of ionic copolymer MALDI-TOF/MS arrays: a new tool for protein identification/profiling. *Electrophoresis* 2006, 27, 4952-9.

[45] Gobets, B., van Grondelle, R., Energy transfer and trapping in photosystem I. *Biochim. Biophys. Acta* 2001, 1507, 80-99.

[46] Ihalainen, J. A., van Stokkum, I. H., Gibasiewicz, K., Germano, M., van Grondell, R., Dekker, J. P., Kinetics of excitation trapping in intact photosystem I of *Chlamydomonas reinhardtii* and *Arabidopsis thaliana*. *Biochim. Biophys. Acta* 2005, 1706, 267-275.

[47] Englemann, E., Zucchelli, G., Casazza, A., P., Brogioli, D., Garlaschi, F., M., Jennings, R., C., Influence of the photosystem I - light harvesting complex I antenna domains on fluorescence decay. *Biochemistry* 2006, 45, 6947 - 6955.

[48] Melkozernov, S., Blankenship, R. E., Structural and functional organization of the peripheral light-harvesting system in photosystem I. *Photosynthesis Research* 2005, 85, 33-50.

[49] Morosinotto, T., Castelletti, S., Breton, J., Bassi, R., Croce, R., Mutational analysis of Lhca1 antenna complex. *J. Biol. Chem.* 2002, 277, 36253-36261.

[50] Kühlbrandt, W., Wang, D., N., Fujiyoshi, Y., Atomic model of plant light-harvesting complex by electron crystallography. *Nature* 1994, 367, 614-621.

[51] Koziol, A. G., Borza, T., Ishida, K.-I., Keeling, P., Lee, R. W., Durnford, D. G., Tracing the evolution of the ligh-harvesting antennae in chlorophyll *a/b*-containing organisms. *Plant Physiol.* 2007, 143, 1802-1816.

[52] Melkozernov, S., Blankenship, R. E., Structural modeling of the Lhca4 subunit of LHCI-730 peripheral antenna in photosystem I based on similarity with LHCII. *J. Biol. Chem.* 2003, 270, 44542-44551.
[53] Melkozernov, A. N., Kargul, J., Barber, J., and Blankenship, R. E., Energy coupling in the PSI-LHCI supercomplex from the green alga *Chlamydomonas reinhardtii*. *J. Phys. Chem. B* 2004, 108, 10547-10555.
[54] Melkozernov, A. N., Kargul, J., Lin, S., Barber, J., Blankenship, R. E., Spectral and kinetic analysis of the energy coupling in the PSI-LHCI supercomplex from the green alga *Chlamydomonas reinhardtii* at 77 K. *Photosynthesis Research* 2005, 86, 203-215.
[55] Gibasiewicz, K., Szrajner, A., Ihalainen, J. A., Germano, M.*, et al.*, Characterization of low-energy chlorophylls in the PSI-LHCI supercomplex from Chlamydomonas reinhardtii. A site-selective fluorescence study. *J Phys Chem B Condens Matter Mater Surf Interfaces Biophys* 2005, 109, 21180-6.
[56] Giglione, C., Boularot, A., Meinnel, T., Protein N-terminal methionine excision. *Cell. Mol. Life Sci.* 2004, 61.
[57] Tokutsu, H., Teramoto, H., Takahashi, Y., Ono, T.-a., Minagawa, J., The light-harvesting complex of photosystem I in *Chlamydomonas reinhardtii*: protein composition, gene structures and phylogenetic implications. *Plant Cell Physiol.* 2004, 45, 138-145.

Figure and Table Legends

Figure 1

The use of stable isotope labelling and tandem mass spectrometry for determining the stoichiometry between photosystem I and its associated light-harvesting sequences as exemplified with PSI-A and Lhca2. Arginine auxotrophic cells are metabolically labelled using the SILAC approach [39] with $^{13}C_6$-arginine. From the cell culture, $^{13}C_6$-labeled photosystem I complex (PSI-LHCI) is biochemically isolated and standard peptides ($^{12}C_6$) are chemically synthesized. PSI-LHCI and synthetic peptides are combined and enzymatically digested with proteases Lys-C and/or trypsin. After sample cleanup, the native ($^{13}C_6$) and internal standard ($^{12}C_6$) peptides are separated by liquid chromatography coupled with mass spectrometry (LC-MS). Use of MS/MS to fragment native and internal standard isotopomers concurrently and subsequent data filtering for arginine containing fragments (heavy isotopomer denoted with an asterix) introduces a high level of specificity. Such specificity allows signals which are several hundred times lower than background signals to be clearly resolved. In the diagram, chromatographic peaks are shown for the transition of IAVDR to its y3 fragment ion and RYEIYK to its b3 fragment ion. For the analyses presented here, multiple fragment ions from each peptide were used (Table I). The chromatographic peaks are then used to determine the stoichiometry between PSI-A and Lhca2.

Figure 2

The figure depicts a comparison among LC-MS/MS traces from proteotypic isotopomers from PSI-LHCI for PSI-A (IAVDR, VAPAIQPR), PSI-C (VYLGSESTR), Lhca2 (RYEIYK), Lhca9 (RYQGFK), and Lhca3 (WLQYSEVIHAR). The mean and standard deviations of multiple product ions are shown after normalizing to the most intense ion and taking into account the deviations between the $^{13}C/^{12}C$ ratios for each product ion pair. For graphing

purposes, the magnitudes of IAVDR, RYEIYK, and RYQGFK were amplified by 200, 8, and 5 respectively.

Figure 3

Protein/chlorophyll ratios (pmol/μg) for each of the different Lhca proteins compared to the PSI core (the mean of the values for PsaA and PsaC). Values are the combined means with the respective combined standard deviations from all three preparations (Table I).

The Lhca proteins can be categorized into three groups: (i) proteins present at a ratio of 1:1 with PSI (Lhca1, Lhca4, and Lhca7); (ii) proteins present at a ratio of approximately 1:2 with PSI (Lhca2, Lhca5, Lhca6, Lhca8 and Lhca9); proteins present at a ratio of approximately 2:1 with PSI (Lhca3).

Figure 4

LC-MS/MS chromatograms for proteotypic products of MTISTPEREAKKVKIAVDR which begins at predicted the N-terminus of the PSI-A. Both IAVDR and MTISTPER (also with oxidized methionine) are detectable by LC-MS/MS, whereas IAVDR-^{13}C is the only product detected from the native protein. For graphing purposes the signal for IAVDR was amplified by a factor of 25.

Incubation of the synthetic peptide MTISTPEREAKKVKIAVDR-^{12}C with trypsin, which begins at position 1 of the predicted *C. reinhardtii* PSI-A sequence, gives rise to the products IAVDR and MTISTPER (also found with an oxidized methionine), which were detected by LC-MS/MS. In contrast, MTISTPER-^{13}C is completely missing, while IAVDR-^{13}C is present, implying that the N-terminus of the PSI-A protein has been modified at a post-translational or post-transcriptional level. Similarly, the Lys-C product MTISTPEREAK-^{12}C was present, the heavy form was absent (data not shown). Formylated forms of either MTISTPER or TISTPER were not identified.

Figure 5

A model comparing the photosystem I complex of *C. reinhardtii* and *A. thaliana* exemplifies the quantitative differences within LHCI. Far-red fluorescing Lhca proteins are denoted with an oval with diagonal lines. A pie chart compares the absolute size of the LHCI antenna between *C. reinhardtii* and *A. thaliana* with the size of the pie chart being proportional to the absolute antenna size. Although *C. reinhardtii* LHCI is larger, only 28 % of the antenna is composed of far-red fluorescing protein pigment complexes (highlighted in gray) while for *A. thaliana*, the proportion is 44 %, assuming a contribution of Lhca5 with about 0.5 copies per PSI core. An alignment from portions of helix B and helix C from *C. reinhardtii* and *A. thaliana* showing the asparigine (N) residue at position A5 that is involved in the formation of red chlorophyll clusters (white characters) [13, 52]. Furthermore, a histidines (H) in Helix C between the B6 and B5 residues (Linker 2) has been implicated in the red shift in vascular plant Lhca4 [48, 52] but is missing from *C. reinhardtii* Lhca4. This histidine is present in *C. reinhardtii* Lhca5 and Lhca6 (which also have significant similarity to vascular plant Lha4) but these proteins lack the asparigine at position A5, which may mean that the overall strength of excitonic coupling in these proteins is lower than in vascular plant Lhca4.

Table 1: Protein/chlorophyll ratios (pmol/µg) obtained for each of the three independent PSI-LHCI purifications. The ratios were determined by dividing the quantity for the native (^{13}C) peptide by the weight of chlorophyll used per enzymatic digestion. By normalizing the ratios for each Lhca to the combined mean of the values for PSI-A and PSI-C from all three preparations, the stoichiometry between each Lhca and PSI was determined.

Protein	**proteolytic peptide**	**Preparation 1**		**Preparation 2**		**Preparation 3**		**combined runs**[a]
		protein/chlorophyll (pmol/µg)	runs/ions (n)	protein/chlorophyll (pmol/µg)	runs/ions (n)	protein/chlorophyll (pmol/µg)	runs/ions (n)	protein/chlorophyll (pmol/µg)
PsaA	VAPAIQPR	5.5 ± 0.5	2 / 10	6.0 ± 0.6	1 / 7			6.5 ± 0.5
PsaB	FSQGLAQDPTTR	5.7 ± 0.4	6 / 42	6.5 ± 1.9	2 / 10	2.5 ± 0.9[b]	4 / 23	4.9 ± 0.9
PsaC	VYLGSESTR			6.8 ± 0.2	2 / 4	4.7 ± 1.8	4 / 14	5.7 ± 1.6
								PSI core: 5.9 ± 1.0 pmol/µg
Lhca1	FTESEVIHGR			10.3 ± 0.6	3 / 8	6.0 ± 1.7	2 / 14	8.3 ± 1.4
Lhca2	RYEIYK			2.8 ± 0.2	2 / 7			2.8 ± 0.2
Lhca3	WLQYSEVIHAR			10.0 ± 0.7	2 / 6	9.8 ± 2.9	7 / 43	9.9 ± 2.7
Lhca4	WYAQAELM(Ox)NAR			8.0 ± 0.2	1 / 2[c]	7.3 ± 2.5	3 / 12[c]	7.7± 2.4
Lhca5	Q(-NH3)SELQHAR	1.0 ± 0.1	2 / 2	2.2 ± 0.3	1 / 3			1.6 ± 0.2
Lhca6	ESEVHLSR			2.9 ± 0.6	2 / 6			2.9 ± 0.6
Lhca7	GLENYPGGR	9.9 ± 1.2	6 / 30	6.2 ± 0.9	4 / 4			
	FFDPMGLSR					4.7 ± 0.6	2 / 3	6.9 ± 1.2
Lhca8	DPVLAR			2.4 ± 0.3	2 / 10			
	WQDIRK			3.1 ± 0.5	2 / 2			2.8 ± 0.4
Lhca9	RYQGFK			2.9 ± 0.1	3 / 6			2.9 ± 0.1
								total Lhca proteins per PSI[d]: 7.8 ± 1.4

[a]shown are the combined means and the respective combined standard deviation,[b]values of the peptide are not included in the PSI core calculations because of partial pseudotryptic cleavage,[c]number of combined pairs of the reduced and respective oxidized y-ion,[d]protein/chlorophyll ratios of all Lhca are added up and divided by the mean for PSI core

Figure 1

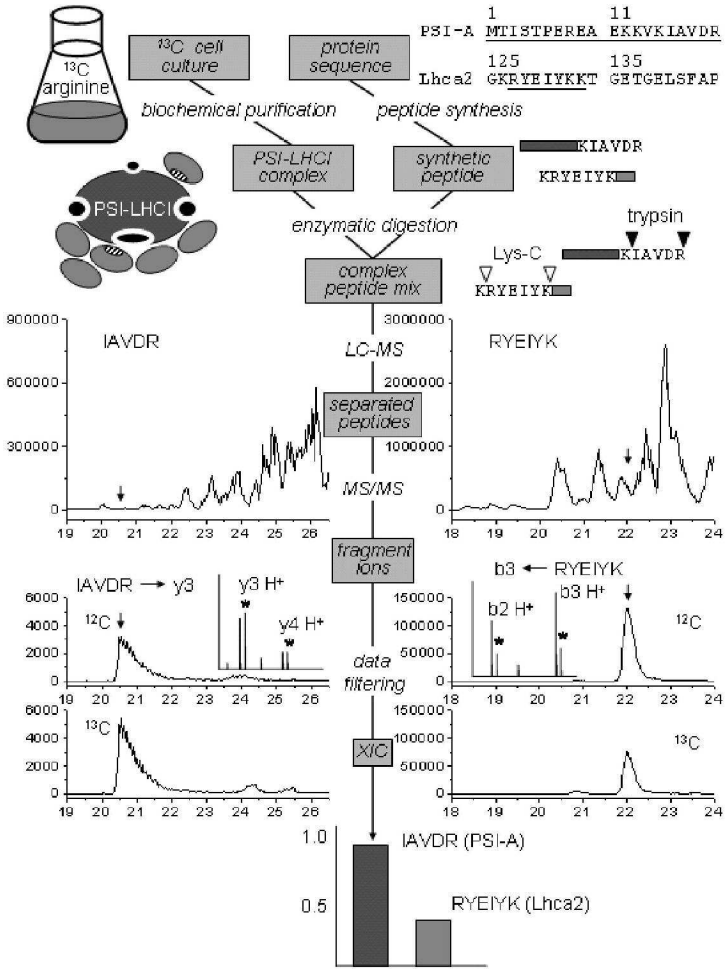

83x138mm (600 x 600 DPI)

Figure 2

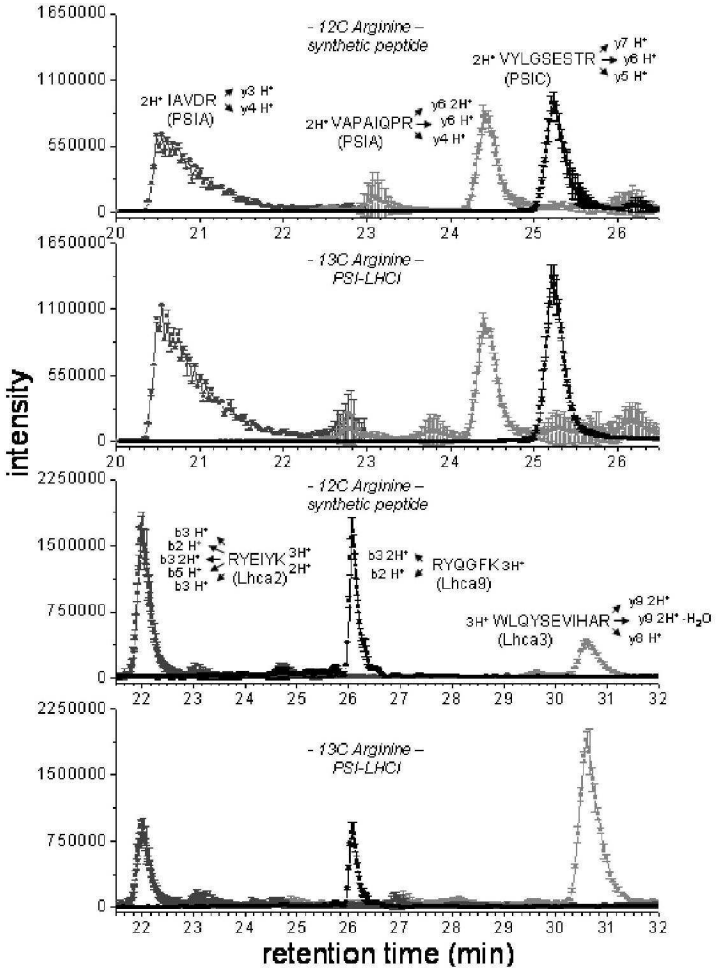

83x138mm (600 x 600 DPI)

Figure 3

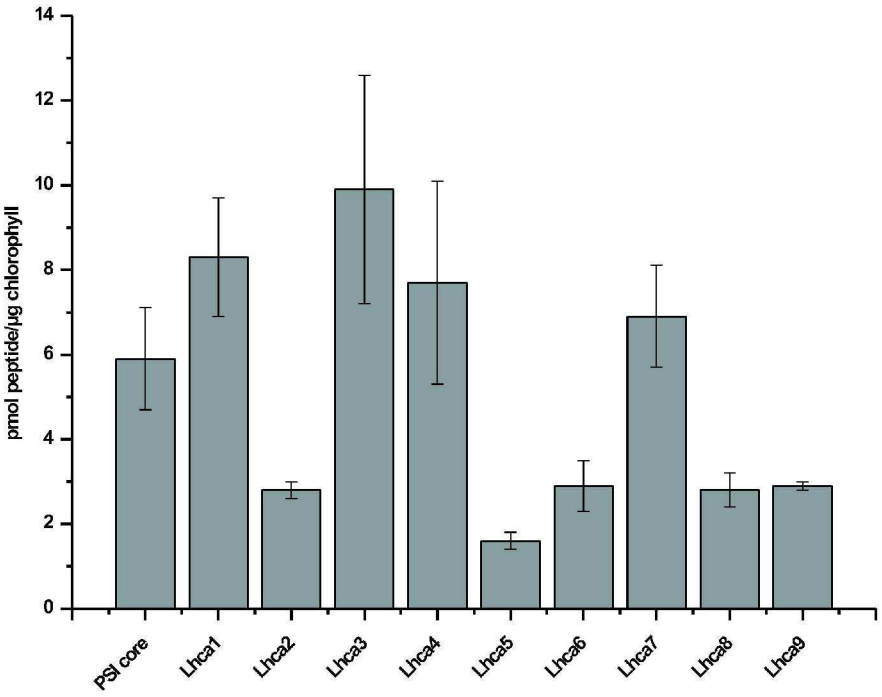

153x171mm (600 x 600 DPI)

Figure 4

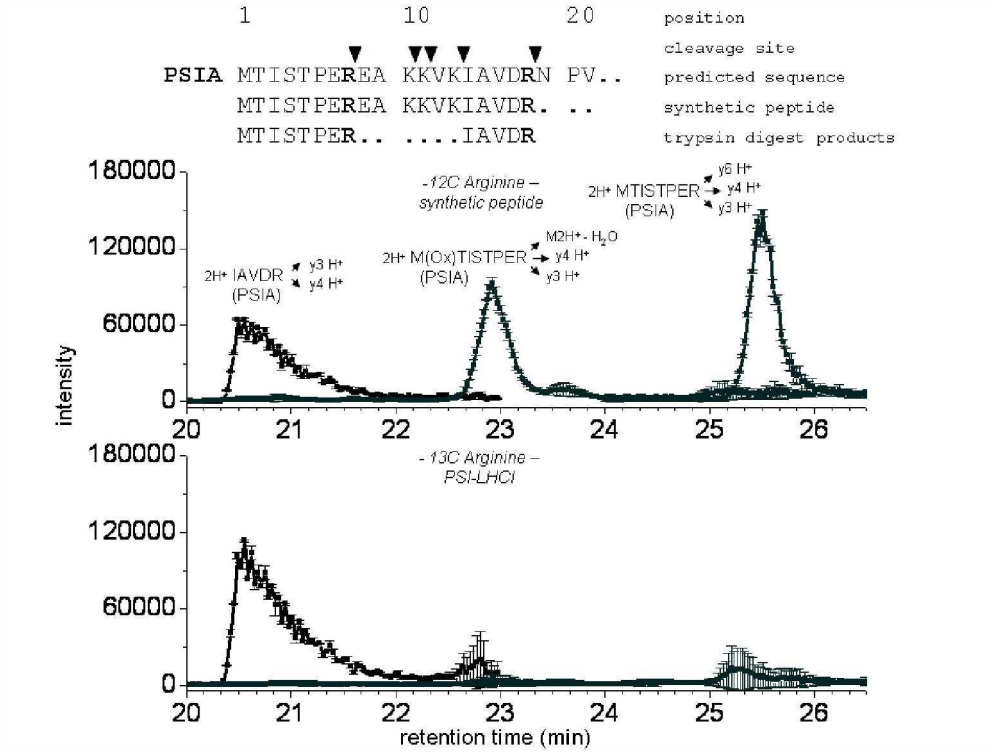

172x172mm (600 x 600 DPI)

Figure 5

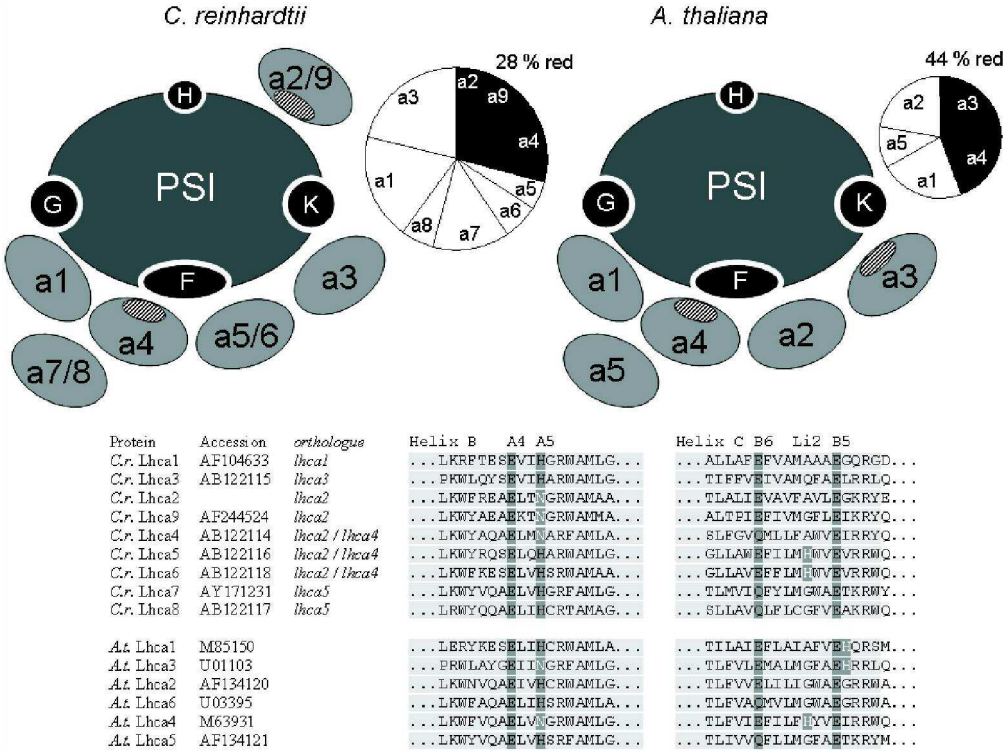

Protein	Accession	*orthologue*	Helix B A4 A5	Helix C B6 Li2 B5
C.r. Lhca1	AF104633	*lhca1*	...LKRFTESEVIHGRWAMLG...	...ALLAFEFVAMAAAEGQRGD...
C.r. Lhca3	AB122115	*lhca3*	...PKWLQYSEVIHARWAMLG...	...TIFFVEIVAMQFAELRRLQ...
C.r. Lhca2		*lhca2*	...LKWFREAELTYGRWAMAA...	...TLALIEVAVFAVLEGKRYE...
C.r. Lhca9	AF244524	*lhca2*	...LKWYAEAEKTYGRWAMMA...	...ALTPIEFIVMGFLEIKRYQ...
C.r. Lhca4	AB122114	*lhca2 / lhca4*	...LKWYAQAELMYARFAMLA...	...SLFGVQMLLFAWVEIRRYQ...
C.r. Lhca5	AB122116	*lhca2 / lhca4*	...LKWYRQSELQHARWAMLG...	...GLLAWEFILMFWVEVRRWQ...
C.r. Lhca6	AB122118	*lhca2 / lhca4*	...LKWFKESELVHSRWAMAA...	...GLLAVEFFLMFWVEVRRWQ...
C.r. Lhca7	AY171231	*lhca5*	...LKWYVQAELVHGRFAMLG...	...TLMVIQFYLMGWAETKRWY...
C.r. Lhca8	AB122117	*lhca5*	...LRWYQQAELIHCRTAMAG...	...SLLAVQLFLCGFVEAKRWQ...
At. Lhca1	M85150		...LERYKESELIHCRWAMLA...	...TILAIEFLAIAFVEFQRSM...
At. Lhca3	U01103		...PRWLAYGEIINGRFAMLG...	...TLFVLEMALMGFAELRRLQ...
At. Lhca2	AF134120		...LKWNVQAEIVHCRWAMLG...	...TLFVVELILIGWAEGRRWA...
At. Lhca6	U03395		...LKWFAQAELIHSRWAMLA...	...TLFVAQMVLMGWAEGRRWA...
At. Lhca4	M63931		...LKWFVQAELVQGRWAMLG...	...TLFVIEFILFIYVEIRRWQ...
At. Lhca5	AF134121		...LKWYVQAELVHSRFAMLG...	...TLIVVQFLLMGFAETKRYM...

167x156mm (600 x 600 DPI)

5. Discussion

5.1. Heterogeneity of light-harvesting complex I in plants

5.1.1. The structure of oligomeric light-harvesting complex I in Chlamydomonas and its association with photosystem I

The first studies of Chlamydomonas LHCI showed that it was a complex composed of several proteins. With the availability of genomic information and proteomic techniques (Manuscript 1), it was established that Chlamydomonas LHCI is composed of nine distinct Lhca proteins (Lhca1-Lhca9; Stauber, 2003) but still relatively little is known about how LHCI associates with PSI. Modelling of the pea PSI-LHCI crystal structure onto electron microscopy images of Chlamydomonas LHCI suggests that several Lhca associate with PSI on the PsaF side of the complex, similar to land plants but that individual proteins also associate with PSI on the side of PsaA between PsaK and PsaL (Dekker, 2005; Kargul, 2005). When purified biochemically, Chlamydomonas LHCI can be isolated as an oligomeric complex (Wollman, 1982; Bassi, 1992) which is different from the case in land plants where Lhca1/Lhca4 purifies as a dimer (Lam, 1984) as does Lhca2/Lhca3 under mild conditions (Croce, 2002). In order to gain insight into the organization of LHCI and its association with PSI, PSI-LHCI from wild-type cells and oligomeric LHCI from the PSI deficient mutant *ΔpsaB* were purified and their protein composition was reexamined using modern techniques (Manuscript 2).

Immunoblot analysis of sucrose density gradient fractions from *ΔpsaB* thylakoids showed that Lhca3 remained at the top of the gradient instead of migrating with oligomeric LHCI (Figure 2A in Manuscript 2). This result was confirmed by 1-DE and immunoblotting which showed that Lhca3 was present in PSI-LHCI preparations but missing from LHCI (Figure 4 in Manuscript 2). Since many of the Lhca can not be adequately separated by 1-DE, 2-DE was used to examine the composition of oligomeric LHCI in detail. Comparison of 2-DE maps of thylakoids and isolated LHCI from *ΔpsaB* cells revealed that Lhca2 and Lhca9 were also absent from oligomeric LHCI. Comparative quantitation of the remaining Lhca from 2DE gels of LHCI and PSI-LHCI showed that Lhca1, Lhca4, Lhca5 and Lhca6 were present at about the same level in both preparations while Lhca7 and Lhca8 were significantly enriched in LHCI. These data provide more insight into the structure of LHCI and its association with PSI. Lhca2, Lhca3 and Lhca9 each require the PSI core for stable association with LHCI. Therefore, they are likely in direct contact with PSI and have weak or no interactions with

other Lhca. Close physical contact with PSI also implies an important role in energy transfer to PSI for these three proteins. The remaining Lhca must have strong enough associations with one another to bind stably with LHCI in the absence of the PSI core.

Crystal structures of plant PSI-LHCI crystals show that Lhca1, Lhca2, Lha3 and Lhca4 form a crescent that cooperatively associates with PSI on the PSI-F side of the complex (Ben-Shem, 2003; Amunts, 2007). The structure indicates that the strongest interactions between LHCI and PSI are through Lhca1 and Lhca3 which associate with the two core subunits PsaG and PsaK, respectively. The association between Lhca1 and PsaG is quite close and is stabilized by hydrophobic interhelical interactions between Lhca1 and PsaG. On the other hand, the orientation of Lhca3 to PsaK precludes interhelical interactions and instead the N-terminus of Lhca3 and the stromal loop of PsaK form electrostatic interactions (Ben-Shem, 2003). Biochemical evidence supports the interaction of PsaK and Lhca3 (Jensen, 2000; Varotto, 2002), however, the nature of the interaction between PsaG and Lhca1 is less clear (Jensen, 2002; Varotto, 2002). Electron microscopy data show that Chlamydomonas LHCI also associates with PSI on one side of the complex but that an additional Lhca likely associates with PsaA between PsaK and PsaL (Germano, 2002; Kargul, 2003; Dekker, 2005; Kargul, 2005). From the electron microscopy data it is not possible to pinpoint the position of individual Lhca, but since both Lhca1 and Lhca3 appear to be true homologues of land plant Lhca1 and Lhca3 (Koziol 2007), they likely have the same positions within Chlamydomonas PSI-LHCI.

Since both Lhca2 and Lhca9 were found to require PSI for stable association into PSI-LHCI both proteins are likely in direct contact with PSI (Manuscript 2). These two proteins may account for the density observed on the surface of PsaA between PsaK and PsaL or on the side of PsaB between PsaG and PsaH by electron microscopy (Germano, 2002; Kargul, 2003; Dekker, 2005; Kargul, 2005). Based on site-selective fluorescence measurements, Gibasiewicz and colleagues (Gibasiewicz, 2005) identified a red pool composed of two to three chlorophyll pairs with absorbance centered at 700 nm. It was suggested that one of the pairs may be located at the periphery of PSI or at the interface between PSI and LHCI but not in oligomeric LHCI since it has less red shifted chlorophylls (Bassi, 1992; Kargul, 2003; Manuscript 2). One possibility is that this red pair is coordinated by Lhca2/9 since these two proteins are not a part of oligomeric LHCI but seem to associate directly with PSI. Besides, they also contain an asparagine at chlorophyll position A5 which is necessary for far red

fluorescence emission in Lhca (Morosinotto, 2003). The results presented in Manuscript 5 indicate that Lhca2 and Lhca9 are each associated with about every other copy of PSI. Both are found widely in green algae, and phylogenetic analyses show that they are likely green algal specific Lhca proteins (Koziol, 2007)).

5.1.2. Stoichiometry of light-harvesting complex I proteins in Chlamydomonas

Using stable isotopes, we were able to directly address the stoichiometry of LHCI in Chlamydomonas (Manuscript 5). Overall, the Lhca subunits fall into three general categories: (i) proteins present at a ratio of about 1:1 with the PSI core complex, (Lhca1, Lhca4, Lhca7); (ii) proteins present at substoichiometric levels with PSI (Lhca2, Lhca5, Lhca6, Lhca8 and Lhca9); and (iii) one protein that may be present at a ratio higher than 1 with PSI (Lhca3). The data indicate that PSI-LHCI of Chlamydomonas binds approximately 196 chlorophyll molecules and contains between six to eight Lhca proteins per PSI core complex (Table I in Manuscript 5), which agrees with the larger size of Chlamydomonas LHCI as compared to land plant LHCI (Germano, 2002; Kargul, 2003; Dekker, 2005; Kargul, 2005). X-ray diffraction of pea PSI-LHCI crystals resolved 168 chlorophyll molecules bound by PSI-LHCI, of which 56 chlorophylls are coordinated by LHCI (Ben-Shem, 2003; Amunts, 2007). Assuming that the number of gap chlorophylls between the PSI core and LHCI as well as the number of chlorophyll molecules bound by each Lhca is conserved, about 30 chlorophyll molecules remain to be distributed, suggesting that likely two additional Lhca are present in Chlamydomonas. If the number of chlorophylls coordinated by the Lhca or the number of gap and linker chlorophylls is not conserved, more than six subunits could be envisioned.

Interestingly, the distinct Lhca polypeptides accumulate at different levels with PSI. The data demonstrate that the population of Chlamydomonas PSI-LHCI in the culture analyzed in this study is highly heterogeneous. In its natural habitat, Chlamydomonas is not exposed to high light in comparison with land plants. A larger antenna might facilitate light capture in low light conditions. As motile organism, Chlamydomonas could be exposed to very different nutrient or light conditions over a relatively short period of time. Flexibility in LHCI compositon would allow adaptation of an antenna configuration suited to the prevailing environmental conditions.

Time resolved fluorescence measurements have shown that Chlamydomonas PSI-LHCI has a lower number of low energy chlorophylls that emit at a higher energy than the land plant complex. The stoichiometric data presented in Manuscript 5 provide insight into this phenomenon. Alignment of the Lhca sequences from *A. thaliana* and Chlamydomonas (Fig. 5) shows that *A. thaliana* Lhca3 and Lhca4 contain an asparagine at position A5 of the first transmembrane helix, a feature which is conserved among land plant Lhca3 and Lhca4. Assuming a 1:1 stoichiometry between Lhca1-Lhca4 and PSI for land plants (Ben-Shem, 2003; Ballottari, 2004; Amunts, 2007) and substoichiometric levels for Lhca5 (Ganeteg, 2004a; Storf, 2005), Lhca3 and Lhca4 would constitute between 44 and 50% of LHCI (assuming that Lhca5 can be expressed at a stoichiometry of up to 0.5:1 with PSI). In contrast, Chlamydomonas has three proteins with an asparagine at the A5 site (Lhca2, Lhca4 and Lhca9) and therefore might well coordinate low energy chlorophylls. Notably, Chlamydomonas Lhca3, which is a clear homologue of land plant Lhca3 (Koziol, 2007), has a histidine rather than an asparagine at this A5 site and therefore is unlikely to coordinate red chlorophylls. Our data indicate that Chlamydomonas Lhca4, which shares similarity with land plant Lhca4, is likely present at a 1:1 ratio with PSI, whereas Lhca2 and Lhca9 are both present at a ratio of slightly less than 0.5:1 with PSI. Together, these three proteins compose about 28% of the LHCI complex.

Time-resolved fluorescence spectroscopy indicated that the fluorescence lifetimes originating from red chlorophylls are shorter for Chlamydomonas than for *A. thaliana* (Ihalainen, 2005b). Similar observations were made in another study (Melkozernov, 2004). This indicates that while Chlamydomonas LHCI is approximately 1.5 to 2 times larger than the *A. thaliana* LHCI, it has a lower proportion of far-red fluorescing chlorophylls. Furthermore, these are less red shifted when compared to land plants. This is in line with the biochemical data presented in Manuscript 5. Using time-resolved absorption spectroscopy at 77K, Melkozernov and coworkers (Melkozernov, 2005) identified two distinct red spectral pools which belong to low-energy pigments in LHCI that absorb at 687 nm and 697 nm. These low energy pigments might be coordinated by Lhca4 and the Lhca2 and Lhca9 which have an asparigine (N) residue at position A5 that is involved in the formation of red chlorophyll clusters.

There are contrasting views as to the stoichiometry of vascular plant LHCI. The two existing crystal structures (Ben-Shem, 2003; Amunts, 2007) show one copy each of Lhca1, Lhca2,

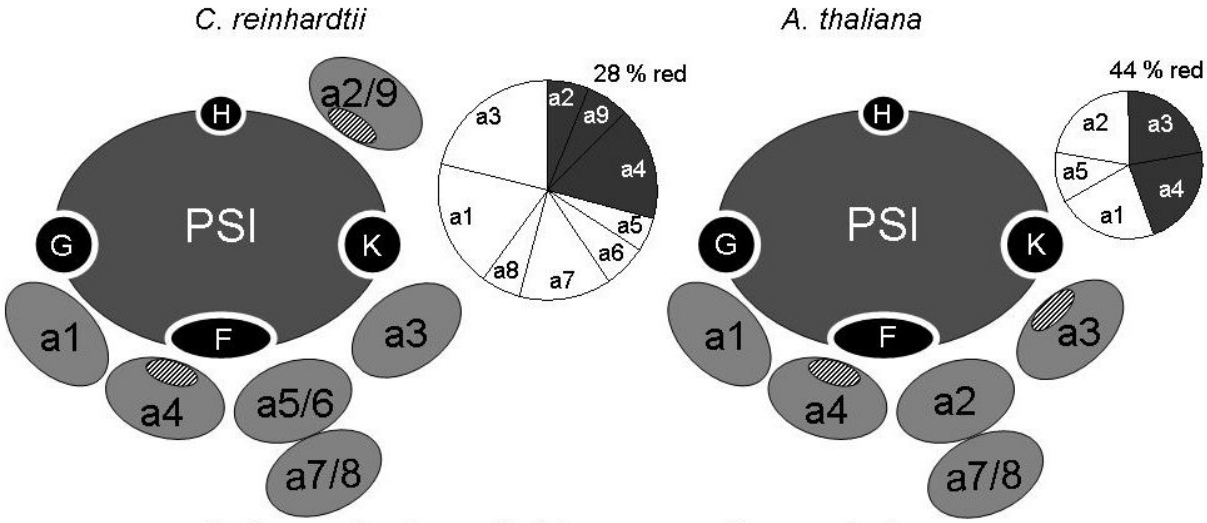

Protein	Accession	Land plant homologue	Helix B A4 A5
C.r. Lhca1	AF104633	Lhca1	...LKRFTESEVIHGRWAMLG...
C.r. Lhca3	AB122115	Lhca3	...PKWLQYSEVIHARWAMLG...
C.r. Lhca2		Lhca2	...LKWFREAELTNGRWAMAA...
C.r. Lhca9	AF244524	Lhca2	...LKWYAEAEKTNGRWAMMA...
C.r. Lhca4	AB122114	Lhca2 / Lhca4	...LKWYAQAELMNARFAMLA...
C.r. Lhca5	AB122116	Lhca2 / Lhca4	...LKWYRQSELQHARWAMLG...
C.r. Lhca6	AB122118	Lhca2 / Lhca4	...LKWFKESELVHSRWAMAA...
C.r. Lhca7	AY171231	Lhca5	...LKWYVQAELVHGRFAMLG...
C.r. Lhca8	AB122117	Lhca5	...LRWYQQAELIHCRTAMAG...
A.t. Lhca1	M85150		...LERYKESELIHCRWAMLA...
A.t. Lhca3	U01103		...PRWLAYGEIINGRFAMLG...
A.t. Lhca2	AF134120		...LKWNVQAEIVHCRWAMLG...
A.t. Lhca6	U03395		...LKWFAQAELIHSRWAMLA...
A.t. Lhca4	M63931		...LKWFVQAELVNGRWAMLG...
A.t. Lhca5	AF134121		...LKWYVQAELVHSRFAMLG...

Figure 5. A model comparing the PSI complex of *C. reinhardtii* and *A. thaliana* exemplifies the quantitative differences within LHCI. LHCI is composed of nine or five Lhca proteins, respectively, in *C. reinhardtii* and *A. thaliana* (marked a1-a9). Far-red fluorescing Lhca proteins are denoted with an oval with diagonal lines. A pie chart compares the absolute size of the LHCI antenna between *C. reinhardtii* and *A. thaliana* with the size of the pie chart being proportional to the absolute antenna size. Although *C. reinhardtii* LHCI is larger, only 28 % of the antenna is composed of far-red fluorescing protein pigment complexes highlighted in gray. For *A. thaliana*, the proportion is 44 %, assuming a contribution of Lhca5 with about 0.5 copies per PSI core. An alignment of portions of Helix 1 (B) from *C. reinhardtii* and *A. thaliana* shows the asparigine (N) residue at position A5 that is involved in the formation of red chlorophyll clusters (white characters) (Morosinotto, 2002, 2003; Croce, 2004; Morosinotto, 2005b; Mozzo, 2006).

Lhca3 and Lhca4 per PSI core. A study using recombinant proteins as standards and Coomassie staining intensity for quantitation, determined one copy each of Lhca1-4 in *A. thaliana* PSI-LHCI (Ballottari, 2004). Later analyses showed that the stoichimetries of the Lhca do not change with different light conditions (Ballottari, 2007). In contrast to this, a different study used immunoblotting to show differences in Lhca expression depending on

light regime (Bailey, 2001). In addition, lack of specific Lhca due to mutation or antisense inhibition can cause differences in accumulation of the remaining proteins (Ganeteg, 2001, 2004b).

Based on the data presented in Manuscript 5, we propose that PsaA has a modified N-terminus (Figure 4). The most likely modification would be N-terminal methionine excision, but until now no evidence has been provided that PsaA undergoes this process (Giglione, 2004). The X-ray diffraction data of pea PSI-LHCI shows that the N-terminus of PsaA is located on the stromal side in the cleft between PSI and Lhca2 and Lhca3 (Ben-Shem, 2003; Amunts, 2007); however, since the structure begins at position 31 of PsaA the precise location of the extreme N-terminus and a possible functional role of N-terminal modification remain to be resolved.

In conclusion, the stoichiometric data presented here provide an explanation for the fluorescence emission properties of the Chlamydomonas PSI-LHCI complex which possesses a lower proportion of red-shifted chlorophylls than the land plant complex. This is likely due to the lower proportion of Lhca with strong chlorophyll coupling in the region of the A5-B5 chlorophylls. In addition, our results suggest that the population of PSI-LHCI in Chlamydomonas is heterogeneously composed with differing LHCI composition. This implies a heterogeneity in energy transfer routes within PSI-LHCI and may be important when acclimating to different environmental conditions.

5.1.3. Composition of light-harvesting complex I in tomato

In contrast to *A. thaliana* which possesses one gene for the Lhca1, Lhca2 , Lhca3 and Lhca4 proteins, tomato LHCI is more complex. There are two *lhca1* genes encoding proteins that differ by one amino acid (*cab6a* and *cab6b*) (Pichersky, 1996). These have also been detected on the protein level (Zolla, 2002). Two *lhca4* genes sharing 93% identity at the amino acid level of the mature proteins (*cab11* and *cab12*) are also present in the tomato genome (Schwartz, 1991). In Manuscript 3, 2-DE and protein sequencing using MS were used to identify both Lhca4 isoforms (cab11 and cab12) on the protein level. In addition Lhca5 (Jansson, 1999) was detected on the protein level as a part of the PSI-LHCI complex. The fact that Lhca5 was found in the Lhca1/Lhca4 fraction but not in the Lhca2/Lhca3 fraction suggests that it associates with Lhca1 or Lhca4 rather than with Lhca2 and Lhca3 (Manuscript

3). Since the completion of the current study, Lhca5 has been further analyzed in other laboratories. Studies of reconstituted Lhca5 show that it can form heterodimers with Lhca1 (Storf, 2005). One possibility is that Lhca5 replaces part of the Lhca4 population and forms heterodimers with Lhca1 under certain growth conditions. However, the finding that plants lacking Lhca4 have very low Lhca1 levels despite elevated levels of Lhca5 provides evidence that Lhca1/Lhca5 heterodimers do not form *in vivo*. Studies with Lhca2 knock-out plants show that Lhca5 levels correlate with Lhca2 levels which suggests an interaction between Lhca2 and Lhca5 (Ganeteg, 2004a; Klimmek, 2005). In cross-linking experiments with wild-type pea and *A. thaliana* as well as with four *A. thaliana* knock-out lines lacking Lhca1, Lhca2, Lhca3, and Lhca4, respectively, it was shown that Lhca5 cross-links with Lhca2 (Luciniski, 2006). In addition, it was also shown that Lhca5 cross-links with itself which indicates that it can also form homodimers. Based on these results, two models were presented (Luciniski, 2006). One possibility is that Lhca5 interacts peripherally with Lhca2 at the Lhca2/Lhca3 dimersurface which would increase the size of LHCI. Another possibility is that it assembles into the Lhca1/Lhca4 binding site of PSI as a homodimeric complex (Luciniski, 2006). Transcript analysis suggests that land plant Lhca5 and Lhca6 are regulated differently than Lhca1, Lhca2, Lhca3, and Lhca4 under various growth conditions (Klimmek, 2006). This suggests that they have distinct roles in acclimating PSI-LHCI to changing environmental conditions (Ganeteg, 2004a).

The existence of two homologous Lhca4 proteins is interesting because Lhca4 has been shown to play a central role in stabilizing land plant LHCI (Morosinotto, 2005a). Studies with mutants lacking or having suppressed levels of Lhca1, Lhca2, Lhca3, and Lhca4 indicate that lack of Lhca4 has the largest contribution to plant fitness (Ganeteg, 2004b). Fifteen amino acids differ between the mature protein sequences of cab 11 and cab 12 (Fig. 6) It is unlikely that they would differ in their mode of interaction with Lhca1, since none of the substitutions are at residues in the second transmembrane helix that are important for dimerization with Lhca1 (Corbet, 2007). The amino acid substitutions in the N-terminal region should also not affect binding with Lhca1 since the N-terminus of Lhca4 is not involved in dimerization with Lhca1 (Schmid, 2002a). Although the extreme N-terminus of Lhca4 is not resolved in the most recent X-ray diffraction model of pea PSI-LHCI, it seems to be located in the cleft between LHCI and PSI (Amunts, 2007). One possibility is that it interacts with gap chlorophylls between LHCI and PSI or with linker chlorophylls between Lhca4 and Lhca2. It is interesting that some species such as tomato and poplar (Klimmek, 2006) possess

homologous genes for major Lhca proteins while *A. thaliana* contains a single copy of each. Light conditions in the natural habitat of tomato might have led to the evolution of two Lhca4 proteins, however, it is also possible that cab11 and cab12 are not functionally different. In studies to answer this question, knock-out plants lacking functional copies of *cab11 and cab12* would be very useful. Quantitation with MS could be used to determine if the expression ratio between the two isoforms is affected by different growth conditions.

By using long gels and an acrylamide gradient, a fifth protein band had been identified in PSI-LHCI and Lhca1/Lhca4 preparations (Schmid, 2002b). In the present study (Manuscript 3), immunoblotting showed a strong reaction of an Lhac1 specific antibody with this band. MS analysis also showed the presence of Lhca1 in this protein band. It is possible that this protein

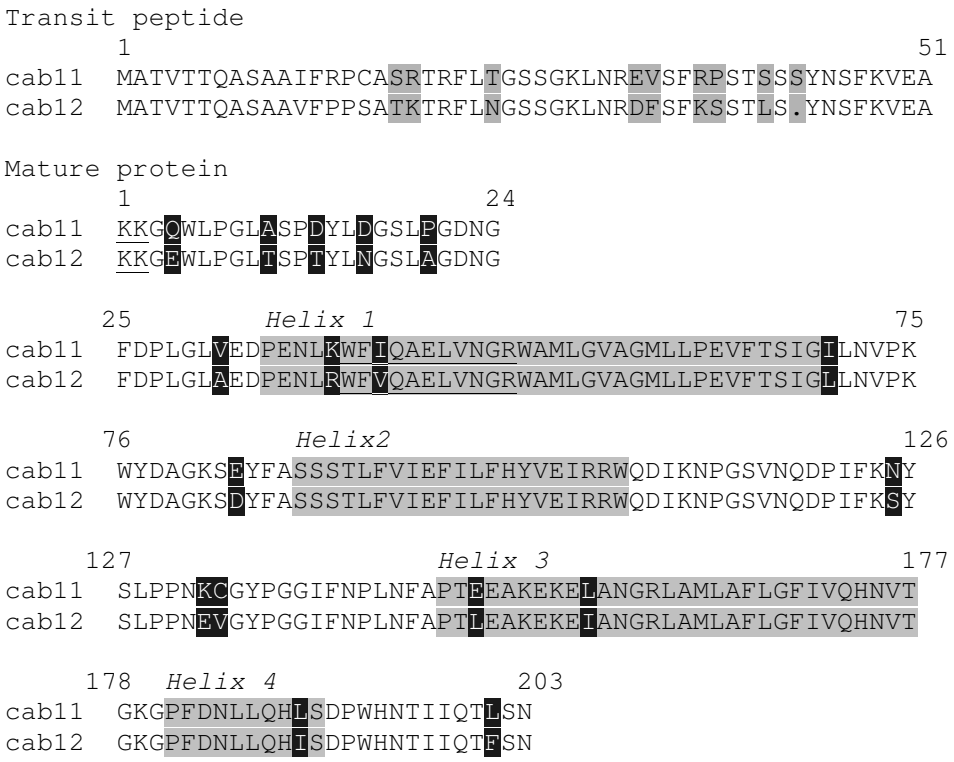

Figure 6. Comparison of the tomato cab11 and cab12 amino acid sequences. The two Lhca4 proteins share 93% identity at the amino acid level of the mature proteins (Schwartz, 1991). The mature protein amino acid sequences begin with the sequence KKG for both proteins (Schwartz, 1991; Pichersky 1996). The α-helices are shown with a grey background. Helices 1-3 are transmembrane spanning (see Fig. 1) while helix 4 is amphiphathic and is located on the luminal side of the thylakoid membrane. Amino acid substitutions are shown in white letters with a black background. The peptides WFIQAELVNGR (cab11) and WFIQAELVNGR (cab12) which differentiate cab11 and cab12 were identified by MS in this study (Manuscript 3).

arises from modification or differential processing of Lhca1. However, no experimental support for this was provided in the current study (Manuscript 3).

In addition to this novel protein band, high resolution 1- and 2-DE in combination with immunoblotting and MS identified several different Lhca1, Lhca2, Lhca3, and Lhca4 polypeptides differing in molecular mass and isoelectric point (Manuscript 3). Immunoblotting with anti-phosphothreonine and anti-phosphoserine antibodies did not reveal any phosphorylation which could have explained the existence of several Lhca isoforms. Another possibility is that Lhca1, Lhca3, and Lhca4, for which different molecular masses were observed, are differentially processed at the N-terminus as has been reported for Lhcb proteins in land plants (Clark, 1989) and in Chlamydomonas (Stauber, 2003). In addition, experimental artifacts such as acetylation or modification of the peptide amino terminus or the side chains of lysine or arginine by isocyanic acid (carbamylation) could explain the different Lhca isoforms. Although none of these modifications were identified by MS (Manuscript 3), recent 2-DE experiments with bacterially overexpressed Lhca proteins revealed spot patterns like those seen in tomato PSI-LHCI preparations (Volkmar Schmid, personal communication). These results indicate that the presence of various protein spots from tomato PSI-LHCI during 2-DE could be an experimental artifact.

5.2. Remodelling of Chlamydomonas photosystem I – light-harvesting complex I under iron deficiency

In Manuscript 4, the mechanism by which PSI-LHCI changes its conformation during iron deficiency was investigated. MS in conjunction with isotopic labelling was applied as a tool to identify and quantify which Lhca was affected by iron deficiency and to detect a processed form of Lhca3. Furthermore, RNA*i* technology was used to suppress Lhca3 levels and determine the function of the processed form of Lhca3 *in vivo*. Previously, immunoblotting of 2DE-separated thylakoids from iron-deficient cells revealed the appearance of a novel protein spot with the onset of iron deficiency (Moseley, 2002a). In Manuscript 4, the protein spot was identified as a lower molecular weight form of Lhca3 based on two internal peptide sequences that were identified by MS (Fig. 1 in Manuscript 4)). The occurrence of the novel form of Lhca3 is interpreted as being due to N-terminal processing because immunoblotting with an N-terminus-specific antibody showed that the larger form disappeared with the onset of iron deficiency and that its disappearance coincided with the appearance of the lower molecular

mass form of Lhca3 (Moseley, 2002a; Fig. 2A in Manuscript 4). The fact that accumulation of the processed form of Lhca3 correlates with a blue shift in the 77K fluorescence emission maximum from 711 nm to 704 nm in isolated thylakoids indicates that it initiates the physical changes that result in altered fluorescence. LHCI that is functionally connected to PSI exhibits a 77K fluorescence emission maximum of between 711 nm and 715 nm (Wollman, 1982; Bassi, 1992; Kargul, 2003; Takahashi, 2004; Gibasiewicz, 2005). A 77K fluorescence emission maximum at 704 nm is characteristic of oligomeric LHCI that is not attached to PSI (Wollman, 1982; Bassi, 1992, Kargul, 2003; Takahashi, 2004). In land plants, uncoupling of LHCI from PSI also results in a blue shift in fluorescence (Jensen, 2000; Morosinotto, 2005a). The cause of the blue shift has not been determined but it has been suggested that gap chlorophylls between PSI and LHCI contribute to the lowest energy states of red chlorophylls (Morosinotto, 2005a; Gibasiewicz, 2005).

Quantitative MS analysis of Fe-deficient (Fe(-)) and Fe-sufficient (Fe(+)) thylakoids and immunoblotting allowed an overview of the changes in the photosynthetic complex induced by iron deficiency. While PSII was largely unaffected, the PSI core was depleted to about 45% as compared to the levels under iron sufficient conditions. The impact on LHCI was more severe than??. The larger form of Lhca3 was the most severely affected, its levels being down to 5-10% of the Fe(+) conditions. Lhca5 also nearly completely disappeared, and the amounts of Lhca1, Lhca7 and Lhca8 were reduced, while Lhca4 and Lhca9 were strongly induced. Previously it had been shown that PsaK is even more sensitive to iron levels than Lhca3 (Moseley, 2002a). Since PsaK is known to stabilize the binding of Lhca3 to PSI (Jensen, 2000), these results suggest together that loss of PsaK exposes the N-terminus of Lhca3 to proteolytic processing (Manuscript 4). Upon addition of iron, the photosynthetic apparatus is quickly reassembled.

In order to investigate the functional association between LHCI and PSI under iron deficient conditions, thylakoids from Fe(+) and Fe(-) cells that had been differentially isotopically labelled were solubilized with detergent. Subsequently, the protein complexes were separated by sucrose gradient centrifugation. QuantitativeMS analysis showed that the truncated form of Lhca3 and the rest of LHCI stably associate with PSI under iron deficient conditions. When PSI particles isolated from Fe(-) and Fe(+) conditions were analyzed by 1-DE on an equal protein basis, the PSI core composed a higher percentage of the total sample than under iron sufficient conditions. Although ratios of all LHCI with respect to PSI were decreased under

iron deficient conditions, levels of Lhca4 and Lhca9 were less affected than other Lhca. These data suggest that the physical association, although somewhat modified, remains intact in the presence of processed Lhca3. Furthermore, the tight association of the processed form of Lhca3 with PSI indicates that it has a functional role.

In order to determine what function the N-terminally processed form of Lhca3 has, RNA*i* technology was used to produce a Chlamydomonas strain (IRLhca3) with depleted Lhca3 expression. In IRLhca3, levels of Lhca3 were reduced to about 10% of wild-type levels. The 77K fluorescence emission spectra of IRLhca3 showed a blue shift and an increase in fluorescence of the PSI-LHCI peak (similar to the case under iron deficiency). The loss of Lhca3 had little effect on the accumulation of the other Lhca proteins in the thylakoid membranes. However, quantitative MS analysis of sucrose gradient fractions of detergent solublized IRLhca3 thylakoids revealed differences in the association of Lhca proteins with PSI. Two PSI fractions were recovered; one containing most of the residual Lhca3 and one that was strongly depleted in Lhca3. Quantitative MS analysis of the two fractions by comparing each with isotopically labelled wild-type PSI-LHCI particles showed that with the exception of Lhca9, the association of Lhca proteins to PSI was severely weakened in the absence of Lhca3 (Tables IV and V in Manuscript 4). Interestingly, the fraction with depleted levels of Lhca3 also had severely depleted levels of PsaK. This suggests that Lhca3 and PsaK mutually stabilize one another or that their assembly into the PSI-LHCI is mutually dependent.

In summary, the N-terminal processing of Lhca3 impairs energy transfer to PSI under iron deficient conditions but does not abolish the physical association of oligomeric LHCI with PSI. Fig. 7 shows a model of the changes that occur to PSI-LHCI during iron deficiency. The dynamic interaction of Lhca3 with PSI may allow it to act as a safety valve to stop the transfer of excitation energy to PSI when the capacity of the electron transport chain is diminished. At the same time the truncated form of Lhca3 acts as a keystone in the interaction between LHCI and PSI. Since LHCI is uncoupled from PSI during iron deficiency, energy transfer to the PSI core is significantly slowed down (as is the case at low temperatures (Melkozernov, 2005)). This decreases delivery of excitation energy to P700. It has been shown that carotenoids bound to recombinant Lhca4 can quench chlorophyll triplet states and thereby prevent the formation of highly reactive singlet oxygen (Carbonera, 2005). It has also been shown using recombinant Lhca3 that the conversion of violaxanthin to zeaxanthin is nearly complete in

Lhca3 which reveals a mechanism for scavenging reactive oxygen species (Wehner, 2004). If these two mechanisms for photoprotection are present in Chlamydomonas, then LHCI that is energetically uncoupled from PSI during iron deficiency could function in photoprotection of the thylakoid membranes. In addition, Lhca4 and Lhca9 are both upregulated during iron deficiency. Further experiments have to be carried out to determine if these two Lhca are involved in photoprotection.

Iron deficiency results in the degradation of several proteins in LHCI which would result in the release of chlorophyll molecules. Upon absorption of light, free chlorophylls give rise to the formation of reactive oxygen species. Therefore, a mechanism for scavenging these chlorophylls must exist. The LI818 proteins can function in scavenging chlorophylls, and it is possible that proteins of this family serve a similar function in Chlamydomonas under iron deficiency (Heddad, 2002).

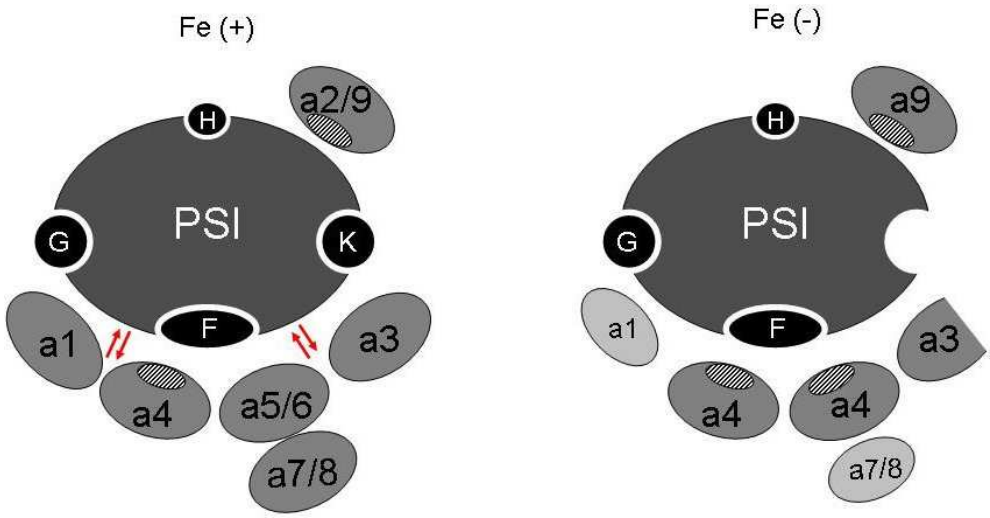

Figure 7. Model of the changes that occur to PSI-LHCI during iron deficiency. Under iron sufficient conditions (left), LHCI is physically and energetically associated with PSI and is composed of nine Lhca proteins (a1-a9). Under iron deficient conditions (right), PsaK becomes susceptible to proteolysis upon loss of its chlorophyll molecule and disappears nearly completely from the thylakoid membranes (Moseley, 2002a). Lack of PsaK exposes Lhca3 (a3) to proteolysis. The energetic connection between LHCI and PSI (shown with arrows) is severed upon N-terminal proteolytic cleavage of Lhca3. Further changes include the loss of Lhca2 (a2), Lhca5 (a5), and Lhca6 (a6) while Lhca4 (a4) and Lhca9 (a9) are upregulated. Levels of Lhca1 (a1), Lhca7 (a7) and Lhca8 (a8) decrease to a lesser extent (shown by smaller light grey ovals). The new conformation of LHCI prevents photo-oxidative damage to the thylakoid membranes during iron deficiency.

The situation is different in the halotolerant alga *Dunaliella salina* where measurements of intact cells showed that iron deficiency results in an increase in 77K chlorophyll fluorescence emission at ~ 708 nm (which is characteristic of PSI-LHCI) relative to emission at 685 nm which might be due to a larger size antenna (Varsano, 2003). In addition, a 45 kDa chlorophyll a/b binding protein (Tidi) induced by thylakoid iron deficiency was induced (Varsano, 2003) and was determined to be an LHCI like protein with a unique proline rich N-terminal extension of 126 amino acids (Varsano, 2006). Purification and single particle electron microscopy analysis of a high molecular weight PSI-LHCI complex which contained Tidi from iron deficient cells indicated that one of the functions of Tidi is to increase the area of LHCI. This is similar to the isiA complex of cyanobacteria which forms a ring of 18 subunits around cyanobacterial PSI and is composed of proteins with high homology to the CP43 protein of PSII (Bibby, 2001; Boekema, 2001; Murray, 2006). The isiA complex likely functions to increase photosynthetic performance (Melkozernov, 2003, 2006; Varsano, 2006). However it is also induced by photoxidative stress (Sandström, 2001; Havaux, 2005) and can function in photoprotection (Ihalainen, 2005a; Kouril, 2005). The contrasting situation between Chlamydomona*s* and *D. salina* may be explained by the fact that *D. salina* can only grow photoautotrophically and thus is forced to maintain photosynthetic performance during iron deficiency. In contrast, for the experiments used in this study, Chlamydomonas was grown photoheterotrophically and could gain energy by mitochondrial metabolism. The photosynthetic apparatus was not required for energy fixation but at the same time needed to be protected from photoinhibition in a poised state to take advantage of conditions in which iron was again abundant. Experiments in which Chlamydomonas grows under photoautotrophic conditions suggest that changes in PSI-LHCI occur much more slowly as compared to photoheterotrophic conditions (Michael Hippler, personal communication).

As a facultative phototroph for which photosynthesis is dispensable in the presence of acetate as a reduced carbon source, Chlamydomonas does not have to be photosynthetically productive. PSI-LHCI is shifted to a dissipative mode and does not disappear completely. As PSI is disassembled so that iron could be re-allocated to the mitochondrial respiratory chain (Naumann, 2007), it might be particularly sensitive and therefore a dissipative state for LHCI might be particularly important. A possibility is that this conformation represents a sort of standby state as has been suggested in a recent study (Naumann, 2007) which can be quickly turned on in the case that iron is added back to the medium again. This would avoid the costs of disassembling and re-synthesizing the photosynthetic apparatus.

5.3. Stable isotope labelling and isotope dilution allow mass-spectrometric protein quantitation

Methods were established in Chlamydomonas for stable isotope labelling for quantitative studies of photosynthetic proteins (Manuscript 1). Using the arginine auxotrophic mutant CC424/425 which lacks a functional arginine succinate lyase, it was possible to introduce arginine containing six ^{13}C atoms into the entire Chlamydomonas proteome (SILAC approach, Fig. 3). Samples from iron-sufficient and iron-deficient samples were combined, separated by 1-DE, hydrolyzed with trypsin and analyzed by LC-MS to quantify changes to PSI-LHCI proteins during iron deficiency (Manuscript 4). For determining stoichiometries between the Lhca and PSI, the endoproteinases Lys-C (from *Lysobacter enzymogenes*) which cleaves with high specificity and efficiency after lysine residues and trypsin which cleaves after lysine and arginine residues were used. The $^{13}C_6$-arginine labelled PSI-LHCI corresponding to a known amount of chlorophyll was incubated with known amounts of synthetic peptides specific for PSI and LHCI subunits together with one of the proteases (Manuscript 5). By comparing the signal intensities in LC-MS chromatograms for native (^{13}C) and synthetic (^{12}C) isotopomers the amount of each protein per microgram chlorophyll could be derived. By normalizing the protein/chlorophyll ratios (prot/chl) for the Lhca to the values for the PSI subunits, the stoichiometries between the Lhca and PSI were determined.

For relative or absolute quantification of proteins, MS-based approaches offer two key advantages over determination of quantity based on staining intensity of 1-DE or 2-DE-separated proteins. MS allows very high selectivity so that even in very complex mixtures, distinct peptides can be sufficiently distinguished for quantitation. A key to achieving high selectivity is the use of tandem mass spectrometry (MS/MS; McLafferty, 1978). MS enables higher levels of accuracy with coefficients of variation (CV, relative standard deviation) ranging between 4 and 10% (Zhu, 1996; Berna, 2006; Uitto, 2007) while CV for specific dye binding range between 20 and 30% (Koller, 2005; Ballottari, 2007; Uitto, 2007). Methods in which two protein samples are marked with distinct dyes and loaded on the same gel (DIGE; Alban, 2003) can reduce CV for relative quantitation of proteins but does not allow overlapping proteins from the same sample to be distinguished (Görg, 2004). Stoichiometric quantitation of ^{14}C-labelled protein subunits in polyacrylamide gels has also been used for analysis of PSI core subunit stoichiometry in Chlamydomonas (Oritz, 1984), *Dunaliella salina* (Bruce, 1988a) and Lemna (Bruce, 1988b). For this method, CV also range between 10

and 30%. Limiting factors are co-migration proteins during electrophoresis, interference of the polyacrylamide gel matrix with detection of ^{14}C isotope decay, and the inability to unambiguosly identify the protein bands on the gel. The use of phosphor-imaging for radioactive detection would increase the accuracy of quantitation with radioisotopes. Protein quantitation with stable isotope labelling and MS complements established methods and offers specificity and selectivity for quantitation of proteins in complex mixtures.

Using specific Coomassie binding as a measure of protein abundance for 1-DE separated samples, Ballottari and colleagues determined a stoichiometry of 1:1 between Lhca1 and Lhca4 in *A. thaliana* (Ballottari, 2004). This technique was further used to determine if variable light or temperature conditions cause changes in Lhca expression levels (Ballottari, 2007). Such an approach would not be feasible for Chlamydomonas Lhca proteins because several proteins have a very similar size (for example Lhca1/9 likely differ from each other by only 7 Da while Lhca5/6 and Lhca7/8, respectively, differ from one another by less than 100 Da). Instead, 2-DE approaches have been used for investigating Chlamydomonas Lhca stoichiometry (Bassi, 1992; Hippler, 2001). Because different proteins solubilize with different efficiencies during isoelectric focusing, determination of protein stoichiometry from 2-DE can result in artifacts. In addition, even with high resolution 2-DE some Lhca co-migrate (Stauber, 2003). Despite its advantages, incomplete proteolysis as well as artifacts introduced by metabolic labelling such as further metabolism of amino acids still need to be addressed for quantitative protein studies with MS.

The establishment of new methods for determining the stoichiometry in multiprotein complexes in Chlamydomonas provides a general means for quantitation of subunit stoichiometries within any multi-protein complex in Chlamydomonas or any other organism that is auxotrophic for one or more amino acids. Once their stoichiometry has been established, $^{13}C_6$-arginine labelled multiprotein complexes from the CC424/425 strain such as PSI-LHCI can serve as references for determining stoichiometries within complexes from other strains or other growth conditions. Such an approach was used to establish absolute protein stoichiometries in brain samples by first determining protein stoichiometries in isotopically labelled neuronal cell cultures and then comparing these with non-labelled whole brain samples (Ishihama, 2005).

5.4. Conclusions and perspectives

In the present study, two eukaryotic organisms, the green alga Chlamydomonas and the land plant tomato, were studied with respect to the composition of their LHCI and the association of LHCI with PSI. A detailed study of Chlamydomonas LHCI was aimed at determining the qualitative composition and the stoichiometry of its Lhca with respect to the PSI core complex. In addition the dynamic changes that occur in Chlamydomonas LHCI under iron deficiency were investigated.

Vascular plant LHCI contains four subunits (Lhca1-Lhca4) that can be isolated as the Lhca1/Lhca4 (Lam, 1984) dimers. Lhca2 and Lhca3 may also purify together as dimers under mild conditions (Ihalainen, 2000; Croce, 2002). The polypeptides encoded by two additional *lhca* genes, Lhca5 and Lhca6 (Jansson, 1999), had not been detected *in planta* before the present study. Analysis of detergent-solubilized tomato PSI-LHCI using immunoblotting, 2-DE and MS (Manuscript 3) revealed that the homologous Lhca4 proteins cab11 and cab12 are both present in the thylakoid PSI-LHCI population. In addition, the Lhca5 polypeptide with a low abundant transcript was identified for the first time and shown to associate with PSI.

Chlamydomonas LHCI is composed of nine distinct Lhca (Lhca1-Lhca9) that constitutively assemble into the PSI-LHCI complex (Hippler, 2001; Stauber, 2003). They associate tightly with PSI and increase photosynthetic capacity by gathering additional light energy. However, during iron deficient conditions when PSI core levels are drastically diminished, LHCI is remodelled and becomes energetically uncoupled from PSI (Moseley, 2002a).

Comparison of oligomeric LHCI isolated from a PSI-deficient Chlamydomonas strain with PSI-LHCI from wildtype cells shows that Lhca3, Lhca2 and Lhca9 require PSI for assembly into LHCI indicating that they are in close contact with PSI and likely important for energy transfer between LHCI and PSI (Manuscript 2). This idea is further supported by correlation of N-terminal processing of Lhca3 with energetic uncoupling of LHCI from PSI during progressing stages of iron deficiency (Manuscript 4). N-terminal processing of Lhca3, however, does not weaken the physical association of LHCI with PSI as does loss of Lhca3 in an RNA*i* strain. Additional changes to LHCI include degradation of Lhca5 and upregulation of Lhca4 and Lhca9. Using isotope dilution MS, Chlamydomonas LHCI was determined to be composed of six to nine subunits (Manuscript 5). Several proteins are not present at 1:1

stoichiometries with PSI which means that the thylakoid LHCI population is heterogeneously composed. The data show that Chlamydomonas LHCI contains a lower proportion of Lhca potentially contributing to far-red fluorescence emission than land plants. As is the case in tomato (Storf, 2004), there is more than one PSI-LHCI population present in the thylakoid membranes at any one time.

Throughout the present study, MS analysis of proteotypic peptides (Manuscript 1) proved to be a powerful tool to study the composition and dynamics of protein complexes. The establishment of the SILAC technique in Chlamydomonas provided a refined means of estimating the stoichiometry of the Lhca proteins and PSI. This provides a general means of quantifying subunit stoichiometries within any multi-protein complex in organisms that are auxotrophic for one or more amino acids.

Future investigations will likely aim at characterizing the different Lhca proteins in more detail and determining if LHCI composition changes under varying environmental conditions apart from iron concentrations. In this context, it would be interesting to conduct site-directed mutagenesis of Lhca2, Lhca4 and Lhca9 to find out if they possess far red chlorophyll forms. Cross-linking or nearest neighbor analysis might allow determination of the location of Lhca2/Lhca9. In order to determine if the isoforms of tomato Lhca4 are expressed at different levels, MS could be used for quantitation. It would be interesting to explore if there are environmental factors that have driven tomato to evolve two closely related Lhca4 genes while *A. thaliana* possesses only one copy. Among the influences that would be interesting to investigate, at least in Chlamydomonas, is the interplay between iron deficiency and acetate levels. In addition, iron deficient PSI-LHCI should be isolated for structural characterization. Measurements of PSI activity and oxygen evolution capability would provide more insight into the physiological status of iron-deficient PSI-LHCI. The extent of cyclic electron flow during iron deficiency would help to clarify how PSI and the cytochrome b_6f complex interact in times of iron scarcity. In addition to laboratory experiments, *in vivo* experiments are required to determine if LHCI composition changes under conditions in which Chlamydomonas is grown in culture tanks exposed to natural light. Such experiments could also help pinpoint the functional significance of Chlamydomonas Lhca.

The N-terminal processing of Lhca3 that takes place in Chlamydomonas under iron deficiency will no doubt be another focus of future studies. In order to determine if N-

terminal processing of Lhca3 would cause an energetic uncoupling of LHCI from PSI, a truncated form of Lhca3 could be overexpressed in an Lhca3 knock-out mutant (which at the moment has not been identified). Overexpression of a truncated form of Lhca3 in the IRLhca3 strain in which Lhca3 levels are suppressed to 10% of wild-type levels is another possibility. This approach could, however, be technically difficult since the newly introduced Lhca3 transgene would likely also be suppressed. Identification of the protease responsible for the cleavage would be greatly facilitated by the determination of the proteolytic site using N-terminal sequencing of the processed form of Lhca3. If processing is required to prevent photoinhibition in Chlamydomonas during iron deficiency, might be tested by overexpression of a mutated form of Lhca3 that is resistant to proteolysis in an Lhca3 knock-out strain.

By identifying a new Lhca in tomato and determining the stoichiometry of Lhca1-Lhca9 with PSI in Chlamydomonas as well as quantifying iron deficiency-induced changes in Chlamydomonas LHCI, we now have a clear and more detailed picture of eukaryotic LHCI. For both organisms, more than one population of LHCI is present in the thylakoids at one time. Furthermore, the results presented here set the stage for functional studies to determine the role of individual Lhca in acclimation the photosynthetic apparatus to varying environmental conditions. The evolution of complexity in both green algae and land plant was likely driven by selective pressures requiring PSI-LHCI to be capable of both light-harvesting and photoprotection (Croce, 2002; Koziol, 2007).

6. Summary

The photosynthetic apparatus of eukaryotic organisms possesses a remarkable ability to adapt to ever changing light conditions and other environmental cues. This is possible because of the modular structure of the apparatus composed of core complexes and antenna complexes. LHCI constitutes an antenna complex of the thylakoid membrane that absorbs solar energy. In this way, it drives photosynthesis, but is also able to protect the thylakoid membrane from damage by excess energy. LHCI consists of up to six polypeptides in land plants (Lha1-6) and nine polypeptides (Lhca1-9) in green algae and is tightly associated with the PSI core complex. The ability to separate and identify the different Lhca and the establishment of methods for absolute quantification of proteins in complexes would enable us to fill in gaps that exist today in our knowledge about the role of individual Lhca proteins and their function in adaptation of photosynthesis to varying environmental conditions.

In the present study, the composition of plant LHCI, its association with PSI and its dynamic changes upon iron deficiency as one environmental variable were investigated by means of qualitative and quantitative proteome analyses using Chlamydomonas and tomato as model organisms.

Eukaryotic LHCI protein-pigment complexes share a similar topology but have distinct spectral properties. A PSI deficient Chlamydomonas mutant strain (*ΔpsaB*) was used to examine the composition of oligomeric LHCI. A combination of detergent solubilization, sucrose density gradient centrifugation and DEAE-sepharose chromatography, allowed purification of intact oligomeric complexes. Immunoblotting after 1-DE separation and 2-DE showed that this complex lacks Lhca2, Lhca3 and Lhca9 indicating that each of these Lhca requires PSI for stable association into LHCI. In order to better understand the composition of Chlamydomonas LHCI, stable isotope labelling and MS were used to determine the stoichiometry of Lhca1-Lhca9 proteins with PSI. With this approach, it was possible to determine the number of Lhca1-Lhca9 that associate with PSI, a task that would not have been possible by 1-DE or 2-DE. The data show that the population of Chlamydomonas LHCI in the thylakoid membranes is heterogeneous. Chlamydomonas LHCI possesses three proteins, Lhca2, Lhca4, and Lhca9, which are predicted to bind low-energy chlorophylls. Together, they compose about 30% of LHCI which is in contrast to land plant LHCI in which about 44 to 50% of the Lhca contribute to far red fluorescence emission.

By applying proteomic techniques to tomato LHCI, new proteins and possible isoforms were discovered. It was demonstrated that both copies of *lhca4* (*cab11* and *cab12*) and the *lhca5* gene are expressed on the protein level, and that the proteins associate with PSI. These results reveal a higher level of LHCI complexity than was previously known in land plants.

Chlamydomonas PSI-LHCI is known to remodel into a dissipative conformation upon iron deficiency during heterotrophic growth conditions. The present study examined the changes that occur on the protein level under iron deficient conditions in detail using isotopic labelling and MS. A processed form of Lhca3 was identified and Lhca4 and Lhca9 were shown to be strongly induced. The use of RNA*i* technology to suppress Lhca3 expression provided evidence that Lhca3 is required for stabilization of the physical interaction and energy transfer between LHCI and PSI. The results of fluorescence emission measurements (77K) and expression analyses are in agreement with the processing of Lhca3 being the mechanism that uncouples the energy transfer between LHCI and PSI.

The establishment of methods for determining the subunit stoichiometry of multiprotein complexes in Chlamydomonas provides a general means for the quantitation of subunit stoichiometries within any multiprotein complex in Chlamydomonas or other organisms that are auxotrophic for one or more amino acids. Also, the approach will enable the comparison of subunit stoichiometries in samples from different growth conditions.

7. Zusammenfassung

Der Photosyntheseapparat eukaryotischer Organismen kann sich in bemerkenswerte Weise an sich verändernde Lichtbedingungen und andere Umweltfaktoren anpassen. Diese Anpassung wird durch den modularen Aufbau des Photosyntheseapparates aus Kernkomplexen und Antennenkomplexen ermöglicht. Lichtsammelkomplex I (LHCI) ist ein Antennenkomplex der Thylakoidmembran, der Sonnenenergie absorbiert. Dadurch treibt er einerseits die Photosynthese an, ist aber andererseits auch in der Lage, die Thylakoidmembran vor Schäden durch überschüssige Energie zu schützen. LHCI besteht in Landpflanzen aus bis zu sechs Polypeptiden (Lhca1-6), in Grünalgen aus neun Polypeptiden (Lhca1-9). Die Lhca-Proteine sind eng mit dem Kernkomplex Photosystem I (PSI) assoziiert. Die Möglichkeit, verschiedene Lhca-Proteine voneinander zu trennen und sie eindeutig zu identifizieren und die Verfügbarkeit von Methoden zur absoluten Quantifizierung von Proteinen in Komplexen würden es erlauben, die Rolle der einzelnen Lhca-Proteine und ihre Funktion bei der Anpassung der Photosynthese an variierende Umweltbedingungen besser zu verstehen.

In der vorliegenden Arbeit wurden die Zusammensetzung des pflanzlichen LHCI, seine Assoziation mit PSI und seine dynamischen Veränderungen unter Eisenmangelbedingungen als einem variablen Umweltfaktor mittels qualitativer und quantitativer Proteomanalyse der Modellorganismen Chlamydomonas und Tomate untersucht.

Die Protein-Pigment-Komplexe des eukaryotischen LHCI besitzen eine ähnliche Topologie, aber verschiedene spektrale Eigenschaften. Um die oligomere Zusammensetzung von LHCI zu untersuchen, wurde ein PSI-defizienter Chlamydomonas-Stamm (*ΔpsaB*) verwendet. Die Kombination von Solubilisierung mit Detergenzien, Saccharose-Dichtegradienten-Zentrifugation sowie Chromatographie an DEAE-Sepharose erlaubte die Isolierung intakter oligomerer Komplexe. Immunodetektion nach eindimensionaler Auftrennung und zweidimensionale Gelelektrophorese zeigten, dass Lhca2, Lhca3 und Lhca9 in diesen Komplexen fehlen. Das deutet darauf hin, dass zur stabilen Assoziation dieser Untereinheiten mit LHCI die Anwesenheit von PSI erforderlich ist. Ein besseres Verständnis der Zusammensetzung des LHCI von Chlamydomonas wurde gewonnen, indem die Stöchiometrie der Untereinheiten Lhca1-Lhca9 nach Markierung mit stabilen Isotopen mittels Massenspektrometrie bestimmt wurde. Mit dieser Methode konnte die Anzahl der Lhca1-Lhca9-Untereinheiten ermittelt werden, die mit PSI assozieren. Dies wäre mittels ein- oder

zweidimensionaler Gelelektrophorese nicht möglich gewesen. Die Ergebnisse zeigen, dass die Population von LHCI in der Thylakoidmembran von Chlamydomonas heterogen aufgebaut ist. Anhand ihrer Aminosäuresequenz kann vorhergesagt werden, dass Lhca2, Lhca4 und Lhca9 Niedrigenergie-Chlorophylle koordineren. Die stöchiometrischen Daten besagen, dass diese Proteine etwa 30% des LHCI ausmachen. Im Vergleich dazu besteht der LHCI der Landpflanzen bis zu 50% aus Lhca mit Niedrigenergie-Chlorophyllen.

Durch die Nutzung von Methoden der Proteomik auf LHCI der Tomate wurden neue Proteine und mögliche Isoformen entdeckt. Es wurde gezeigt, dass beide Kopien von *lhca4* (*cab11* und *cab12*) auf dem Proteinniveau exprimiert werden und dass die cab11 und cab12 mit PSI assozieren. Aus diesen Ergebnissen kann geschlossen werden, dass der LHCI der Landpflanzen komplexer aufgebaut ist als bisher angenommen wurde.

Es ist bekannt, dass es unter Eisenmangel und heterotrophen Wachstumsbedingungen in Chlamydomonas zur Entkopplung des LHCI von PSI kommt. Dabei erfolgt der Umbau in eine Konformation, die die Abgabe von überschüssiger Energie ermöglicht. In der vorliegenden Untersuchung wurden die Veränderungen, die auf dem Proteinniveau unter Eisenmangel stattfinden, mittels Isotopenmarkierung und Massenspektrometrie detailliert untersucht. Dabei gelang die Identifizierung einer prozessierten Form von Lhca3 und der Nachweis einer Induktion des Expressionsniveaus von Lhca4 und Lhca9. Die Analyse einer RNA*i*-Mutante mit verminderter Lhca3-Expression zeigte, dass Lhca3 die physikalische Wechselwirkung von LHCI und PSI stabilisert und für die energetische Kopplung von LHCI und PSI nötig ist. Fluoreszenz-Emissionsmessungen (77K) und Expressionsanalysen lieferten Hinweise darauf, dass die Prozessierung von Lhca3 den Mechanismus zur Entkopplung der energetischenVerbindung zwischen LHCI und PSI darstellt.

Die hier etablierte Methode zur Bestimmung der Stöchiometrie der Untereinheiten von Multiproteinkomplexen in Chlamydomonas kann als generelle Methode zur Analyse der Stöchiometrie von Multiproteinkomplexen in Chlamydomonas angesehen werden. Sie lässt sich außerdem zur Analyse anderer Organismen anwenden, die in Bezug auf eine oder mehrere Aminosäuren auxotroph sind. Zusätzlich bietet die Methode die Möglichkeit, Stöchiometrien innerhalb von Multiproteinkomplexen in Abhängigkeit von den Wachstumsbedingungen zu bestimmen.

References

Aebersold, R., Mann, M. (2003). Mass spectrometry-based proteomics. Nature **422,** 198-207.

Alban, A., Olu David, S., Bjorkesten, L., Andersson, C., Sloge, E., Lewis, S., Currie, I. (2003). A novel experimental design for comparative two-dimensional gel analysis: Two-dimensional difference gel electrophoresis incorporating a pooled internal standard. Proteomics **3,** 36-44.

Amunts, A., Omri, Drory, Nelson, N. (2007). The structure of a plant photosystem I supercomplex at 3.4 Å resolution. Nature **447,** 50-63.

Bailey, S., Walters, R. G., Jansson, S., Horton, P. (2001). Acclimation of *Arabidopsis thaliana* to the light environment: the existence of seperate low light and high light responses. Planta **213,** 794-801.

Ballottari, M., Dal´Òsto, L., Morosinotto, T., Bassi, R. (2007). Contrasting behaviour of higher plant photosystem I and II antenna systems during acclimation. J. Biol. Chem. **282,** 8947-8958.

Ballottari, M., Govoni, C., Caffari, S., Morosinotto, T. (2004). Stoichiometry of LHCI antenna polypeptides and characterization of gap and linker pigments in higher plants Photosystem I. Eur. J. Biochem. **271,** 4659 - 4665.

Barndridge, D.R., Dratz, E. A., Martin, T., Bonilla, L. E., Moran, L. B., Lindall, A. (2003). Absolute quantification of the G-protein coupled receptor rhodopsin by LC/MS/MS using proteolysis product peptides and synthetic peptide standards. Analytical Chemistry **75,** 445 - 451.

Bassi, R., Soen, S., Y., Frank, G., Zuber, H., Rochaix, J., D. (1992). Characterization of chlorophyll a/b proteins of photosystem I from *Chlamydomonas reinhardtii*. J. Biol. Chem. **267,** 25714-25721.

Ben-Shem, A., Frolow, F., Nelson, N. (2003). Crystal structure of plant photosystem I. Nature **426,** 630-635.

Berna, M., Schmalz, C., Duffin, K., Mitchell, P., Chambers, M., Ackermann, B. (2006). Online immunoaffinity liquid chromatography/tandem mass spectrometry determination of a type II collagen peptide biomarker in rat urine: Investigation of the impact of collision-induced dissociation fluctuation on peptide quantitation. Anal. Biochem. **356,** 235-243.

Bibby, T.S., Mary, I., Nield, J., Partensky, F., Barber, J. (2003). Low-light-adapted *Prochlorococcus* species possess specific antennae for each photosystem. Nature **424,** 1051-1054.

Bibby, T.S., Nield, J., Barber, J. (2001). Iron deficiency induces the formation of an antenna ring around trimeric photosystem I in cyanobacteria. Nature**,** 473-475.

Boekema, E.J., Hifney, A., Yakushevska, A. E., Piotrowski, M., Keegstra, W., Berry, S., Michel, K.-P., Pistorius, E. K., Kruip, J. (2001). A giant chlorophyll-protein complex induced by iron deficiency in cyanobacteria. Nature **412,** 745-748.

Bruce, B., D., Malkin, R. (1988a). Structural aspects of photosystem I from *Dunaliella salina*. Plant Physiol. **88,** 1201-1206.

Bruce, B., D., Malkin, R. (1988b). Subunit stoichiometry of the chloroplast photosystem I complex. J. Biol. Chem. **263,** 7302-7308.

Byrdin, M., Jordan, P., Krauss, N., Fromme, P., Stehlik., Schlodder, E. (2002). Low energy chlorophylls. Biophysical Journal **83,** 433-.

Carbonera, D., Giancarlo, A., Morosinotto, T., Bassi, R. (2005). Quenching of chlorophyll triplet states by carotenoids in reconstituted Lhca4 subunit of peripheral light-harvesting complex of photosystem I. Biochemistry **44,** 8337-8346.

Clark, S.E., Abad, M. S, Lamppa, G. K. (1989). Mutations at the transit peptide-mature protein junction separate two cleavage events during chloroplas import of the chlorophyll a/b-binding protein. J. Biol. Chem. **264,** 17544-17550.

Corbet, D., Schweikardt, T., Paulsen, Schmid, V. H. R. (2007). Amino acids in the second transmembrane helix of the Lhca4 subunit are important for formation of stable heterodimeric light-harvesting complex LHCI-730. J. Mol. Biol. **370,** 170-182.

Cramer, W.A., Zhang, H., Yan, J., Kurisu, G., Smith, J. L. (2006). Transmembrane traffic in the cytochrome b_6f complex. Annu. Rev. Biochem. **75,** 769-790.

Croce, R., Morosinotto, T., Castelletti, S., Bassi, R. (2002). The Lhca antenna complexes of higher plants photosystem I. Biochim. Biophys. Acta **1556,** 19-40.

Croce, R., Morosinotto, T., Ihalainen, J. A., Chojnicka, A., Breton, J.., Dekker, J. P., van Grondelle, R., Bassi, R. (2004). Origin of the 701-nm fluorescence emission of the Lhca2 subunit of higher plant photosystem I. J. Biol. Chem. **280,** 48543-48549.

Croce, R., Zucchelli, G., Garlaschi, F., M., Bassi, R., Jennings, R., C. (1996). Excited-state equilibration in the photosystem I light harvestin I complex: P700 is almost isoenergetic with its antenna. Biochemistry **35,** 8572-8579.

Dekker, J.P., Boekema, E. J. (2005). Supramolecular organization of thylakoid membrane proteins in green plants. Biochim. Biophys. Acta **1706,** 12-39.

Dolganov, N.A., Bhaya, D., Grossman, A. R. (1995). Cyanobacterial protein with similarity tothe chlorophyll *a/b* binding proteins of higher plants: evolution and regulation. Proc. Natl. Acad. Sci. USA **92,** 636-640.

Eng, J., K., McCormack, A., L., Yates, J., R., 3rd. (1994). An approach to correlate tandem mass spectral data of peptides with amino acids in a protein database. J. Am. Soc. Mass. Spectrom. **5,** 976-989.

Englemann, E., Zucchelli, G., Casazza, A., P., Brogioli, D., Garlaschi, F., M., Jennings, R., C. (2006). Influence of the photosystem I - light harvesting complex I antenna domains on fluorescence decay. Biochemistry **45,** 6947 - 6955.

Finazzi, G. (2004). The central role of the green alga *Chlamydomonas reinhardtii* in revealing the mechanism of state transitions. J. Exp. Bot. **56,** 383-388.

Ganeteg, U., Klimmek, F., Jansson, S. (2004a). Lhca5 - an LHC - type protein associated with photosystem I. Plant Molecular Biology **54,** 641-651.

Ganeteg, U., Kühlheim, C., Andersson, J., Jansson, S. (2004b). Is each light-harvesting complex protein important for plant fitness? Plant Physiology **134,** 502-509.

Ganeteg, U., Strand, Å., Gustafsson, P., Jansson, S. (2001). The properties of the chlorophyll *a/b*-binding proteins Lhca2 and Lhca3 studied *in vivo* using antisense inhibition. Plant Physiol. **127,** 150-158.

Gerber, S.A., Rush, J., Stemman, O., Kirschner, M. W., Gygi, S. P. (2003). Absolute quantification of proteins and phosphoproteins from cell lysates by tandem MS. Proc. Natl. Acad. Sci. USA **12,** 6940-6945.

Germano, M., Yakushevska, A. E., Keegstra, W., van Gorkom, J. J., Dekker, J. P., Boekema, E. J. (2002). Supramolecular organization of photosystem I and light harvesting complex I in *Chlamydomonas reinhardtii*. FEBS Lett. **525,** 121-125.

Gibasiewicz, K., Szrajner, A., Ihalainen, J. A., Germano, M., Dekker, J. P., van Grondelle, R. (2005). Characterization of low-energy chorophylls in the PSI-LHCI supercomplex from *Chlamydomonas reinhardtii*. A site-selective fluorescnece study. J. Phys. Chem. B **109,** 21180-21186.

Giglione, C., Boularot, A., Meinnel, T. (2004). Protein N-terminal methionine excision. Cell. Mol. Life Sci. **61**, 1455-1474.

Gobets, B., Valkunas, L., van Grondelle, R. (2003). Bridging the gap between structural and lattice models: a parameterization of energy transfer and trapping in photosystem I. Biophysical Journal **85,** 3872-3882.

Gobets, B., van Grondelle, R. (2001). Energy transfer and trapping in photosystem I. Biochim. Biophys. Acta **1507,** 80-99.

Görg, A., Weiss, W., Dunn, M. J. (2004). Current two-dimensional electrophoresis technology for proteomics. Proteomics **4,** 3665-3685.

Grossman, A.R., Harris, E. E., Hauser, C., Lefebvre, P. A., Martinez, D., Rokhsar, D., Shrager, Silflow, C. D., Stern, D., Vallon, O., Zhang, Z. (2003). *Chlamydomonas reinhardtii* at the crossroads of genomics. Eukaryotic Cell **2,** 1137-1150.

Gygi, S.P., Rist, B., Gerber, S. A., Turecek F., Gelb, M. H., Aebersold, R. (1999). Quantitative analysis of complex protein mixtures using isotope-coded affinity tags. Nature Biotechnology **17,** 994 - 999.

Harris, E. (2001). *Chlamydomonas* as a model organism. Annu. Rev. Plant Physiol. Plant Mol. Biol. **52,** 363-406.

Havaux, M.e.a. (2005). The chlorophyll-binding protein IsiA is inducible by high light and protects the cyanobacterium *Synechocystis* PCC 6803 from photooxidative stress. FEBS Lett. **579,** 2289-2293.

Heddad, M., Adamska, I. (2002). The evolution of light stress proteins in photosynthetic organisms. Comparative and Functional Genomics **3,** 504-510.

Hippler, M., Biehler, K., Krieger-Liszkay A., van Dillewjin, J., Rochaix, J.-D. (2000). Limitation of electron transfer in photosystem I donor side mutants of *Chlamydomonas reinhardtii*. J. Biol. Chem. **275,** 5852-5859.

Hippler, M., Klein, J., Fink, A., Allinger, T., Hoerth, P. (2001). Towards functional proteomics of membrane protein complexes: analysis of thylakoid membranes from *Chlamydomonas reinhardtii*. Plant Journal **28,** 595-606.

Hippler, M., Redding, K., Rochaix, J.-D. (1998). *Chlamydomonas* genetics, a tool for the study of bioenergetic pathways. Biochim. Biophys. Acta **1367,** 1-62.

Hoffman, N.E., Pichersky, E., Malik, V. S., Castresana, C., Ko, K., Darr, S. C., Cashmore, A. R. (1987). The nucleotide sequence of a tomato cDNA clone encoding a photosystem I protein with hmology to photosystem II chlorophyll a/b-binding polypeptides. Proc. Natl. Acad. Sci. USA **84,** 8844-8848.

Ihalainen, J.A., D'Haene, S., Yeremenko, N., van Roon, H., Arteni, A. A., Boekema, E. J., van Grondelle, R., Matthijs, H. C., Dekker, J. P. (2005a). Aggregates of the

chlorophyll-binding protein isiA (CP43') dissipate energy in cyanobacteria. Biochemistry **44**,10846-10853.

Ihalainen, J.A., Gobets, B., Kinga, S., Brazzoli, M., Croce, R., Bassi, R., van Grondelle, R., Korppi-Tommola, J. E. I., Dekker, J. P. (2000). Evidence for two spectroscopically different dimers of light-harvesting complex I from green plants. Biochemistry **39,** 8625-8631.

Ihalainen, J.A., van Stokkum, I. H., Gibasiewicz, K., Germano, M., van Grondell, R., Dekker, J. P. (2005b). Kinetics of excitation trapping in intact photosystem I of *Chlamydomonas reinhardtii* and *Arabidopsis thaliana*. Biochim. Biophys. Acta **1706,** 267-275.

Ishihama, Y., Sato, T., Tabata, T., Miyamoto, N., Sagane, K., Nagasu, T., Oda, Y. (2005). Quantitative mouse brain proteomics using culture-derived isotope tags as internal standards. Nature Biotechnology **23,** 617-621.

Jansson, S. (1999). A guide to the Lhc genes and their relatives in *Arabidopsis*. Trends Plant Sci. **4,** 236-240.

Jensen, P.E., Bassi, R., Boekema, E. J., Dekker, J. P., Jansson, S., Leister, D., Robinson, C., Vibe Scheller, H. (2007). Structure, function and regulation of plant photosystem I. Biochim. Biophys. Acta **1767,** 335-352.

Jensen, P.E., Gilpin, M., Knoetzel, J., Vibe Scheller, H. (2000). The PSI-K subunit of photosystem I is involved in the interaction between light-harvesting complex I and the photosystem I reaction center core. J. Biol. Chem. **275,** 24701-24708.

Jensen, P.E., Rosgaard, L., Knowetzel, J., Scheller, H. V. (2002). Photosystem I activity is increased in the absence of the PSI-G subunit. J. Biol. Chem. **277,** 2798-2803.

Jordan, P., Fromme, P., Witt, H., T., Klukas, O., Saenger, W., Krauß, N. (2001). Three-dimensional structure of cyanobacterial photosystem I at 2.5 Å resolution. Nature **411,** 909-917.

Kargul, J., Nield, J., Barber J. (2003). Three dimensional reconstruction of a light harvesting complex I photosystem I (LHCI-PSI) supercomplex from the green alga *Chlamydomonas reinhardtii*. J. Biol. Chem. **278,** 16135-16141.

Kargul, J., Turkina, M. V., Nield, J., Benson, S., Vener, A. V., Barber J. (2005). Light harvesting complex II protein CP29 binds to photosystem I of *Chlamydomonas reinhardtii* under state 2 conditions. FEBS Journal **272,** 4797-4806.

Klimmek, F., Ganeteg, U., Ihalainen, J. A., van Roon, H., Jensen, P. E., Scheller, H. V., Dekker, J. P., Jansson, S. (2005). Structure of the higher plant light harvesting

complex I: in vivo characterization and structural interdependence of the Lhca proteins. Biochemistry **44,** 3065-3073.

Koller, A., Wätzig, H. (2005). Precision and variance components in quantitative gel electrophoresis. Electrophoresis **26,** 2470-2475.

Kouril, R., Arteni, A. A., Lax, J., Yeremenko, N., D'Haene, S., Rögner, M., Matthijs, H. C. P., Dekker, J. P., Boekema, E. J. (2005). Structure and functional role of supercomplexes of IsiA and photosystem I in cyanobacterial photosynthesis. FEBS Lett. **579,** 3253-3257.

Koziol, A.G., Borza, T., Ishida, K.-I., Keeling, P., Lee, R. W., Durnford, D. G. (2007). Tracing the evolution of the ligh-harvesting antennae in chlorophyll *a/b*-containing organisms. Plant Physiol. **143,** 1802-1816.

Krieger-Liszkay, A. (2005). Singlet oxygen production in photosynthesis. J. Exp. Bot. **56,** 337-346.

Kühlbrandt, W., Wang, D., N., Fujiyoshi, Y. (1994). Atomic model of plant light-harvesting complex by electron crystallography. Nature **367,** 614-621.

La Roche, J., Boyd, P. W., McKay, R. M. L., Geider, R. J. (1996). Flavodoxin as an *in situ* marker for iron stress in phytoplankton. Nature **382,** 802-805.

Lam, E., Oritz, W., Malkin, R. (1984). Chlorophyll a/b proteins of photosystem I. FEBS Lett. **525,** 121-125.

Larbi, A., Abadia, A., Abadia, J., Morales, M. (2006). Down co-regulation of light absorption, photochemistry, and carboxylation in Fe-deficient plants growing in different environments. Photosynthesis Research **89,** 113-126.

Laudenbach, D.E., Reith, M. E., Straus, N. A. (1988a). Isolation, sequence analysis and transcriptional studies of the flavodoxin gene from *Anacystis nidulans* R2. J. Bacteriol. **170,** 258-265.

Laudenbach, D.E., Straus, N. A. (1988b). Characterization of a cyanobacterial iron stress-induced gene similar to psbC. J. Bacteriol. **170,** 5018-5026.

Liu, Z., Yan, H., Wang, K., Kuang, T., Zhang, J., Gui, L., An, X., Chang, W. (2004). Crystal structure of spinach major light-harvesting complex at 2.72 Å resolution. Nature **428,** 287-292.

Luciniski, R., Schmid, V. H., Jansson, S., Klimmek, F. (2006). Lhca5 interaction with plant photosystem I. FEBS Lett **580,** 6485-6488.

Luck, D., Piperno, G., Ramanis, Z., Huang, B. (1977). Flagellar mutants of *Chlamydomonas*: studies of radial spoke-defective strains by dikaryon and revertant analysis. Proc. Natl. Acad. Sci. USA **74,** 3456-3460.

McLafferty, F.W., Bockhoff, F., M. (1978). Separation/identification system for complex mixtures using mass separation and mass spectral characterization. Anal. Chem. **50,** 69-76.

Melkozernov, A.N., Barber, J., and Blankenship, R. E. (2006). Light Harvesting in Photosystem I Supercomplexes. Biochemistry **45,** 331-345.

Melkozernov, A.N., Bibby T. S., Lin, S., Barber, J. (2003). Time-resolved absorption and emission show that the CP43´ antenna ring of iron-stressed *Synechocystis* sp. PCC6803 is efficiently coupled to the photosystem I reaction center core. Biochemistry **42,** 3893-3903.

Melkozernov, A.N., Kargul, J., Barber, J., and Blankenship, R. E. (2004). Energy coupling in the PSI-LHCI supercomplex from the green alga *Chlamydomonas reinhardtii*. J. Phys. Chem. B **108,** 10547-10555.

Melkozernov, A.N., Kargul, J., Lin, S., Barber, J., Blankenship, R. E. (2005). Spectral and kinetic analysis of the energy coupling in the PSI-LHCI supercomplex from the green alga *Chlamydomonas reinhardtii* at 77 K. Photosynthesis Research **86,** 203-215.

Merchant, S.S., Allen, M. D., Kropat, J., Moseley, J. L., Long, J. C., Tottey, S., Terauchi, A. M. (2006). Between a rock and a hard place: Trace element nutrition in Chlamydomonas. Biochim. Biophys. Acta **1763,** 578-594.

Montané, H.-M., Kloppstech, K. (2000). The family of light-harvesting-related proteins (LHCs, ELIPs, HLIPs): was the harvesting of light their primary function? Gene **258,** 1-8.

Morosinotto, T., Ballotari, M., Klimmek, F., Jansson, S., Bassi, R. (2005a). The association of the antenna system to photosystem I in higher plants. J. Biol. Chem. **280,** 31050-31058.

Morosinotto, T., Breton, J., Bassi, R., Croce, C. (2003). The nature of a chlorophyll ligand in Lhca proteins determines the far red fluorescence emission typical of photosystem I. J. Biol. Chem. **278,** 49223-49229.

Morosinotto, T., Castelletti, S., Breton, J., Bassi, R., Croce, R. (2002). Mutational analysis of Lhca1 antenna complex. J. Biol. Chem. **277,** 36253-36261.

Morosinotto, T., Mozzo, M., Bassi, R., Croce, R. (2005b). Pigment-pigment interactions in Lhca4 antenna complex of higher plants photosystem I. J. Biol. Chem. **280,** 20612-20619.

Moseley, J., L., Allinger, T., Herzog, S., Hoerth, P., Wehinger, E., Merchant, S., Hippler, M. (2002a). Adaptation to Fe-deficiency requires remodeling of the photosynthetic apparatus. EMBO J. **21,** 6709-6720.

Moseley, J.L., Page, M. D., Alder, N. P., Eriksson, M., Quinn, J., Soto, F., Theg, S. M., Hippler, M., Merchant, S. (2002b). Reciprocal expression of two candidate di-iron enzymes affecting photosystem I and light-harvesting complex accumulation. Plant Cell **14,** 673-688.

Mozzo, M., Morosinotto, T., Bassi, R., Croce, R. (2006). Probing the structure of Lhca3 by mutation analysis. Biochim. Biophys. Acta **1757,** 1607-1613.

Mullet, J.E., Burke, J. J., Arntzen, C. J. (1980). Chlorophyll proteins of photosystem I. Plant Physiol. **1980,** 814-822.

Murray, J.W., Duncan, J., Barber, J. (2006). CP43-like chlorophyll binding proteins: structural and evolutionary implications. Trends Plant Sci. **11,** 152-158.

Naumann, B., Busch, A., Allmer, J., Ostendorf, E., Zeller, M., Kirchhoff, H., Hippler, M. (2007). Comparitive quantitative proteomics to investigate the remodelling of bioenergetic pathways under iron-deficiency in *Chlamydomonas reinhardtii*. Proteomics **In Press**.

Naumann, B., Stauber E. J., Busch, A., Sommer, F., Hippler, M. (2005). N-terminal processing of Lhca3 is a key step in remodelling of the photosystem-I-light-harvesting complex under iron deficiency in *Chlamydomonas reinhardtii*. J. Biol. Chem. **280,** 20431-20441.

Nelson, N., Yocum, C., F. (2006). Structure and function of photosystems I and II. Annu. Rev Plant. Biol. **57,** 521 - 565.

Nield, J., Redding, K., Hippler M. (2004). Remodeling of light-harvesting protein complexes in *Chlamydomonas* in response to environmental changes. Eukaryotic Cell **3,** 1370-1380.

Nishio, J.N., Adabía J., Terry, N. (1985). Chlorophyll-proteins and electron transport during iron nutrition-mediated chloroplast development. Plant Physiol. **78,** 296-299.

Ong, S.-E., Blagoev, B., Kratchmarova, I., Kristensen, D. B., Steen H., Pandey, A., Mann, M. (2002). Stable isotope labeling by amino acids in cell culture, SILAC, as a simple and accurate approach to expression proteomics. Proteomics **1,** 376-386.

Ong, S.-E., Mann, M. (2005). Mass Spectrometry-based proteomics turns quantitative. Nature Chemical Biology **1,** 252-262.

Paulsen, H. (2001). Pigment assembly-transport and ligation. In Rgulation of photosynthesis, E.M. Aro, Andersson, B., ed (Dordrecht, the Netherlands: Kluwer academic publishers), pp. 219-233.

Peers, G., Price, N. M. (2006). Copper-containing plastocyanin used for electron transport by an oceanic diatom. Nature **441,** 341-344.

Perkins, D., N., Pappin, D., J., C., Creasy, D., M., Cottrell, J., S. (1999). Probability-based protein identification by searching sequence databases using mass spectrometry data. Electrophoresis **20,** 3551-3567.

Pichersky, E., Hoffman, N. E., Bernatzky, R., Piechulla, B., Tanksley, S. D., Cashmore, A. R. (1987). Molecular characterization and genetic mapping of DNA sequences encoding type I chlorophyll *a/b*-polypeptide of photosystem I in *Lycopersicon esculentum* (tomato). Plant Mol. Biol. **9,** 205-216.

Pichersky, E., Jansson, S. (1996). The light-harvesting chlorophyll a/b-binding polypeptides and their genes in angiosperm and gymnosperm species. In Oxygenic photosynthesis: the light reactions, D.R. Ort, Yocum, C. F., ed (Dordrecht, the Netherlands: Kluwer Academic Publishers), pp. 507-521.

Redding, K., Cournac, L., Vassiliev, I. R., Goldbeck, J. H., Peltier, G., Rochaix, J.-D. (1999). Photosystem I is indispensable for photoautotrophic growth, CO_2 fixation, and H_2 photoproduction in *Chlamydomonas reinhardtii*. J. Biol. Chem. **274,** 10466-10473.

Richly, E., Leister, D. (2004). An improved prediction of chloroplast proteins reveals diversities and commonalities in the chloroplast proteomes of Arabidopsis and rice. Gene **329,** 11-16.

Rochaix, J.-D. (2001). Assembly, function, and dynamics of the photosynthetic machinery in *Chlamydomonas reinhardtii*. Plant Physiol. **127,** 1394-1398.

Rochaix, J.-D. (2007). Role of thylakoid protein kinases in photosynthetic acclimation. FEBS Lett **581,** 2768-2755.

Rochaix, J.-D., Fischer, N., Hippler, M. (2000). Chloroplast site-directed mutagenesis of photosystem I in *Chlamydomonas*: Electron transfer reactions and light sensitivity. Biochimie **82,** 635-645.

Sandström, S., Park, Y. I., Öquist, G., Gustafsson, P. (2001). CP43', the *isiA* gene product, functions as an excitation energy dissipator in the cyanobacterium *Synechococcus* sp. PCC 7942. Photochem. Photobiol. **74,** 431-437.

Santoni, V., Molloy, M., Rabilloud.,T. (2000). Membrane proteins and proteomics: un amour impossible? Electrophoresis **21**.

Schmid, V.H.R., Paulsen, H., Ruprecht, J. (2002a). Identification of N- and C-terminal amino acids of Lhca1 and Lhca4 required for formation of the heterodimeric peripheral photosystem I antenna LHCI-730. Biochemistry **41,** 9126-9131.

Schmid, V.H.R., Potthast, S., Wiener, M., Bergauer, V., Paulsen, H., Storf, S. (2002b). Pigment binding of photosystem I light-harvesting proteins. J. Biol. Chem. **277,** 37307-37314.

Schwartz, E., Shen, D., Aebersold, R., McGrath, J.M., Pichersky, E., and Green, B.R. (1991). Nucleotide sequence and chromosomal location of cab11 and cab12, the genes for the fourth polypeptide of the photosystem I light-harvesting antenna. FEBS Lett **280,** 229-234.

Schwartz, J.C., Senko, M. W., Syka, J. E. P. (2002). A two-dimensional quadrupole ion trap mass spectrometer. J. Am. Soc. Mass. Spectrom. **13,** 659-669.

Sommer, F., Hippler, M. (2003a). Photosystem I: structure/function and assembly of a transmembrane light-driven plastocyanin/cytochrome c_6-ferredoxin oxidoreductase. In Handbook of Photochemistry and Photobiology, H.S. Nalwa, ed (American Scientific Publishers), pp. 269-294.

Sommer, F., Hippler, M., Biehler, K., Fischer, N., Rochaix, J.-D. (2003b). Compariative analysis of photosensitivity in photosystem I donor and acceptor side mutants of *Chlamydomonas reinhardtii*. Plant Cell and Environ. **26,** 1881-1892.

Spiller, S., Terry, N. (1980). Limiting factors in phtosynthesis. II. Iron stress diminisches photochemical capacity by reducing the number of photosynthetic units. Plant Physiol. **65,** 121-125.

Spreitzer, R.J., Mets, L. (1981). Photosynthesis-deficient mutants of *Chlamydomonas reinhardtii* with associated light-sensitive phenotypes. Plant Physiol. **67,** 565-569.

Standfuss, J., Terwisscha van Scheltinga, A. C., Lamborghini, M., Kühlbrandt, W. (2005). Mechanisms of photoprotection and nonphotochemical quenching in pea light-harvesting complex at 2.5 angstrom resolution. EMBO J. **24,** 919-928.

Stauber, E., J., Busch, A., Naumann, B, Svatoš, A., Hippler, M. (2007). Proteotypic peptide of LHCI from *Chlamydomonas reinhardtii* provides new insights into structure and function of the complex. Submitted to Proteomics.

Stauber, E., J., Hippler, M. (2004). *Chlamydomonas reinhardtii* proteomics. Plant Phys. Biochem. **42,** 989-1001.

Stauber, E.J., Fink, A., Markert, K., Kruse, O., Johanningmeier, U., Hippler, M.,. (2003). Proteomics of *Chlamydomonas reinhardtii* light-harvesting proteins. Eukaryotic Cell **2,** 978-994.

Storf, S., Jansson S., Schmid, V. H. R. (2005). Pigment binding, fluorescence properties, and oligomerization behaviour of Lhca5. a novel light-harvesting protein. J. Biol. Chem. **280**, 5163-5168.

Storf, S., Stauber, E. J., Hippler, M., Schmid, V. H. R. (2004b). Proteomic analysis of phtosystem I light-harvesting antenna in tomato (*Lycopersicon esculentum*). Biochemistry **43,** 9214-9224.

Takahashi, Y., Yasui, T.-a., Stauber, E. J., Hippler, M. (2004). Comparison of the subunit compositions of the PSI-LHCI supercomplex and the LHCI in the green alga *Chlamydomonas reinhardtii*. Biochemistry **43,** 7816-7823.

Terry, N. (1980). Limiting factors in photosynthesis I. use of iron stress to control photochemical capacity *in vivo*. Plant Physiol. **65,** 114-120.

Uitto, P.M., Lance, B. K., Wood, G. R., Sherman, J., Baker, M. S., Molloy, M. P. (2007). Comparing SILAC and two-dimensional gel electrophoresis image analysis for profiling urokinase plasminogen activatior signaling in ovarian cancer cells. J. Prot. Res. **In press**.

Varotto, C., Pesaresi, P., Jahns, P., Leßnick, A., Tizzano, M., Schiavon, F., Salamini, F., Leister, D. (2002). Single and double knockouts of the genes for photosystem I subunits G, K, and H of arabidopsis, effects on photosystem I composition, photosynthetic electron flow, and state transitions. Plant Physiol. **129,** 616-624.

Varsano, T., Kaftan, D., Pick, U. (2003). Effects of iron deficiency on thylakoid membrane structure and composition in the Alga *Dunaliella salina*. J. Plant Nutr. **26,** 2197-2210.

Varsano, T., Wolf, S. G., Pick, U. (2006). A chlorophyll *a*/*b*-binding protein homolog that is induced by iron deficiency is associated with enlarged photosystem I units in the eucaryotic Alga *Dunaliella salina*. J. Biol. Chem. **281,** 10305-10315.

Vasil'ev, S., Bruce, D. (2004). Optimization and evolution of light harvesting in photosynthesis: the role of antenna chlorophyll conserved between photosystem II and photosystem II. Plant Cell **16,** 3059-3068.

Wagner, V., Fiedler, M., Markert, C., Hippler, M., Mittag, M. (2004). Functional proteomics of circadian expressed proteins from *Chlamydomonas reinhardtii*. FEBS Lett. **559**, 129-135.

Wehner, A., Storf, S., Jahns, P., Schmid, V. H. R. (2004). De-epoxidation of vilaxanthin in light-harvesting complex I proteins. J. Biol. Chem. **279,** 26823-26829.

Weigel, M., Varotto, C., Pesaresi, P., Finazzi, G., Rappaport, F. (2003). Plastocyanin is indispensable for photosynthetic electron flow in *Arabidopsis thaliana*. J. Biol. Chem. **278,** 31286-31289.

Westbrook, J.A., Yan, J. X., Wait, R., Welson, S. Y., Dunn, M. J. (2001). Zooming-in on the proteome: very narrow-range immobilised pH gradients reveal more protein species and isoforms. Electrophoresis **22,** 2865-2871.

Wollman, F.-A., Bennoun, P. (1982). A new chlorophyll-protein complex related to photosystem I in *Chlamydomonas reinhardtii*. Biochim. Biophys. Acta **680,** 352-360.

Zhang, S., Vibe Scheller, H. (2004). Photoinhibition of photosystem I at chilling temperature and subsequent recovery in *Arabidopsis thaliana*. Plant Cell Physiol. **45**, 1595-1602.

Zhu, X., Desiderio, D., M. (1996). Peptide quantification by tandem mass spectrometry. Mass Spectrom. Rev. **15,** 213-240.

Zolla, L., Rinalducci, S., Timperio, A. M., Huber, C. G. (2002). Proteomics of light-harvesting proteins in different plant species. analysis and comparison by liquid chromatography-electrospray ionization mass spectrometer. photosystem I. Plant Physiol. **130,** 1938-1950.

Eigenständigkeitserklärung

Ich erkläre hiermit, dass ich die vorliegende Dissertation selbständig verfasst, keine Textabschnitte eines Dritten ohne Kennzeichnung übernommen und keine anderen als die angegebenen Quellen, persönlichen Mitteilungen und Hilfsmittel verwendet habe.

Braunschweig, den 25. November 2007 .....

Einar J. Stauber

Curriculum vitae

Einar Jamandre Stauber
born on 22.08.1973 in Moscow (Idaho, USA)
married, one son (born on 05.09.2004)

Current occupation

since 01.09.2006	Scientist at the Institute of Pharmaceutical Biology, Braunschweig University of Technology

Undergraduate and graduate studies

02/2003-10/2006	Graduate Student at the Institute of Plant Physiology, Friedrich-Schiller-University Jena
10/2000-02/2003	Student of Biology at the FSU Jena, Diploma 22 February 2003
11/1999-09/2000	Language certificate „German as a second language“, FSU Jena
11/1999-02/2003	Various employments as research and teaching assistant at the Max Planck Institute for Chemical Ecology, Jena, and the FSU Jena
08/1998-10/1999	Research training at the Max Planck Institute for Chemical Ecology, Jena
09/1991-08/1998	Student at the Washington State University, Pullman (Washington, USA) 05/1998 Bachelor of Science (Chemistry) 12/1996 Bachelor of Science (Physical Science)

School education

1986-1991	High school in Genesee (Idaho, USA)
1985-1986	Realschule in Unterschleißheim (Germany)
1979-1985	Grade school in Genesee (Idaho, USA)

Research stipends

03/2005-02/2006	Research stipend at the Max Planck Institute for Chemical Ecology Jena, Mass Spectrometry Research Group
08/1998-10/1999	Research stipend at the Max Planck Institute for Chemical Ecology Jena, Department of Biochemistry
01/1992-05/1993	Howard Hughes Research Fellowship at the Department of Biochemistry, Washington State University

Acknowledgements

The experimental part of this PhD thesis was accomplished at the Institute of Plant Physiology at the Friedrich-Schiller-Universität in Jena and at the Mass Spectrometry Unit of the Max Planck Institute for Chemical Ecology in Jena from March 2003 to February 2006. I am grateful to my scientific supervisor Prof. Dr. Michael Hippler who gave me the possiblility to work on this project. I would like to thank Michael for many inspiring discussions on theoretical and practical subjects which contributed greatly to all aspects of my thesis work.

Prof. Dr. Maria Mittag was generous in acting as my academic supervisor at the FSU in Jena. In addition, I appreciate that she kept me involved in the Chlamydomonas Forschergruppe during the last year of the experimental work.

I am grateful to Dr. Aleš Svatoš for supporting me during the last year of experimental work. I really enjoyed working in his laboratory at the MPI for Chemical Ecology in Jena. Aleš' suggestions on peptide chromatography and the use of mass spectrometry for peptide quantification were very valuable for the stoichiometric measurements of the Lhca with PSI.

I wish to thank to all my collaborators and coauthors of the manuscripts for their contributions that greatly extended the insights into the composition and function of Lhca proteins that I could gain in this project. I thank Dr. Volkmar H. R. Schmid for his good insights and critical comments to the discussion of tomato LHCI. I am grateful to Prof. Dr. Poul Erik Jensen for taking the time to critically read this thesis, and I thank him for his good comments.

I thank Prof. Dr. Ralf Oelmüller for generating an inspiring scientific atmosphere at the Institute of Plant Physiology at the FSU and for his interest and support throughout my thesis work. All my coworkers at the Institute of Plant Physiology at the FSU and the Mass Spectrometry Unit of the MPI are thanked for making this work a valuable scientific and personal experience.

I would like to thank Ute Wittstock for her support, her comments and suggestions on the thesis and for help with the German translation of the summary and theses. I am grateful to my parents who have continued to encourage me throughout the course of my studies.